Title	Microbial community dynamics of farmed Atlantic salmon gill microbiomes during amoebic gill disease episodes
Author(s)	Birlanga, Victor B.
Publication Date	2022-06-14
Publisher	NUI Galway
Item record	http://hdl.handle.net/10379/17210

MICROBIAL COMMUNITY DYNAMICS OF FARMED ATLANTIC SALMON GILL MICROBIOMES DURING AMOEBIC GILL DISEASE EPISODES

A thesis submitted in partial fulfilment of the requirements for

the degree of Doctor of Philosophy

by

Victor B. Birlanga

Microbial Communities Laboratory,

School of Natural Sciences,

National University of Ireland Galway

May 2022

Head of School: Prof. Adrienne Gorman

Head of Discipline: Prof. Conor O'Byrne

Research Supervisor: Dr. Gavin Collins

Table of Contents

Acknowledgments

I would like to thanks my supervisor, Dr. Gavin Collins, who gave me the opportunity to work with him in my PhD, providing his support, guidance and expertise since the beginning. I would also like to thank my graduate research committee, Dr. Anne Marie Power, Dr. Aoife Boyd, and Dr. Florence Abram for their advice and supervision. Additionally, I want to thank Dr. Eugene MacCarthy, Dr. Grace McCormack, and Professor Cindy Smith for their guidance and wise advice.

I am very grateful for all the help and mentoring I got from Dr. Umer Zeeshan Ijaz on bioinformatics and data visualisation, his help was highly valuable. Thank you to all of the other people who helped with different aspects of this thesis; Catherine McManus for provide useful data, Dr. Neil Ruan for qPCR analyses, Dr. Victoria Valdenegro for her help and insight in chapter 5, and Dr. Luca Mirimin for his help in water sampling.

A huge thank you to all of the members of the Microbial Communities Lab in NUIG, for their professional and moral support, including: Octavi, Joe, Anna, Simon and Marco. Thanks to everyone else in the Microbiology Department at NUIG especially those in the technical staff; Mike, Anne and Maurice.

I would also like to thank all researchers in the same project working in GMIT; Dr. Anita Talbot and Kerrie Ni Dhufaigh for their help with sampling optimisation and the lab trial.

I would like to dedicate special thanks to the Latin dance community in Ireland, your warm welcome and smile, along with all our dancing experiences, healed my mental and emotional status. All of you mean a lot to me.

Thank you to my dear family; papá, mama, Ángela, Juanvi, and all my friends in Spain; Adrián, Marcos, Inma, Noelia, Natalia and Leti, all of you encouraged and loved me in the distance during the hardest times. Os quiero mucho a todos.

Finally, I would like to thank Huong, your love and patience made this thesis possible. Your constant support, along with Mimi and Nheonheo, made this experience an amazing adventure, especially during the pandemic. Tôi yêu bạn.

Abstract

Gill pathologies, especially the Amoebic Gill Disease (AGD), present one of the main health concerns for marine aquaculture worldwide. In Ireland alone, Atlantic salmon (*Salmo salar* L.) production in fish farms was 12,000 tonnes worth €114.5 million in 2018, but the mortality of the livestock in marine farms due to AGD reaches an average between 10-20% every year. As of yet, the most common means to reduce AGD is to control the abundance of its first aetiological agent, the free-living amoeba *Neoparamoeba perurans*, that typically produces white mucoid patches on infected gills. There are two main ways to diagnose AGD: **i)** by scoring gills based on the abundance of white patches on them; **ii)** quantifying *N. perurans* abundance on gills using quantitative-PCR assays. However, these diagnosis tools are only useful in confirming the amoeba colonisation on gills, being unable to determine the vulnerability to AGD prior to the colonisation. Indeed, our understanding of AGD is far from complete; specifically, the role of the gill microbiome from seawater farmed salmon and how it responds to an AGD episode is limited.

The present thesis mainly aimed to characterise the prokaryotic gill microbiome from farmed Atlantic salmon (*Salmo salar* L.) before and during an AGD episode using high-throughput sequencing approaches. A first sampling campaign was carried out in a single Irish fish farm, where gill and mucus from gills were sampled from Atlantic salmon from May to October in 2017. A novel DNA extraction procedure was optimised and used to get the microbiome DNA from entire gill arches, with the objective to avoid under-sampling and taxa under-representation that could happen as a result of characterising the gill microbiome from part of a gill arch. On the other hand, the microbiome DNA in mucus samples was extracted and isolated aiming to test the efficacy of mucus sampling as a suitable alternative source to gills for AGD microbiome analyses. A set of variables, such as AGD gill scores, *N. perurans* abundance on gills, fish condition factor, water temperature, salinity, oxygen, and turbidity, was monitored to track the development of the AGD episode and environmental variations. After an AGD onset, the prokaryotic community on salmon gills shifted towards lower diversity and less balance. In addition, the possible correlation between the development of AGD and the prokaryotic microbiome from gill and mucus samples was suggested after an AGD episode. Bacterial communities from gill and mucus samples presented close similarities, establishing mucus scrapings as a suitable non-lethal substitute for gill sampling for partial characterisation of the whole-gill prokaryotic community.

Average AGD-associated mortalities in certain fish farms have been punctually reported to reach a 60-80% loss in stocks, higher than the annual average between 10-20% every year in most of the farm locations. In addition, frequency of AGD outbreaks seemed to differ between salmon-producing regions. A second sampling campaign aimed to characterise the prokaryotic microbiome on gills from farmed Atlantic salmon at six disparate fish farms before and during AGD. Thus, from June to December 2018, salmon gills were sampled from each of the six farms along the West coast of Ireland at various sampling points. The gill microbiome DNA was extracted and isolated from following the DNA extraction optimised in the previous sampling campaign. Additionally, a set of variables was monitored during the campaign to track the AGD development and environmental variations. AGD severity was similar between farms; but, the AGD development was still correlated with changes in gill microbiome from every fish farm. However, the strong influence of the different environmental factors made it difficult to discern patterns. During the hottest time of the year, we found a decreasing gradient in gill microbiome diversity from northern to southern fish farms. In addition, the location of each fish farm significantly influenced the bacterial community, in combination with the AGD development.

Variations in the environmental factors greatly impacted the gill microbiome, but there were evidence suggesting the connection between the gill microbiome and AGD. Hence, a third sampling campaign aimed to further investigate the possible connection between the gill microbiome and AGD by describing the impact of the disease on the bacterial community on gills, but in a controlled laboratory challenge. Additionally, functional diets were also recently shown to have a positive impact on the survival and physiological response to AGD on salmon. Therefore, we also tested the effect of various functional diets on AGD severity and the gill microbiome in AGD-affected Atlantic salmon. Atlantic salmon were separated and treated distinctly in four tanks, sampling gills at each timepoint. The gill microbiome DNA was extracted and isolated following the DNA extraction optimised in the first sampling campaign. In addition, water samples were taken from each experimental tank to compare the gill and water microbiome, and to determine the effect of the functional diets on the surrounding seawater microbiome. The fish condition factor, AGD gill scores, and *N. perurans* abundance on gills were tracked. Unexpectedly, the diversity and evenness of the prokaryotic gill microbiome increased in AGD-affected salmon. Additionally, a tested functional diet impacted the gill microbiome before AGD, while the various diets differentiate the water microbiome during the whole laboratory trial. Bacterial communities were distinct between gill and water samples. These results further evidenced the impact of the AGD on the gill microbiome of Atlantic

salmon, and also provided some initial evidence of the influence of the diet on both, the gill and the water microbiome.

Our knowledge about the AGD onset and development is still far from complete; however, results in the present thesis proved that the AGD impacted the gill microbiome from farmed Atlantic salmon along the Irish West coast, and in laboratory conditions.

CHAPTER 1

Introduction, Scope and Structure of Thesis

1.1 - Introduction to Thesis

Global aquaculture production has been increasing gradually over the past 40 years, and now almost exceeds the biomass captured in worldwide fisheries (SOFIA, 2020). Aquaculture production is expected to continue rising over the coming years, becoming the primary source of fish protein for the growing human population. Atlantic salmon (*Salmo salar* L.) aquaculture production is also expected to increase, representing a very important part of the global aquaculture sector. In Ireland alone, there were around 30 fish farms producing salmon in 2018, with a production worth €114.5 million (BIM Annual Aquaculture Survey 2019). However, the impact of various diseases constrains the benefits associated with Atlantic salmon aquaculture. In fact, infectious diseases affecting fish gills could represent 12% of the losses in marine fish farms (Rodger, 2007), with amoebic gill disease (AGD) perhaps the most concerning gill disorder with respect to economic impact. The impact of AGD on Atlantic salmon aquaculture has been estimated to increase production costs by 10-20% (Munday *et al*., 2001; Downes, 2017).

Fish affected by AGD experience various behavioural changes, including lethargy, reduced appetite, increased ventilation rates, increased gill mucus production, and tend to congregate close to the surface of the water. Infected fish also exhibit microscopic signs after the colonisation of the AGD first aetiological agent, the marine amoeba *Neoparamoeba perurans* (Young *et al.*, 2007), on gills, namely: hyperplasia, lamellar fusion, and the development of interlamellar vesicles. However, the most recognisable AGD macroscopic sign is the presence of white mucoid patches on gills, as a result of the hyperplasia and lamellar fusion. The abundance and size of these patches are used as a quantitative sign of the AGD severity in gross pathological assessment of the gills, especially when compared to an already established guideline (Taylor *et al*., 2009). Other techniques have been developed to track AGD development ahead of the appearance of any observable signs. Indeed, a quantitative Polymerase Chain Reaction (qPCR) targeting *N. perurans* was optimised (Bridle *et al*., 2010; Downes *et al*., 2015), allowing researchers to detect and quantify the amoeba after it colonised the gills. However, these diagnosis methods cannot predict the susceptibility of an Atlantic salmon cohort to AGD prior to colonisation of gills with *N. perurans*. The resistance to AGD of some hybrid Atlantic salmons was confirmed (Maynard *et al*., 2016), and genetic factors involved in the resistance of non-hybrids were identified (Robledo *et al*., 2020). The establishment of a susceptibility status of farmed fish would allow producers to treat the susceptible salmon to help prevent an AGD episode.

There are many factors influencing the development of AGD on Atlantic salmon, of which salmon genetics, farming practices, and environmental conditions are among the most important (Crosbie *et al*., 2010; Oldham *et al*., 2016; Boerlage *et al*., 2020; Robledo *et al*., 2020). Nevertheless, little is known about the possible role of the gill microbiome in the onset and development of AGD in farmed Atlantic salmon (Nowak & Archibald, 2018). In particular, there is a paucity of data from field studies. Additionally, the gill microbiome is still poorly understood in healthy Atlantic salmon, making it more difficult to interpret the role of specific bacteria in AGD-affected gills. With improved understanding of the interactions between the gill microbiome and AGD development, or severity, the abundance of key species may be used to indicate the susceptibility of salmon cohorts to AGD episodes.

One of the main sets of influencing factors in the development of AGD relates to environmental conditions, which will differ between fish farms depending on geographical location. This may partially explain why, although typical AGD outbreaks cause mortalities between 10 and 20% in salmon stocks, mortality sometimes could reach 80% in certain locations, such as in Scotland, Norway and Ireland (Shinn *et al.*, 2015). These differences in environmental factors also select for the microbial communities in seawater, very likely influencing the composition of the gill microbiome of farmed salmon in those waters and their possible relationship with AGD. Thus, studying and comparing the gill microbiome of Atlantic salmon from disparate farms would improve understanding of the gill disease as well as the dynamics of key bacterial taxa, or niches, in the gill microbiome. On the other hand, recent testing on the influence of various diets showed an improvement in survival and physiological response of Atlantic salmon to AGD (Oldham *et al*., 2016; Mullins *et al*., 2020), opening a new field to treat AGD in less-invasive and inexpensive ways. Further research in this field may lead to the identification of a diet formula suitable for at least partial treatment of AGD and to complement existing treatments.

Traditionally, microbial ecology studies have relied on culture-dependent techniques. However, it has been suggested that only 0.1 – 1% of all microorganisms have yet been cultured under laboratory conditions i.e. classical microbiology is constrained by the Plate Count Anomaly (Staley and Konopka, 1985). The development of culture-independent approaches, such as high-throughput amplicon sequencing, targeting the 16S rRNA genes of bacteria and archaea, has revolutionised Microbiology and allowed the *in situ* study of microbial ecology across a vast range of environments (Thompson *et al*., 2017). To date, only one published paper has applied

high-throughput amplicon sequencing to study the bacterial microbiome on gills from AGD-affected Atlantic salmon (Slinger *et al*., 2020), and, thus, further research should be done in this field.

Previous studies that aimed to characterise the gill microbiome from Atlantic salmon regularly have used part of an excised gill arch, or gill swabs in their DNA extraction procedures to isolate microbiome nucleic acids. However, it is still not determined whether genetic material extracted from a part of the gill or from gill swabs would be representative of the microbiome from an entire gill arch. Other literature described extracting the microbiome DNA from whole gill arches (Hess *et al*., 2015; Lowrey *et al*., 2015), but their extractions required a disruption of fish tissue, aiming the lysis and disintegration of the microbiome cells, but it also affects gill cells. Thus, this approach typically cannot allow for complete separation of nucleic acids originating from the microbiome and the host, hence the host DNA may compete with microbiome DNA for PCR amplification during sequencing, limiting the number of reads from the microbiome, and possibly obscuring patterns in downstream microbiome analyses (Lefèvre *et al*., 2020; Reigel *et al.*, 2020). In conclusion, an optimised DNA extraction procedure from entire gill arches and a step to isolate and concentrate the microbial cells prior to DNA extraction is desirable for use in gill microbiome studies. Additionally, testing mucus swabbing as a non-lethal, less invasive and suitable substitute for gill sampling would provide the basis for more attractive sampling techniques in gill microbiome research.

1.2 - Structure of Thesis

This thesis comprises of a literature review (Chapter 2) documenting the research to date on the aetiology, diagnosis, distribution, treatment and management of AGD, as well as the potential role(s) of microbial communities, and in particular the gill microbiome, in AGD onset and development. Chapter 2 concludes with the development of the hypotheses, and presentation of research questions, underpinning this thesis. This is followed by three experimental chapters focused on the microbiomics of salmon gills – Chapter 3 on a field-scale sampling campaign, Chapter 4 on geographically disparate field campaigns, and Chapter 5 on a laboratory-scale trial. The thesis closes with a final chapter (Chapter 6) offering a general discussion on the work of this thesis, as well as conclusions, and recommendations for future research in this area.

1.3 - References

BIM (Bord IascaighMhara) Annual Aquaculture Survey (2019) Ireland's Seafood Development Agency. http://www.bim.ie/our-publications/aquaculture/

Boerlage, A. S., Ashby, A., Herrero, A., Reeves, A., Gunn, G. J., & Rodger, H. D. (2020) Epidemiology of marine gill diseases in Atlantic salmon (*Salmo salar*) aquaculture: a review. *Reviews in Aquaculture*, 1-20.

Bridle, A. R., Crosbie, P. B. B., Cadoret, K., & Nowak, B. F. (2010). Rapid detection and quantification of *Neoparamoeba perurans* in the marine environment. *Aquaculture*, 309(1-4), 56-61.

Crosbie, P. B., Bridle, A. R., Leef, M. J., & Nowak, B. F. (2010). Effects of different batches of *Neoparamoeba perurans* and fish stocking densities on the severity of amoebic gill disease in experimental infection of Atlantic salmon, *Salmo salar* L. *Aquaculture Research*, 41(10), e505-e516.

Downes, J. K., Henshilwood, K., Collins, E. M., Ryan, A., Connor, I. O., Rodger, H. D., MacCarthy, E., & Ruane, N. M. (2015). A longitudinal study of amoebic gill disease on a marine Atlantic salmon farm utilising a real-time PCR assay for the detection of *Neoparamoeba perurans*. *Aquaculture Environment Interactions*, 7(3), 239-251.

Downes, J. K. (2017). Gill disease in finfish aquaculture with emphasis on amoebic gill disease (Doctoral dissertation, Galway-Mayo Institute of Technology).

Hess, S., Wenger, A. S., Ainsworth, T. D., & Rummer, J. L. (2015). Exposure of clownfish larvae to suspended sediment levels found on the Great Barrier Reef: impacts on gill structure and microbiome. *Scientific reports*, 5, 10561.

Lefèvre, E., Gardner, C.M. and Gunsch, C.K. (2020). A novel PCR-clamping assay reducing plant host DNA amplification significantly improves prokaryotic endo-microbiome community characterization. *FEMS Microbiology Ecology*, 96(7), p.fiaa110.

Lowrey, L., Woodhams, D. C., Tacchi, L., & Salinas, I. (2015). Topographical mapping of the rainbow trout (*Oncorhynchus mykiss*) microbiome reveals a diverse bacterial community with antifungal properties in the skin. *Applied and Environmental Microbiology*, 81(19), 6915-6925.

Maynard, B. T., Taylor, R. S., Kube, P. D., Cook, M. T., & Elliott, N. G. (2016). Salmonid heterosis for resistance to amoebic gill disease (AGD). *Aquaculture*, 451, 106-112.

Mullins, J., Nowak, B., Leef, M., Røn, Ø., Eriksen, T. B., & McGurk, C. (2020). Functional diets improve survival and physiological response of Atlantic salmon (*Salmo salar*) to amoebic gill disease. *Journal of the World Aquaculture Society*, 51(3), 634-648.

Munday, B. L., Zilberg, D., & Findlay, V. (2001). Gill disease of marine fish caused by infection with *Neoparamoeba pemaquidensis*. *Journal of Fish Diseases*, 24(9), 497-507.

Nowak, B. F., & Archibald, J. M. (2018). Opportunistic but lethal: the mystery of paramoebae. *Trends in parasitology*, 34(5), 404-419.

Oldham, T., Rodger, H., & Nowak, B. F. (2016). Incidence and distribution of amoebic gill disease (AGD)—an epidemiological review. *Aquaculture*, 457, 35-42.

Reigel, A.M., Owens, S.M. and Hellberg, M.E. (2020). Reducing host DNA contamination in 16S rRNA gene surveys of anthozoan microbiomes using PNA clamps. *Coral Reefs*, 39(6), 1817-1827.

Robledo, D., Hamilton, A., Gutiérrez, A. P., Bron, J. E., & Houston, R. D. (2020). Characterising the mechanisms underlying genetic resistance to amoebic gill disease in Atlantic salmon using RNA sequencing. *BMC genomics*, 21, 1-11.

Rodger, H. D. (2007). Gill disorders: an emerging problem for farmed Atlantic salmon (*Salmo salar*) in the marine environment. *Fish Veterinary Journal*, 9, 38-48.

Shinn, A. P., Pratoomyot, J., Bron, J. E., Paladini, G., Brooker, E. E., Brooker, A. J., &Timi, J. (2015). Economic costs of protistan and metazoan parasites to global mariculture. *Parasitology*, 142(1), 196.

Slinger, J., Adams, M. B., & Wynne, J. W. (2020). Bacteriomic profiling of branchial lesions induced by *Neoparamoeba perurans* challenge reveals commensal dysbiosis and an association with *Tenacibaculum dicentrarchi* in AGD-affected Atlantic salmon (*Salmo salar* L.). *Microorganisms*, 8(8), 1189.

SOFIA (2020) Fisheries and Aquaculture topics. The State of World Fisheries and Aquaculture. Food and Agricultural Organization of the United Nations. http://www.fao.org/documents/card/en/c/ca9229en

Staley, J. T., & Konopka, A. (1985). Measurement of in situ activities of nonphotosynthetic microorganisms in aquatic and terrestrial habitats. *Annual review of microbiology*, 39(1), 321-346.

Thompson, L. R., Sanders, J. G., McDonald, D., Amir, A., Ladau, J., Locey, K. J., Prill, R.J., Tripathi, A., Gibbons, S.M., Ackermann, G. & Knight, R. (2017). A communal catalogue reveals Earth's multiscale microbial diversity. *Nature*, 551(7681), 457-463.

Taylor, R. S., Muller, W. J., Cook, M. T., Kube, P. D., & Elliott, N. G. (2009). Gill observations in Atlantic salmon (*Salmo salar*, L.) during repeated amoebic gill disease (AGD) field exposure and survival challenge. *Aquaculture*, 290(1-2), 1-8.

Young, N. D., Crosbie, P. B. B., Adams, M. B., Nowak, B. F., & Morrison, R. N. (2007). *Neoparamoeba perurans* n. sp., an agent of amoebic gill disease of Atlantic salmon (*Salmo salar*). *International journal for parasitology*, 37(13), 1469-1481.

CHAPTER 2

Literature Review

2.1 - Aquaculture from a global perspective

Global aquaculture production from inland and marine farms has been increasing since 1950, reaching an estimated value of 82 million tonnes (**Fig. 2.1**), worth over US$ 400 billion. This trend is the consequence of increasing human population as well as rising demand for fish consumption, from 5.2 kg per capita in 1961 to 19.4 kg in 2017 (SOFIA, 2020). It is expected global fish production will continue to expand and is projected to grow by 15% to a total of 204 million tonnes by 2030 (SOFIA 2020). Specifically, aquaculture fish production is expected to reach an increase in the annual production of 109 million tonnes in 2030, 32% more than 2018 (SOFIA 2020). In comparison, fish production in aquaculture is expected to continue growing in the upcoming years, while fisheries captures are expected to be stable (SOFIA, 2020).

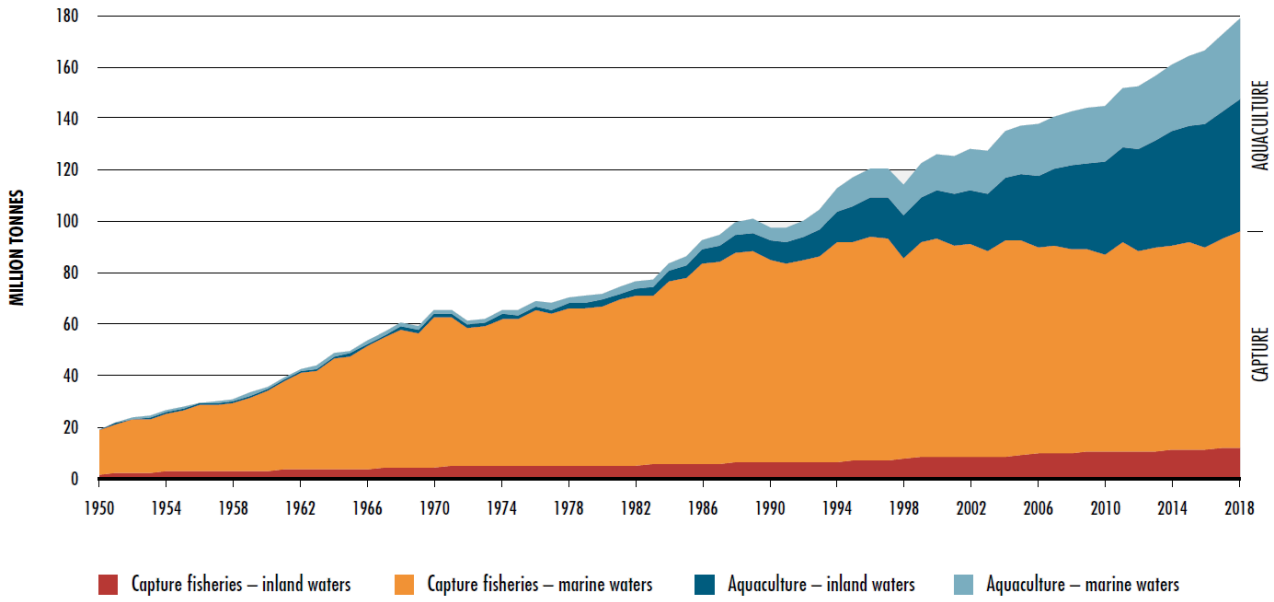

NOTE: Excludes aquatic mammals, crocodiles, alligators and caimans, seaweeds and other aquatic plants.
SOURCE: FAO.

Figure 2.1. Global capture fisheries and aquaculture production in inland and marine waters 1950-2018 (SOFIA, 2020).

Global aquaculture production of Atlantic salmon (*Salmo salar* L.) has also increased since 2010 (1.4 million tonnes), reaching 2.4 million tonnes in 2018 driven by rising demand in both developed and developing markets (SOFIA, 2020). In fact, the salmonid production industry accounted for around 19% of the total value of internationally traded fish products in 2018 (SOFIA 2020). In Ireland alone, Atlantic salmon production in fish farms in 2018 was 12,000 tonnes worth €114.5 million (BIM Annual Aquaculture Survey 2019) (**Fig. 2.2**). The number of fish farms in Ireland increased from 22 active sites in 2016 to34 in 2019 (BIM Annual

Aquaculture Survey 2019), and may change in future due to variations in management practices (O'Donohoe *et al.*, 2017).

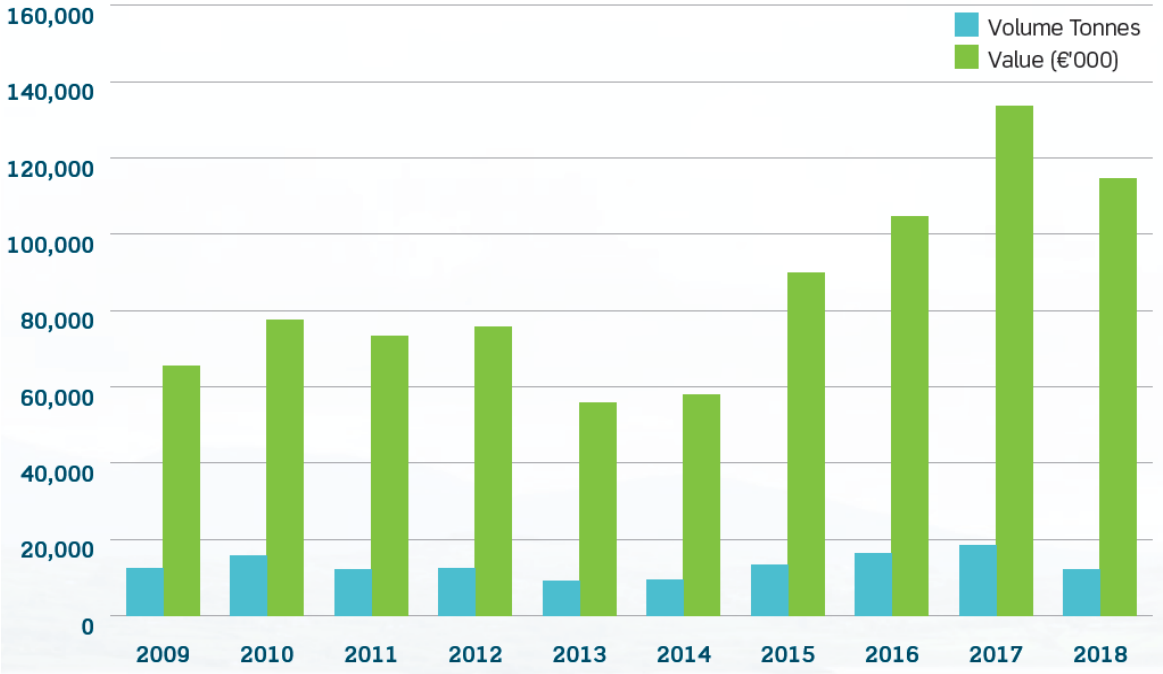

Figure 2.2. Irish Atlantic salmon production from aquaculture and its value from 2009 to 2018 (Source: BIM, 2019).

However, the expected growth of the global salmonid industry faces several limitations likely to strain productivity and increase costs, such as the adoption of increasingly stringent environmental regulations; fewer feasible sites for farming; adverse, and changing, environmental conditions; and increasingly prevalent aquatic animal diseases. Gill pathologies, especially infectious gill diseases, present one of the main health concerns for marine salmons worldwide (Marcos-López *et al.*, 2017).

2.2 - Infectious gill diseases in salmon

The essential role of the gills in gas exchange, osmoregulation, nitrogen excretion, pH regulation and hormone synthesis in fish make gill disorders highly harmful and costly in the aquaculture industry. Between 2003 and 2005 gill infectious diseases increased the mortality of the livestock in marine farms to an average of 12% (Rodger, 2007). In addition to the fish losses, the poor food conversion of the infected survivors, along with the cost of treating such disorders, has increased substantially the financial investment required at fish farms to maintain production.

Therefore, there has been a great effort in recent decades to better diagnose, understand and treat gill infectious disorders, especially in salmonid fish farms.

Marine gill infections in salmonids can be classified by aetiology-based types. Within disorders with one causative agent, it possible to distinguish six different categories (Boerlage *et al*. 2020): (i) parasitic gill diseases, (ii) viral gill diseases, (iii) bacterial gill diseases, (iv) zooplankton-associated gill diseases, (v) harmful algal gill diseases, and (vi) amoebic gill diseases (**Table 2.1**). In addition, direct consequences of these gill infections could lead to higher vulnerabilities to other pathogens (Rodger, 2007), especially in marine fish farms where co-infections on salmon are more common (Downes *et al.*, 2018a). One of the most common parasitic gill disorders with, probably, multiple aetiological agents is the recently re-named Complex Gill Disease (CGD) (Herrero *et al*., 2018). This disease has been described as encompassing the Proliferative Gill Disease (PGD) and the Proliferative Gill Inflammation (PGI), with non-specific signs of any gill dysfunctionality, and a variable histopathology and gross pathology (Herrero *et al*., 2018). On the other hand, Amoebic Gill Disease (AGD) can be classified as a parasitic or amoebic gill disease, but, among the most common gill infectious disorders, AGD represents perhaps the most relevant gill disorder in terms of economic impact and gill health (Bustos *et al.*, 2011; Nowak *et al.*, 2014; Marcos-López *et al.*, 2017; Rozas-Serri, 2019), and is thus the main focus of the present thesis.

Table 2.1. Types of gill infectious pathologies and a representative disease from each type.

Type of gill infection	Representative disease	Pathogen	Reference
Parasitic	Proliferative Gill Inflammation (PGI)	*Desmozoon lepeophtherii*	Nylund *et al*. 2011
Viral	Salmon gill poxvirus disease	Salmon gill poxvirus (SGPV)	Thoen *et al.* 2020
Bacterial	Tenacibaculosis	*Tenacibaculum maritimum*	Avendaño-Herrera *et al.* 2006
Zooplankton-associated	Gill injuries due to stings	*Muggiaea atlantica*	Purcell *et al.* 2013
Harmful algal	Gill irritation and bleeding	*Chaetoceros concavicornis*	Rensel & Whyte 2003
Amoebic	Amoebic Gill Disease	*Neoparamoeba perurans*	Oldham *et al.* 2016

2.3 - Amoebic gill disease (AGD)

The first described AGD episode occurred in Tasmania, Australia in the 1980s (Munday, 1986) on salmon caged in sea water. Since then, this pathology has been reported in the USA (Kent *et al.*, 1988), France (Findlay *et al.*, 1995), Spain (Rodger & McArdle, 1996), Ireland (Rodger & McArdle, 1996), Chile (Nowak *et al.*, 2002), Norway (Steinum *et al.*, 2008), Scotland (Rodger, 2014), South Africa (Mouton *et al.*, 2014), New Zealand (Young *et al.*, 2008a), Japan (Crosbie *et al.*, 2010a), Faroe Islands (Oldham *et al.*, 2016), Canada (Oldham *et al.*, 2016) and South Korea (Kim *et al.*, 2017). However, although the average AGD-associated mortalities around the world range between 10 and 20%, some fish farms have been reported to reach a 60-80% loss in stocks (Shinn *et al.*, 2015). A combination of multiple factors might explain these differences, including variations in intrinsic resistance to AGD among different salmon cohorts (Vincent *et al.*, 2006; Taylor *et al.*, 2007; Wynne *et al.*, 2007); the availability of proven AGD treatments; the density of salmon populations in the fish farms (Crosbie *et al.*, 2010b); and the site-specific environmental conditions at the farms.

Some fish species other than Atlantic salmon (*Salmo salar* L.) that were reported to be affected by AGD are coho salmon (*Oncorhynchus kisutch*; Kent, 1988), rainbow trout (*Oncorhynchus mykiss*; Munday *et al.*, 2001), chinook salmon (*Oncorhynchus tshawytscha*; Findlay *et al.*, 1995; Young *et al.*, 2008a), brown trout (*Salmo trutta*; Munday *et al*., 2001; Rodger, 2014), turbot (*Scophthalmus maximus*; Dyková *et al.*, 1998; Dyková *et al.*, 2000; Dyková & Novoa, 2001), sea bass (*Dicentrarchus labrax*; Dyková *et al.*, 2000), sharpsnout seabram (*Diplodu spuntazzo*; Dyková & Novoa, 2001), ayu (*Plecoglossus altivelis*; Crosbie *et al.*, 2010a), olive flounder (*Paralichthy solivaceus*; Kim *et al.*, 2005), blue warehou (*Seriolella brama*; Adams *et al*., 2008), horse mackerel (*Trachurus trachurus*; Stagg *et al.*, 2015), ballan wrasse (*Labrus bergylta*; Karlsbakk *et al*., 2013), corkwing wrasse (*Symphodus melops*; Hjeltnes, 2013), lumpsucker (*Cyclopterus lumpus*; Haugland *et al*., 2017) and halibut (*Hippoglossus hippoglossus*; Rodger, 2019).

In the specific case of Atlantic salmon farming in Ireland, the first confirmed episode of AGD was described in 1995 (Rodger & McArdle, 1996). Salmons in 10 farms showed clear signs of AGD and associated amoeba on gills, with an average mortality at three farms of 5% and 10% at two others (Rodger & McArdle, 1996). Since then and until 2010, there were some sporadic and minor episodes of AGD in Ireland (Palmer *et al*., 1997; Mitchell & Rodger, 2011; Downes,

2017). However, the incidence of AGD in Irish fish farms increased from 2011, reaching 50% in 2016 (Downes, 2017) and presenting a recurring problem with up to 10% mortality in Atlantic salmon stocks (Oldham *et al.*, 2016). In the early 2000s, production costs associated with AGD increased by 10-20% (Munday *et al.*, 2001), making this gill disease one of the most concerning Atlantic salmon disorders (Marcos-Lopez *et al.*, 2017; Boerlage *et al.*, 2020).

2.4 - AGD pathology

The behavioural signs of an AGD infection on Atlantic salmon include lethargy, decreased appetite (resulting in anorexia), increased ventilation rates, increased production of gill mucus, and congregation of the fish close to the surface of the water (Kent *et al.*, 1988; Munday *et al.*, 1990; Marcos-López *et al.*, 2017). These clinical signs of AGD are a consequence of the microscopic changes on the gill epithelium, namely: hyperplasia, lamellar fusion, the development of interlamellar vesicles, oxidative stress in gill cells and necroses (Kent *et al.*, 1988; Munday *et al.*, 1990; Dyková *et al.*, 1995; Clark & Novak, 1999; Adams & Novak, 2003; Marcos-López *et al.*, 2017). These microscopic consequences lead to a reduction in the number of chloride cells and an increase in mucus cells on gills (Munday *et al.*, 1990; Nowak & Munday, 1994), which compromises the capacity to maintain ionic homeostasis and gas exchange in salmon (Hvas *et al.*, 2017). However, the most recognisable sign of an AGD infection is the presence of observable white mucoid patches on the gills (**Fig. 2.3**), as a macroscopic result of the hyperplasia and lamellar fusion (Clark & Novak, 1999; Taylor *et al.*, 2009a; Bridle *et al.*, 2010; Oldham *et al.*, 2016).

Figure 2.3. Left) Healthy Atlantic salmon gill. **Right)** AGD-infected Atlantic salmon gill, that shows white patches and interlamellar fusion.

2.5 - The first aetiological agent of AGD

Although AGD was firstly described in 1986 in Tasmania (Munday, 1986), the causative agent was not identified as the genus *Paramoeba* until three years later by Roubal *et al.* (1989). In the intervening period Kent *et al.* (1988) described AGD occurring in coho salmon (*O. kisutch*) in the US states of Washington and California, classifying the causative agent as *Paramoeba pemaquidensis* based on morphology, although Page (1987) had described it as *Neoparamoeba pemaquidensis*. Thanks to the immunohistochemical techniques developed by Howard & Carson (1993), the identification of the amoeba became simpler and more widely affordable (Munday *et al.*, 2001). The normalisation of molecular characterisation confirmed *N. pemaquidensis* to be one causative agent (Wong *et al.*, 2004), although *N. branchiphila* was proposed to share the aetiology of AGD (Dyková *et al.*, 2005). However, further research with molecular approaches suggested that the causative agent should be described as a new species. Therefore it was proposed as *Neoparamoeba perurans* (Young *et al.*, 2007). In addition, *N. perurans* was corroborated as the first aetiological agent of AGD after fulfilling Koch's postulates (Crosbie *et al.*, 2012).

The aetiological agent of AGD was first proposed to belong to the family Vexillifaridae (Phylum – Amoebozoa, Class – Discosea, Subclass – Flavellinia, Order – Dactylopodida) by Page (1987), as this amoeba has a dense surface coverage of glycocalyx. Later on, the causative agent of AGD was described as a new genus (*Neoparamoeba*) in the same family, based on species specific oligonucleotide probes developed for a non-cultured gill-derived amoebae (Young *et al.*, 2007). This new genus was then corroborated as the only detectable amoeba associated with AGD-infected gills since this disease was first reported, and in AGD outbreaks in five countries (Young *et al.*, 2008a). In addition, cultured *N. perurans* successfully induced AGD in healthy Atlantic salmon (Crosbie *et al.*, 2012), with gradually decreasing virulence over three years, becoming avirulent after 200 passages (Bridle *et al.*, 2015).

There is quite little information about the life cycle and biology of *N. perurans* beyond that they are free-living and facultative ectoparasites. However, when it is removed from a freshly infected gill and observed under the microscope, the pathogen appears as a subspherical, naked and globose amoeba (15 – 40 μm) (Kent *et al.*, 1988; Munday *et al.*, 1990; Rodger & McArdle, 1996; Munday *et al.*, 2001), but cannot be classified in the genus *Neoparamoeba* on the basis of morphology alone (Dyková *et al.*, 2005; Young *et al.*, 2007). The cells from these microorganisms could range from round under stressful conditions (Wiik-Nielsen *et al.*, 2016) to an irregular (typically amoeboid) shape with many pseudopodia (**Fig. 2.4**), a stage they use to move or to engulf (Crosbie *et al.*, 2012; Wiik-Nielsen *et al.*, 2016). One of the most characteristic features of the genus *Neoparamoeba* is that the cells contain one or more parasomes (≈ 4 μm), described as *Perkinsiella amoebae*-like organisms (PLOs), around the nucleous. The parasomes are eukaryotic endosymbionts phylogenetically related to flagellated, parasitic, marine, protozoans of the genus *Ichthyobodo* (Dyková *et al.*, 2000; Dyková *et al.*, 2003).

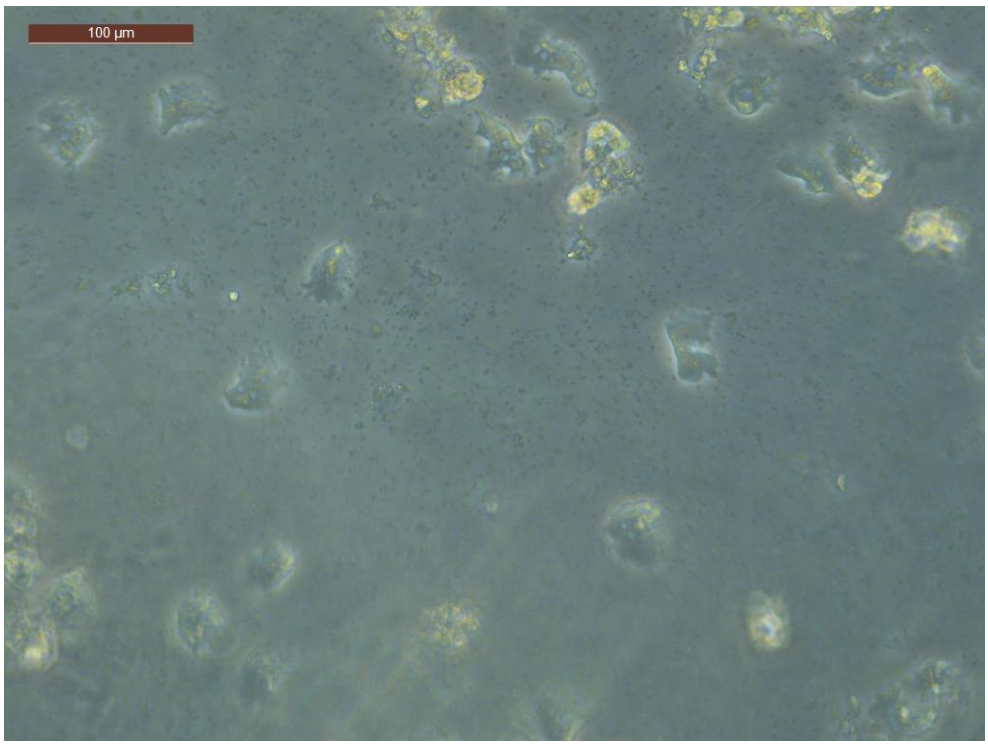

Figure 2.4. *Neoparamoeba perurans* viewed using an inverted microscope.

The presence of naked and globose amoeba has been confirmed in a wide variety of habitats, including the open ocean, coastal environments, marine sediments (Page, 1983; Rogerson & Laybourn-Parry, 1992; Crosbie *et al.*, 2002), and the surrounding waters of marine fish cages (Bridle *et al.*, 2010; Wright *et al.*, 2015; Wright *et al.*, 2017). The abundance of these naked amoeba has been estimated to be as many as 1,350 amoeba/L on the surface of the North Atlantic (Sieburth *et al.*, 1976), and 3,000-23,000 amoeba/L on macro-aggregates suspended on the surface of the Sargasso Sea (Caron *et al.*, 1982). However, the *Neoparamoeba perurans* abundance in sea water was determined to be much lower, with a mean of 4.7 ± 2.0 cells/L around commercial salmon cages in southern Tasmania during the early autumn (Wright *et al.*, 2015). Although it seemed that *N. perurans* tended to concentrate in the water close to the surface and around sea-cages (Wright *et al.*, 2015), no further evidence could be found to support this stratification of the amoeba in the water column near salmon cages (Wright *et al.*, 2017). Despite the low concentrations of *N. perurans* in waters near salmon cages, the minimum concentration of the amoeba to induce a laboratory-based amoebic gill disease was determined to be 10 cells/L (Morrison *et al.*, 2004), suggesting that even low *N. perurans* concentrations in seawater could indeed induce the onset of AGD.

Amoebozoa have been typically assumed to be asexual, unless direct sexual behaviour is observed (Page, 1983, 1987). However, it has been considered that this phylum could be

anciently sexual, still currently having some orders with sexual reproduction. Nonetheless, the Order Dactylopodida, to which *N. perurans* belongs, is not one of them (Lahr *et al.*, 2011). Therefore, the complete life cycle of *N. perurans* is yet to be fully described.

2.6 - Diagnosis of AGD

Traditional approaches for the diagnosis of AGD have included AGD scoring, histological observations of sectioned gills, and PCR-analysis of gene targets.

Histological observations include wet preparation of gill tissue, where it is possible to see large cysts under light microscopy (Nowak & LaPatra, 2006; Mitchell & Rodger, 2011), or, more frequently, histopathological preparations, where epithelial hyperplasia, lamellar fusion, inflammation, cell death, presence of interlamellar vesicles and the presence of *N. perurans* are easier to identify (Adams & Nowak, 2003; Adams & Nowak, 2004; Adams *et al.*, 2004). Histopathological analyses are normally conducted using a haematoxylin and eosin stain on pre-fixed gills excised from the fish (Zilberg *et al.*, 1999; Adams *et al.*, 2004), making it impossible to follow the development of the disease *in situ* and from the same individuals.

On the other hand, molecular approaches that include PCR amplification typically have targeted the 18S rRNA gene of *N. perurans* (Young *et al.*, 2008b). Template DNA is normally obtained from excised gill material, but non-lethal gill swabs may provide a suitable and less-invasive alternative (Bridle *et al.*, 2010; Downes *et al.*, 2015; Downes *et al.*, 2017). PCR amplification-based approaches have allowed researchers around the world confirm the global distribution of *N. perurans* (Young *et al.*, 2008) and to implicate *N. perurans* in samples from AGD infections previously assumed to be associated with other organisms (Downes *et al.*, 2018b).Quantitative PCR assays to allow tracking of the abundance of *N. perurans* on gills and surrounding waters have also been developed (Fringuelli *et al.*, 2012; Downes *et al.*, 2015; Wright *et al.*, 2017). However, in the case of both histological observations and PCR-based methods, diagnosis is typically achieved only after 1-2 days of laboratory work, meaning that these approaches do not provide inexpensive, *in situ* or immediate diagnosis of AGD.

The cheapest and most common tool to support *in situ* AGD diagnosis is a gross pathological assessment of the gills (Adams & Nowak, 2001; Taylor *et al.*, 2009a; Rodger, 2014). Various gross assessments of gills have been used as a non-destructive, quantitative measurement of the

severity of AGD and are based upon the abundance and size of white patches on gills (Taylor *et al.*, 2009a). This approach has been shown to be a reliable tool to monitor the gill condition in routine checking when performed by an experienced examiner (Bridle *et al.*, 2010; Rozas *et al.*, 2011; Nowak *et al.*, 2014; Rodger, 2014). However, gross pathological assessment is unable to identify the causative agent, and therefore to diagnose the specific disorder since most common gill diseases share similar signs (Rozas-Serri, 2019).

During the last years more diagnostic methodologies have been developed, especially those that are non-lethal and less invasive than gill sampling (Downes *et al.*, 2017; Cano *et al.*, 2020). Cano *et al*. (2020) developed a loop-mediated isothermal amplification (LAMP) assay targeting the 18S rRNA gene from *N. perurans*, and EF1α gene from Atlantic salmon, which could be applied using non-lethal gill swabs. The inventors suggested this LAMP-based approach as a good candidate for on-site confirmation of *N. perurans* on salmons with high AGD gill scores. Indeed, similar conclusions were provided by Downes *et al*. (2017) in relation to results from salmon with low AGD gill scores. However, none of the diagnostics techniques mentioned in this section can predict the susceptibility of Atlantic salmon to AGD prior to colonisation of *N. perurans* on gills.

2.7 - Environmental factors influencing the AGD

Although some common farming practices, such as high stock densities and proximity to an infected site, are risk factors for an AGD outbreak, environmental parameters such as temperature and salinity are considered the main influencers of AGD prevalence and severity (Oldham *et al.*, 2016; Boerlage *et al.*, 2020). This pathology has been typically associated with the summer season, when the average water temperature and salinity in the northern hemisphere rise (Munday *et al.*, 1990; Clark & Novak, 1999). However, the temperature range that researchers categorise as suitable for an AGD episode has been changed over the years, decreasing the temperature minima from 12ºC (Munday *et al.*, 1990) to 7ºC (Steinum *et al.*, 2008; Rodger, 2014) and even to 2.5ºC [in a masters thesis] (Mertz, 2020). On the other hand, the earliest reported AGD outbreaks suggested that the temperature maxima may be relevant in the development of the gill disease (Douglas-Helders *et al.*, 2001; Oldham *et al.*, 2016). The role of the water temperature in AGD needs further evidence to explain the huge variability in the results, but AGD is still considered as a seasonal disease, as it is mainly present during the warmest period of the year.

Salinity is the environmental factor most clearly affecting AGD. Since Kent *et al.* (1988) found that AGD was almost eradicated from the tanks used in a laboratory-scale study after a temporal reduction in salinity, more studies reported that AGD prevalence and severity negatively correlate with salinity (Munday *et al.*, 1990; Rodger & McArdle, 1996; Clark & Nowak, 1999). Further literature that included rainfall data found that lower-than-average rainfall normally preceded AGD episodes (Palmer *et al*., 1997; Bustos *et al.*, 2011; Rozas *et al.*, 2012). Based on these studies, further publications have addressed the possibility of using commercial freshwater bathing to treat AGD in Atlantic salmon (Parsons *et al.*, 2001; Clark *et al.*, 2003; Powell *et al*., 2015).

It was also suggested that other environmental factors, such as biofouling of solid structures (Tan *et al.*, 2002) and the presence of cleaner-fish (Haugland *et al.*, 2017), or microbial dysbiosis (a disturbance or imbalance of the gill microbiome)(Nowak & Archibald, 2018), may contribute to AGD in fish farms. Each of the possible environmental factors would likely be different across various geographical locations, likely differently influencing *N. perurans* colonisation of gills and the subsequent severity of the AGD. This may partially explain why, although typical AGD outbreaks cause mortalities between 10 and 20% in salmon stocks, mortality sometimes could reach 80% in certain locations, such as in Scotland, Norway and Ireland (Shinn *et al*., 2015).

2.8 - Infection trials

The high variability of factors influencing the onset and development of AGD in Atlantic salmon underpin experimenting with the disease in controlled environments, such as laboratories. Initial laboratory trials to induce AGD on AGD-naïve salmon using cultured amoeba were unsuccessful (Kent *et al.*, 1988; Howard *et al.*, 1993; Findlay, 2001). Those studies typically cultured amoeba classified as *Paramoeba* sp. (Findlay, 2001), but subsequent literature, that included data from molecular approaches and better culturing techniques, identified *Neoparamoeba pemaquidensis* as the agent of amoebic gill disease and proceeded to culture the organism (Wong *et al*., 2004; Morrison *et al.*, 2004, Lee *et al.*, 2006). However, it was still not possible to induce AGD on naïve Atlantic salmon in a laboratory trial using *N. pemaquidensis* cultures (Morrison *et al*., 2005). After the reclassification of the first aetiological agent of AGD to *Neoparamoeba perurans* (Young *et al.*, 2007), the first laboratory-induced AGD on Atlantic salmon using an amoeba culture was successfully reported, including fulfilling Koch's postulates (Crosbie *et al.*,

2012). Challenged salmon in this study were exposed to a *N. perurans* concentration in water of 5,000 cells/L, whereas part of the cohort were maintained as negative controls throughout the trial. This concentration of amoeba was more than three times higher than the estimated concentration of naked amoeba on the surface of the North Atlantic (1,350 cells/L, Sieburth *et al.*, 1976), and many times higher than the maximum measured concentration of *N. perurans* cells close to commercial salmon cages during early autumn in Tasmania (62.3 cells/L, Wright *et al.*, 2017). However, other successful laboratory trials have found gross and histological gill lesions after inoculation with concentrations ranging from 1,000 down to 10 amoeba/L (Morrison *et al.*, 2004; Oldham *et al.*, 2016; Pennacchi *et al*., 2016; Haugland *et al*., 2017; Slinger *et al.*, 2020a), after co-habitation of naïve fish with AGD-affected ones (Munday *et al.*, 2001; Chang *et al*., 2019) or after placing debris from scraping the gills of AGD-affected fish into fish-holding systems (Zilberg *et al.*, 2001). Further evidence demonstrated *N. perurans* cultures maintained for extended periods were less virulent (Collins *et al.*, 2017), and eventually lost capacity to induce AGD (Bridle *et al.*, 2015).

The main advantage of such laboratory trials is the opportunity to reduce the number of variables that may influence complex interactions between organisms, thus isolating the effect of the targeted factors and providing clearer results. However, this advantage also represents one of the inherent limitations of this approach, since the environmental parameters that influence the onset, and development, of AGD in nature are still not completely clear, and laboratory trials thus may not provide the ideal conditions for establishment, and spread, of the gill disease as it would in the environment. Patterns from controlled environments, as in laboratory trials, are more difficult to extrapolate to stocks in fish farms or to wild populations of fish because they do not include the possible effect of the variability of environmental factors on the measured indicator. Therefore, a combination of the results from both laboratory trials and field-based studies would help improve our understanding of this important gill disorder.

2.9 - Prevention and treatment of AGD

Firstly, various strategic adjustments may be made at fish farms to reduce the chance of future AGD episodes in salmon cohorts. Reduced salmon stocking densities from, for example, 5 to 1.7 kg/m^3, or even to 0.8 kg/m^3, has been shown to have a significantly positive impact on salmon survival after an AGD challenge, but also to reduce the AGD prevalence (Douglas-Helders *et al*., 2004; Crosbie *et al.*, 2010b). Micro-environments developed on biofouled cage nets, which were

not changed over long periods, also appeared to have a positive relationship with AGD prevalence in Tasmania (Clark & Nowak, 1999; Nowak, 2001).A similar situation was reported in fish farms in Europe, and was found to reduce water exchange in cages and to significantly increase the number of AGD cases (Rodger, 2014).

Another prevention strategy has been to increase the genetic resistance of salmon to AGD. Since Findlay *et al.* (1995) noticed a huge variation in the survival following an AGD challenge, the genetic resistance to AGD in Atlantic salmon has been assessed and better described in many studies (Findlay, 2001; Taylor *et al*., 2007; Taylor *et al*., 2009b; Boison *et al.*, 2019; Aslam *et al.*, 2020; Robledo *et al.*, 2020). AGD resistance can manifest in two different ways: innate resistance of AGD naïve fish to an initial infection, and adaptative resistance to a second infection after surviving the first (Kube *et al.*, 2012). The innate resistance could be enhanced by selectively breeding resistant salmon (Kube *et al.*, 2012; Robledo *et al.*, 2020), or by hybridising Atlantic salmon with brown trout individuals (Maynard *et al.*, 2016). The adaptative resistance could also be improved by selective breeding (Kube *et al.*, 2012), and vaccination and immunostimulants were also tested but found to have very little effect on survival of AGD (Nowak *et al.*, 2014; Valdenegro-Vega *et al.*, 2015).

A recent study has shown that specific functional diets to have a positive impact on survival, and physiological, response to AGD in Atlantic salmon (Mullins *et al*., 2020). Such diets are formulated as inexpensive preventive treatments for various disorders and diseases (Mullins *et al*., 2020; Waagbø & Remø, 2020). Thus, further research on their effect on AGD would be desirable.

However, treatments for an already AGD-affected fish population have been reported in the literature and have included: freshwater bathing (Clark *et al*., 2003; Douglas-Helders *et al*., 2004), softened freshwater bathing (Roberts and Powell, 2003), hydrogen peroxide bathing (Powell and Clark, 2004; Adams *et al.*, 2012; Wynne *et al*., 2020), chlorine dioxide bathing (Powell and Clark, 2004), chloramine-T bathing (Powell and Clark, 2004; Harris *et al.*, 2005), formalin bathing (Rodger and McArdle, 1996), levamisole bathing (Clark and Nowak, 1999; Findlay and Munday, 2000), potassium permanganate bathing (Embar-Gopinath *et al*., 2005a), peracetic acid bathing (Lazado *et al*., 2019), bithionol bathing and oral deliveries (Florent *et al*., 2007a; Florent *et al*., 2007b), narasin oral delivery (Cameron, 1992), L-cysteine ethyl esther oral delivery (Roberts and Powell, 2003), N-acetyl cysteine oral delivery (Powell *et al*., 2007), garlic

extracts (Peyghan *et al*., 2008), and metronidazole (Peyghan *et al*., 2008). Among these, freshwater bathing is the main treatment of choice against AGD in regions where access to freshwater is more affordable, such as in Ireland, Scotland, Norway or Tasmania (Oldham *et al.*, 2016). Freshwater bathing comprises submerging the AGD-affected salmon into a water bath with salinity below 3 ppt, for between 2 and 4 hours, before returning to seawater cages. The efficiency of freshwater baths in treating AGD and reducing *N. perurans* abundance on gills has been widely demonstrated (Parsons *et al.*, 2001; Clark *et al.*, 2003; Powell *et al.*, 2015), although it is normally labour-intensive and expensive. The treatment requires multiple freshwater baths so as to be effective, as it alleviates but does not eliminate AGD (Parsons *et al.*, 2001; Clark *et al.*, 2003), partially because of the continuous presence of the amoeba in the seawater (Boerlage *et al.*, 2020). For that reason, Wright *et al*. (2018) created a permanent freshwater surface layer in snorkel sea-cages in attempting to reduce AGD prevalence and lice levels in Atlantic salmon, and by continuously applying treatment to reduce the abundance of *N. perurans* on gills. However, Wright *et al*. (2018) did not observe a significant reduction in AGD prevelance, concluding that the fish probably did not spend enough time in contact with the freshwater surface.

2.10 - Fish microbiomes and their connection with diseases

It is widely accepted that the microbial community (microbiome) on a biological tissue usually plays an important role in the health status and protection of hosts (Gómez & Balcázar, 2008), by influencing the development and maturation of the immune system (Hooper *et al.*, 2012; Kelly & Salinas, 2017), and through competitive exclusion mechanisms (Balcázar *et al*., 2006; Stecher & Hardt, 2008). This connection has been shown to exist in teleost species, including Atlantic salmon, where a perturbation of the normal commensal microbiome (which results in dysbiosis) could enhance the susceptibility of the fish to diseases (Gómez & Balcázar, 2008; Llewellyn *et al*., 2014). Dysbiosis in the microbiome of the fish gut, skin, mucus or gill increases the chance of developing various disorders (Llewellyn *et al*., 2017; Piazzon *et al.*, 2017; Reid *et al.*, 2017; Reverter *et al.*, 2020). Therefore, a detailed understanding of the microbiome of susceptible fish prior to the onset of disease could be used as a reference for future prediction tools that target key microbial taxa.

2.11 - Microbial ecology: a continually developing field

Current studies involving a description of a microbiome involve molecular techniques to characterise and quantify the different microbial taxa (Steinum *et al*., 2009; Schmidt *et al*., 2016; Minich *et al*., 2020a; Minich *et al*., 2020b; Slinger *et al.*, 2020a; Slinger *et al.*, 2020b; Slinger *et al.*, 2021). Culture-dependent approaches to study microbial communities likely miss relevant taxa since many microorganisms in nature are unculturable, and thus culture-independent methodologies based on nucleic acid isolation and description/quantification are currently preferred and are able to provide a representative insight into microbiomes, (Schloss & Handelsman, 2005;).

The quantification of certain microbes may be accomplished by Polymerase Chain Reaction (PCR)-based procedures, such as quantitative PCR. One of the first characterisations of microbial communities from environmental samples using a PCR-based approach was conducted by Schmidt *et al.* (1991), who constructed clonal libraries from picoplankton DNA for 16S ribosomal RNA gene screening and sequencing. Since then, the techniques available to study microbial ecology have changed drastically, not requiring a clonal library preparation to isolate each of the community members.

In a quantitative PCR, a fluorescent molecule is attached to the amplicon generated using specific oligonucleotides targeting a DNA region of the microorganism of interest (Downes *et al.*, 2015). Thus, the number of amplicons may be quantified using the intensity of the fluorescence signal. Later, the initial abundance of the targeted taxa could be inferred with the equation of a regression curve from known concentrations of the targeted DNA fragment.

The identification of the members in a microbiome was traditionally done by biochemically characterising each of the microbiome isolates; but this required isolation and culture of individual microorganisms (Grondona *et al.*, 1997), once again underscoring the limitations of culture-based approaches to study vastly unculturable samples. Hence, PCR-based methodologies offer an approach to better represent the microbiome. The amplification and subsequent sequencing of certain regions of the genome (usually the ones coding for ribosome proteins), or the whole genome (metagenome), of the different taxa in the microbiome allow researchers to identify them and to compare their relative abundances (Schloss & Handelsman,

2005; Slinger *et al.*, 2020a; Slinger *et al.*, 2020b).Thus, many microbiome features can be inherited from such data, including the richness, structure and diversity of communities.

The rapid pace of discoveries over the past decade has enhanced the development of new methodologies to study microbial ecology. This has allowed researchers to, for example, integrate metagenomic data with other ‘omics, to better understand the microbial response to different perturbations (Feng *et al.*, 2019; Moskowitz *et al.*, 2020) or their relationships in different environments (Bikel *et al*., 2015; Wang *et al*., 2020). The development of accessible sequencing based on microfluidics, such as Nanopore and long-read sequencing, has also contributed to address different questions in microbial ecology (Deamer *et al*., 2016; Amarasinghe *et al*., 2020) and to the discovery of new candidate phyla (Brown *et al*., 2015). The next decade will be very exciting in this field, as the accessibility of such technologies widens, thus promoting further discoveries.

2.12 - Microbiome on Atlantic salmon gills

Any culture-independent gill microbiome study inherently requires a DNA extraction step, but there is no international consensus and standardisation in these procedures. Many of the published procedures extract the microbiome nucleic acids from part of an excised gill arch (Steinum *et al*., 2009; Schmidt *et al*., 2016; Pratte *et al.*, 2018; Brown *et al.*, 2019; Lim *et al.*, 2019), from a single filament of the arch (Slinger *et al.*, 2020a; Slinger *et al.*, 2020b) or from gill swabs (Legrand *et al*., 2018; Rosado *et al*., 2019a; Rosado *et al*., 2019b; Minich *et al*., 2020a; Minich *et al*., 2020b; Slinger *et al.*, 2021), using a commercially-available extraction kit to ensure simplicity and reproducibility. However, it is still not determined whether genetic material extracted from a part of the gill or from gill swabs would be representative of the microbiome from the entire gill arch. On the other hand, procedures to extract nucleic acids from whole gill arches normally require disruption of fish tissue, as well as a disintegration step with bead-beating (Lowrey *et al.*, 2015), digesting agents (Bowman & Nowak, 2004; Hess *et al.*, 2015) or by crushing the gill after snap-freezing in liquid nitrogen (Brito *et al*., 2018). However, these approaches typically cannot allow for complete separation of nucleic acids from the microbiome and the host. During DNA sequencing, host DNA may compete with microbiome DNA for PCR amplification, obscuring patterns in microbial community analyses (Marotz *et al*., 2018). Thus, a step to isolate and concentrate the microbial cells from entire gills prior to DNA extraction is desirable in gill microbiome studies.

Two of the first studies describing the gill microbiome of salmonids were conducted by Horsley (1973) and by Trust (1975). Wild Atlantic salmon from coastal, estuarine and river waters were sampled, and culture-based methodologies were applied to grow the gill bacterial community. Subsequently, biochemical tests were conducted to describe the metabolic and morphological characteristics of the isolates. Even though these studies sampled Atlantic salmon from a variety of environments (coastal, estuarine and river waters), very similar predominant bacterial taxa were identified in all individuals: *Moraxella*, *Acinetobacter*, *Pseudomonas*, *Flavobacterium*, *Cytophaga*, *Enterobacteriaceae*, *Micrococcaceae*, *Bacillus*, *Vibrio* and *Aeromonas*. Many of these bacteria were also present in the surrounding water (Horsley, 1977). Since then, no study has tried to again describe the complete prokaryotic gill microbiome from Atlantic salmon, until an experimental study was published by Bowman and Nowak (2004). They characterised the bacterial community of AGD-affected and healthy Atlantic salmon by digesting gills, isolating the DNA, amplifying the 16S rRNA genes, creating a clone library with the obtained amplicons, and finally sequencing and comparing their sequences with the GenBank database using BLAST-n. The most common bacterial taxa were: *Gammaproteobacteria* spp., *Flavobacteriaceae* spp., *Marinobacter*, *Desulfosarcina*, *Psychroserpens*, *Pseudomonas*, *Pseudoalteromonas*, *Photobacterium*, *Propionibacterium*, *Streptococcus* and *Staphylococcus*. The genus *Psychroserpens* was consistently detected in samples from AGD-affected salmon, and this genus was thus proposed to be a potential opportunistic pathogen associated with salmonid AGD.

A subsequent laboratory-based challenge (Embar-Gopinath *et al*., 2005b) suggested that high occurrence of the bacterial genus *Winogradskyella*, cultured from AGD-affected gills, was able to influence the prevalence of severe AGD on Atlantic salmon. Further challenges (Embar-Gopinath *et al*., 2006; Embar-Gopinath *et al*., 2008) supported that *Winogradskyella* and *Staphylococcus* could be associated with AGD in Atlantic salmon. Most of the previously mentioned studies tested the possible connection between individual genus and *N. perurans* and relied on cultured-based techniques (Embar-Gopinath *et al*., 2006; Embar-Gopinath *et al*., 2008), limited by unculturable free-living bacteria. Later studies tried to focus more on the possible connection between the whole gill microbiome and AGD, also trying to find key taxa, using culture-independent approaches. Some studies included the characterisation of the gill microbiome from partial gill samples (Steinum *et al*., 2009; Schmidt *et al*., 2016), detecting bacteria belonging to *Burkholderia*-like microorganisms, *Psychrobacter*, *Propionibacterium* and *Enterobacteriales*on healthy Atlantic salmon gills. The latest studies involving the

characterisation of the gill microbiome from AGD-affected Atlantic salmon in a laboratory challenge were conducted by Slinger *et al.* (2020a, and 2021).

Slinger *et al.* (2020a) described the bacterial community from gill filaments affected by AGD, and compared it with the microbiome from non-affected filaments from the same fish, and with the microbiome from gill filaments of naïve salmon. They sequenced the V1-V3 hypervariable region of the 16S rRNA gene of the bacterial community using an Illumina MiSeq platform. The most abundant taxa belonged to the genera: *Colwellia*, *Propionibacterium*, *Pseudoalteromona*, *Rubritalea*, *Burkholderia*, *Vibrio*, *Maribacter* and *Sphingomonas*. All mentioned taxa were also present in the surrounding water of the tanks. However, the bacteria *Tenacibaculum dicentrachi* and *Flavobacterium* appeared to be highly abundant in the AGD-affected gills. In addition, *T. dicentrachi* abundance showed a moderately positive correlation with *N. perurans* abundance (Slinger *et al.*, 2020a), suggesting this organism could play a role in AGD. These differences in the most common genera in the Atlantic salmon gill microbiome could be partially due to the combined effect of distinct environmental parameters and historical colonisations on each cohort, as could be reflected from skin and gut samples (Uren Webster *et al.*, 2020).

Previous reports describing the gill and skin microbiomes from fish usually include water sampling in their methodologies so as to obtain an insight to the environmental ecology and the contribution of free-living microorganisms to the exposed surface. The connection between the surrounding water and the gill and skin microbiome was suggested in some literature (Kuang *et al.*, 2020; Minich *et al*., 2020a). However, it is sometimes not clear whether the water was the initial reservoir of certain taxa present on the studied organ, as both systems had significantly different bacterial communities (Karlsen *et al.*, 2017; Minniti *et al.*, 2017). Minniti *et al*. (2017) suggested that these differences could be the result of the specific adaptation of some of the taxa to live on the mucus-skin.

2.13 - Knowledge gaps

Our current understanding of the *Neoparamoeba perurans* biology and life-cycle, in aquaculture and in the environment, is very limited (Oldham *et al.*, 2016; Rozas-Serri; 2019). The relationship between *N. perurans* and environmental parameters, such as temperature, turbidity and dissolved nutrients, as well as with free-living bacteria, is still uncertain and further evidence is required for a clear understanding of its ecophysiology (Oldham *et al.*, 2016; Rozas-Serri;

2019). This information will be also relevant in the future identification of natural reservoirs of *N. perurans* (Oldham *et al.*, 2016), where the amoeba would typically reside. However, climate change may alter the global distribution and severity of AGD (Nowak & Archibald, 2018; Rozas-Serri, 2019; Boerlage *et al*. 2020), underscoring the need to better understand the gill disorder. Indeed, a changing climate will add complexity to the AGD research on farmed Atlantic salmon, making more difficult to interpret results in field-based AGD trials. Thus, the combination of data from (i) laboratory challenges performed under controlled and stable physico-chemical conditions, and (ii) samples collected under real-world conditions at AGD- affected fish farms, would provide more comprehensive insights in the possible connection between AGD and the gill microbiome, and also in the role of various environmental factors in that relationship.

Although there is a considerable success in selective breeding and nutrition as mitigation agents of AGD, further research should be done in relation to health management of fish stocks, either for prevention or treatment of the AGD. Treatments other than freshwater or hydrogen peroxide bathing should be also investigated and tested at commercial scales (Oldham *et al.*, 2016). However, it is possible that AGD will not be eliminated from global Atlantic salmon production. Hence, mitigation efforts may need to focus on control of AGD to a level that is admissible for animal welfare and from production perspectives (Boerlage *et al*. 2020).

Different aspects of the AGD onset in farmed Atlantic salmon are still not clear. The possibility of various vectors, such as sea lice or cleaner-fish, that spread the causative agent remains uncertain (Oldham *et al.*, 2016). Many of the causative agents of distinct gill pathologies appear to be present in the sea water and as part of the gill microbiome (Slinger *et al.*, 2020a). Therefore, there is a high chance that the consequences of one gill disorder would trigger the development of another one. One of the least studied aspects of AGD is its possible co-occurrence with other gill pathologies in Atlantic salmon (Oldham *et al.*, 2016; Rozas-Serri; 2019). It is not uncommon that co-infections impact fish farms around the globe, probably having synergistic or antagonistic effects on the host, and/or reducing the effects of immunomodulation or applied treatments (Oldham *et al.*, 2016; Rozas-Serri; 2019).

Equally, the relationship between *N. perurans* and other microorganisms on the gills is also still mostly unknown (Nowak & Archibald, 2018; Rozas-Serri; 2019). Some microbes could impact the colonisation and development of *N. perurans* on fish gills, thus influencing the prevalence and severity of AGD. A dysbiosis event on the gills could then facilitate the appearance of

clinical signs of AGD (Rozas-Serri; 2019). At the same time, the occurrence of AGD could also perturb the gill microbiome, along with impacting on other functional aspects of the gill(Chang *et al*., 2019). If this mutual relationship is confirmed and described, a microbiome characterisation from gill samples could suggest the susceptibility or resistance of a certain Atlantic salmon cohort to develop AGD, even before the *N. perurans* colonisation on gills. In addition, the manipulation of the gill microbiome structure, to increase the abundance of key microbial taxa, could enhance the resistance of those salmon to AGD, preventing or even treating the gill disorder. For example, prebiotics or probiotics may be included in the fish diet, or the gill may be inoculated by exposing the fish to bathing waters containing desirable microbial species.

2.14 - Objectives and Hypothesis

The overall goal of this doctoral thesis was to determine whether AGD development and the prokaryotic microbiome on the farmed Atlantic salmon gills were linked, and to identify bacterial taxa that could be used as early warning indicators of disease outbreaks. To these ends, the project initially aimed to create and optimise an extraction procedure for the recovery of total microbiome genomic DNA and RNA using entire gill arches. Furthermore, we used this methodology and mucus sampling, in conjunction with a longitudinal study on a fish farm, to address the main goal in a field study. However, the conclusions from this study were based on a single AGD episode on one fish farm. Therefore, our second objective was to characterise the gill microbiome from Atlantic salmon before and during AGD, but including a total of six different farms along the Irish coast and using the newly optimised DNA extraction methodology. We hypothesised for both field trials that AGD onset and development would have an impact on the gill microbiome in all locations, but its influence on the bacterial community would be different due to the geographical dependency of the microbiome. Nevertheless, the variability in the environmental parameters increased the complexity of the data interpretation. Thus, an additional objective was to design a study to corroborate the results from the previous field campaigns, and to evaluate the impact of various functional diets on the AGD development, and on the gill microbiome. It consisted of a laboratory trial involving the optimised DNA extraction method; water sampling and negative controls. We hypothesised that the appearance of the disease would impact the gill microbiome in a controlled environment, changing the microbiome structure on the gill with bacteria from the surrounding water. We also hypothesised that the various functional diets would differently drive the gill microbiome, possibly reducing the AGD severity on salmon gills.

This work brought together many novel and relevant information in the understanding of AGD from the perspective of the gill microbiome. In addition, the findings from this thesis could mean the first steps towards a better prevention, monitoring and even treatment of the AGD in farmed Atlantic salmon.

2.15 - Summary of Chapters

This dissertation comprises five chapters, including a literature review and a discussion with conclusions. The body of the thesis includes three chapters; one of them is under peer-revision in a scientific journal.

Chapter 3: Dynamic gill and mucus microbiomes track an Amoebic Gill Disease episode in farmed Atlantic salmon.

There is no consensus in the DNA extraction procedure to study the gill microbiome. Thus, this chapter describes a new method for the microbiome DNA extraction from fish gills. In addition, it characterises the gill microbiome before and during an AGD episode in an Atlantic salmon farm in Ireland. As it is still unknown whether mucus sampling could be a suitable substitute for gill sampling in gill microbiome studies, complementary mucus samples were obtained to compare this type of sampling with entire gill sampling. Some environmental data were also added in order to have a more complete understanding of the changes in the microbiome.

Part of this chapter was presented to the following conference:
Birlanga, V. B. (2018). Optimisation of a new method to extract genetic material from microbes on gills. First step of an early Amoebic Gill Disease detection. 6th Gill Health Initiative, Marine Institute, Galway, Ireland, 11-12 April, 2018.

Part of this chapter was presented to the following conference:
Birlanga, V. B., McCormack, G., Smith, C., & Collins, G. (2018). Characterisation of the Atlantic salmon microbial community on gills during an Amoebic Gill Disease outbreak. First step of an early AGD detection. 3rd UK & Ireland EAFP Branch Meeting, Marine Institute, Galway, Ireland, 11-12 September, 2018.

Part of this chapter was presented to the following conference:
Birlanga, V. B., McCormack, G., Ijaz, U. Z., McCarthy, E., Smith, C., & Collins, G. (2019). Farmed Atlantic salmon microbiome on gills and mucous samples during an Amoebic Gill Disease episode: Towards an early prediction. 19th EAFP International Conference on Diseases of Fish and Shellfish, Porto, Portugal, 9-12 September, 2019.

The chapter has been accepted to be published in the scientific journal "*Scientific Reports*":
Birlanga, V. B., McCormack, G., Ijaz, U. Z., McCarthy, E., Smith, C., & Collins, G. (2022). Dynamic Gill and Mucus Microbiomes During a Gill Disease Episode in Farmed Atlantic Salmon. *Sci. Rep*.

Chapter 4: Description of the farmed Atlantic salmon gill microbiome during an Amoebic Gill Disease episode along the West Coast of Ireland.

The microbiome on biological tissues is highly influenced by the environmental conditions, being the gill microbiome not an exception. Therefore, different environments would partially determine how different the gill community is, probably influencing the AGD onset and development. As the previous chapter only had samples from one location, this chapter includes data from six different Irish farms along the West coast, describing and comparing the gill microbiome from all of them while they were impacted by AGD. Salmon from the same farm that was sampled in the previous chapter were included in this part, thus a comparison between the gill microbiome from salmon from both sampling campaigns was carried out. Some environmental data were also added in order to have a more complete understanding of the changes in the microbiome.

Part of this chapter was presented to the following conference:
Birlanga, V. B., Ijaz, U. Z., McCarthy, E., Smith, C., & Collins, G. Geographical gradient in gill microbiome diversity of farmed Atlantic salmon during an Amoebic Gill Disease episode. International Workshop of PhDs and Post-doctoral Fellows on Anadromous Salmonids 2021 online meeting, March, 2021.

Chapter 5: Amoebic Gill Disease and functional diets alter the gill microbiome in Atlantic salmon.

Results in previous chapters were highly influenced by the instability of environmental factors, making more difficult to discern patterns in the AGD-affected gill microbiome. Hence, we investigated the connection between the whole-gill microbiome and AGD by describing the impact of the disease on the bacterial community on gills over a controlled laboratory trial. As literature demonstrated the positive impact of functional diets on the survival, and physiological response to AGD, of Atlantic salmon; we also tested the effect of various functional diets on fish performance, AGD severity and the gill microbiome in Atlantic salmon during an AGD episode. Water samples were taken to compare the gill and water microbiome, and determine the effect of the functional diets on the bacterial communities in surrounding seawater.

Chapter 6: General discussion.

In the concluding chapter, the main findings of this thesis are summarised and discussed, including possible future lines of research in this field.

2.16 - References

Adams, M. B., & Nowak, B. F. (2001). Distribution and structure of lesions in the gills of Atlantic salmon, *Salmo salar* L., affected with amoebic gill disease. *Journal of fish diseases*, 24(9), 535-542.

Adams, M. B., & Nowak, B. F. (2003). Amoebic gill disease: sequential pathology in cultured Atlantic salmon, *Salmo salar* L. *Journal of fish diseases*, 26(10), 601-614.

Adams, M. B., & Nowak, B. F. (2004). Sequential pathology after initial freshwater bath treatment for amoebic gill disease in cultured Atlantic salmon, *Salmo salar* L. *Journal of Fish Diseases*, 27(3), 163-173.

Adams, M. B., Ellard, K., & Nowak, B. F. (2004). Gross pathology and its relationship with histopathology of amoebic gill disease (AGD) in farmed Atlantic salmon, *Salmo salar* L. *Journal of Fish Diseases*, 27(3), 151-161.

Adams, M. B., Villavedra, M., & Nowak, B. F. (2008). An opportunistic detection of amoebic gill disease in blue warehou, *Seriole llabrama* Günther, collected from an Atlantic salmon, *Salmo salar* L., production cage in south eastern Tasmania. *Journal of fish diseases*, 31(9), 713-717.

Adams, M. B., Crosbie, P. B. B., & Nowak, B. F. (2012). Preliminary success using hydrogen peroxide to treat Atlantic salmon, *Salmo salar* L., affected with experimentally induced amoebic gill disease (AGD). *Journal of Fish Diseases*, 35(11), 839-848.

Amarasinghe, S. L., Su, S., Dong, X., Zappia, L., Ritchie, M. E., & Gouil, Q. (2020). Opportunities and challenges in long-read sequencing data analysis. *Genome biology*, 21(1), 1-16.

Aslam, M. L., Boison, S. A., Lillehammer, M., Norris, A., &Gjerde, B. (2020). Genome-wide association mapping and accuracy of predictions for amoebic gill disease in Atlantic salmon (*Salmo salar*). *Scientific reports*, 10(1), 1-9.

Avendaño-Herrera, R., Toranzo, A. E., &Magariños, B. (2006). Tenacibaculosis infection in marine fish caused by *Tenacibaculum maritimum*: a review. *Diseases of aquatic organisms*, 71(3), 255-266.

Balcázar, J. L., De Blas, I., Ruiz-Zarzuela, I., Cunningham, D., Vendrell, D., & Múzquiz, J. L. (2006). The role of probiotics in aquaculture. *Veterinary microbiology*, 114(3-4), 173-186.

BIM (Bord IascaighMhara) Annual Aquaculture Survey (2019) Ireland's Seafood Development Agency. http://www.bim.ie/our-publications/aquaculture/

Bikel, S., Valdez-Lara, A., Cornejo-Granados, F., Rico, K., Canizales-Quinteros, S., Soberón, X., Del Pozo-Yauner, L. & Ochoa-Leyva, A. (2015). Combining metagenomics, metatranscriptomics and viromics to explore novel microbial interactions: towards a systems-level understanding of human microbiome. *Computational and structural biotechnology journal*, 13, 390-401.

Boerlage, A. S., Ashby, A., Herrero, A., Reeves, A., Gunn, G. J., & Rodger, H. D. (2020) Epidemiology of marine gill diseases in Atlantic salmon (*Salmo salar*) aquaculture: a review. *Reviews in Aquaculture*, 1-20.

Boison, S. A., Gjerde, B., Hillestad, B., Makvandi-Nejad, S., & Moghadam, H. K. (2019). Genomic and transcriptomic analysis of amoebic gill disease resistance in Atlantic salmon (*Salmo salar* L.). *Frontiers in genetics*, 10, 68.

Bowman, J. P., & Nowak, B. (2004). Salmonid gill bacteria and their relationship to amoebic gill disease. *Journal of Fish Diseases*, 27(8), 483-492.

Bridle, A. R., Carter, C. G., Morrison, R. N., & Nowak, B. F. (2005). The effect of β-glucan administration on macrophage respiratory burst activity and Atlantic salmon, *Salmo salar* L., challenged with amoebic gill disease–evidence of inherent resistance. *Journal of fish diseases*, 28(6), 347-356.

Bridle, A. R., Crosbie, P. B. B., Cadoret, K., & Nowak, B. F. (2010). Rapid detection and quantification of *Neoparamoeba perurans* in the marine environment. *Aquaculture*, 309(1-4), 56-61.

Bridle, A. R., Davenport, D. L., Crosbie, P. B., Polinski, M., & Nowak, B. F. (2015). *Neoparamoeba perurans* loses virulence during clonal culture. *International journal for parasitology*, 45(9-10), 575-578.

Brito, T. L., Campos, A. B., Bastiaan von Meijenfeldt, F. A., Daniel, J. P., Ribeiro, G. B., Silva, G. G., Wilke, D.V., De Moraes, D.T., Dutilh, B.E., Meirelles, P.M. & Trindade-Silva, A. E. (2018). The gill-associated microbiome is the main source of wood plant polysaccharide hydrolases and secondary metabolite gene clusters in the mangrove shipworm *Neoteredoreynei*. *PloS one*, 13(11), e0200437.

Brown, C. T., Hug, L. A., Thomas, B. C., Sharon, I., Castelle, C. J., Singh, A., Wilkins, M.J., Wrighton, K.C., Williams, K.H. & Banfield, J. F. (2015). Unusual biology across a group comprising more than 15% of domain Bacteria. *Nature*, 523(7559), 208-211.

Brown, R. M., Wiens, G. D., & Salinas, I. (2019). Analysis of the gut and gill microbiome of resistant and susceptible lines of rainbow trout (*Oncorhynchus mykiss*). *Fish & shellfish immunology*, 86, 497-506.

Bustos, P. A., Young, N. D., Rozas, M. A., Bohle, H. M., Ildefonso, R. S., Morrison, R. N., & Nowak, B. F. (2011). Amoebic gill disease (AGD) in Atlantic salmon (*Salmo salar*) farmed in Chile. *Aquaculture*, 310(3-4), 281-288.

Cameron, D. E. (1992). Amoebic gill disease field research 1991/92. *In Proceedings of the Saltas Research and Development Review Seminar*. Hobart, Tasmania (pp. 123-133).

Cano, I., McCullough, R., Mulhearn, B., Gunning, S., Waine, A., Joiner, C., & Paley, R. (2020). Non-lethal loop-mediated isothermal amplification assay as a point-of-care diagnostics tool for *Neoparamoeba perurans*, the causative agent of amoebic gill disease. *Journal of Fish Diseases*.

Caron, D. A., Davis, P. G., Madin, L. P., &Sieburth, J. M. (1982). Heterotrophic bacteria and bacterivorous protozoa in oceanic macroaggregates. *Science*, 218(4574), 795-797.

Chang, Y. C., Hamlin-Wright, H., Monaghan, S., Herath, T., Baily, J., Del Pozo, J., Downes, J., Preston, A., Chalmers, L., Jayasuriya, N., &Bron, J. E. (2019). Changes in distribution, morphology and ultrastructure of chloride cell in Atlantic salmon during an AGD infection. *Journal of fish diseases*, 42(10), 1433-1446.

Clark, A., & Nowak, B. F. (1999). Field investigations of amoebic gill disease in Atlantic salmon, *Salmo salar* L., in Tasmania. *Journal of Fish Diseases*, 22(6), 433-443.

Clark, G., Powell, M., & Nowak, B. (2003). Effects of commercial freshwater bathing on reinfection of Atlantic salmon, *Salmo salar*, with amoebic gill disease. *Aquaculture*, 219(1-4), 135-142.

Collins, C., Hall, M., Bruno, D., Sokolowska, J., Duncan, L., Yuecel, R., McCarthy, U., Fordyce, M.J., Pert, C.C., McIntosh, R., & MacKay, Z. (2017). Generation of *Paramoeba perurans* clonal cultures using flow cytometry and confirmation of virulence. *Journal of fish diseases*, 40(3), 351-365.

Crosbie, P. B. B., Carson, J., & Nowak, B. F. (2002). Detection of *Neoparamoeba pemaquidensis* in marine sediments in Tasmania. *In Aquafin CRC Conference* (p. 17).

Crosbie, P. B. B., Ogawa, K., Nakano, D., & Nowak, B. F. (2010a). Amoebic gill disease in hatchery-reared ayu, *Plecoglossus altivelis* (Temminck & Schlegel), in Japan is caused by *Neoparamoeba perurans*. *Journal of fish diseases*, 33(5), 455-458.

Crosbie, P. B., Bridle, A. R., Leef, M. J., & Nowak, B. F. (2010b). Effects of different batches of *Neoparamoeba perurans* and fish stocking densities on the severity of amoebic gill disease in experimental infection of Atlantic salmon, *Salmo salar* L. *Aquaculture Research*, 41(10), e505-e516.

Crosbie, P. B. B., Bridle, A. R., Cadoret, K., & Nowak, B. F. (2012). In vitro cultured *Neoparamoeba perurans* causes amoebic gill disease in Atlantic salmon and fulfils Koch's postulates. *International journal for parasitology*, 42(5), 511-515.

Deamer, D., Akeson, M., &Branton, D. (2016). Three decades of nanopore sequencing. *Nature biotechnology*, 34(5), 518-524.

Douglas-Helders, M., Saksida, S., Raverty, S., & Nowak, B. F. (2001). Temperature as a risk factor for outbreaks of amoebic gill disease in farmed Atlantic salmon (*Salmo salar*). *Bulletin of the European Association of Fish Pathologists*, 21(3), 114-116.

Douglas-Helders, G. M., Weir, I. J., O'brien, D. P., Carson, J., & Nowak, B. F. (2004). Effects of husbandry on prevalence of amoebic gill disease and performance of reared Atlantic salmon (*Salmo salar* L.). *Aquaculture*, 241(1-4), 21-30.

Downes, J. K., Henshilwood, K., Collins, E. M., Ryan, A., Connor, I. O., Rodger, H. D., MacCarthy, E., & Ruane, N. M. (2015). A longitudinal study of amoebic gill disease on a marine Atlantic salmon farm utilising a real-time PCR assay for the detection of *Neoparamoeba perurans*. *Aquaculture Environment Interactions*, 7(3), 239-251.

Downes, J. K. (2017). Gill disease in finfish aquaculture with emphasis on amoebic gill disease (Doctoral dissertation, Galway-Mayo Institute of Technology).

Downes, J. K., Rigby, M. L., Taylor, R. S., Maynard, B. T., MacCarthy, E., O'Connor, I., Marcos-Lopez, M., Rodger, H.D., Collins, E., Ruane, N.M. & Cook, M. T. (2017). Evaluation of Non-destructive Molecular Diagnostics for the Detection of *Neoparamoeba perurans*. *Frontiers in Marine Science*, 4 (61).

Downes, J. K., Yatabe, T., Marcos-Lopez, M., Rodger, H. D., MacCarthy, E., O'Connor, I., Collins, E. & Ruane, N. M. (2018a). Investigation of co-infections with pathogens associated with gill disease in Atlantic salmon during an amoebic gill disease outbreak. *Journal of fish diseases*, 41(8), 1217-1227.

Downes, J. K., Collins, E. M., Morrissey, T., Hickey, C., O'Connor, I., Rodger, H. D., MacCarthy, E., Palmer, R., Ruttledge, M. & Ruane, N. M. (2018b). Confirmation of *Neoparamoeba perurans* on the gills of Atlantic salmon during the earliest outbreaks of amoebic gill disease in Ireland. *Bull. Eur. Assoc. Fish Pathol*, 38(1).

Dyková, I., Figueras, A., Novoa, B., & Casal, J. F. (1998). *Paramoeba* sp., an agent of amoebic gill disease of turbot *Scophthalmus maximus*. *Diseases of Aquatic Organisms*, 33(2), 137-141.

Dyková, I., Figueras, A., & Peric, Z. (2000). Neoparamoeba Page, 1987: light and electron microscopic observations on six strains of different origin. *Diseases of aquatic organisms*, 43(3), 217-223.

Dyková, I., & Novoa, B. (2001). Comments on diagnosis of amoebic gill disease (AGD) in turbot, *Scophthalmus maximus*.

Dyková, I., Fiala, I., Lom, J., & Lukeš, J. (2003). *Perkinsiella amoebae*-like endosymbionts of *Neoparamoeba* spp., relatives of the kinetoplastid *Ichthyobodo*. *European Journal of Protistology*, 39(1), 37-52.

Dyková, I. B. F. N., Nowak, B. F., Crosbie, P. B. B., Fiala, I., Peckova, H., Adams, M. B., Macháčková, B., & Dvořáková, H. (2005). *Neoparamoeba branchiphila* n. sp., and related species of the genus Neoparamoeba Page, 1987: morphological and molecular characterization of selected strains. *Journal of fish diseases*, 28(1), 49-64.

Embar-Gopinath, S., Crosbie, P. B. B., & Nowak, B. F. (2005a). Use of potassium permanganate to disinfect Atlantic salmon (*Salmo salar*) gills. *Bulletin European Association of Fish Pathologists*, 25(6), 291-296.

Embar-Gopinath, S., Butler, R., & Nowak, B. (2005b). Influence of salmonid gill bacteria on development and severity of amoebic gill disease. *Diseases of aquatic organisms*, 67(1-2), 55-60.

Embar-Gopinath, S., Crosbie, P., & Nowak, B. F. (2006). Concentration effects of *Winogradskyella* sp. on the incidence and severity of amoebic gill disease. *Diseases of aquatic organisms*, 73(1), 43-47.

Embar-Gopinath, S., Bowman, J., Carson, J., Crosbie, P., & Nowak, B. (2008). A culture-dependent 16S rRNA gene-based approach to identify gill bacteria associated with amoebic gill disease in Atlantic salmon. *BULLETIN-EUROPEAN ASSOCIATION OF FISH PATHOLOGISTS*, 28(1), 27.

Feng, Y., Ramnarine, V. R., Bell, R., Volik, S., Davicioni, E., Hayes, V. M., Ren, S. & Collins, C. C. (2019). Metagenomic and metatranscriptomic analysis of human prostate microbiota from patients with prostate cancer. *BMC genomics*, 20(1), 1-8.

Findlay, V. L., Helders, M., Munday, B. L., & Gurney, R. (1995). Demonstration of resistance to reinfection with *Paramoeba* sp. by Atlantic salmon, *Salmo salar* L. *Journal of Fish Diseases*, 18(6), 639-642.

Findlay, V. L., & Munday, B. L. (2000). The immunomodulatory effects of levamisole on the nonspecific immune system of Atlantic salmon, *Salmo salar* L. *Journal of Fish Diseases*, 23(6), 369-378.

Findlay, V. L. (2001). Demonstration and manipulation of acquired resistance to amoebic gill disease in Atlantic salmon, *Salmo salar* L (*Doctoral dissertation*, University of Tasmania).

Florent, R. L., Becker, J. A., & Powell, M. D. (2007a). Efficacy of bithionol as an oral treatment for amoebic gill disease in Atlantic salmon *Salmo salar* (L.). *Aquaculture*, 270(1-4), 15-22.

Florent, R. L., Becker, J. A., & Powell, M. D. (2007b). Evaluation of bithionol as a bath treatment for amoebic gill disease caused by *Neoparamoeba* spp. *Veterinary parasitology*, 144(3-4), 197-207.

Fringuelli, E., Gordon, A. W., Rodger, H., Welsh, M. D., & Graham, D. A. (2012). Detection of *Neoparamoeba perurans* by duplex quantitative Taqman real-time PCR in formalin-fixed, paraffin-embedded Atlantic salmonid gill tissues. *Journal of fish diseases*, 35(10), 711-724.

Gómez, G. D., &Balcázar, J. L. (2008). A review on the interactions between gut microbiota and innate immunity of fish. *FEMS Immunology & Medical Microbiology*, 52(2), 145-154.

Grondona, I., Hermosa, R., Tejada, M., Gomis, M. D., Mateos, P. F., Bridge, P. D., Monte, E. & Garcia-Acha, I. (1997). Physiological and biochemical characterization of *Trichoderma harzianum*, a biological control agent against soilborne fungal plant pathogens. *Applied and Environmental Microbiology*, 63(8), 3189-3198.

Haugland, G. T., Olsen, A. B., Rønneseth, A., & Andersen, L. (2017). Lumpfish (*Cyclopterus lumpus* L.) develop amoebic gill disease (AGD) after experimental challenge with *Paramoeba perurans* and can transfer amoebae to Atlantic salmon (*Salmo salar* L.). *Aquaculture*, 478, 48-55.

Fiskehelserapporten 2013. In: Hjeltnes, B. (Ed.), Report. Norwegian Veterinary Institute, Oslo, Norway (42 pp. (http://www.vetinst.no/nor/Publikasjoner/Fiskehelserapporten/Fiskehelserapporten-2013).

Harris, J. O., Powell, M. D., Attard, M. G., &DeHayr, L. (2005). Clinical assessment of chloramine-T and freshwater as treatments for the control of gill amoebae in Atlantic salmon, *Salmo salar* L. *Aquaculture research*, 36(8), 776-784.

Herrero, A., Thompson, K. D., Ashby, A., Rodger, H. D., &Dagleish, M. P. (2018). Complex gill disease: an emerging syndrome in farmed Atlantic salmon (*Salmo salar* L.). *Journal of comparative pathology*, 163, 23-28.

Hess, S., Wenger, A. S., Ainsworth, T. D., & Rummer, J. L. (2015). Exposure of clownfish larvae to suspended sediment levels found on the Great Barrier Reef: impacts on gill structure and microbiome. *Scientific reports*, 5, 10561.

Hooper, L. V., Littman, D. R., & Macpherson, A. J. (2012). Interactions between the microbiota and the immune system. *Science*, 336(6086), 1268-1273.

Horsley, R. W. (1973). The bacterial flora of the Atlantic salmon (*Salmo salar* L.) in relation to its environment. *Journal of Applied Bacteriology*, 36(3), 377-386.

Horsley, R. W. (1977). A review of the bacterial flora of teleosts and elasmobranchs, including methods for its analysis. *Journal of Fish biology*, 10(6), 529-553.

Howard, T., & Carson, J. (1993). Are there alternatives to freshwater treatment of AGD. In *Proceedings of the SALTAS Research and Development Review Seminar. SALTAS, Hobart, Tasmania* (pp. 81-87).

Howard, T. S., Carson, J., & Lewis, T. (1993). Development of a model of infection for amoebic gill disease. *In SALTAS Research and Development Seminar* (pp. 103-111). SALTAS.

Hvas, M., Karlsbakk, E., Mæhle, S., Wright, D. W., & Oppedal, F. (2017). The gill parasite *Paramoeba perurans* compromises aerobic scope, swimming capacity and ion balance in Atlantic salmon. *Conservation physiology*, 5(1), cox066.

Karlsbakk, E., Olsen, A. B., Einen, A. C. B., Mo, T. A., Fiksdal, I. U., Aase, H., Kalgraff, C., Skår, S.Å. & Hansen, H. (2013). Amoebic gill disease due to *Paramoeba perurans* in ballan wrasse (*Labrus bergylta*). *Aquaculture*, 412, 41-44.

Karlsen, C., Ottem, K. F., Brevik, Ø. J., Davey, M., Sørum, H., & Winther-Larsen, H. C. (2017). The environmental and host-associated bacterial microbiota of Arctic seawater-farmed Atlantic salmon with ulcerative disorders. *Journal of fish diseases*, 40(11), 1645-1663.

Kelly, C., & Salinas, I. (2017). Under pressure: interactions between commensal microbiota and the teleost immune system. *Frontiers in immunology*, 8, 559.

Kent, M. L., Sawyer, T. K., & Hedrick, R. P. (1988). *Paramoeba pemaquidensis* (Sarcomastigophora: Paramoebidae) infestation of the gills of coho salmon *Oncorhynchus kisutch* reared in sea water. *Diseases of Aquatic Organisms*, 5(3), 163-169.

Kim, H. J., Cho, J. B., Lee, M. K., Do Huh, M., & Kim, K. H. (2005). *Neoparamoeba* sp. infection on gills of olive flounder, *Paralichthy solivaceus* in Korea. 한국어병학회지제, 18(2).

Kim, W. S., Kong, K. H., Kim, J. O., Jung, S. J., Kim, J. H., & Oh, M. J. (2017). Amoebic gill disease outbreak in marine fish cultured in Korea. *Journal of Veterinary Diagnostic Investigation*, 29(3), 357-361.

Kuang, T., He, A., Lin, Y., Huang, X., Liu, L., & Zhou, L. (2020). Comparative analysis of microbial communities associated with the gill, gut, and habitat of two filter-feeding fish. *Aquaculture Reports*, 18, 100501.

Kube, P. D., Taylor, R. S., & Elliott, N. G. (2012). Genetic variation in parasite resistance of Atlantic salmon to amoebic gill disease over multiple infections. *Aquaculture*, 364, 165-172.

Lahr, D. J., Parfrey, L. W., Mitchell, E. A., Katz, L. A., & Lara, E. (2011). The chastity of amoebae: re-evaluating evidence for sex in amoeboid organisms. *Proceedings of the Royal Society B: Biological Sciences*, 278(1715), 2081-2090.

Lazado, C. C., Timmerhaus, G., Pedersen, L. F., Pittman, K., Soleng, M., Haddeland, S., Johansen, L.H., Breiland, M.S.W., Rørmark, L., Mohammad, S., & Hytterød, S. (2019). Peracetic acid as a potential treatment for amoebic gill disease (AGD) in Atlantic salmon-Stage 1. *Nofimarapportserie*.

Lee, L. E. J., Van Es, S. J., Walsh, S. K., Rainnie, D. J., Donay, N., Summerfield, R., & Cawthorn, R. J. (2006). High yield and rapid growth of *Neoparamoeba pemaquidensis* in co-culture with a rainbow trout gill-derived cell line RTgill-W1. *Journal of fish diseases*, 29(8), 467-480.

Legrand, T. P., Catalano, S. R., Wos-Oxley, M. L., Stephens, F., Landos, M., Bansemer, M. S., Stone, D.A., Qin, J.G. & Oxley, A. (2018). The inner workings of the outer surface: skin and gill microbiota as indicators of changing gut health in yellowtail kingfish. *Frontiers in microbiology*, 8, 2664.

Lim, S. J., Davis, B. G., Gill, D. E., Walton, J., Nachman, E., Engel, A. S., Anderson, L.C. & Campbell, B. J. (2019). Taxonomic and functional heterogeneity of the gill microbiome in a symbiotic coastal mangrove lucinid species. *The ISME journal*, 13(4), 902-920.

Llewellyn, M. S., Boutin, S., Hoseinifar, S. H., & Derome, N. (2014). Teleost microbiomes: the state of the art in their characterization, manipulation and importance in aquaculture and fisheries. *Frontiers in microbiology*, 5, 207.

Llewellyn, M. S., Leadbeater, S., Garcia, C., Sylvain, F. E., Custodio, M., Ang, K. P., Powell, F., Carvalho, G.R., Creer, S., Elliot, J. & Derome, N. (2017). Parasitism perturbs the mucosal microbiome of Atlantic Salmon. *Scientific reports*, 7, 43465.

Lowrey, L., Woodhams, D. C., Tacchi, L., & Salinas, I. (2015). Topographical mapping of the rainbow trout (*Oncorhynchus mykiss*) microbiome reveals a diverse bacterial community with antifungal properties in the skin. *Applied and Environmental Microbiology*, 81(19), 6915-6925.

Marcos-López, M., Ruiz, C. E., Rodger, H. D., O'Connor, I., MacCarthy, E., & Esteban, M. Á. (2017). Local and systemic humoral immune response in farmed Atlantic salmon (*Salmo salar* L.) under a natural amoebic gill disease outbreak. *Fish & shellfish immunology*, 66, 207-216.

Marotz, C. A., Sanders, J. G., Zuniga, C., Zaramela, L. S., Knight, R., & Zengler, K. (2018). Improving saliva shotgun metagenomics by chemical host DNA depletion. *Microbiome*, 6(1), 1-9.

Maynard, B. T., Taylor, R. S., Kube, P. D., Cook, M. T., & Elliott, N. G. (2016). Salmonid heterosis for resistance to amoebic gill disease (AGD). *Aquaculture*, 451, 106-112.

Mertz, N. (2020). eDNA metabarcoding of amoebic gill disease (AGD) pathogens exposes potential vectors and reservoirs (*Master's thesis, UiTNorgesarktiskeuniversitet*).

Minich, J. J., Poore, G. D., Jantawongsri, K., Johnston, C., Bowie, K., Bowman, J., Knight, R., Nowak, B. & Allen, E. E. (2020a). Microbial ecology of Atlantic salmon (*Salmo salar*) hatcheries: impacts of the built environment on fish mucosal microbiota. *Applied and Environmental Microbiology*, 86(12).

Minich, J. J., Petrus, S., Michael, J. D., Michael, T. P., Knight, R., & Allen, E. E. (2020b). Temporal, environmental, and biological drivers of the mucosal microbiome in a wild marine fish, *Scomber japonicus*. *Msphere*, 5(3).

Minniti, G., Hagen, L. H., Porcellato, D., Jørgensen, S. M., Pope, P. B., & Vaaje-Kolstad, G. (2017). The skin-mucus microbial community of farmed Atlantic salmon (*Salmo salar*). *Frontiers in Microbiology*, 8, 2043.

Mitchell, S. O., & Rodger, H. D. (2011). A review of infectious gill disease in marine salmonid fish. *Journal of fish diseases*, 34(6), 411-432.

Mouton, A., Crosbie, P., Cadoret, K., & Nowak, B. (2014). First record of amoebic gill disease caused by *Neoparamoeba perurans* in South Africa. *Journal of Fish Diseases*, 37(4), 407-409.

Morrison, R. N., Crosbie, P. B. B., & Nowak, B. F. (2004). The induction of laboratory-based amoebic gill disease revisited. *Journal of Fish Diseases*, 27(8), 445-449.

Morrison, R. N., Crosbie, P. B. B., Cook, M. T., Adams, M. B., & Nowak, B. F. (2005). Cultured gill-derived *Neoparamoeba pemaquidensis* fails to elicit amoebic gill disease (AGD) in Atlantic salmon *Salmo salar*. *Diseases of aquatic organisms*, 66(2), 135-144.

Moskowitz, J. E., Doran, A. G., Lei, Z., Busi, S. B., Hart, M. L., Franklin, C. L., Sumner, L.W., Keane, T.M. & Amos-Landgraf, J. M. (2020). Integration of genomics, metagenomics, and metabolomics to identify interplay between susceptibility alleles and microbiota in adenoma initiation. *BMC cancer*, 20(1), 1-16.

Mullins, J., Nowak, B., Leef, M., Røn, Ø., Eriksen, T. B., & McGurk, C. (2020). Functional diets improve survival and physiological response of Atlantic salmon (*Salmo salar*) to amoebic gill disease. *Journal of the World Aquaculture Society*.

Munday, B. L. (1986). Diseases of salmonids. In Proceedings of the workshop on diseases of Australian fish and shellfish (pp. 127-141). *Australian Fish Health Reference Laboratory*.

Munday, B. L., Foster, C. K., Roubal, F. R., & Lester, R. J. G. (1990). Paramoebic gill infection and associated pathology of Atlantic salmon, *Salmo salar* and rainbow trout, *Salmo gairdneri* in Tasmania. In Pathology in marine science. *Proceedings of the Third International Colloquium on Pathology in Marine Aquaculture, held in Gloucester Point, Virginia, USA, October 2-6, 1988.* (pp. 215-222). Academic Press Inc..

Munday, B. L., Zilberg, D., & Findlay, V. (2001). Gill disease of marine fish caused by infection with *Neoparamoeba pemaquidensis*. *Journal of Fish Diseases*, 24(9), 497-507.

Nowak, B. F., & Munday, B. L. (1994). Histology of gills of Atlantic salmon during the first few months following transfer to sea water. *Bulletin of the European Association of Fish Pathologists*, 14(3), 77-81.

Nowak, B. F. (2001). Qualitative evaluation of risk factors for amoebic gill disease in cultured Atlantic salmon. *In Risk analysis in aquatic animal health* (pp. 148-155).

Nowak, B.F., Carson, J., Powell, M.D., Dyková, I. (2002). Amoebic gill disease in the marine environment. *Bull. Eur. Assoc. Fish Pathol.* 22, 144–147.

Nowak, B. F., & LaPatra, S. E. (2006). Epitheliocystis in fish. *Journal of fish diseases*, 29(10), 573-588.

Nowak, B., Valdenegro-Vega, V., Crosbie, P., & Bridle, A. (2014). Immunity to amoeba. *Developmental & Comparative Immunology*, 43(2), 257-267.

Nowak, B. F., & Archibald, J. M. (2018). Opportunistic but lethal: the mystery of paramoebae. *Trends in parasitology*, 34(5), 404-419.

Nylund, S., Andersen, L., Sævareid, I., Plarre, H., Watanabe, K., Arnesen, C. E., Karlsbarkk, E., & Nylund, A. (2011). Diseases of farmed Atlantic salmon (*Salmo salar*) associated with infections by the microsporidian *Paranucleos poratheridion*. *Diseases of Aquatic Organisms*, 94(1), 41-57.

O'Donohoe, P., Kane, F., Kelly, S., McDermott, T., D'Arcy, J., Casserly, J., Downes, J. K. & Jackson, D. (2018). National survey of sea lice (*Lepeophtheirus salmonis* Krøyer and *Caligus elongatus* Nordmann) on fish farms in Ireland-2017. *Marine Insitute*.

Oldham, T., Rodger, H., & Nowak, B. F. (2016). Incidence and distribution of amoebic gill disease (AGD)—an epidemiological review. *Aquaculture*, 457, 35-42.

Page, F. C. (1983). Marine Gymnamoebae. Institute of Terrestrial Ecology. *Culture Collection of Algae and Protozoa Cambridge, England*.

Page, F. C. (1987). The classification of 'naked' amoebae (Phylum Rhizopoda). *ArchivfürProtistenkunde*, 133(3-4), 199-217.

Palmer, R., Carson, J., Ruttledge, M., Drinan, E., & Wagner, T. (1997). Gill disease associated with *Paramoeba*, in sea reared Atlantic salmon in Ireland. *Bulletin of the European Association of Fish Pathologists*, 17(3/4), 112-114.

Parsons, H., Nowak, B., Fisk, D., & Powell, M. (2001). Effectiveness of commercial freshwater bathing as a treatment against amoebic gill disease in Atlantic salmon. *Aquaculture*, 195(3-4), 205-210.

Pennacchi, Y., Adams, M. B., Nowak, B. F., & Bridle, A. R. (2016). Immune gene expression in the gills of Atlantic salmon (*Salmo salar* L.) following experimental reinfection with *Neoparamoeba perurans*. *Aquaculture*, 464, 410-419.

Peyghan, R., Powell, M. D., & Zadkarami, M. R. (2008). In vitro effect of garlic extract and metronidazole against *Neoparamoeba pemaquidensis*, page 1987 and isolated amoebae from Atlantic salmon. *Pakistan journal of biological sciences*: PJBS, 11(1), 41-47.

Piazzon, M. C., Calduch-Giner, J. A., Fouz, B., Estensoro, I., Simó-Mirabet, P., Puyalto, M., Karalazos, V., Palenzuela, O., Sitjà-Bobadilla, A. & Pérez-Sánchez, J. (2017). Under control: how a dietary additive can restore the gut microbiome and proteomic profile, and improve disease resilience in a marine teleostean fish fed vegetable diets. *Microbiome*, 5(1), 164.

Powell, M. D., & Clark, G. A. (2004). Efficacy and toxicity of oxidative disinfectants for the removal of gill amoebae from the gills of amoebic gill disease affected Atlantic salmon (*Salmo salar* L.) in freshwater. *Aquaculture Research*, 35(2), 112-123.

Powell, M. D., Ransome, J., Barney, M., Duijf, R. M., & Flik, G. (2007). Effect of Dietary Inclusion of N-Acetyl Cysteine on Mucus Viscosity and Susceptibility of Rainbow Trout, *Oncorhynchus mykiss*, and Atlantic Salmon, *Salmo salar*, to Amoebic Gill Disease. *Journal of the World Aquaculture Society*, 38(3), 435-442.

Powell, M. D., Reynolds, P., & Kristensen, T. (2015). Freshwater treatment of amoebic gill disease and sea-lice in seawater salmon production: Considerations of water chemistry and fish welfare in Norway. *Aquaculture*, 448, 18-28.

Pratte, Z. A., Besson, M., Hollman, R. D., & Stewart, F. J. (2018). The gills of reef fish support a distinct microbiome influenced by host-specific factors. *Applied and environmental microbiology*, 84(9).

Purcell, J. E., Baxter, E. J., & Fuentes, V. L. (2013). Jellyfish as products and problems of aquaculture. In Advances in aquaculture hatchery technology (pp. 404-430). *Woodhead Publishing*.

Reid, K. M., Patel, S., Robinson, A. J., Bu, L., Jarungsriapisit, J., Moore, L. J., & Salinas, I. (2017). Salmonid alphavirus infection causes skin dysbiosis in Atlantic salmon (*Salmo salar* L.) post-smolts. *PLoS One*, 12(3), e0172856.

Rensel, J. E., & Whyte, J. N. C. (2003). Finfish mariculture and harmful algal blooms. Manual on harmful marine microalgae. *Monographs on oceanographic methodology*, 11, 693-722.

Reverter, M., Sasal, P., Suzuki, M. T., Raviglione, D., Inguimbert, N., Pare, A., Banaigs, B., Voisin, S.N., Bulet, P. & Tapissier-Bontemps, N. (2020). Insights into the Natural Defenses of a Coral Reef Fish Against Gill Ectoparasites: Integrated Metabolome and Microbiome Approach. *Metabolites*, 10(6), 227.

Roberts, S. D., & Powell, M. D. (2003). Reduced total hardness of fresh water enhances the efficacy of bathing as a treatment for amoebic gill disease in Atlantic salmon, *Salmo salar* L. *Journal of Fish Diseases*, 26(10), 591-599.

Robledo, D., Hamilton, A., Gutiérrez, A. P., Bron, J. E., & Houston, R. D. (2020). Characterising the mechanisms underlying genetic resistance to amoebic gill disease in Atlantic salmon using RNA sequencing. *BMC genomics*, 21, 1-11.

Rodger, H. D., & McArdle, J. F. (1996). An outbreak of amoebic gill disease in Ireland. *Veterinary record*, 139, 348-348.

Rodger, H. D. (2007). Gill disorders: an emerging problem for farmed Atlantic salmon (*Salmo salar*) in the marine environment. *Fish Veterinary Journal*, 9, 38-48.

Rodger, H. D. (2014). Amoebic gill disease (AGD) in farmed salmon (*Salmo salar*) in Europe. *Fish Veterinary Journal*, (14), 16-27.

Rodger, H. D. (2019). Amoebic gill disease in farmed halibut (*Hippoglossus hippoglossus*) in the United Kingdom. *Veterinary Record Case Reports*, 7(1).

Rogerson, A., &Laybourn-Parry, J. (1992). The abundance of marine naked amoebae in the water column of the Clyde Estuary. *Estuarine, Coastal and Shelf Science*, 34(2), 187-196.

Rosado, D., Perez-Losada, M., Severino, R., Cable, J., & Xavier, R. (2019a). Characterization of the skin and gill microbiomes of the farmed seabass (*Dicentrarchu slabrax*) and seabream (*Sparus aurata*). *Aquaculture*, 500, 57-64.

Rosado, D., Xavier, R., Severino, R., Tavares, F., Cable, J., & Pérez-Losada, M. (2019b). Effects of disease, antibiotic treatment and recovery trajectory on the microbiome of farmed seabass (*Dicentrarchus labrax*). *Scientific reports*, 9(1), 1-11.

Roubal, F. R., Lester, R. J. G., & Foster, C. K. (1989). Studies on cultured and gill-attached *Paramoeba* sp.(Gymnamoebae: Paramoebidae) and the cytopathology of paramoebic gill disease in Atlantic salmon, *Salmo salar* L., from Tasmania. *Journal of Fish Diseases*, 12(5), 481-492.

Rozas, M., Bohle, H., Ildefonso, R., & Bustos, P. (2011). Development of PCR assay for detection of *Neoparamoeba perurans* and comparison of histological diagnosis. *Bull. Eur. Assoc. Fish Pathol*, 31, 211-218.

Rozas, M., Bohle, H., Grothusen, H., & Bustos, P. (2012). Epidemiology of amoebic gill disease (AGD) in Chilean salmon industry between 2007 and 2010. *Bull. Eur. Assoc. Fish Pathol*, 32, 181-188.

Rozas-Serri, M. (2019). Gill diseases in marine salmon aquaculture with an emphasis on amoebic gill disease. *Atlantic*, 32(33), 34-35.

Schloss, P. D., &Handelsman, J. (2005). Metagenomics for studying unculturable microorganisms: cutting the Gordian knot. *Genome biology*, 6(8), 1-4.

Schmidt, T. M., DeLong, E. F., & Pace, N. R. (1991). Analysis of a marine picoplankton community by 16S rRNA gene cloning and sequencing. *Journal of bacteriology*, 173(14), 4371-4378.

Schmidt, V., Amaral-Zettler, L., Davidson, J., Summerfelt, S., & Good, C. (2016). Influence of fishmeal-free diets on microbial communities in Atlantic salmon (*Salmo salar*) recirculation aquaculture systems. *Applied and environmental microbiology*, 82(15), 4470-4481.

Shinn, A. P., Pratoomyot, J., Bron, J. E., Paladini, G., Brooker, E. E., Brooker, A. J., & Timi, J. (2015). Economic costs of protistan and metazoan parasites to global mariculture. *Parasitology*, 142(1), 196.

Sieburth, J. M., Willis, P. J., Johnson, K. M., Burney, C. M., Lavoie, D. M., Hinga, K. R., Caron, D. A., French, F. W., Johnson, P. W. & Davis, P. G. (1976). Dissolved organic matter and heterotrophic microneuston in the surface microlayers of the North Atlantic. *Science*, 194(4272), pp.1415-1418.

SOFIA (2020) Fisheries and Aquaculture topics. The State of World Fisheries and Aquaculture. Food and Agricultural Organization of the United Nations. http://www.fao.org/documents/card/en/c/ca9229en

Slinger, J., Adams, M. B., & Wynne, J. W. (2020a). Bacteriomic profiling of branchial lesions induced by *Neoparamoeba perurans* challenge reveals commensal dysbiosis and an association with *Tenacibaculum dicentrarchi* in AGD-affected Atlantic salmon (*Salmo salar* L.). *Microorganisms*, 8(8), 1189.

Slinger, J., Adams, M. B., & Wynne, J. W. (2020b). Comparison of bacterial diversity and distribution on the gills of Atlantic salmon (*Salmo salar* L.); an evaluation of sampling techniques. *Journal of Applied Microbiology*.

Slinger, J., Adams, M. B., Stratford, C. N., Rigby, M., & Wynne, J. W. (2021). The Effect of Antimicrobial Treatment upon the Gill Bacteriome of Atlantic Salmon (*Salmo salar* L.) and Progression of Amoebic Gill Disease (AGD) In Vivo. *Microorganisms*, 9(5), 987.

Stagg, H. E. B., Hall, M., Wallace, I. S., Pert, C. C., Garcia Perez, S., & Collins, C. (2015). Detection of *Paramoeba perurans* in Scottish marine wild fish populations. *Bull. Eur. Assoc. Fish Pathol*, 35, 217-226.

Stecher, B., & Hardt, W. D. (2008). The role of microbiota in infectious disease. *Trends in microbiology*, 16(3), 107-114.

Steinum, T., Kvellestad, A., Rønneberg, L. B., Nilsen, H., Asheim, A., Fjell, K., Nygård, S.M.R., Olsen, A.B. & Dale, O. B. (2008). First cases of amoebic gill disease (AGD) in Norwegian seawater farmed Atlantic salmon, *Salmo salar* L., and phylogeny of the causative amoeba using 18S cDNA sequences. *Journal of fish diseases*, 31(3), 205-214.

Steinum, T., Sjåstad, K., Falk, K., Kvellestad, A., & Colquhoun, D. J. (2009). An RT PCR-DGGE survey of gill-associated bacteria in Norwegian seawater-reared Atlantic salmon suffering proliferative gill inflammation. *Aquaculture*, 293(3-4), 172-179.

Tan, C. K., Nowak, B. F., & Hodson, S. L. (2002). Biofouling as a reservoir of *Neoparamoeba pemaquidensis* (Page, 1970), the causative agent of amoebic gill disease in Atlantic salmon. *Aquaculture*, 210(1-4), 49-58.

Taylor, R. S., Wynne, J. W., Kube, P. D., & Elliott, N. G. (2007). Genetic variation of resistance to amoebic gill disease in Atlantic salmon (*Salmo salar*) assessed in a challenge system. *Aquaculture*, 272, S94-S99.

Taylor, R. S., Muller, W. J., Cook, M. T., Kube, P. D., & Elliott, N. G. (2009a). Gill observations in Atlantic salmon (*Salmo salar*, L.) during repeated amoebic gill disease (AGD) field exposure and survival challenge. *Aquaculture*, 290(1-2), 1-8.

Taylor, R. S., Kube, P. D., Muller, W. J., & Elliott, N. G. (2009b). Genetic variation of gross gill pathology and survival of Atlantic salmon (*Salmo salar* L.) during natural amoebic gill disease challenge. *Aquaculture*, 294(3-4), 172-179.

Thoen, E., Tartor, H., Amundsen, M., Dale, O. B., Sveinsson, K., Rønning, H. P., Estelle Grønneberg, E., Dahle, M. K. & Gjessing, M. C. (2020). First record of experimentally induced salmon gill poxvirus disease (SGPVD) in Atlantic salmon (*Salmo salar* L.). *Veterinary Research*, 51, 1-10.

Trust, T. J. (1975). Bacteria associated with the gills of salmonid fishes in freshwater. *Journal of Applied Bacteriology*, 38(3), 225-233.

Uren Webster, T. M., Rodriguez-Barreto, D., Castaldo, G., Gough, P., Consuegra, S., & Garcia de Leaniz, C. (2020). Environmental plasticity and colonisation history in the Atlantic salmon microbiome: a translocation experiment. *Molecular ecology*, 29(5), 886-898.

Valdenegro-Vega, V. A., Cook, M., Crosbie, P., Bridle, A. R., & Nowak, B. F. (2015). Vaccination with recombinant protein (r22C03), a putative attachment factor of *Neoparamoeba perurans*, against AGD in Atlantic salmon (*Salmo salar*) and implications of a co-infection with *Yersinia ruckeri*. *Fish & shellfish immunology*, 44(2), 592-602.

Vincent, B. N., Morrison, R. N., & Nowak, B. F. (2006). Amoebic gill disease (AGD)-affected Atlantic salmon, *Salmo salar* L., are resistant to subsequent AGD challenge. *Journal of fish diseases*, 29(9), 549-559.

Waagbø, R., & Remø, S. C. (2020). Functional diets in fish health management. In Aquaculture Health Management (pp. 187-234). Academic Press.

Wang, Y., Hu, Y., Liu, F., Cao, J., Lv, N., Zhu, B., Zhang, G. & Gao, G. F. (2020). Integrated metagenomic and metatranscriptomic profiling reveals differentially expressed resistomes in human, chicken, and pig gut microbiomes. *Environment international*, 138, 105649.

Wiik-Nielsen, J., Mo, T. A., Kolstad, H., Mohammad, S. N., Hytterød, S., & Powell, M. D. (2016). Morphological diversity of *Paramoeba perurans* trophozoites and their interaction with Atlantic salmon, *Salmo salar* L., gills. *Journal of Fish Diseases*, 39(9), 1113-1123.

Wong, F. Y., Carson, J., & Elliott, N. G. (2004). 18S ribosomal DNA-based PCR identification of *Neoparamoeba pemaquidensis*, the agent of amoebic gill disease in sea-farmed salmonids. *Diseases of aquatic organisms*, 60(1), 65-76.

Wright, D. W., Nowak, B., Oppedal, F., Bridle, A., & Dempster, T. (2015). Depth distribution of the amoebic gill disease agent, *Neoparamoeba perurans*, in salmon sea-cages. *Aquaculture Environment Interactions*, 7(1), 67-74.

Wright, D. W., Nowak, B., Oppedal, F., Bridle, A., & Dempster, T. (2017). Free-living *Neoparamoeba perurans* depth distribution is mostly uniform in salmon cages, but reshaped by stratification and potentially extreme fish crowding. *Aquaculture Environment Interactions*, 9, 269-279.

Wright, D. W., Geitung, L., Karlsbakk, E., Stien, L. H., Dempster, T., Oldham, T., Nola, V., & Oppedal, F. (2018). Surface environment modification in Atlantic salmon sea-cages: effects on amoebic gill disease, salmon lice, growth and welfare. *Aquaculture Environment Interactions*, 10, 255-265.

Wynne, J. W., Cook, M. T., Nowak, B. F., & Elliott, N. G. (2007). Major histocompatibility polymorphism associated with resistance towards amoebic gill disease in Atlantic salmon (*Salmo salar* L.). *Fish & shellfish immunology*, 22(6), 707-717.

Wynne, J. W., Stratford, C., Slinger, J., Samsing, F., Rigby, M., McCulloch, R., Quezada-Rodriguez, P., & Taylor, R. S. (2020). The interaction between temperature and dose on the efficacy and biochemical response of Atlantic salmon to hydrogen peroxide treatment for amoebic gill disease. *Journal of Fish Diseases*, 43(1), 39-48.

Young, N. D., Crosbie, P. B. B., Adams, M. B., Nowak, B. F., & Morrison, R. N. (2007). *Neoparamoeba perurans* n. sp., an agent of amoebic gill disease of Atlantic salmon (*Salmo salar*). *International journal for parasitology*, 37(13), 1469-1481.

Young, N. D., Dyková, I., Snekvik, K., Nowak, B. F., & Morrison, R. N. (2008a). *Neoparamoeba perurans* is a cosmopolitan aetiological agent of amoebic gill disease. *Diseases of aquatic organisms*, 78(3), 217-223.

Young, N. D., Dyková, I., Nowak, B. F., & Morrison, R. N. (2008b). Development of a diagnostic PCR to detect *Neoparamoeba perurans*, agent of amoebic gill disease. *Journal of Fish Diseases*, 31(4), 285-295.

Zilberg, D., Nowak, B., Carson, J., & Wagner, T. (1999). Simple gill smear staining for diagnosis of amoebic gill disease. *Bulletin of the European Association of Fish Pathologists*, 19, 186-189.

Zilberg, D., Gross, A., & Munday, B. L. (2001). Production of salmonid amoebic gill disease by exposure to *Paramoeba* sp. harvested from the gills of infected fish. *Journal of Fish Diseases*, 24(2), 79-82.

CHAPTER 3

Dynamic Gill and Mucus Microbiomes Track an Amoebic Gill Disease Episode in Farmed Atlantic Salmon

*A version of this chapter has been accepted to be published at *Scientific Reports*

3.1 - Introduction

Global fish production was 179 million tonnes in 2018, of which aquaculture represented 46% (FAO, 2020) and approximately 2.4 million tonnes were production of Atlantic salmon (*Salmo salar* L.) (FAO, 2020). The average annual growth of worldwide fish consumption was 3.2% between 1961 and 2016, which was twice the rate of human population growth and significantly more than the growth in meat consumption (FAO, 2018). Although capture fisheries are predicted to keep a stable trend in their live captures until 2030, aquaculture production is expected to expand from 179 million tons in 2018 to 204 million tons in 2030 (FAO, 2020). The aquaculture production would represent then more than 50% of the total obtained fish protein in 2030 (FAO, 2020).

However, the aquaculture industry faces several production challenges, including those related to infectious diseases (Dittmann *et al*., 2017). Particularly, rates of gill disorders in salmon have increased in many countries (Rodger *et al*., 2011), resulting in significant burdens on the sector due to lower growth rates, and increased susceptibility to other pathogenic agents and mortality. Amoebic gill disease (AGD) is currently one of the most important among the gill pathologies (Oldham *et al.*, 2016; Marcos-López *et al.*, 2017), resulting in a significant economic impact for the industry (Rodger, 2014; Nowak & Archibald, 2018).

The most prevalent signs of AGD include uncontrolled proliferation of fish gill cells (hyperplasia), overproduction of gill mucus, respiratory distress, and, in some cases, fish death, mainly due to reduced gas exchange (Munday *et al*., 2001). The first aetiological agent of AGD is the free-living amoeba *Neoparamoeba perurans* (Young *et al.*, 2007). As of yet, the most common means to reduce AGD is to control the abundance of *N. perurans*, with, for example, the application of freshwater baths (Oldham *et al.*, 2016; Nowak & Archibald, 2018). The clearest sign of *N. perurans* infection is the presence of white patches on gills, allowing classification of gill health using an AGD gill score describing the extent of the patches and thus the disease (Taylor *et al.*, 2009). In addition, a suite of molecular diagnostic tools is now available (Young *et al.*, 2007; Downes *et al.*, 2015), which allow the aetiological agent to be directly targeted from community DNA from water or gill samples. However, and despite inherent sensitivity and specificity, quantitative-PCR assays targeting *N. perurans* are only useful in confirming the colonisation of the gill by the amoeba, being unable to determine the vulnerability to AGD prior to the colonisation by *N. perurans*. Indeed, our understanding of

several aspects of AGD and similar gill disorders is incomplete, including regarding the density of parasites and pathogens required to provoke signs; the involvement of other microorganisms, such as viruses, bacteria and zooplankton; and environmental parameters (Steinum *et al*., 2009).

It is well documented that the microbiome of plant and animal tissue plays important potential roles in several diseases of various macro-eukaryotes, variously affecting the severity of signs (Gómez & Balcázar, 2008; Berendsen *et al.*, 2012; Cho & Blaser, 2012; Llewellyn *et al.*, 2014; Voreades *et al*., 2014). Indeed, fish are known to harbour natural microflora (Smith *et al.*, 2007) that play a role in host defenses against pathogens (Oldham *et al*., 2016). The impact of AGD on the microbiome of the salmon gill, and *vice versa,* lacks many information. To date, only some studies have reported on AGD and associated bacteria (Bowman & Nowak, 2004; Embar-Gopinath *et al.*, 2005; Embar-Gopinath *et al.*, 2006; Slinger *et al*., 2020; MacPhail *et al.*, 2021), identifying the presence of a various bacterial taxa only in AGD-affected fish. However, those studies were either constrained by the relatively low-throughput nature of the culture-independent approaches or by the inherent limitations of a laboratory trial, with a low variation of the environmental factors and a low diversity of free-living microorganisms in the surrounding water. Thus, our understanding of the role of the gill microbiome in gill health from seawater farmed salmon, and how it responds during AGD outbreaks, is limited (Nowak & Archibald, 2018). We hypothesise that the gill microbiome may influence the onset and development of AGD in farmed salmon. Equally, we hypothesise that specific bacterial taxa will be associated with AGD and may, in turn, be useful in predicting probable AGD outbreaks in the farmed salmon stocks.

We undertook a longitudinal study with the main objective of characterising the gill prokaryotic microbiome of farmed Atlantic salmon (*Salmo salar* L.), and to quantify *N. perurans* markers, before, and during, an AGD episode.

To achieve this, we also pursued two methodological objectives. First, we needed to develop an approach to reliably sample the gill microbiome. Although previous studies have described extracting nucleic acids from, and applying molecular tools to study gills (Steinum *et al*., 2009; Lowrey *et al.*, 2015; Schmidt *et al*., 2016; Slinger *et al*., 2020), typically only partial gills (sometimes less than 10% total gill arch weight) have been used as samples. Equally, there are few data available on the efficiency of gill microbiome DNA recovery techniques. Thus, we first undertook to optimise the extraction based on sampling of entire gill arches. In that way we

avoided extrapolation of results from partial gills to the whole gill microbiome, as well as under-sampling and under-representation of taxa in the microbiome.

Finally, as gill sampling is inherently invasive, a non-lethal and less invasive sampling approach would provide the basis for more attractive monitoring tools. Thus, our second methodological objective was to test the efficacy of mucus sampling as a suitable alternative source to gills for AGD microbiome analyses.

3.2 - Materials and Methods

3.2.1 - Longitudinal Atlantic Salmon Gill Microbiome Sampling

Salmon gill samples were collected from a fish farm in Bertraghboi Bay (western coast of Ireland; 53°22’03.1”N, 9°51’47.5”W), with the collaboration of MOWI Ireland. Sampling was started in Spring (T0, May 2017) using freshwater pre-smolts and followed the cohort for six months (T1, June – T6, October) in seawater cages (**Fig. 3.1**), during and after the summer months (**Table 1**), when AGD is more likely to appear (Oldham *et al.*, 2016). At each of the seven timepoints (T0-T6), five salmon were sampled from each of three cages (**Table 1**), all of them under the same environmental and farming conditions. All salmon were sampled after attracting them to the edge of the cage with food and simply dip-netted. The fish were then over-anesthetised (tricaine methanosulfonate MS-222, 200 mg/L). The weight and length of each fish was measured, and the AGD gill score was recorded by the same person in every timepoint, following the published guidelines (Taylor *et al.*, 2009). The condition factor (K) of each fish was calculated using the given formula (Alne *et al.*, 2011):

$K = 100 \times [\text{Weight (g)} * (\text{Length (cm)}^{3})]^{-1}$

The gill microbiome was sampled as follows: first, the operculum was aseptically removed using sterile scissors; second, mucus was collected (only mucus samples from T2 to T6 were included in the study, as samples from T0 and T1 showed very low DNA yield after the extraction) from the first brachial arch of the left side of the fish by gently scraping using a sterile spatula, so only mucus was obtained. Mucus was sampled in this way from each of the five fish from the respective cages and pooled in 200 µl TE buffer (10 mM Tris-Cl, pH 7.5; 1 mM EDTA) in order to have enough DNA concentration after the extraction. When there was enough volume of sample, each of the three mucus pools (one from each cage) was then divided into two or three

technical replicates for further processing. However all mucus samples from the same timepoint were considered as biological replicates in the statistical analyses. After the mucus sampling, the second brachial arch of the left side of the fish was excised using sterile scissors and forceps, and placed in respective sterile, labelled, tubes prior to flash freezing (n = 15).

Water temperature (ºC), salinity (‰), dissolved oxygen (%) and turbidity (Secchi depth, metres), were each measured daily throughout the sampling campaign at a depth of 5 m using a Conductivity-Temperature-Depth (CTD) measuring device (YSI 2030 device; ID: 12391).

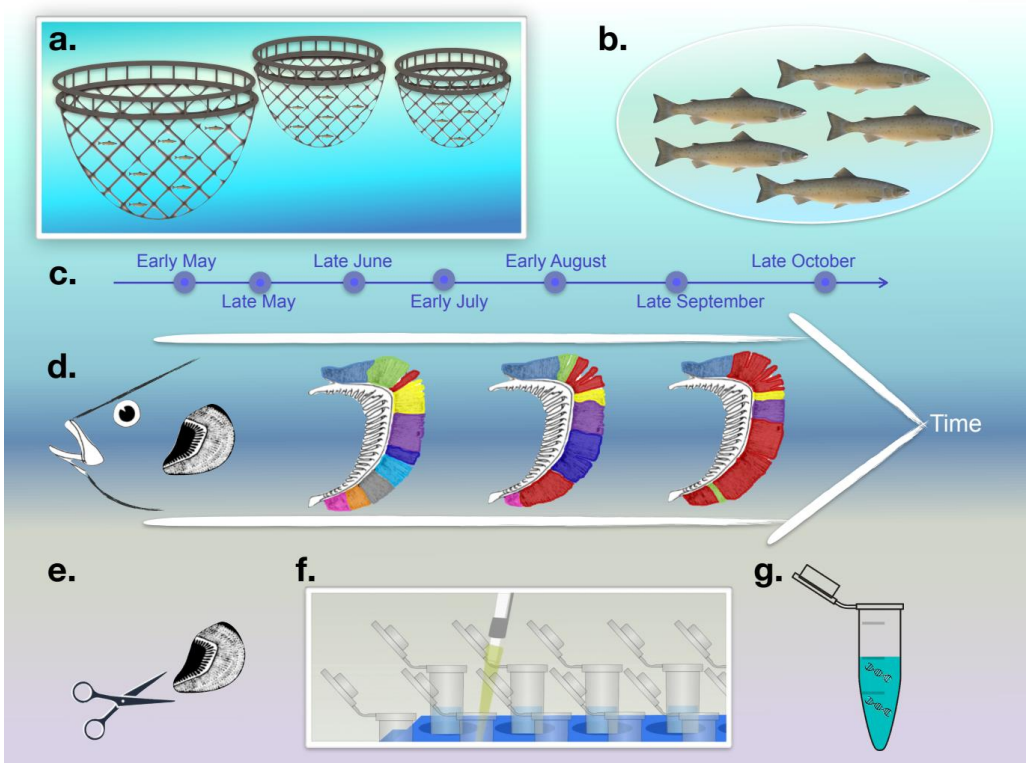

Figure 3.1. Overview of the sampling campaign and analytical approach. (a) Three cages were sampled to retrieve (b) five fish from each (n = 15) at each of (c) seven timepoints (n = 105) from May through October. (d) The hypothesis underpinning the study was that the amoebic gill disease (AGD) episode and abundance of *N. perurans* (red shading) would be associated with a shifting microbiome. The analytical approach included (e) sampling of gill and mucus samples, (f) a newly optimised DNA extraction protocol incorporating several successive washes, and (g) downstream analyses of nucleic acids.

3.2.2 - Optimisation of nucleic acids extraction from gills

To extract the DNA from gill samples, a three-step procedure was developed. First, 50 µl trypsin-EDTA (0.5% trypsin [w/v] in 6.8 mM EDTA; Sigma-Aldrich, Saint Louis, USA) were added along with 450 µl 0.5 M EDTA to a gill in a 2-ml microcentrifuge tube prior to sonication for 5 min (Kerry Ultrasonic Baths, model PUL-125). The gill was then removed to a fresh tube and the process was repeated multiple (seven) times. The number of washes required to optimally detach bacterial cells was determined based on the concentration of prokaryotic cells in the liquid phase from each successive wash measured using a hemocytometer (10 central squares [0.20 mm x 0.20 mm] were considered in each of three replicates for each wash).

Second, the liquid phase from each wash step was pooled in a 15-ml tube, and the gill was discarded. An equal volume of ice-cold isopropanol was added along with a 0.1 volume of 3 M sodium acetate to precipitate free DNA, which was then recovered with microbial cells by centrifuging for 30 min at > 8,000 g (4°C) to form three layers. The top and middle layers were discarded.

Third, an extraction kit (AllPrep DNA/RNA extraction kit, QIAGEN, Hilden, Germany) was used to recover nucleic acids from the bottom layer containing the pellet following the manufacturer's instructions without any modifications.

To determine the efficacy of the second step in enhancing DNA extraction efficiency, DNA recovery was compared with and without the precipitation stage. DNA yield was measured as ng DNA recovered per mg wet gill, so as to ensure a fair comparison of DNA recovery across different gill weights.

3.2.3 - DNA extraction from gills and mucus samples

DNA was extracted from the gills at each of the seven timepoints (n = 105) according to the optimised protocol. Mucus samples, including the possible replicates, from each of T2-T6 (n = 30) were processed using the extraction kit (AllPrep DNA and RNA extraction kit, QIAGEN, Hilden, Germany) according to the manufacturer's instructions. Concentrations of double-stranded DNA were determined using a Qubit dsDNA BR Assay Kit (ThermoFisher Scientific, Paisley, UK), following the instructions provided.

3.2.4 16S rRNA gene sequencing and *N. perurans* 18S rRNA gene quantification

The V4 and OutTS1-spanning regions of 16S rRNA genes from gill and mucus DNA samples were amplified using the oligonucleotide primers 515F (5'-GTGCCAGCMGCCGCGGTAA-3') and 806R (5'-GGACTACHVGGGTWTCTAAT-3') (Caporaso *et al.*, 2011; Dittmann *et al.*, 2019; Dittmann *et al*., 2020). PCR mixtures (25 µl final volume) contained: 12.5 ng genomic DNA, 0.2 µM (final concentration) of each primer (515F and 806R), and 12.5 µl 2X KAPA HiFi Hot Start Ready Mix (0.25 U; Roche). The PCR comprised of initial denaturation at 95°C for 3 min; 25 cycles of 95°C for 30 s, 55°C for 30 s and 72°C for 30 s; and a final incubation at 72°C for 5 min. PCR products were purified (AMPure XP for PCR Purification, Beckman Coulter, USA) before adding Illumina sequencing adapters and indices using a Nextera XT Index Kit (Cambridge, United Kingdom) following the manufacturer's instructions. A second PCR purification was done before quantifying the DNA using a 2100 Bioanalyzer system (Agilent Technologies), normalising the DNA concentration (to 4 nM) and pooling the libraries with unique indices. Pooled libraries were denatured (0.2 N NaOH), diluted and heat-denatured before sequencing. Amplicons were sequenced using an Illumina MiSeq platform (Caporaso *et al.*, 2012) using 5% PhiXas as internal control, following Illumina's recommendations.

The concentration of *N. perurans* in gill and mucus samples was estimated in quantitative PCR assays targeting partial 18S rRNA gene sequences specific to the amoeba and using the primers NP1 (5'-AAAAGACCATGCGATTCGTAAAGT-3') and NP2 (5'-CATTCTTTTCGGAGAGTGGAAATT-3'), with the NPP (6-FAM-ATCATGATTCACCATATGTT-MGB) probe, according to the procedure as described in detail by Downes *et al.* (2015). Each PCR mixture (25 µl) contained 5 µl microbial genomic DNA (5 ng/µl), 12.5 µl TaqMan® Universal 2 Master Mix (Applied Biosystems), and final concentrations of 300 nM primer NP1, 900 nM primer NP2 and 200 nM probe NPP. Each qPCR program comprised of an initial denaturation at 95°C for 15 min, followed by 45 cycles of 95°C for 15 s and 56°C for 30 s in a real-time PCR thermocycler (Applied Biosystems AB7500). Positive and negative controls were added into each run, as well as internal and external process controls (Downes *et al.*, 2015).

3.2.5 - Bioinformatics and Statistical Analyses

The software VSEARCH v2.3.4 (steps documented in http://github.com/torognes/vsearch/wiki/VSEARCH-pipeline) was used to generate the abundance table by constructing operational taxonomic units (OTUs), a proxy for species. Prior to using VSEARCH, the paired-end reads were preprocessed according to the recommendations given in author's recent publications (Schirmer *et al*., 2015; D'Amore *et al*., 2016) which results in significant reduction of substitution errors. Briefly, the paired-end reads were trimmed and filtered using Sickle v1.200 (Joshi & Sickle, 2011) by using a sliding window approach and trimming the reads where the average base quality drops below 20. Only the reads that were above 10 bp length were kept after trimming. Next, BayesHammer (Nikolenko *et al*., 2013) was used from the Spades v2.5.0 assembler, which error-corrected the paired-end reads. Following this, pandaseqv(2.4) (Masella *et al*., 2012) was used to assemble the forward and reverse reads into a single sequence spanning the entire V4 region with a minimum overlap of 10 bp. The preprocessed reads (overlapped) from each sample were pooled together while barcodes were added to keep track of which sample the read originated from. The reads were then dereplicated, sorted in order of decreasing abundance and singletons were discarded. Next, the reads were clustered based on 97% similarity followed by a removal of clusters which had chimeric models built from more abundant reads (--uchime_denovo option in vsearch). To remove any chimeras that may have been missed, particularly in the case that they had parents that were absent from the reads or were present in very low abundance, a reference-based chimera filtering step (--uchime_ref option in vsearch) using a gold database (https://www.mothur.org/w/images/f/f1/Silva.gold.bacteria.zip) was applied. Finally, the OTU table was generated by matching the original barcoded reads against clean OTUs (a total of 17,428 OTUs for n=135 samples) at 97% similarity (a proxy for species-level separation). Having obtained the OTUs, we then used DeConseq (Schmieder & Edwards, 2011) to identify OTUs that were contaminants, hitting on *Salmo salar* reference genome. This step identified 13,211 OTUs as contaminants bringing the total OTUs down to 4,217 OTUs. Then, the OTUs were manually checked against NCBI for further contaminants and filtered out some that were still hitting *Salmo salar* reference genome even after DeConseq and others to mitochondria leading to 3,852 OTUs For ensuing statistical analysis, any sample was dropped with total reads <2000 (6 samples in this dataset) and that resulted in a 129 (samples) X 3,834 (OTUs) abundance table.

The assign_taxonomy.py script from the Qiime workflow (Caporaso *et al*., 2010) was used to taxonomically classify the representative OTUs against the SILVA SSU Ref NR database release v123 database. After, the OTUs were multisequence aligned using MAFFT v 7.3 (Katoh & Standley, 2013) and were used in FastTree v2.1.7 (Price *et al*., 2010) to generate the phylogenetic tree in NEWICK format. The biom file for the OTUs was then generated by combining the abundance table with taxonomy information using make_otu_table.py from the Qiime workflow.

Statistical analyses were performed in R using the combined data generated from the bioinformatics as well as meta data associated with the study (environmental factors, fish features, and qPCR results). The vegan package (Oksanen *et al*., 2007) was used for alpha and beta diversity analyses. For alpha diversity measures we have used: Shannon entropy – a commonly used index to measure balance within a community, and rarefied richness (exponential of Shannon entropy) – the estimated number of species, and both indices after rarefying the abundance table to minimum library size. Ordination of OTU table in reduced space (beta diversity) was done using Principal Coordinate Analysis (PCoA) plots of OTUs.Three different distance measures were made using Vegan's cmdscale() function: (1) Bray-Curtis is a distance metric which considers only OTU abundance counts, (2) Unweighted Unifrac is a phylogenetic distance metric which calculates the distance between samples by taking the proportion of the sum of unshared branch lengths in the sum of all the branch lengths of the phylogenetic tree for the OTUs observed in two samples, and without taking into account their abundances and, (3) Weighted Unifrac is a phylogenetic distance metric combining phylogenetic distance with relative abundances. This places emphasis on dominant OTUs or taxa. Unifrac distances were calculated using the phyloseq package (McMurdie & Holmes, 2013).

Analysis of variance for explanatory variables (or sources of variation) was performed using Vegan's adonis() against distance matrices (Bray-Curtis/UnweightedUniFrac/Weighted UniFrac). This function, referred to as PERMANOVA, fit linear models to distance matrices and used a permutation test with pseudo-F ratios. To give an account of environmental filtering (phylogenetic overdispersion versus clustering), phylogenetic distances within each sample were further characterised by calculating the nearest taxa index (NTI) and net relatedness index (NRI). This analysis helped determine whether the community structure was stochastic (overdispersion and driven by competition among taxa) or deterministic (clustering and driven by strong

environmental pressure). The NTI was calculated using mntd() and ses.mntd(), and the mean phylogenetic diversity (MPD) and NRI were calculated using mpd() and ses.mpd() functions from the picante package (Kembel *et al*., 2010). NTI and NRI represent the negatives of the output from ses.mntd() and ses.mpd(), respectively. Additionally, they quantify the number of standard deviations that separate the observed values from the mean of the null distribution (999 randomisation using null.model-'richness' in the ses.mntd() and ses.mpd() functions and only considering taxa as either present or absent regardless of their relative abundance). Based upon the recommendations given (Stegen *et al*., 2012), only the top 1000 most abundant OTUs were used for the calculations.

Discriminant analyses were performed for two cases: longitudinal comparison of gill microbiome, and cross-sectional comparison of microbiome between Gill and Mucous samples. For the first case, Sparse Projection to Latent Structure – Discriminant Analysis (sPLS-DA) was used with the R's mixOmics package (Rohart *et al*., 2017) The procedure constructs artificial latent components of the predicted dataset (genera table denoted as $X(N \times P)$collated at genus level) and the response variable (denoted as $Y$with categorical information of samples, e.g. T0, T1, T2, T3, T4, T5, and T6 for longitudinal analysis) by factorizing these matrices into scores and loading vectors in a new space such that the covariance between the scores of these two matrices$cov(X_h a_h, Y_h b_h)$ in this space is maximized under two constraints: $\|a_h\|_2 = 1$; and $\|a_h\|_1 \leq \lambda$, where a_h and $b_h$are the corresponding loading vectors for X and Y, and h represents the number of components (akin to PCA analysis). The first constraint ensures the loading vector to have unit magnitude (requirement of the procedure) and the second constraint (also called l_1 penalty) to ensure that for the features that do not vary between the categories, the corresponding loading vector coefficients go to zero. This is done by using the sparsity control parameter λ in the above equation, and by adjusting it enforces shrinkage of loading vector coefficients. According to the recommendations given in mixOmics package (http://www.mixomics.org), before applying the procedure splsda(), we pre-filter 1% of the lowest abundant genera and then perform TSS+CLR (Total Sum Scaling followed by Centralised Log Ratio) normalisation. To predict the number of latent components (associated loading vectors) and the number of discriminants, the perf.plsda() and tune.splsda() functions were used, respectively. In the latter case, we fine tune the model was applied using leave-one-out cross-validation by splitting the data into training and testing sets and then finding the classification error rates employing two metrics, overall error rates and balanced error rates (BER), between the predicted latent variables

with the centroid of the class labels (categories considered in this study) using the centroid distance. BER accounts for differences in number of samples between different categories.

For the second case (Gill vs Mucous), the Multivariate Integration (MINT) algorithm (Rohart *et al*., 2017) was used, which is an extension of the multi-group Projection to Latent Structure (mgPLS), and it attempts to find a common projection space across all studies, defined on a small subset of discriminative variables that consistently discriminate the outcome classes (timepoints T2 to T6). In MINT, we have combined $M = 2$ datasets denoted $X^{(1)}(N_1 \times P)$, $X^{(2)}(N_2 \times P)$ for Gill and Mucous, respectively, where both the datasets share the P OTUs whilst the number of samples differ, i.e., N_1, N_2. Both studies have associated dummy indicator outcome $Y^{(1)}$, $Y^{(2)}$ in which all the timepoints (T2, T3, T4, T5, and T6 only as T0, and T1 were not available for Mucous samples) are represented. MINT then solves the problem: $\max_{a_h, b_h} \sum_{m=1}^{M} N_m \mathrm{cov}\left(X_h^{(m)} a_h, Y_h^{(m)} b_h\right)$, with the previous constrains $\|a_h\|_2 = 1$ and $\|a_h\|_1 \leq \lambda$, where the covariance of scores between the datasets are maximised by finding the global loading vectors a_h and b_h common to all studies. The prefiltering and the cross-validation procedure is similar to the previous case (sPLS-DA).

The "BVSTEP" routine (Clarke & Ainsworth, 1993) was used to search for the highest correlation, in a Mantel test, between dissimilarities of fixed and multivariate datasets. To run this algorithm, bvStep() (from the sinkr package) (Taylor, 2017) was used. It permuted through 2n-1 possible combinations of features in the variable dataset. Rather than testing all possible OTU subsets (for n=3,834) which is intractable, the top 1000 most abundant OTUs (Ijaz *et al.*, 2018) were used to best correlate dissimilarities (Bray-Curtis distance) of samples using subsets against dissimilarities of the samples given to all the OTUs. This analysis is complementary to the sPLS-DA and MINT which identified the OTUs causing major shifts in beta diversity but without considering their labelling (i.e., timepoints) with the intention to identify OTUs that change markedly in the sample space.

Subset regression analysis of the microbial community was also performed using the leaps package (Lumley & Miller, 2009), which performs exhaustive search for the best subsets of the explanatory variables (meta data recorded in this study) for predicting the dependent variable in linear regression using an efficient branch-and-bound algorithm. For cross-validation, CVlm() from R's DAAG package was used (Maindonald & Braun, 2015). Other than TSS+CLR

normalisation for the abundance table, Log10 normalisation for qPCR data was used, and Arcsinh normalisation for the cell count data as is the general practice.

In majority of the figures displaying boxplots, pair-wise ANOVA was performed taking two categories at a time, and where significant ($p \leq 0.05$), joined them together by a line and plotting significance on top (*: $0.01 \leq p < 0.05$; **: $0.001 \leq p < 0.01$; ***: $p < 0.001$).

The sequencing data are available in the European Nucleotide Archive under the study accession number PRJEB32307 (http://www.ebi.ac.uk/ena/data/view/PRJEB32307), with further detail in the supplementary files.

3.3 - Results

3.3.1 - Representative nucleic acids extraction method from fish gills

The number of prokaryotic cells in the liquid phase increased across the first five of the successive washes. However, significantly fewer cells were counted after the sixth and seventh washes, suggesting that five such washes sufficiently recovered the majority of the prokaryotic cells on the gills (**Fig. 3.2**). Alpha and beta-diversity (supported by PERMANOVA $p > 0.05$) were not significantly different between each wash, similarly resolving the prokaryotic communities (**Fig. 3.3**). Rarefaction curves (**Fig. 3.4**) indicated DNA sequencing was close to the saturation limit (or plateau) in each of the separate washes after host DNA removal (~75% of the reads).

The second step of the DNA extraction procedure (i.e. the precipitation step) resulted in a four-fold increase in DNA recovery (**Fig. 3.2**). The average DNA recovery from gill samples was 3 ng DNA/mg wet gill.

Quantitative PCR assays indicated abundant amoeba along the washes (**Fig. 3.2**). Although the concentration of *N. perurans* 18S rRNA genes was relatively low after the fifth wash, the abundance was higher again after the sixth and seventh washes.

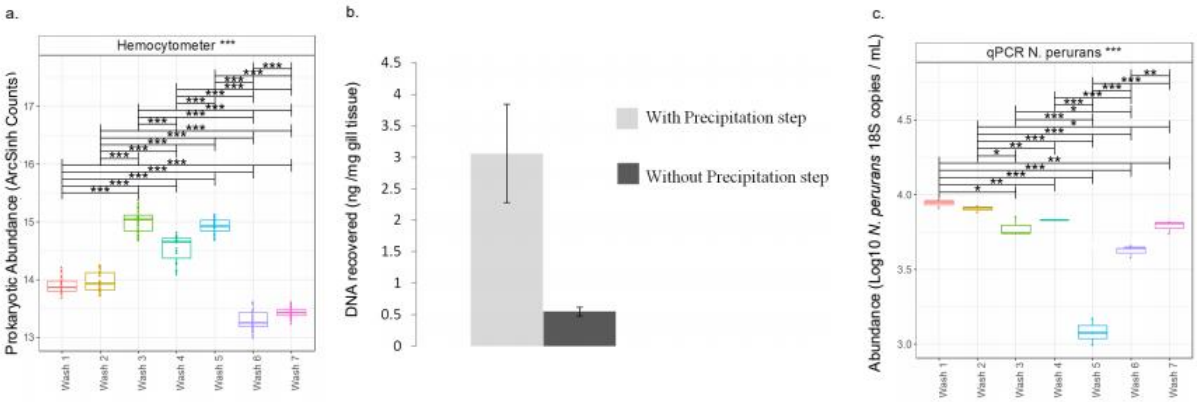

Figure 3.2. ANOVA of pair-wise comparison of extrinsic metadata considered in this study, and after applying appropriate normalization (where necessary). Lines connect two categories where the differences were significant with * ($P < 0.05$), ** ($P < 0.01$), or *** ($p < 0.001$). (a) ArcSinh normalisation was used for prokaryote cells from each wash); (b) comparison of DNA yield from extractions with and without isopropanol and acetic acid precipitation (replicate treatments); (c) qPCR data from each wash transformed using Log10 of the original results for *N. perurans*.

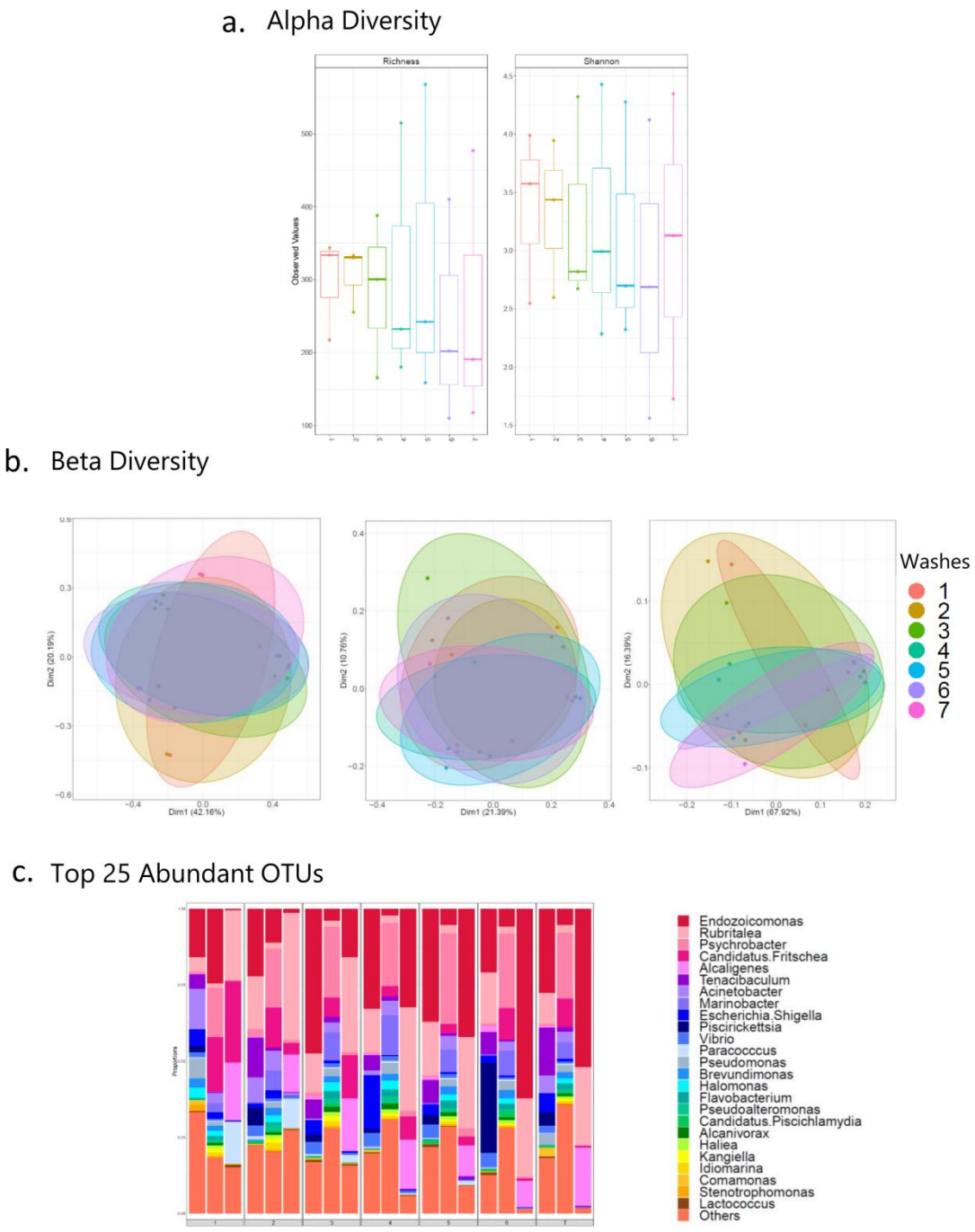

Figure 3.3. Microbial diversity and community structure for the First step of the Nucleic acid extraction protocol optimisation. **(a)** and **(b)** represent alpha diversity and beta diversity indices, respectively. In (b), the ellipses are drawn at 95% confidence interval of standard error with lines going from Wash number 1 to Wash number 7 plotted at mean of the ordination values at each wash. From the left graphic until the right one: Bray-Curtis; UniFrac; Weighted UniFrac. **(c)** shows bacterial community structure based on relative abundance of the top-25 most abundant OTUs from across each Wash, where 'others' refers to all

OTUs not included in the 'top-25'; no significant difference where found in the alpha diversity analyses between washes.

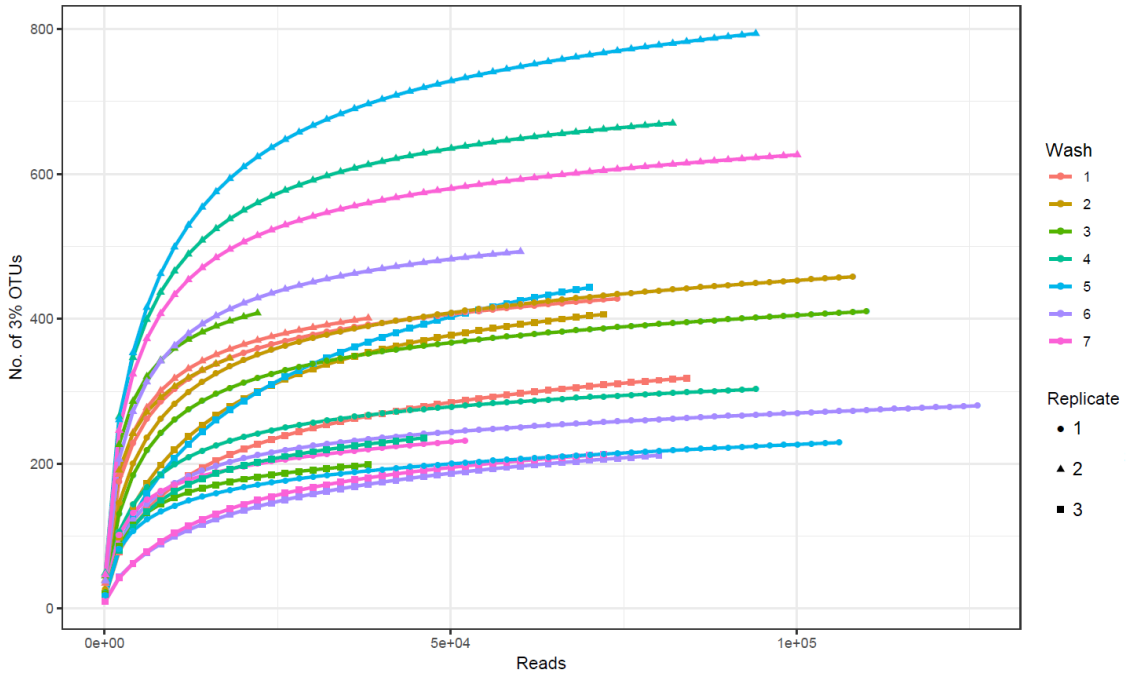

Figure 3.4. Rarefaction curves for 3% OTUs. These curves were generated by using rarefy() function from R's vegan package that gives the expected species richness in random subsamples of OTU table.

3.3.2 - Fish features and appearance of the AGD

The length and weight of the salmon cohort increased progressively over the sampling campaign (**Fig. 3.5**) but had increased significantly by the final sampling point (T6). The mean length and weight at T0 were 19.5 cm and 72.6 g respectively, and at T6 were 36.4 cm and 847.3 g respectively (**Table 3.1**). Based on AGD scoring, no clear signs were apparent until T3 (**Fig. 3.5**). Equally, no *N. perurans* 18S rRNA genes were detected in any of the gill samples from any of the cages before T3 (**Fig. 3.6**). *N. perurans* was detected in two samples at T2 but only after 39 PCR amplification cycles, very close to the limit of detection of the assay (Ct = 40.13) (Downes *et al.*, 2015). Based on this and their AGD gill scores, both fish were considered to be AGD-negative. The first AGD signs on gills were detected one week before T3. Considering this, the farm decided to apply freshwater baths to the salmon stocks three weeks before T4, and two weeks before T6 (**Table 3.1**). All salmon from the same cage were freshwater bathed at the same time for three hours in a bath with salinity between 0.1 and 0.6‰.

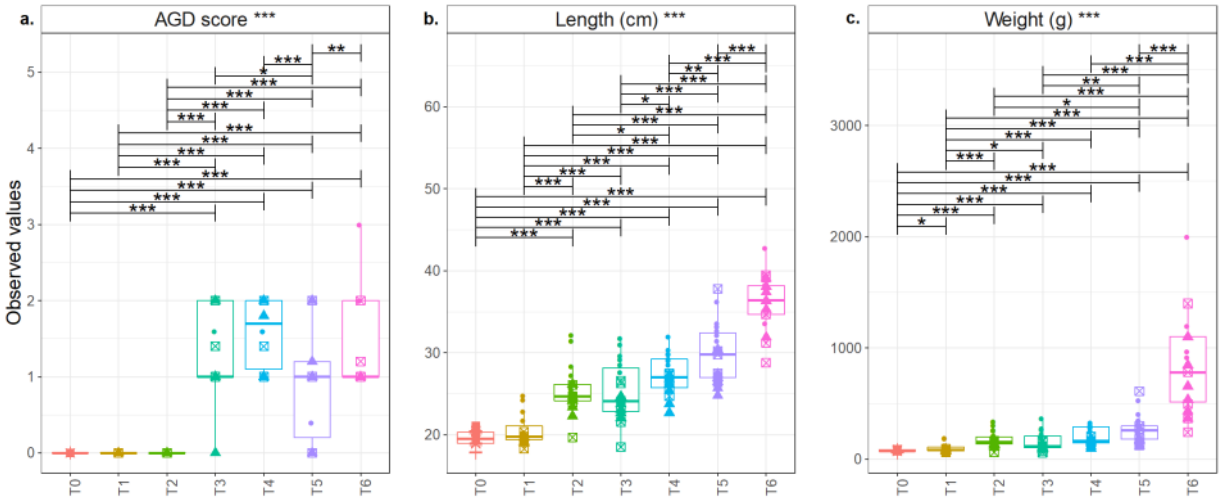

Figure 3.5. ANOVA of pair-wise comparison of extrinsic metadata considered in this study, and after applying appropriate normalization (where necessary). Lines connect two categories where the differences were significant with * (P < 0.05), ** (P < 0.01), or *** (p < 0.001). Mean (a) weight (g), (b) length (cm), and (c) AGD gill score at each of the timepoints.

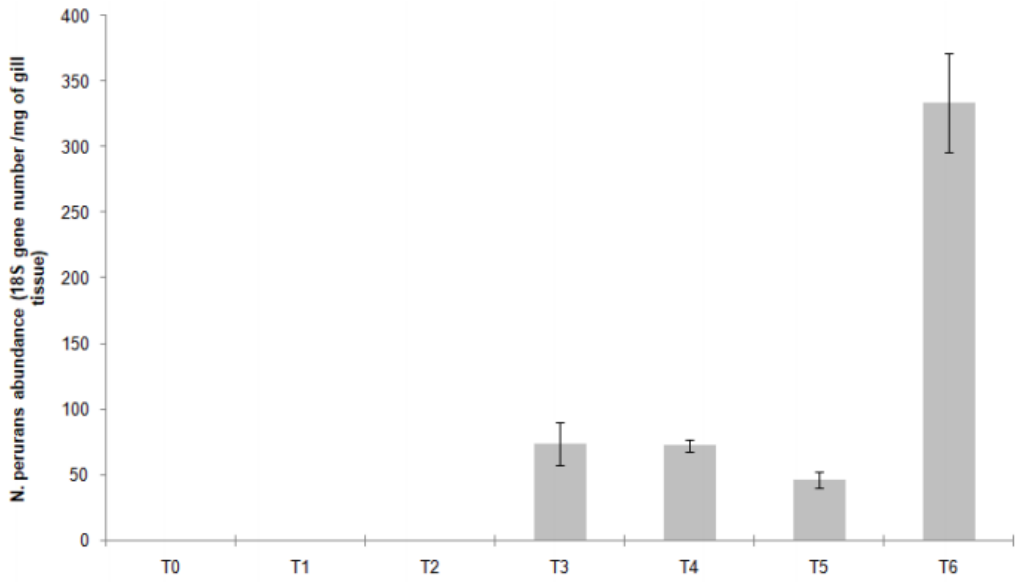

Figure 3.6. Concentrations of *N. perurans* 18S rRNA genes in DNA extractions from salmon gills measured by qPCR assays.

Table 3.1. Mean and standard deviation (in brackets) values of the weight (g), length (cm), condition factor and AGD scores of the 5 salmon from each of the cages in each timepoint. Each timepoint includes the date and the events in each of the important dates of the sampling campaign.

Date	Timepoint	Event	Cage ID	Weight (g)	Length (cm)	Condition Factor	AGD gill scores
05 May 2017	T0	Pre-smolted salmon sampling	44	82.2 (7.5)	20.2 (0.6)	0.99 (0.04)	0 (0)
			58	79.4 (6.6)	19.7 (0.7)	1.03 (0.06)	0 (0)
			75	67.0 (11.0)	18.5 (0.7)	1.02 (0.06)	0 (0)
26 May 2017	T1	Post-smolted salmon sampling	1	144.5 (42.9)	22.8 (1.8)	1.18 (0.1)	0 (0)
			4	80.4 (6.0)	19.5 (0.3)	1.08 (0.05)	0 (0)
			6	75.8 (11.9)	19.4 (0.7)	1.02 (0.12)	0 (0)
22 June 2017	T2	Post-smolted salmon sampling	1	260.2 (68.8)	28.3 (3.2)	1.14 (0.25)	0 (0)
			4	137.3 (25.8)	24.1 (1.4)	0.96 (0.02)	0 (0)
			6	135.4 (41.7)	23.9 (2.4)	0.95 (0.08)	0 (0)
11 July 2017	T3	AGD-affected Post-smolted salmon sampling	1	267.7 (66.8)	29.6 (1.6)	1.01 (0.1)	1.6 (0.5)
			4	105.9 (20.9)	23.0 (1.1)	0.85 (0.03)	1.0 (0.7)
			6	117.4 (50.2)	23.4 (3.4)	0.86 (0.06)	1.4 (0.5)
18 July 2017		First freshwater bath	1 and 4				
19 July 2017		First freshwater bath	6				
10 August 2017	T4	AGD-affected Post-smolted salmon sampling	1	295.0 (30.0)	29.8 (1.3)	1.1 (0.08)	1.6 (0.5)
			4	158.4 (29.7)	26.3 (1.1)	0.86 (0.05)	1.8 (0.4)
			6	158.4 (29.7)	26.3 (1.1)	0.85 (0.07)	1.4 (0.5)
25 September 2017	T5	AGD-affected Post-smolted salmon sampling	1	347.7 (122.5)	33.2 (1.8)	0.91 (0.14)	0.4 (0.2)
			4	181.6 (58.0)	26.9 (2.1)	0.9 (0.09)	1.2 (0.8)
			6	274.8 (199.5)	29.8 (4.6)	0.91 (0.18)	1.0 (1.0)

09 October 2017		Second freshwater bath	1 and 4				
10 October 2017		Second freshwater bath	6				
26 October 2017	T6	AGD-affected Post-smolted salmon sampling	1	1103.7 (574.4)	38.1 (3.4)	1.85 (0.45)	2.0 (0.2)
			4	657.1 (308.1)	36.3 (2.8)	1.31 (0.37)	1.0 (0.0)
			6	781.1 (572.0)	34.6 (4.7)	1.6 (0.57)	1.2 (0.4)

3.3.3 - Impact of AGD on salmon gill microbiome

After the removal of the reads from the host DNA, all samples from the longitudinal gill microbiome part of the study showed the next statistics related with the number of reads: 1st Quantile: 6,063, Median: 27,684, Mean: 41,221, 3rd Quantile: 65,769, Max: 210,382. On the other hand, all samples from the gill and mucus comparison part of the study showed the next statistics related with the number of reads: 1st Quantile: 4,774, Median: 22,601, Mean: 43,180, 3rd Quantile: 71,340, Max: 210,382. During the sample processing, any sample with total reads below 2,000 was dropped, thus six samples (4 gill and 2 mucus samples) were removed before final analyses and resulting in a total of 129 samples (101 gill and 28 mucus samples). In the final analysis, a total of 3,834 clean OTUs from the n=129 samples were included.

The richness and Shannon index of the prokaryotic community on gills increased between T0 and T3 (**Fig. 3.7a, b**). By T3, with the first signs of AGD, and the prevalence of *N. perurans,* the microbiome changed significantly toward reduced diversity and lower NRI (environmental filtering). However, this was reversed following the application of the first (between T3 and T4) and second (between T5 and T6) freshwater baths.

Beta-diversity analyses (**Fig. 3.7c**) using the Bray-Curtis metric indicated the gill microbiome of pre-smolted salmon was completely different to the community on gills of post-smolted salmon. This is consistent with beta-diversity using UniFrac and Weighted UniFrac metrics. Once all salmon were transferred to sea water, the bacterial community did not sharply change until the first AGD signs were detected by T3. The gill microbiomes on T5 and T6 separately clustered from the earlier samples.

The genus *Rubritalea* was found to be consistently present in microbiomes from gill samples through the whole sampling campaign, except at T0 (**Fig. 3.7d**). The gill microbiome from pre-smolted salmon was predominantly composed of bacteria from the genus *Albidiferax* and *Flavobacterium*. However, after smoltification and during the rest of the sampling period, more prokaryotes were very abundant on gills, such as *Shewanella*, *Synechococcus*, *Marinobacter*, *Endozoicomonas*, *Tenacibaculum*, *Pelomonas*, *Alcanivorax* and *Staphylococcus*. A less diverse community was present on gills during the AGD, where bacteria from *Vibrio*, *Pseudomonas* or *Psychrobacter* seemed to be more abundant. Some other genera were found mainly from AGD-affected gills, including C. *Branchiomonas cisticola*, *Tenacibaculum maritimum*, *Piscirickettsia salmonis*, *Piscichlamydia* sp., *Psychroserpens* sp. and C. *Fritschea* sp. These are known as opportunistic species that have previously been detected in diseased Atlantic salmon (**Table S3.1**).

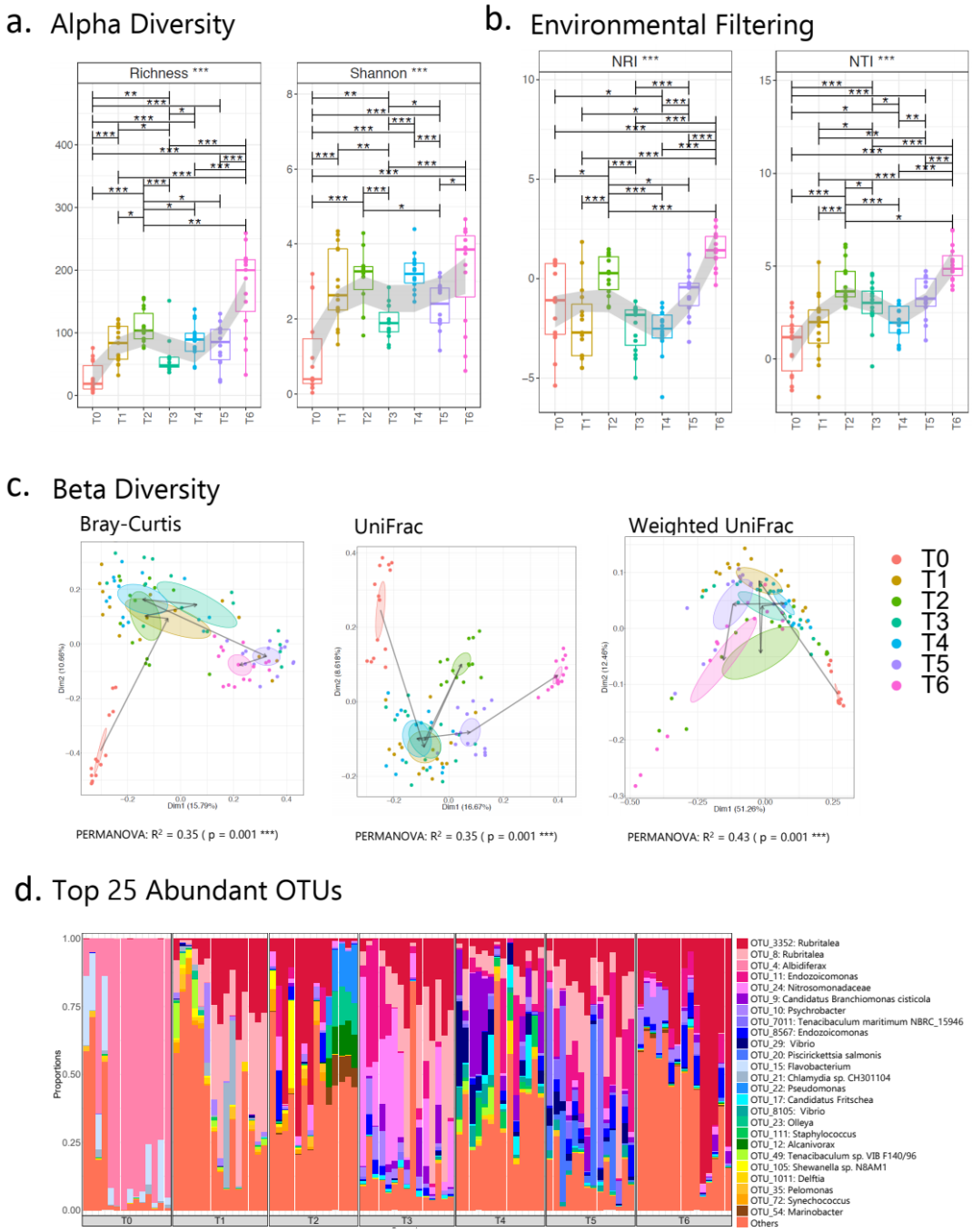

Figure 3.7. Microbial diversity and community structure from temporal gill analyses. **(a)**, **(b)** and **(c)** represent alpha diversity, environmental filtering, and beta diversity indices, respectively. In **(a)** and **(b)**, the regions have been shaded using LOESS smoothing in geom_smooth() when plotting using R'sggplot(). In **(c)**, ellipses are drawn at 95% confidence interval of standard error with lines from T0 to T6 plotted at the mean of the ordination values at each timepoint. **(d)** shows community structure based on relative abundance of the top 25 most abundant OTUs from across each timepoint, where 'others'

refers to all OTUs not included in the top 25; lines for figures **(a)** and **(b)** connect two categories where the differences were significant (ANOVA) with * (P < 0.05), ** (P < 0.01), or *** (p < 0.001).

Based on sPLS-DA analyses of discriminating genera (**Fig. 3.8e**), gill samples from the same timepoint clustered together, except those from T1 and T2. Some genera (e.g., *Albidiferax*, *Altererythrobacter*, *Pedobacter*, *Dyadobacter* and *Shewanella*) were maximally abundant immediately prior to the onset of AGD (at T2 and almost two weeks before the first AGD signs were detected), which was not observable at any of the remaining timepoints.

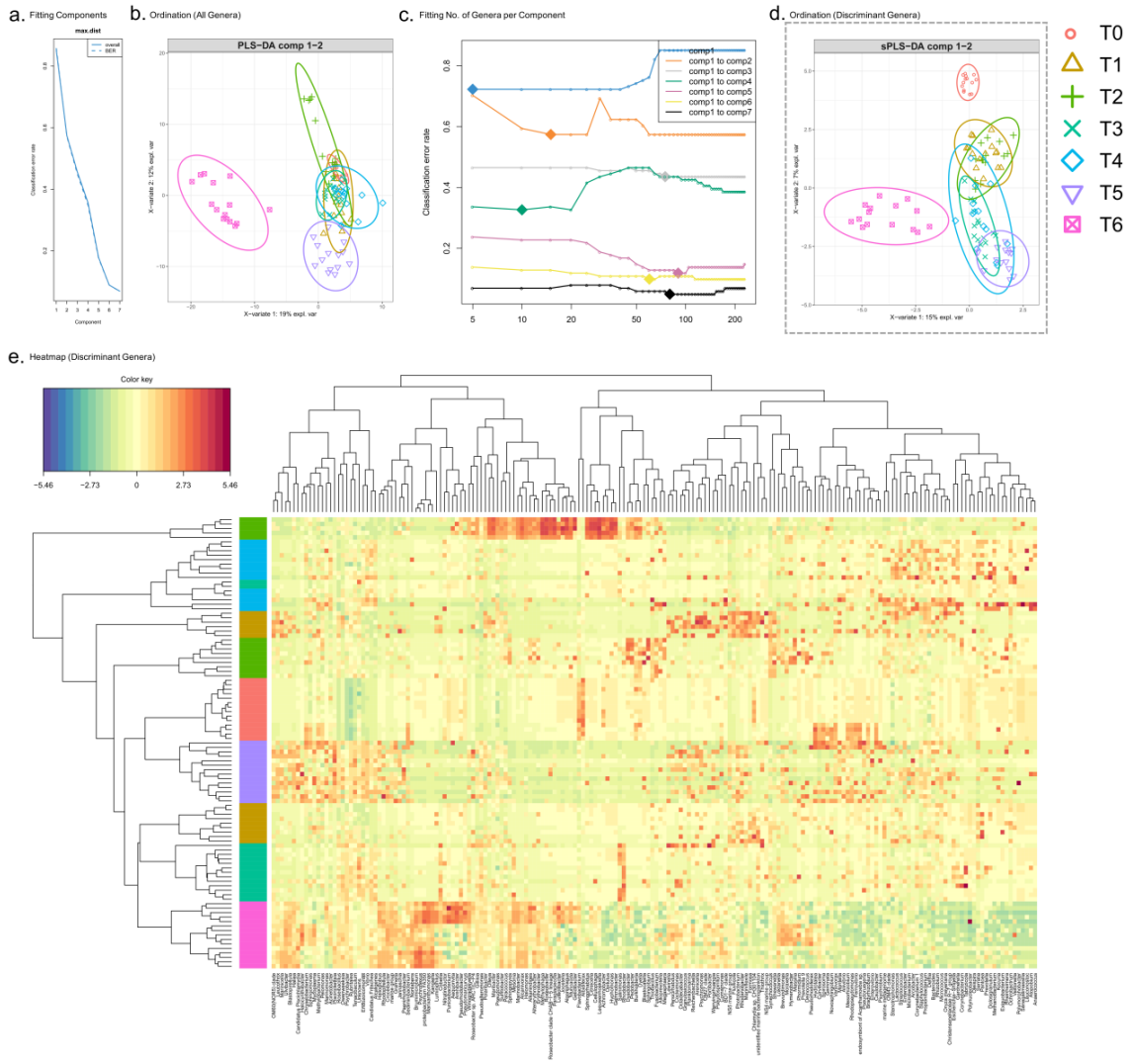

Figure 3.8. sPLS-DA Gill Longitudinal Data Analysis. The algorithm is a two-step process where **(a)** seven components were found reducing the classification error rates (using max.dist in the function) in the algorithm, with **(b)** showing the ordination of samples using all the genera in the first two components (PLS-DA) with ellipses representing 95% confidence interval and percentage variations explained by these components in axes labels. In step two, **(c)** the number of discriminating genera were found for each

component, highlighted as diamonds. **(d)** is similar to **(b)** however the ordination was considered using the discriminants from all seven components (sPLS-DA); **(e)** shows the heatmaps of these discriminant genera, with both rows and columns ordered using hierarchical (average linkage) clustering to identify blocks of genera of interest. Heatmap depicts TSS+CLR normalised abundances: high abundance (red) and low abundance (blue).

3.3.4 - Feasibility of non-lethal mucus scraping to approximate gill microbiomes

The alpha-diversity profiles of gill and mucus microbiomes were similar before the first appearance of AGD (**Fig. 3.9a**). Shannon diversity indices of gill and mucus samples deviated significantly after the first detection of signs (T3), and mucus microbiomes were significantly less balanced than gill microbiomes at both T3 and T4.

No distinguishable patterns were apparent in gill or mucus samples using environmental filtering or beta-diversity analyses (**Fig. 3.9b, c**). The genus *Rubritalea*, as well as the previously described variety of bacteria, which were apparent in gill samples (previous section), were also found in all corresponding mucus samples (**Fig. 3.9d**) at the same timepoints. Microbiome variability in both gill and mucus samples was significantly affected by both time (23%) and sample type (mucus or gill; 3%), and mucus samples appeared to provide at least a partial characterisation of corresponding gill microbiomes (**Fig. 3.9c**).

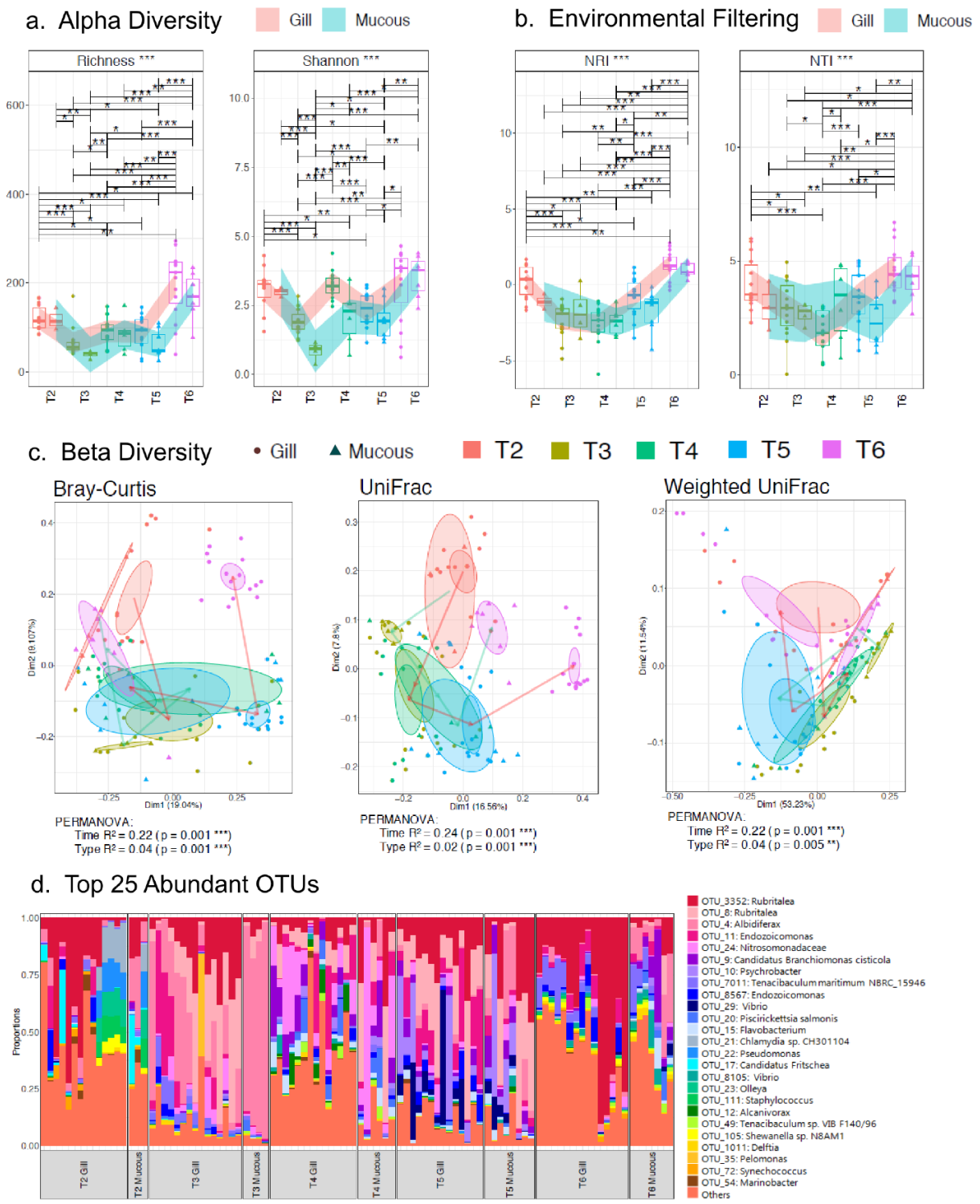

Figure 3.9. Microbial diversity and community structure from for cross-sectional 'gill vs mucus' analyses. (a), (b) and (c) represent alpha diversity, environmental filtering, and beta diversity indices, respectively. In (a) and (b), that LOESS smoothing was performed separately on gill and mucus samples, and PERMANOVA now considers both *Time* and *Type* parameters. In (c), ellipses are drawn at 95% confidence interval of standard error with lines from T2 to T6 plotted at the mean of the ordination values. (d) shows community structure based on relative abundance of the top25 most abundant OTUs;

lines for figures (a) and (b) connect two categories where the differences were significant (ANOVA) with * ($P < 0.05$), ** ($P < 0.01$), or *** ($p < 0.001$).

3.3.5 - Sources of variation in *N. perurans* abundance

The abundance of *N. perurans* was strongly related to the water temperature and the sample type (gill or mucus) (**Table S3.2**). The abundance of the amoeba was negatively associated with the water temperature, that ranged between 12.2 and 16.0 ºC during the sampling campaign. On the other hand, there was a significantly higher chance to detect more abundant *N. perurans* from mucus samples than from gill samples. No relationship was apparent between fish features (i.e. weight and length, or AGD gill score) and *N. perurans* abundance. Negative associations were observed between the abundance of *N. perurans* and salinity, oxygen concentrations and water clarity.

3.3.6 - Influence of *N. perurans*, and environmental factors, on the gill microbiome

A subset of nine OTUs could explain 92% of dissimilarity (Bray-Curtis distance) between gill samples (**Table S3.3**). Time could explain 35% of variability amongst all gill OTUs in the study but only 20% of variability in this OTU sub-set. Similarly, *N. perurans* abundance could explain 5% of variability across all OTUs but only 3.7% in those nine OTUs.

Observing only data from gill microbiomes, only one group – *Stenotrophomonas* sp. – was correlated (negatively) with any of the environmental metadata (water clarity) (**Table S3.3**).

Considering both mucus and gill samples, a sub-set of 12 OTUs accounted for 91% of all dissimilarities across all OTUs (**Table S3.3**). In this case, sample type (mucus or gill) was also considered in PERMANOVA analyses. Time could explain 22% of variability amongst all OTUs but only 20% of variability in this sub-set. *N. perurans* abundance could explain 2.4% of variability in the sub-set.

Again, considering mucus and gill data collectively, four OTUs from both gill and mucus microbiomes correlated with environmental metadata, of which only two OTUs correlated with fish features. One OTU – *Gardnerella* sp. –was positively correlated in the gill dataset with AGD gill scores, but negatively correlated with fish weight in both gill and mucus datasets.

MINT analysis of gill and mucus samples to determine possible indicators of AGD susceptibility found *Altererythrobacter*, *Dyadobacter*, *Shewanella* and *Pedobacter* showed their maximum abundance on gills and in mucus samples at T2 (**Fig. 3.10**), which was 12 days prior to the first detection of AGD signs and when qPCR detected fewest *N. perurans* (**Fig. 3.6**).

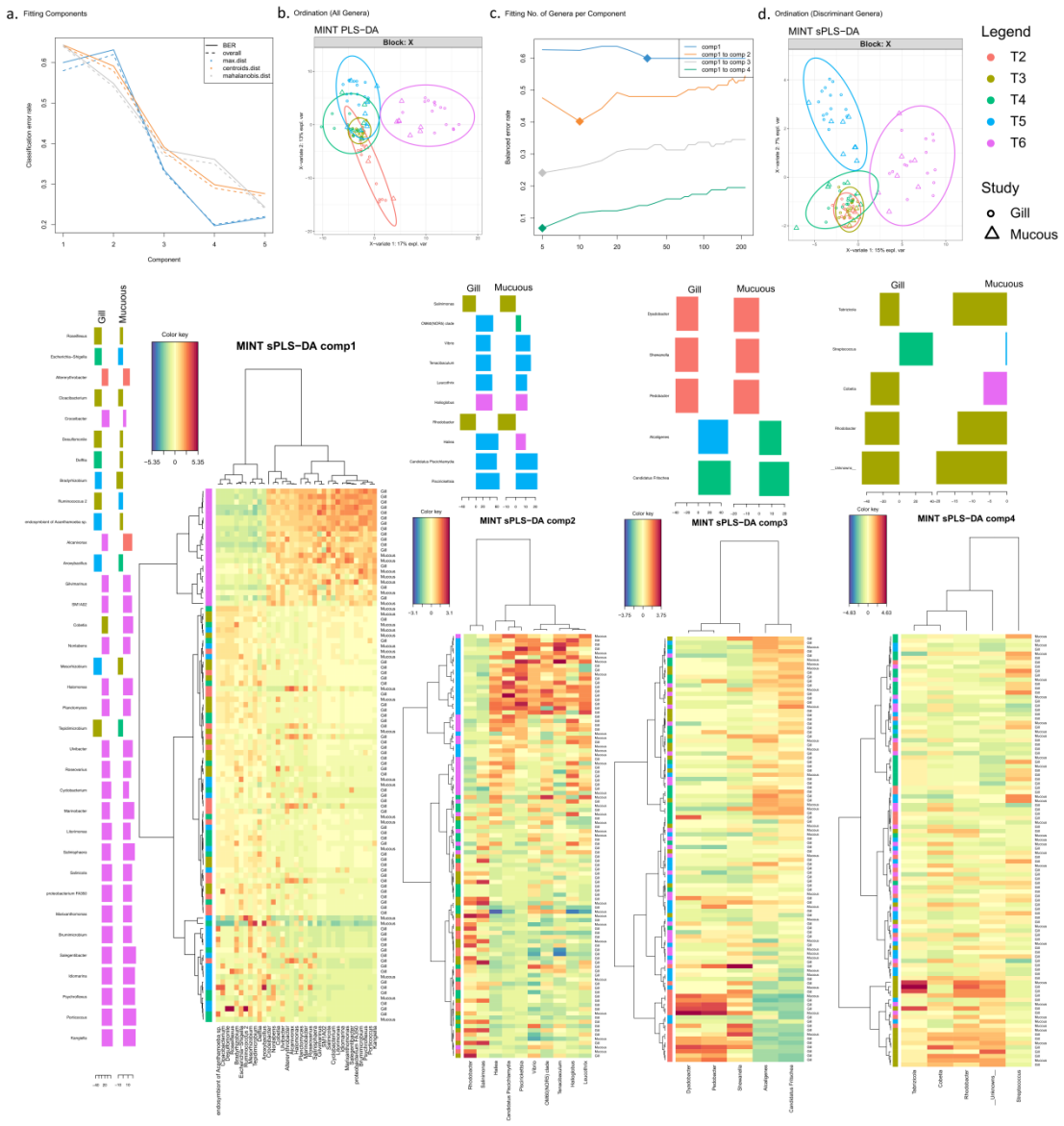

Figure 3.10. MINT study-wise discriminant analysis (Gill vs Mucous). The algorithm is a two-step process where **(a)** four components were found that reduce the classification error rates (using max.dist in the function) in the algorithm, with **(b)** showing the ordination of samples using all the genera in the first two components (MINT PLS-DA) with ellipse representing 95% confidence interval and percentage variations explained by these components in axes labels. In step two, **(c)** the number of discriminating genera were found for each component, highlighted as diamonds. **(d)** is similar to **(b)** however the ordination was considered using the discriminants from all four components (MINT sPLS-DA); **(e)** shows the MINT

sPLS loading vectors a_1,a_2,a_3, and $a_4$with non-zero weights for component 1, 2, 3, and 4 for both Gill and Mucous together, along with the heatmaps of these discriminant genera, with both rows and columns ordered using hierarchical (average linkage) clustering to identify blocks of genera of interest. Heatmap depicts TSS+CLR normalised abundances: high abundance (red) and low abundance (blue). Loading vectors are coloured by time points with maximal abundance.

3.4 - Discussion

3.4.1 - Advantages of the extraction protocol and scope for improvement

Representativeness in sampling has been widely addressed across different fields (Paoletti & Esbensen, 2015), and including in contaminants degradation (Peter *et al.*, 2004), macroorganism ecology (Dufrêne & Legendre, 1997) and microbial ecology (Ranjard *et al.*, 2003), since under-sampling reduces the reliability of observed patterns. Microbial analyses from field samples normally indicate high spatial and temporal heterogeneity, making representativeness critical in microbial ecology. There is currently no evidence indicating how representative partial gill arches are of the overall gill microbiome. Previous studies, such as Steinum *et al.* (2009), Schmidt *et al*. (2016) and Slinger *et al*. (2020) have characterised bacterial communities from partial gills, but the approach may underestimate diversity in the microbiome. Commonly used nucleic acids extraction kits limit the volume, or mass, of tissue in extraction preparations to normally between 30 and 100 mg, which would preclude the use of entire gill arches (which typically exceed 100 mg).

Although it is also possible to extract DNA and RNA from whole gills using in-house purification protocols (Lowrey *et al.*, 2015), commercially available isolation kits offer more reproducibility and, usually, user-friendly workflows. In addition, nucleic acids extraction protocols commonly incorporate a tissue disintegration step with bead-beating (Lowrey *et al.*, 2015), resulting in high relative concentrations of host DNA in final extracts. Host DNA competes with microbiome DNA for PCR amplification, and sequencing depth, limiting the number of reads from the microbiome, and possibly obscuring patterns in microbiome results (Lefèvre *et al*., 2020; Reigel *et al.*, 2020). Thus, a step to allow for isolation, and concentration, of microbial cells from whole gill arches is desirable. The DNA and RNA extraction protocol presented in this study included this critical step prior to the use of a commercially available extraction kit. This ensured DNA extractions comprised the nucleic acids from a representative

part of the microbiome on gills, and that all of the abundant bacterial taxa were included, by extracting DNA from five pooled gill washes. Although additional *N. perurans* could be detected after the fifth wash, the first step of the protocol was thus established as a series of *five* washes in order to keep the DNA extraction as simple and cheap as possible. In addition, this study was focused on the role of the prokaryotic microbiome in AGD and not in the prevalence of *N. perurans* on farmed salmon gills. Therefore, although there was a loss in the amount of recovered amoeba from the gills, every sample probably lost a similar number of amoebic cells. Hence, significant correlations involving the *N. perurans* abundance were still valid.

Salmon DNA was present in extractions and roughly three quarters of reads were from host genes. Nevertheless, after removing host DNA from the analyses, the saturation of the rarefaction curves from bacterial sequences indicated no significant loss of measured bacterial diversity despite host contamination. Nonetheless, competition from high concentrations of host DNA could inhibit amplification of prokaryotic targets. Further modifications to the proposed DNA extraction procedure could be considered, including to deplete as much host DNA as possible using, for instance, blocking primers (Arenz *et al.*, 2015), propidium monoazide (Marotz *et al*., 2018) or methylation-based enrichments (Chiou & Bergey, 2018).

3.4.2 - Impact of AGD and possible influence of freshwater bathing on the gill microbiome

It was reasonable to consider that the AGD episode started between T2 (June) and T3 (July) as the first signs were detected in early July and continued until T6. The *N. perurance* abundance and AGD gill scoring during this period supports the previous statement (**Fig. 3.5 and 3.6**). It was possible that the recovered amount of *N. perurans* in the DNA samples was limited by its detachment from gills due to the used anaesthesia (MS-222) (Chance *et al.*, 2018). In addition, a larger sampling area would allow us to recover more amoebas from the gills (Downes *et al.*, 2017), being able to detect more of them at an early stage like T2. However, the salmon cohort did not show any sign of a gill disease until T3 (**Fig. 3.5**), suggesting that the stock was not affected by AGD until that timepoint. Hence, even if *N. perurans* already colonised those salmon at T1 or T2, we cannot conclude that the AGD episode started until T3.

Some bacterial taxa, for example *Rubritalea*, *Endozoicomonas*, *Nitrosomonas*, C. *Branchiomonas cysticola*, *Psychrobacter*, *Tenacibaculum*, *Piscirickettsia*, *Flavobacterium*, *Shewanella*, *Synechococcus*, *Pseudomonas*, C. *Fritschea*, *Staphylococcus*, *Alcanivorax* and

Winogradskyella, that were found in the microbiome from gill and mucus samples, were already described in previous gill microbiome studies (**Table S3.1**). However, this was the first field study that detect the genus *Rubritalea* from Atlantic salmon gill samples. Being very abundant in all the gill and mucus samples from farmed seawater salmon. Its prevalence in this study suggested that *Rubritalea* would play an important role in the Atlantic salmon gill microbiome. Further research should be conducted for a better comprehension of this bacterial genus.

Previous studies suggested that some bacteria (*Psychroserperns*, *Winogradskyella* and *Tenacibaculum dicentrarchi*) could have a connection with the AGD on Atlantic salmon gills (Bowman & Nowak, 2004; Embar-Gopinath *et al*., 2005; Embar-Gopinath *et al*., 2006; Slinger *et al.*, 2020). However, *Winogradskyella* did not appear to have difference abundance between gill samples before and during the AGD episode, supporting that its possible connection would not be related with the onset of AGD, but more with the severity of the gill disorder (Embar-Gopinath *et al.*, 2006). A species from the *Tenacibaculum* genus (*Tenacibaculum maritimum*) and *Psychroserperns* were more abundant during the AGD, supporting the idea that both genera could be associated with AGD-affected gills (Bowman & Nowak, 2004; Downes *et al.*, 2018; Slinger *et al.*, 2020). Other paper observed a close association between *in vitro* cultured *N. perurans* and *Vibrio* species (MacPhail *et al.*, 2021). In this study, species form the genus *Vibrio* were much more abundant during the AGD episode in gill and mucus samples (**Fig. 3.9d**), when the *N. perurans* abundance increased (**Fig. 3.6**), adding more evidence to their possible connection, but now from field samples.

Other opportunistic bacteria associated with various gill diseases were prominent on gills during the AGD episode. Those included: C. *Branchiomonas cisticola*, *Piscirickettsia salmonis*, *Piscichlamydia* sp., and C. *Fritschea* sp. (**Table S3.1**), the presence of which on salmon gills during the AGD episode may have contributed to gill damage, increasing the severity of the already existing gill lesions, as was suggested previously by Steinum *et al.* (2009). Due to circumstances beyond the authors' control, it was not possible to continue sampling after T6, when AGD gill scores and qPCR data indicated the salmon population was still affected.

Principally, the study provided a temporal profile of the microbiome on Atlantic salmon gills by focusing emphasis on microbial diversity metrics. Prokaryotic richness and community balance on gills of pre-smolted salmon were the lowest across the dataset. The gill microbiome may follow a similar trajectory to the gut microbiome (Romero & Navarrete, 2006; Llewellyn *et al*.,

2014), whereby an initial phase characterised by low diversity in the microbial community transitions, with changes in salmon lifestyle, toward a richer and balanced community. After smoltification, there was a marked change in prokaryotic diversity on salmon gills, preserving balance and richness. The shifting salinity during the smoltification, however, can change the gill microbiome, as described previously for skin microbiomes (Lokesh & Kiron, 2016). Nonetheless, the environmental filtering analysis in our study, which considers phylogenetic clustering as a cue for environmental pressure, suggests that changes in the prokaryotic microbiome on the pre-smolted salmon gills may have inherent stochasticity, driven by competition with other taxa.

The alpha diversity of the prokaryotic gill microbiome continued to increase after smoltification, as was also observed by Llewellyn *et al.* (2014). In addition, the environmental filtering analysis suggested the main environmental pressure was around T2 (which was also supported by beta-diversity analyses). However, 7 days after the salmon showed the first signs (T3), the environmental pressure was eased, and the structure of the microbial communities appeared less deterministic, driven instead by a competitive exclusion principle (the ecological principle whereby community assembly is unhindered, and is driven by competition amongst taxa). Those trends were previously observed in the literature, albeit in connection with a *Helicobacter pylori* gastric infection in human and its gut microbiome (Das *et al*., 2017). At the same time, *N. perurans* concentrations, determined by qPCR profiles, sharply increased by T3. Thus, it is likely that changes in the microbial community structure were due to the influence of AGD. The results give credence to the hypothesis that the development of AGD and the dynamic gill microbiome are related. Slinger *et al.* (2020) demonstrated that the alpha-diversity (measured like Shannon diversity) from AGD-affected gills was significantly higher than gills from AGD-naïve salmon. Although the present study had no negative controls, the same trend between AGD-naïve gills and AGD-affected gills was observed between samples from T2 and T3 (**Fig. 3.7**).

After the first AGD-affected timepoint, freshwater treatments were applied (between T3 and T4; and between T5 and T6) and alpha diversity (including phylogenetic measures) increased (**Fig. 3.7**). Based on these results, the intervention appeared successful, and the gill microbiomes reverted to a growing state in diversity, obtaining the highest richness at T6. Thus, freshwater treatment likely affected microbial community assembly more than other physico-chemical parameters. Nevertheless, further time-course research on the gill microbiome from freshwater

exposed and unexposed AGD-affected salmon should be carried out to have a better understanding of its impact on gill communities.

An alternative scenario immediately after the freshwater treatment would see a less diverse gill microbiome prevailing, with fewer commensal bacteria. This would have two consequences: a short-term and a long-term one. The first is the immediate reduction of the inhibitory effect of commensal bacteria on pathogen colonisation, either passively or actively (Llewellyn *et al.*, 2014). The second is a decelerated development of the vertebrate adaptive immune system (Hooper *et al.*, 2012) due to reduced gill bacterial loads that otherwise enhance this phenomenon. Both outcomes could elevate the AGD susceptibility of the salmon, but previous literature already concluded that re-infected salmon are more resistant to AGD (Findlay *et al.*, 1995; Kube *et al*., 2012). Therefore, as there is no specific treatment available against *N. perurans*, freshwater baths are still the most feasible option in AGD treatment.

3.4.3 - Comparing gill and mucus microbiomes

None of the predominant bacterial taxa were found to be unique to either of the sample types (**Fig. 3.9d**). This was not unexpected, as the DNA extraction from gill samples could be considered as a DNA co-extraction from both mucus and gills. The mucus on gills is likely to detach from the gill to the wash solution during the DNA extraction protocol; hence, communities can intermingle with more homogenised microbial community structures for the two sample types. Thus, our null hypothesis was that there is a degree of similarity in the bacterial communities from mucus and gill samples. However, when we performed diversity analysis, we found significant differences in Shannon entropy between gill and mucus samples at T3 and T4. One possible explanation is that the mucus on gills could act as an insulator, limiting the impact of environmental factors on the organ and the underlying microbial community. Thus, the bacteria in mucus samples were likely better adapted to the changing environment, and both more resistant and resilient than taxa on gills. Nevertheless, bacterial communities on gill and mucus samples were equally affected by freshwater baths, which eventually increased diversity after each treatment.

Although some differences between gill and mucus samples were found, the similarity of the sample types with respect to prokaryotic diversity (**Fig. 3.9**) means mucus scrapings appear

suitable as a non-lethal alternative for partial characterisation of the whole-gill prokaryotic microbiome.

Furthermore, three bacterial genera (*Shewanella* sp., *Dyadobacter* sp. and *Pedobacter* sp.) were most relatively abundant 12 days before the first AGD signs in gill and mucus samples (**Fig. 3.10**). The genera were previously found on intestine, skin, eggs and gill microbiomes from various fish (**Table S3.1**). Of these, *Shewanella* sp. were amongst the most abundant OTUs in this study and were widely detected on skin and gill microbiomes in the literature (Steinum *et al.*, 2009; Svanevik & Lunestad, 2011; Brown *et al.*, 2019). Since its abundance was affected by the onset of AGD, *Shewanella* sp. is a candidate marker (in either gill or mucus samples) for early detection of AGD. This should be investigated further.

3.4.4 - Freshwater bathing appears to regulate response of *N. perurans* to environmental drivers

The available literature on the life details of *N. perurans* is patchy, and the relationship with other microorganisms in distinct environments, such as fish gills, is still mostly unknown (Oldham *et al.*, 2016). However, it is known that unicellular microeukaryotes, such as *N. perurans*, feed on other microorganisms, such as bacteria or archaea (Thaler & Lovejoy, 2012). The gill microbiome, and the interaction with *N. perurans*, may thus shape the host's immunological machinery and response to infection (Gómez & Balcázar, 2008). As in the case of other fish pathologies associated with microbiomes (Talwar *et al.*, 2018), AGD is thus a multifactorial gill disease (Oldham *et al.*, 2016), requiring complex interactions between environmental factors (such as salinity), the host's metabolism, the pathogen and probably the gill microbiome. This is not new between gill disorders, as they are generally complex and involve multiple factors (Rozas-Serri, 2019).

Despite this, quantification of *N. perurans*, combined with AGD scoring, is the most reliable approach currently available to track the progress of the disease. Therefore, changes in *N. perurans* abundance on gills were used to find correlations explaining the development of AGD (**Table S3.2**). *N. perurans* abundance profiles did not, however, reveal any significant correlations with AGD gill scores or any other fish features (e.g., weight or length) in any subset regression model. Such results could be explained by the application of, and interruption by, freshwater treatments during the sampling period. Whilst the size of individual fish continued to increase throughout the sampling campaign, the AGD outbreak impacted the stocks and the fish

farm decided to apply a freshwater treatment. This reduced the abundance of *N. perurans* on gills (**Fig. 3.6**). The sharp increase observed in fish size at the last timepoint (**Fig. 3.5**) could also be part of the reason why the lack of correlation between the *N. perurans* abundance and any fish feature. This increase could mean that salmon grew and gained weight during autumn, also increasing the condition factor at T6 (**Table 3.1**). Another possible explanation is that this unexpected event would be the result of the introduction of salmon from a different cohort, bigger in size, to the salmon cohort that we focused on during this study. Being the administration of the fish farm the responsible for that decision. However, this possible explanation could not be corroborated, and we decided to not remove all the results from the last timepoint.

On the other hand, *N. perurans* abundance appeared significantly correlated with environmental factors in most of the subset regression models (**Table S3.2**). Breaking with convention (Oldham *et al*., 2016), *N. perurans* abundance was negatively correlated with seawater temperature in many of the subset regression models. This unexpected result could be explained by the application of freshwater baths over the summer, which reduced *N. perurans* abundance on gills whilst the seawater temperature continued to increase. Importantly, the influence on *N. perurans* in this way, suggests freshwater baths are still the most viable intervention strategy to treat AGD.

Finally, *N. perurans* abundance was also significantly positively correlated with mucus samples in every subset regression model (**Table S3.2**). This confirms it was more likely to quantify more *N. perurans* in the mucus than in the gill samples, making non-lethal mucus scraping more reliable in targeting *N. perurans* from salmon gills. This would be supported by the study from Downes *et al*. (2017), which found gill swabs to show a higher proportion of AGD-positive results than filament biopsies from gills.

3.4.5 - Sources of variation of the microbiome on salmon gills

Microbiome subset analyses of gill and mucus samples found several positive and negative correlations between the most variable part of the prokaryotic community and the environmental factors considered (**Table S3.3**). Nevertheless, only one bacterial taxon correlated with fish features. *Gardnerella* sp. significantly, positively correlated with the AGD gill score, but negatively correlated with salmon weight. The results suggest those bacteria typically appear on

less developed prokaryotic communities from immature salmon, or from AGD-affected salmon. The influence of freshwater treatments on those correlations was not clear.

Several intrinsic and extrinsic sources of variation shape microbial communities, from study design to environmental factors. Environmental parameters explained for 31% of the variability in community structure (**Table S3.3**). *N. perurans* explained 5% of the variability in the whole prokaryotic community from gills and mucus. Thus, the connection between the development of AGD (*N. perurans* quantification) and the prokaryotic microbiome on farmed Atlantic salmon gills was significant, despite the apparent impact of the freshwater treatments.

Furthermore, *N. perurans* abundance significantly correlated with subsets of the microbiome (**Table S3.3**). It is likely that taxa, including *Lactobacillus, Turicibacter, Bifidobacterium, Allobaculum, Clostridium* and *Stenotrophomonas,* play a role in *N. perurans* predominance on the salmon gills. However, further studies will be required to better understand the relationships between the bacterial microbiome and AGD on salmon gills. Metagenomics of the prokaryotic community on AGD-affected gills, combined with *N. perurans* transcriptomics, would further elucidate the relationship.

3.5 - Conclusions

In this study, a new procedure was optimised to representatively recover DNA from the microbiome of fish gills. Applying this optimised procedure, we were able to determine that, after the onset of an AGD episode, the prokaryotic community on salmon gills shifted toward lower diversity and less balance. In addition, the possible correlation between the development of AGD (*N. perurans* abundance) and the prokaryotic microbiome from gill and mucus samples was confirmed after an AGD episode in one Irish fish farm, explaining 5% of the bacterial community variability. Declining bacterial diversity was reversed after freshwater treatments, increasing the richness and community balance.

Three different bacteria were found to be maximally relatively abundant on gills and mucus samples 12 days before first AGD signs appeared. Among them, *Shewanella*, appeared to be in the top 25 most abundant OTUs, indicating this genus as a possible target for early AGD prediction assays. Bacterial communities from gill and mucus samples from this study presented

very close similarities, establishing mucus scrapings as a suitable non-lethal substitute for gill sampling for partial characterisation of the whole-gill prokaryotic community.

Combined laboratory and field trials would allow for more complete understanding of the connection between AGD and the gill microbiome. Nonetheless, the results could mean a point toward the potential for earlier, more efficient, and less invasive diagnoses and treatment of AGD.

3.6 - References

Alne, H., Oehme, M., Thomassen, M., Terjesen, B., & Rørvik, K. A. (2011). Reduced growth, condition factor and body energy levels in Atlantic salmon *Salmo salar* L. during their first spring in the sea. *Aquaculture Research*, 42(2), 248-259.

Arenz, B. E., Schlatter, D. C., Bradeen, J. M., & Kinkel, L. L. (2015). Blocking primers reduce co-amplification of plant DNA when studying bacterial endophyte communities. *Journal of microbiological methods*, 117, 1-3.

Berendsen, R. L., Pieterse, C. M., & Bakker, P. A. (2012). The rhizosphere microbiome and plant health. *Trends in plant science*, 17(8), 478-486.

Bowman, J. P., & Nowak, B. (2004). Salmonid gill bacteria and their relationship to amoebic gill disease. *Journal of Fish Diseases*, 27(8), 483-492.

Brown, R. M., Wiens, G. D., & Salinas, I. (2019). Analysis of the gut and gill microbiome of resistant and susceptible lines of rainbow trout (*Oncorhynchus mykiss*). *Fish & shellfish immunology*, 86, 497-506.

Caporaso, J. G., Kuczynski, J., Stombaugh, J., Bittinger, K., Bushman, F. D., Costello, E. K., Fierer, N., Pena, A.G., Goodrich, J.K., Gordon, J.I. & Knight, R. (2010). QIIME allows analysis of high-throughput community sequencing data. *Nature methods*, 7(5), 335-336.

Caporaso, J. G., Lauber, C. L., Walters, W. A., Berg-Lyons, D., Lozupone, C. A., Turnbaugh, P. J., Fierer, N. & Knight, R. (2011). Global patterns of 16S rRNA diversity at a depth of millions of sequences per sample. *Proceedings of the national academy of sciences*, 108(Supplement 1), 4516-4522.

Caporaso, J. G., Lauber, C. L., Walters, W. A., Berg-Lyons, D., Huntley, J., Fierer, N., Owens, S.M., Betley, J., Fraser, L., Bauer, M. & Knight, R. (2012). Ultra-high-throughput microbial community analysis on the Illumina HiSeq and MiSeq platforms. *The ISME journal*, 6(8), 1621-1624.

Chance, R. J., Allcock, Z., Secombes, C. J., Collet, B., & Collins, C. (2018). Effect of repeated exposure to AQUI-S® on the viability and growth of *Neoparamoeba perurans*. *Journal of fish diseases*, 41(2), 291-298.

Chiou, K. L., & Bergey, C. M. (2018). Methylation-based enrichment facilitates low-cost, noninvasive genomic scale sequencing of populations from feces. *Scientific reports*, 8(1), 1-10.

Cho, I., & Blaser, M. J. (2012). The human microbiome: at the interface of health and disease. *Nature Reviews Genetics*, 13(4), 260-270.

Clarke, K. R., & Ainsworth, M. (1993). A method of linking multivariate community structure to environmental variables. *Marine Ecology-Progress* Series, 92, 205-205.

D'Amore, R., Ijaz, U. Z., Schirmer, M., Kenny, J. G., Gregory, R., Darby, A. C., Shakya, M., Podar, M., Quince, C. & Hall, N. (2016). A comprehensive benchmarking study of protocols and sequencing platforms for 16S rRNA community profiling. *BMC genomics*, 17(1), 1-20.

Das, A., Pereira, V., Saxena, S., Ghosh, T. S., Anbumani, D., Bag, S., Das, B., Nair, G.B., Abraham, P. & Mande, S. S. (2017). Gastric microbiome of Indian patients with *Helicobacter pylori* infection, and their interaction networks. *Scientific reports*, 7(1), 1-9.

Dittmann, K. K., Rasmussen, B. B., Castex, M., Gram, L., & Bentzon-Tilia, M. (2017). The aquaculture microbiome at the centre of business creation.

Dittmann, K. K., Sonnenschein, E. C., Egan, S., Gram, L., & Bentzon-Tilia, M. (2019). Impact of *Phaeobacter inhibens* on marine eukaryote-associated microbial communities. *Environmental microbiology reports*, 11(3), 401-413.

Dittmann, K. K., Rasmussen, B. B., Melchiorsen, J., Sonnenschein, E. C., Gram, L., & Bentzon-Tilia, M. (2020). Changes in the microbiome of mariculture feed organisms after treatment with a potentially probiotic strain of *Phaeobacter inhibens*. *Applied and environmental microbiology*, 86(14), e00499-20.

Downes, J. K., Henshilwood, K., Collins, E. M., Ryan, A., Connor, I. O., Rodger, H. D., MacCarthy, E. & Ruane, N. M. (2015). A longitudinal study of amoebic gill disease on a marine Atlantic salmon farm utilising a real-time PCR assay for the detection of *Neoparamoeba perurans*. *Aquaculture Environment Interactions*, 7(3), 239-251.

Downes, J. K., Rigby, M. L., Taylor, R. S., Maynard, B. T., MacCarthy, E., O'Connor, I., Marcos-Lopez, M., Rodger, H.D., Collins, E., Ruane, N.M. & Cook, M. T. (2017). Evaluation of Non-destructive Molecular Diagnostics for the Detection of *Neoparamoeba perurans.Frontiers in Marine Science*, 4, 61.

Downes, J. K., Yatabe, T., Marcos-Lopez, M., Rodger, H. D., MacCarthy, E., O'Connor, I., Collins, E. & Ruane, N. M. (2018). Investigation of co-infections with pathogens associated with gill disease in Atlantic salmon during an amoebic gill disease outbreak. *Journal of fish diseases*, 41(8), 1217-1227.

Dufrêne, M., & Legendre, P. (1997). Species assemblages and indicator species: the need for a flexible asymmetrical approach. *Ecological monographs*, 67(3), 345-366.

Embar-Gopinath, S., Butler, R., & Nowak, B. (2005). Influence of salmonid gill bacteria on development and severity of amoebic gill disease. *Diseases of aquatic organisms*, 67(1-2), 55-60.

Embar-Gopinath, S., Crosbie, P., & Nowak, B. F. (2006). Concentration effects of *Winogradskyella* sp. on the incidence and severity of amoebic gill disease. *Diseases of aquatic organisms*, 73(1), 43-47.

FAO. 2018. The State of World Fisheries and Aquaculture 2018. Meeting the sustainable development goals. Rome.

FAO. 2020. The State of World Fisheries and Aquaculture 2020. Sustainability in action. Rome. https://doi.org/10.4060/ca9229enFood and Agriculture Organization of the United Nations. Fisheries Department. The state of world fisheries and aquaculture. Food and Agriculture Organization of the United Nations. 2020

Findlay, V. L., Helders, M., Munday, B. L., & Gurney, R. (1995). Demonstration of resistance to reinfection with *Paramoeba* sp. by Atlantic salmon, *Salmo salar* L. *Journal of Fish Diseases*, 18(6), 639-642.

Gómez, G. D., & Balcázar, J. L. (2008). A review on the interactions between gut microbiota and innate immunity of fish. *FEMS Immunology & Medical Microbiology*, 52(2), 145-154.

Hooper, L. V., Littman, D. R., & Macpherson, A. J. (2012). Interactions between the microbiota and the immune system. *Science*, 336(6086), 1268-1273.

Ijaz, U. Z., Sivaloganathan, L., McKenna, A., Richmond, A., Kelly, C., Linton, M., Stratakos, A.C., Lavery, U., Elmi, A., Wren, B.W & Gundogdu, O. (2018). Comprehensive longitudinal microbiome analysis of the chicken cecum reveals a shift from competitive to environmental drivers and a window of opportunity for *Campylobacter*. *Frontiers in microbiology*, 9, 2452.

Joshi, N. A., & Sickle, F. J. N. a sliding-window, adaptive, quality-based trimming tool for FastQ files (Version 1.33)[Software]. 2011.

Katoh, K., & Standley, D. M. (2013). MAFFT multiple sequence alignment software version 7: improvements in performance and usability. *Molecular biology and evolution*, 30(4), 772-780.

Kembel, S. W., Cowan, P. D., Helmus, M. R., Cornwell, W. K., Morlon, H., Ackerly, D. D., Blomberg, S.P. & Webb, C. O. (2010). Picante: R tools for integrating phylogenies and ecology. *Bioinformatics*, 26(11), 1463-1464.

Kube, P. D., Taylor, R. S., & Elliott, N. G. (2012). Genetic variation in parasite resistance of Atlantic salmon to amoebic gill disease over multiple infections. *Aquaculture*, 364, 165-172.

Lefèvre, E., Gardner, C.M. and Gunsch, C.K. (2020). A novel PCR-clamping assay reducing plant host DNA amplification significantly improves prokaryotic endo-microbiome community characterization. *FEMS Microbiology Ecology*, 96(7), p.fiaa110.

Llewellyn, M. S., Boutin, S., Hoseinifar, S. H., & Derome, N. (2014). Teleost microbiomes: the state of the art in their characterization, manipulation and importance in aquaculture and fisheries. *Frontiers in microbiology*, 5, 207.

Lokesh, J., & Kiron, V. (2016). Transition from freshwater to seawater reshapes the skin-associated microbiota of Atlantic salmon. *Scientific reports*, 6(1), 1-10.

Lowrey, L., Woodhams, D. C., Tacchi, L., & Salinas, I. (2015). Topographical mapping of the rainbow trout (*Oncorhynchus mykiss*) microbiome reveals a diverse bacterial community with antifungal properties in the skin. *Applied and environmental microbiology*, 81(19), 6915-6925.

Lumley, T., & Miller, A. (2009). Leaps: regression subset selection. *R package version*, 2, 2366.

MacPhail, D. P., Koppenstein, R., Maciver, S. K., Paley, R., Longshaw, M., & Henriquez, F. L. (2021). Vibrio species are predominantly intracellular within cultures of *Neoparamoeba perurans*, causative agent of Amoebic Gill Disease (AGD). *Aquaculture*, 532, 736083.

Maindonald, J. H., & Braun, W. J. (2015). DAAG: data analysis and graphics data and functions. *R package version* 1.22.

Marcos-López, M., Ruiz, C. E., Rodger, H. D., O'Connor, I., MacCarthy, E., & Esteban, M. Á. (2017). Local and systemic humoral immune response in farmed Atlantic salmon (*Salmo salar* L.) under a natural amoebic gill disease outbreak. *Fish & shellfish immunology*, 66, 207-216.

Masella, A. P., Bartram, A. K., Truszkowski, J. M., Brown, D. G., & Neufeld, J. D. (2012). PANDAseq: paired-end assembler for illumina sequences. *BMC bioinformatics*, 13(1), 1-7.

McMurdie, P. J., & Holmes, S. (2013). phyloseq: an R package for reproducible interactive analysis and graphics of microbiome census data. *PloS one*, 8(4), e61217.

Munday, B. L., Zilberg, D., & Findlay, V. (2001). Gill disease of marine fish caused by infection with *Neoparamoeba pemaquidensis*. *Journal of Fish Diseases*, 24(9), 497-507.

Nikolenko, S. I., Korobeynikov, A. I., & Alekseyev, M. A. (2013, January). BayesHammer: Bayesian clustering for error correction in single-cell sequencing. *In BMC genomics* (Vol. 14, No. 1, pp. 1-11). *BioMed Central*.

Nowak, B. F., & Archibald, J. M. (2018). Opportunistic but lethal: the mystery of paramoebae. *Trends in Parasitology*, 34(5), 404-419.

Oksanen, J., Kindt, R., Legendre, P., O'Hara, B., Stevens, M. H. H., Oksanen, M. J., & Suggests, M. A. S. S. (2007). The vegan package. Community ecology package, 10(631-637), 719.

Oldham, T., Rodger, H., & Nowak, B. F. (2016). Incidence and distribution of amoebic gill disease (AGD)—an epidemiological review. *Aquaculture*, 457, 35-42.

Paoletti, C., & Esbensen, K. H. (2015). Distributional assumptions in food and feed commodities—development of fit-for-purpose sampling protocols. *Journal of AOAC International*, 98(2), 295-300.

Peter, A., Steinbach, A., Liedl, R., Ptak, T., Michaelis, W., & Teutsch, G. (2004). Assessing microbial degradation of o-xylene at field-scale from the reduction in mass flow rate combined with compound-specific isotope analyses. *Journal of contaminant hydrology*, 71(1-4), 127-154.

Price, M. N., Dehal, P. S., & Arkin, A. P. (2010). FastTree 2–approximately maximum-likelihood trees for large alignments. *PloS one*, 5(3), e9490.

Ranjard, L., Lejon, D. P., Mougel, C., Schehrer, L., Merdinoglu, D., & Chaussod, R. (2003). Sampling strategy in molecular microbial ecology: influence of soil sample size on DNA fingerprinting analysis of fungal and bacterial communities. *Environmental microbiology*, 5(11), 1111-1120.

Reigel, A.M., Owens, S.M. and Hellberg, M.E. (2020). Reducing host DNA contamination in 16S rRNA gene surveys of anthozoan microbiomes using PNA clamps. *Coral Reefs*, 39(6), 1817-1827.

Rodger, H. D., Henry, L., & Mitchell, S. O. (2011). Non-infectious gill disorders of marine salmonid fish. *Reviews in Fish Biology and Fisheries*, 21(3), 423-440.

Rodger, H. D. (2014). Amoebic gill disease (AGD) in farmed salmon (*Salmo salar*) in Europe. *Fish Veterinary Journal*, (14), 16-27.

Rohart, F., Gautier, B., Singh, A., & Lê Cao, K. A. (2017). mixOmics: An R package for 'omics feature selection and multiple data integration. *PLoS computational biology*, 13(11), e1005752.

Rohart, F., Eslami, A., Matigian, N., Bougeard, S., & Le Cao, K. A. (2017). MINT: a multivariate integrative method to identify reproducible molecular signatures across independent experiments and platforms. *BMC bioinformatics*, 18(1), 1-13.

Romero, J., & Navarrete, P. (2006). 16S rDNA-based analysis of dominant bacterial populations associated with early life stages of coho salmon (*Oncorhynchus kisutch*). *Microbial ecology*, 51(4), 422-430.

Rozas-Serri, M. (2019). Gill diseases in marine salmon aquaculture with an emphasis on amoebic gill disease. *Atlantic*, 32(33), 34-35.

Schirmer, M., Ijaz, U. Z., D'Amore, R., Hall, N., Sloan, W. T., & Quince, C. (2015). Insight into biases and sequencing errors for amplicon sequencing with the Illumina MiSeq platform. *Nucleic acids research*, 43(6), e37-e37.

Schmidt, V., Amaral-Zettler, L., Davidson, J., Summerfelt, S., & Good, C. (2016). Influence of fishmeal-free diets on microbial communities in Atlantic salmon (*Salmo salar*) recirculation aquaculture systems. App*lied and Environmental Microbiology*, 82(15), 4470-4481.

Schmieder, R., & Edwards, R. (2011). Fast identification and removal of sequence contamination from genomic and metagenomic datasets. *PloS one*, 6(3), e17288.

Slinger, J., Adams, M. B., & Wynne, J. W. (2020). Bacteriomic profiling of branchial lesions induced by *Neoparamoeba perurans* challenge reveals commensal dysbiosis and an association with *Tenacibaculum dicentrarchi* in AGD-affected Atlantic salmon (*Salmo salar* L.). *Microorganisms*, 8(8), 1189.

Smith, C. J., Danilowicz, B. S., & Meijer, W. G. (2007). Characterization of the bacterial community associated with the surface and mucus layer of whiting (*Merlangius merlangus*). *FEMS microbiology ecology*, 62(1), 90-97.

Stegen, J. C., Lin, X., Konopka, A. E., & Fredrickson, J. K. (2012). Stochastic and deterministic assembly processes in subsurface microbial communities. *The ISME journal*, 6(9), 1653-1664.

Steinum, T., Sjåstad, K., Falk, K., Kvellestad, A., & Colquhoun, D. J. (2009). An RT PCR-DGGE survey of gill-associated bacteria in Norwegian seawater-reared Atlantic salmon suffering proliferative gill inflammation. *Aquaculture*, 293(3-4), 172-179.

Svanevik, C. S., & Lunestad, B. T. (2011). Characterisation of the microbiota of Atlantic mackerel (*Scomber scombrus*). *International Journal of Food Microbiology*, 151(2), 164-170.

Talwar, C., Nagar, S., Lal, R., & Negi, R. K. (2018). Fish gut microbiome: current approaches and future perspectives. *Indian journal of microbiology*, 58(4), 397-414.

Taylor, R. S., Muller, W. J., Cook, M. T., Kube, P. D., & Elliott, N. G. (2009). Gill observations in Atlantic salmon (*Salmo salar*, L.) during repeated amoebic gill disease (AGD) field exposure and survival challenge. *Aquaculture*, 290(1-2), 1-8.

Taylor, M. (2017). sinkr: Collection of functions with emphasis in multivariate data analysis. *R Package Version* 0.6.

Thaler, M., & Lovejoy, C. (2012). Distribution and diversity of a protist predator Cryothecomonas (Cercozoa) in Arctic marine waters. *Journal of Eukaryotic Microbiology*, 59(4), 291-299.

Voreades, N., Kozil, A., & Weir, T. L. (2014). Diet and the development of the human intestinal microbiome. *Frontiers in microbiology*, 5, 494.

Young, N. D., Crosbie, P. B. B., Adams, M. B., Nowak, B. F., & Morrison, R. N. (2007). *Neoparamoeba perurans* n. sp., an agent of amoebic gill disease of Atlantic salmon (*Salmo salar*). *International journal for parasitology*, 37(13), 1469-1481.

3.7 - Supplementary Figures and Tables

Table S3.1. Most Abundant and Relevant OTUs (Operational Taxonomical Units) Description. This table only show the top 25 most abundant OTUs/Genus and the most relevant taxa that appear to consistently being selected in subsets of species explaining the variability in sample space (beta diversity), as well as their OTU identification numbers. The time when the OTU was more abundant is showed in the "Significance" column. The type of sample where the OTU abundance was higher is showed in the "Type of sample" column.

OTU ID	OTU/Genera	Significance	Type of sample	Description
3352	Rubritalea	Present during the whole period, decrease in T4	Gill & Mucous	Was found on salmon, seabram and seabass gills, skin and guts [1, 2, 3], even on some salmon affected by epitheliocystis [1]
4	Albidiferax	Abundance increases during AGD, but seems like freshwater bath treatments reduce its abundance	More abundant in Mucous	This genus appeared very commonly on rainbow trout eggs [4], and associated with biofilms [5]
11	Endozoicomonas	Abundance increases during AGD	More abundant on Gills	First described as a causative agent for epitheliocystis [6], even on Atlantic salmon gills [7, 8]
24	Nitrosomonas	Abundance increases after the AGD, in T4	Gill & Mucous	Was found more often in water samples [9]. But this genus was detected on Atlantic salmon gills in a Epitheliocystis outbreak [10]
9	C. Branchiomonas cysticola	Only found during the AGD outbreak	Gill & Mucous	Very common agent of Epitheliocystis on Atlantic salmon gills [11]. This genus was found associated with "Proliferative Gill Inflammation" (PGI) and "Complex Gill Disease" (CGD) [12]
10	Psychrobacter	Only appeared during the AGD, and abundance increases in T5 and T6	Gill & Mucous	This genus was found on affected and non-affected AGD Atlantic salmon gills [7], gut [13], skin [14], and even kidney [15]
7011	Tenacibaculum maritimum	Mainly present during the AGD outbreak	Gill & Mucous	Is the causative agent of tenacibaculisis, especially at low water temperatures [12]. Was found on skin, gill and salmon fins [16], even in

				freshwater [14]. Another species from the same genus was associated with AGD in a laboratory trial [52]
29	Vibrio	Mostly present during AGD outbreak	Gill & Mucous	*Vibrio* sp. was found to appear on Atlantic salmon epidermal mucous [17] and gastrointestinal microbiome [18]. Also closely associated with *N. perurans*in *in vitro* cultures [51]
20	Piscirickettsia salmonis	Mainly present during the AGD outbreak	Gill & Mucous	It causes Piscirickettsiosis in Atlantic salmon [19], common to find on gills [20]
15	Flavobacterium	Only appeared during the AGD, and abundance increases in T4 and T5	Gill & Mucous	This genus appeared before on Atlantic salmon gills [7], gut [2], and skin [14]
22	Pseudomonas	Present during the whole period	Gill & Mucous	Was present in Atlantic salmon gut [2], gills [7], and even in freshwater salmon skin [14]
17	C. Fritschea	Present during the whole period in low abundance, but abundance increases at T2	Gill & Mucous	Was found to be very close to other gill pathogens in Atlantic salmon [21], such as *Candidatus* Syngnamydia venezia and *Candidatus* Syngnamydia salmonis [22, 23], associated with *Paramoeba perurans*
23	Olleya	Abundance increases at T2 in one of the cages	Gill & Mucous	Typically present in seawater [24], was not related with any Atlantic salmon microbiome before
111	Staphylococcus	Present during the whole period in low abundance, but abundance increases at T2	Gill & Mucous	This genus was found on Atlantic salmon skin [14] and AGD affected gills [7]
12	Alcanivorax	Present during the whole period in low abundance, but abundance increases at T4	More abundant on Gills	Was found in gut microbiome of *Epinepheluscoioides* before and after a probiotic treatment with *Psychrobacter*[25]. Was detected in marine sediments [26]
477	Winogradskyella	In low abundance during the AGD outbreak, maximum at T6	Gill & Mucous	This genus was suggested to enhance the severity of the AGD [27], but a further study discarded the idea of that connection [28]
105	Shewanella	Present during the whole period in low abun-	Gill & Mucous	This genus was found in Atlantic cod intestine [29], and in other fish skin and

		dance, but abundance increases at T2 and T6		gill microbiome studies [30, 31]
1011	Delftia	Present in low abundance during the AGD outbreak, maximum at T6	Gill & Mucous	Was found in the Atlantic salmon intestine, and skin microbiome [32]
35	Pelomonas	Present in low abundance during the AGD outbreak, maximum at T6	Gill & Mucous	This genus is part of the proposed core microbiome in intestine of fish [33, 34], being present in the *Gambusia affinis* skin microbiome [35]
1970	Pedobacter	Present in low abundance during the AGD outbreak, maximum at T2	Gill & Mucous	This genus appears in the gut microbiome of some tropical fish [34] with *Bacillus* and *Vibrio* species too
72	Synechococcus	Present in low abundance in the AGD, maximum at T6	Gill & Mucous	This genus was found in Atlantic mackerel gills [30], and in Chinook salmon gut microbiome [36]
54	Marinobacter	Present during the whole period	Gill &Mucous	This genus was detected in AGD affected and non-affected Atlantic salmon gills [7]. In another study [37], was associated with *Paramoeba perurans* cultures
268	Lactobacillus	Significant due to being selected in subsets of species explaining the variability in beta diversity	Gill & Mucous	Is a genus very commonly present with high abundance in skin [33] and gut [38] microbiome of different fish
145	Turicibacter	Significant due to being selected in subsets of species explaining the variability in beta diversity	Gill & Mucous	Was found in the intestine of different fish [39, 40]
62	Stenotrophomonas	Significant due to being selected in subsets of species explaining the variability in beta diversity	Gill & Mucous	Can be found in Atlantic salmon skin [14] and intestine [41] microbiome
136	Bifidobacterium	Significant due to being selected in subsets of species explaining the variability in beta di-	Gill & Mucous	This bacteria was not related with fish microbiome before, but is commonly used as a potential probiotic for fish [42]

		versity		
347	Allobaculum	Significant due to being selected in subsets of species explaining the variability in beta diversity	Gill & Mucous	Was detected in sediment and water samples in China [43], but could not be found in any fin-fish microbiome study
248	Propionibacterium	Significant due to being selected in subsets of species explaining the variability in beta diversity	Gill & Mucous	Was found before on AGD affected and non-affected Atlantic salmon gills [7]. This genus was detected widely across mucous and tissue samples of Atlantic salmon, seabass, and seabream gut [3, 41]
188	Gardnerella	Significant due to being selected in subsets of species explaining the variability in beta diversity	Gill & Mucous	Could not be found in any fish microbiome study
3156	Illumatobacter	Significant due to being selected in subsets of species explaining the variability in beta diversity	Gill & Mucous	This uncultured actinobacteria was found in coastal and oceanic sediments [44], and in a wide range of marine organisms [45]
305	Altererythrobacter	Significant due to being selected in subsets of species explaining the variability in beta diversity	Gill &Mucous	This genus was found in Atlantic salmon gut microbiome after a fermented soybean meal diet [46]
1802	Dyadobacter	Significant due to being selected in subsets of species explaining the variability in beta diversity	Gill & Mucous	This genus was found on the surface of Lake Sturgeon eggs after an iodine disinfection treatment [47]
1344	Rhodobacter	Significant of being in subsets of species explaining the variability in beta diversity	Gill & Mucous	Are abundant in fresh and seawater samples and in intestine, skin, and gills from Atlantic salmon [2, 7, 14]
3149	Psychroserpens	Significant due to being selected in subsets of species explaining the variability in beta diversity	Gill & Mucous	Was mainly found in AGD affected Atlantic salmon gills [7], and it was proposed to be an opportunistic pathogen associated with AGD.

522	Salinimonas	Significant due to being selected in subsets of species explaining the variability in beta diversity	Gill & Mucous	Was previously found in marine sediments [48], but could not be found in any fish microbiome study
754	Burkholderia	Significant due to being selected in subsets of species explaining the variability in beta diversity	Gill & Mucous	This genus was found in healthy gut [2, 41], skin [14], and on gills during a "Proliferative gill inflammation" [8] from Atlantic salmon
807	Dyella	Significant due to being selected in subsets of species explaining the variability in beta diversity	Gill & Mucous	This bacteria was found in the digestive cavity of the jellyfish *Cotylorhiza tuberculata* [49], but could not be found in any fin-fish microbiome study
73	Piscichlamydia	Significant due to being selected in subsets of species explaining the variability in beta diversity	Gill & Mucous	This genus was found to have a positive association with the "Proliferative Gill Inflammation" [8] on Atlantic salmon gills. Was also related with Epitheliocystis [50]

References

1. Soto MG, Vidondo B, Vaughan L, Seth-Smith HM, Nufer L, Segner H, Rubin JF, Schmidt-Posthaus H. The emergence of epitheliocystis in the upper Rhone region: evidence for Chlamydiae in wild and farmed salmonid populations. Archives of microbiology. 2016;198(4):315-24.

2. Wang C, Sun G, Li S, Li X, Liu Y. Intestinal microbiota of healthy and unhealthy Atlantic salmon *Salmo salar* L. in a recirculating aquaculture system. Journal of Oceanology and Limnology. 2018;36(2):414-26.

3. Rosado D, Perez-Losada M, Severino R, Cable J, Xavier R. Characterization of the skin and gill microbiomes of the farmed seabass (*Dicentrarchus labrax*) and seabream (*Sparus aurata*). Aquaculture. 2019;500:57-64.

4. Heikkinen J, Tiirola M, Mustonen SM, Eskelinen P, Navia-Paldanius D, von Wright A. Suppression of *Saprolegnia* infections in rainbow trout (*Oncorhynchus mykiss*) eggs using protective bacteria and ultraviolet irradiation of the hatchery water. Aquaculture research. 2016;47(3):925-39.

5. Lyons PP, Turnbull JF, Dawson KA, Crumlish M. Phylogenetic and functional characterization of the distal intestinal microbiome of rainbow trout *Oncorhynchus mykiss* from both farm and aquarium settings. Journal of Applied Microbiology. 2017;122(2):347-63.ç

6. Mendoza M, Güiza L, Martinez X, Caraballo X, Rojas J, Aranguren LF, Salazar M. A novel agent (*Endozoicomonas elysicola*) responsible for epitheliocystis in cobia *Rachycentrum canadum* larvae. Diseases of aquatic organisms. 2013;106(1):31-7.

7. Bowman JP, Nowak B. Salmonid gill bacteria and their relationship to amoebic gill disease. Journal of Fish Diseases. 2004;27(8):483-92.

8. Steinum T, Sjåstad K, Falk K, Kvellestad A, Colquhoun DJ. An RT PCR-DGGE survey of gill-associated bacteria in Norwegian seawater-reared Atlantic salmon suffering proliferative gill inflammation. Aquaculture. 2009;293(3-4):172-9.

9. Elizondo-Patrone C, Hernández K, Yannicelli B, Olsen LM, Molina V. The response of nitrifying microbial assemblages to ammonium (NH4+) enrichment from salmon farm activities in a northern Chilean Fjord. Estuarine, Coastal and shelf science. 2015;166:131-42.

10. Wiik-Nielsen J, Solheim HT, Steinum TM, Bornø G, Skjelstad HR, Olsen AB, Colquhoun DJ. A novel epitheliocystis associated bacterium in Atlantic salmon.

11. Mitchell SO, Steinum TM, Toenshoff ER, Kvellestad A, Falk K, Horn M, Colquhoun DJ. '*Candidatus* Branchiomonas cysticola'is a common agent of epitheliocysts in seawater-farmed Atlantic salmon *Salmo salar* in Norway and Ireland. Diseases of aquatic organisms. 2013;103(1):35-43.

12. Herrero A, Thompson KD, Ashby A, Rodger HD, Dagleish MP. Complex gill disease: an emerging syndrome in farmed Atlantic salmon (*Salmo salar* L.). Journal of comparative pathology. 2018;163:23-8.

13. Askarian F, Zhou Z, Olsen RE, Sperstad S, Ringø E. Culturable autochthonous gut bacteria in Atlantic salmon (*Salmo salar* L.) fed diets with or without chitin. Characterization by 16S rRNA gene sequencing, ability to produce enzymes and in vitro growth inhibition of four fish pathogens. Aquaculture. 2012;326:1-8.

14. Lokesh J, Kiron V. Transition from freshwater to seawater reshapes the skin-associated microbiota of Atlantic salmon. Scientific reports. 2016;6:19707.

15. McCarthy Ú, Stagg H, Donald K, Garden A, Weir SJ. *Psychrobacter* sp. isolated from the kidney of salmonids at a number of aquaculture sites in Scotland. Bull Eur Assoc Fish Pathol. 2013;33:67-72.

16. Downes JK, Collins EM, Morrissey T, Hickey C, O'Connor I, Rodger HD, MacCarthy E, Palmer R, Ruttledge M, Ruane NM. Confirmation of *Neoparamoeba perurans* on the gills of Atlantic salmon during the earliest outbreaks of amoebic gill disease in Ireland. Bull. Eur. Assoc. Fish Pathol.. 2018;38(1).

17. Llewellyn MS, Leadbeater S, Garcia C, Sylvain FE, Custodio M, Ang KP, Powell F, Carvalho GR, Creer S, Elliot J, Derome N. Parasitism perturbs the mucosal microbiome of Atlantic Salmon. Scientific reports. 2017;7:43465.

18. Zarkasi KZ, Abell GC, Taylor RS, Neuman C, Hatje E, Tamplin ML, Katouli M, Bowman JP. Pyrosequencing-based characterization of gastrointestinal bacteria of Atlantic salmon (*Salmo salar* L.) within a commercial mariculture system. Journal of applied microbiology. 2014;117(1):18-27.

19. Olsen AB, Melby HP, Speilberg L, Evensen Ø, Håstein T. Piscirickettsia salmonis infection in Atlantic salmon *Salmo salar* in Norway--epidemiological, pathological and microbiological findings. Diseases of aquatic organisms. 1997;31(1):35-48.

20. Bustos PA, Young ND, Rozas MA, Bohle HM, Ildefonso RS, Morrison RN, Nowak BF. Amoebic gill disease (AGD) in Atlantic salmon (*Salmo salar*) farmed in Chile. Aquaculture. 2011;310(3-4):281-8.

21. Pawlikowska-Warych M, Deptuła W. Characteristics of chlamydia-like organisms pathogenic to fish. Journal of applied genetics. 2016;57(1):135-41.

22. Nylund S, Steigen A, Karlsbakk E, Plarre H, Andersen L, Karlsen M, Watanabe K, Nylund A. Characterization of '*Candidatus* Syngnamydia salmonis'(Chlamydiales, Simkaniaceae), a bacterium associated with epitheliocystis in Atlantic salmon (*Salmo salar* L.). Archives of microbiology. 2015;197(1):17-25.

23. Nylund A, Pistone D, Trösse C, Blindheim S, Andersen L, Plarre H. Genotyping of Candidatus Syngnamydia salmonis (chlamydiales; Simkaniaceae) co-cultured in *Paramoeba perurans* (amoebozoa; Paramoebidae). Archives of microbiology. 2018;200(6):859-67.

24. Nichols CM, Bowman JP, Guezennec J. *Olleya marilimosa* gen. nov., sp. nov., an exopolysaccharide-producing marine bacterium from the family Flavobacteriaceae, isolated from the Southern Ocean. International journal of systematic and evolutionary microbiology. 2005;55(4):1557-61.

25. Yang HL, Sun YZ, Ma RL, Li JS, Huang KP. Probiotic *Psychrobacter* sp. improved the autochthonous microbial diversity along the gastrointestinal tract of grouper *Epinephelus coioides*. J Aquac Res Development S. 2011;1:001.

26. Liu C, Shao Z. Alcanivorax dieselolei sp. nov., a novel alkane-degrading bacterium isolated from sea water and deep-sea sediment. International Journal of Systematic and Evolutionary Microbiology. 2005;55(3):1181-6.

27. Embar-Gopinath S, Butler R, Nowak B. Influence of salmonid gill bacteria on development and severity of amoebic gill disease. Diseases of aquatic organisms. 2005;67(1-2):55-60.

28. Embar-Gopinath S, Crosbie P, Nowak BF. Concentration effects of *Winogradskyella* sp. on the incidence and severity of amoebic gill disease. Diseases of aquatic organisms. 2006;73(1):43-7.

29. Riiser ES, Haverkamp TH, Borgan Ø, Jakobsen KS, Jentoft S, Star B. A single Vibrionales 16S rRNA oligotype dominates the intestinal microbiome in two geographically separated Atlantic cod populations. Frontiers in Microbiology. 2018;9:1561.

30. Svanevik CS, Lunestad BT. Characterisation of the microbiota of Atlantic mackerel (*Scomber scombrus*). International Journal of Food Microbiology. 2011;151(2):164-70.

31. Brown RM, Wiens GD, Salinas I. Analysis of the gut and gill microbiome of resistant and susceptible lines of rainbow trout (*Oncorhynchus mykiss*). Fish & shellfish immunology. 2019;86:497-506.

32. Udoye C. Analytical challenges and characterization of skin and gut microbiota of Atlantic salmon fry in a commercial smolt production facility (Master's thesis, NTNU).

33. Nikouli E, Meziti A, Antonopoulou E, Mente E, Kormas KA. Gut bacterial communities in geographically distant populations of farmed sea bream (*Sparus aurata*) and sea bass (*Dicentrarchus labrax*). Microorganisms. 2018;6(3):92.

34. Rasheeda MK, Rangamaran VR, Srinivasan S, Ramaiah SK, Gunasekaran R, Jaypal S, Gopal D, Ramalingam K. Comparative profiling of microbial community of three economically important fishes reared in sea cages under tropical offshore environment. Marine genomics. 2017 Aug 1;34:57-65.

35. Carlson JM, Leonard AB, Hyde ER, Petrosino JF, Primm TP. Microbiome disruption and recovery in the fish *Gambusia affinis* following exposure to broad-spectrum antibiotic. Infection and drug resistance. 2017;10:143.

36. Ciric M, Waite D, Draper J, Jones JB. Characterisation of gut microbiota of farmed Chinook salmon using metabarcoding. bioRxiv: The Preprint server for Biology. 2018.

37. Benedicenti, O., Secombes, C.J. and Collins, C., 2019. Effects of temperature on *Paramoeba perurans* growth in culture and the associated microbial community. Parasitology, 146(4), pp.533-542.

38. Hovda MB, Fontanillas R, McGurk C, Obach A, Rosnes JT. Seasonal variations in the intestinal microbiota of farmed Atlantic salmon (*Salmo salar* L.). Aquaculture Research. 2012;43(1):154-9.

39. Tan CK, Natrah I, Suyub IB, Edward MJ, Kaman N, Samsudin AA. Comparative study of gut microbiota in wild and captive Malaysian Mahseer (*Tor tambroides*). MicrobiologyOpen. 2019;8(5):e00734.

40. Tran NT, Zhang J, Xiong F, Wang GT, Li WX, Wu SG. Altered gut microbiota associated with intestinal disease in grass carp (*Ctenopharyngodon idellus*). World Journal of Microbiology and Biotechnology. 2018;34(6):71.

41. Gajardo K, Rodiles A, Kortner TM, Krogdahl Å, Bakke AM, Merrifield DL, Sørum H. A high-resolution map of the gut microbiota in Atlantic salmon (*Salmo salar*): a basis for comparative gut microbial research. Scientific Reports. 2016;6:30893.

42. Tacchi L, Bickerdike R, Douglas A, Secombes CJ, Martin SA. Transcriptomic responses to functional feeds in Atlantic salmon (*Salmo salar*). Fish & shellfish immunology. 2011;31(5):704-15.

43. Hou D, Huang Z, Zeng S, Liu J, Weng S, He J. Comparative analysis of the bacterial community compositions of the shrimp intestine, surrounding water and sediment. Journal of applied microbiology. 2018;125(3):792-9.

44. Liu H, Wang B, Hu X. Sediment bacterial communities are more complex in coastal shallow straits than in oceanic deep straits. Journal of Oceanology and Limnology. 2018;36(5):1643-54.

45. Valliappan K, Sun W, Li Z. Marine actinobacteria associated with marine organisms and their potentials in producing pharmaceutical natural products. Applied microbiology and biotechnology. 2014;98(17):7365-77.

46. Catalán N, Villasante A, Wacyk J, Ramírez C, Romero J. Fermented soybean meal increases lactic acid bacteria in gut microbiota of Atlantic Salmon (*Salmo salar*). Probiotics and antimicrobial proteins. 2018;10(3):566-76.

47. Chalupnicki M, Dittman D, Starliper CE, Iwanowicz DD. Efficacy of iodine for disinfection of lake sturgeon eggs from the St. Lawrence River, New York. North American Journal of Aquaculture. 2015;77(1):82-9.

48. Tuncer I, Bizsel N. Antibiotic resistance and phylogeny of bacterial isolates with biogeochemical analysis from sediments of Eastern Mediterranean Sea in association with environmental parameters. Journal of Clinical & Experimental Immunology. 2016;1(2):15-20.

49. Cortés-Lara S, Urdiain M, Mora-Ruiz M, Prieto L, Rosselló-Móra R. Prokaryotic microbiota in the digestive cavity of the jellyfish *Cotylorhiza tuberculata*. Systematic and applied microbiology. 2015;38(7):494-500.

50. Draghi A, Popov VL, Kahl MM, Stanton JB, Brown CC, Tsongalis GJ, West AB, Frasca S. Characterization of "*Candidatus* Piscichlamydia salmonis"(order Chlamydiales), a chlamydia-like bacterium associated with epitheliocystis in farmed Atlantic salmon (*Salmo salar*). Journal of clinical microbiology. 2004;42(11):5286-97.

51. MacPhail DP, Koppenstein R, Maciver SK, Paley R, Longshaw M, Henriquez FL. Vibrio species are predominantly intracellular within cultures of *Neoparamoeba perurans*, causative agent of Amoebic Gill Disease (AGD). Aquaculture. 2020, 736083.

52. Slinger J, Adams MB, Wynne JW. Bacteriomic profiling of branchial lesions induced by *Neoparamoeba perurans* challenge reveals commensal dysbiosis and an association with *Tenacibaculum dicentrarchi* in AGD-affected Atlantic salmon (*Salmo Salar* L.). Microorganisms. 2020, 8(8), 1189.

Table S3.2. Subset regression to link *N. perurans* to explanatory data.The linear regression was fitted to the form, $Y_i = \beta_0 + \beta_1 X1_i + \beta_2 X2_i + \beta_3 X3_i + \varepsilon_i$, where Y_i is the Log10 (qPCR of *N. perurans*). Using leaps package in the regression model, the subsets of explanatory variables X_i were permuted, and report the top 20 subsets ranked by adjusted R^2. Furthermore, cross-validation for linear regression was performed using CVlm() from R's DAAG package. Ten folds in the function were used whereby data are randomly assigned to the number of folds, each fold is removed, and in turn, the remaining data issued to re-fit the regression model and to predict at the deleted observations. Mean Squared Error (MSE) between cross-validated prediction and the predicted values using all observations is thus reported in the table. Predictors with positive β-coefficients (that are significant) and are causing *N. perurans* to increase are shaded as red, and those with negative β-coefficients (that are significant) and are causing *N. perurans* to decrease are shaded as blue. If the explanatory variable is not selected in the subset regression, the cell is empty. A consistent red or blue pattern (in column) for a predictor frequently selected in a regression model can serve as a clue for its importance. Note that of all the explanatory variables considered, Type (Gill and Mucous) and Time (point1, point2, point3, point4, point5, point6) are categorical variables were internally supplied to the regression model in R as factors. Also, in R when a categorical variable is considered, it is expanded to the number of factors (presence/absence) in that variable each with the iron β-coefficients. If Type:Mucous comes out to be significant and has a positive β-coefficient then it is read as more likely the sample comes from Mucous, more likely it increases *N. perurans*. In subset regression analysis, Type:Gill, Time:point1,Time:point5, and Time:point6 were not selected in any of the models and therefore are dropped from the list below.

Subsets	S1	S2	S3	S4	S5
Adjusted R^2	0.8052	0.8052	0.8052	0.8052	0.8052
MSE (cross-validation)	0.4508	0.4508	0.4508	0.4508	0.4508
Intercept	-402 ($p < 0.001$ ***)	1359 ($p < 0.001$ ***)	1546 ($p < 0.001$ ***)	1577 ($p < 0.001$ ***)	383 ($p < 0.001$ ***)
β - Coefficient					
Weight of the salmon	-0.0001757 ($p = 0.916$)	-0.0001757 ($p = 0.916$)	-0.0001757 ($p = 0.916$)	-0.0001757 ($p = 0.916$)	-0.0001757 ($p = 0.916$)
Length of the salmon	-0.0112 ($p = 0.920$)	-0.01128 ($p = 0.920$)	-0.01128 ($p = 0.920$)	-0.01128 ($p = 0.920$)	-0.01128 ($p = 0.920$)
AGD score (salmon)	0.478 ($p = 0.344$)	0.4783 ($p = 0.344$)	0.4783 ($p = 0.344$)	0.4783 ($p = 0.344$)	0.4783 ($p = 0.344$)
Temp. °C (same day)	-6.185 ($p < 0.001$ ***)	-27.81 ($p < 0.001$ ***)	-27.81 ($p < 0.001$ ***)	-6.555 ($p < 0.001$ ***)	-1.312 ($p = 0.0223$ *)
Sal. ‰ (same day)	9.499 ($p < 0.001$ ***)	-32.03 ($p < 0.001$ ***)	-32.03 ($p < 0.001$ ***)	-15.03 ($p < 0.001$ ***)	-9.455($p < 0.001$ ***)
O2 % (same day)					1.906 ($p < 0.001$ ***)
Clarity (same day)			-31.18 ($p < 0.001$ ***)		
Temp. (prev. month)	13.45 ($p < 0.001$ ***)				
Sal. (prev. month)					
O2 (prev. month)					-2.710 ($p < 0.001$ ***)
Clarity (prev. month)				-172.1 ($p < 0.001$ ***)	
Type:Mucous	2.846 ($p < 0.001$ ***)	2.846 ($p < 0.001$ ***)	2.846 ($p < 0.001$ ***)	2.846 ($p < 0.001$ ***)	2.846 ($p < 0.001$ ***)
Time:point 2	18.58 ($p < 0.001$ ***)	-31.18 ($p < 0.001$ ***)		-56.69 ($p < 0.001$ ***)	-23.73 ($p < 0.001$ ***)
Time:point 3	11.58 ($p < 0.001$ ***)	17.08 ($p < 0.001$ ***)	17.08 ($p < 0.001$ ***)	8.863 ($p < 0.001$ ***)	
Time:point 4		51.01 ($p < 0.001$ ***)	51.01 ($p < 0.001$ ***)		

	S6	S7	S8	S9	S10	S11
	0.8052	0.8052	0.8052	0.8052	0.8052	0.8052
	0.4508	0.4508	0.4508	0.4508	0.4508	0.4508
	195.3 ($p < 0.001$ ***)	-239.6 ($p < 0.001$ ***)	383 ($p < 0.001$ ***)	383 ($p < 0.001$ ***)	383 ($p < 0.001$ ***)	844 ($p < 0.001$ ***)
	-0.0001757 ($p = 0.916$)	-0.0001757 ($p = 0.916$)	-0.0001757 ($p = 0.916$)	-0.0001757 ($p = 0.916$)	-0.0001757 ($p = 0.916$)	-0.0001757 ($p = 0.916$)
	-0.01128 ($p = 0.920$)	-0.01128 ($p = 0.920$)	-0.01128 ($p = 0.920$)	-0.01128 ($p = 0.920$)	-0.01128 ($p = 0.919$)	-0.01128 ($p = 0.920$)
	0.4783 ($p = 0.344$)	0.4783 ($p = 0.344$)	0.4783 ($p = 0.344$)	0.4783 ($p = 0.344$)	0.4783 ($p = 0.343$)	0.4783 ($p = 0.344$)
	1.113 ($p = 0.0146$ *)	2.496 ($p < 0.001$ ***)	-1.312($p = 0.0223$ *)	-1.312 ($p = 0.0223$ *)	-1.312 ($p = 0.0223$ *)	
	1.982 ($p < 0.001$ ***)	-1.772 ($p = 0.006$ **)	-9.455 ($p < 0.001$ ***)	-9.455 ($p < 0.001$ ***)	-9.455 ($p < 0.001$ ***)	
	-0.06139 ($p = 0.621$)	1.786 ($p < 0.001$ ***)	1.906 ($p < 0.001$ ***)	1.906 ($p < 0.001$ ***)	1.906 ($p < 0.001$ ***)	
						5.433 ($p < 0.001$ ***)
	-5.876 ($p < 0.001$ ***)					
	-0.9131 ($p < 0.001$ ***)	-3.309 ($p < 0.001$ ***)	-2.710 ($p < 0.001$ ***)	-2.710 ($p < 0.001$ ***)	-2.710 ($p < 0.001$ ***)	-2.710 ($p < 0.001$ ***)
		6.774 ($p < 0.001$ ***)				-1.545 ($p < 0.001$ ***)
	2.846 ($p < 0.001$ ***)	2.846 ($p < 0.001$ ***)	2.846 ($p < 0.001$ ***)	2.846 ($p < 0.001$ ***)	2.846 ($p < 0.001$ ***)	2.846 ($p < 0.001$ ***)
			-23.73 ($p < 0.001$ ***)	-23.73 ($p < 0.001$ ***)	-23.73 ($p < 0.001$ ***)	-33.98 ($p < 0.001$ ***)
						7.481 ($p < 0.001$ ***)
						-15.37 ($p < 0.001$ ***)

S12	S13	S14	S15	S16	S17
0.807	0.807	0.807	0.807	0.807	0.807
0.4355	0.4355	0.4355	0.4355	0.4355	0.4355
-54.40 (p = 0.014 *)	-184.2 (p < 0.001 ***)	315.8 (p < 0.001 ***)	-440 (p < 0.001 ***)	-499 (p < 0.001 ***)	266 (p < 0.001 ***)
-0.0002916 (p = 0.808)	-0.0002916 (p = 0.808)	-0.0002916 (p = 0.808)	-0.0002916 (p = 0.808)	-0.0002916 (p = 0.808)	-0.0002916 (p = 0.808)
0.485 (p = 0.330)	0.485 (p = 0.330)	0.485 (p = 0.330)	0.485 (p = 0.330)	0.485 (p = 0.330)	0.485 (p = 0.330)
		2.475 (p = 0.0083 **)	14.69 (p < 0.001 ***)	22.20 (p < 0.001 ***)	-5.3 (p < 0.001 ***)
9.207 (p < 0.001 ***)	9.207 (p < 0.001 ***)	-0.3015 (p = 0.0412*)	-1.281 (p < 0.001 ***)	-3.112 (p < 0.001 ***)	1.247 (p < 0.001 ***)
-2.362 (p < 0.001 ***)	-2.362 (p < 0.001 ***)				
	21.63(p < 0.001 ***)				
			7.848 (p < 0.001 ***)		
		-11.99 (p < 0.001 ***)			
					-2.341 (p < 0.001 ***)
2.846 (p < 0.001 ***)	2.845 (p < 0.001 ***)	2.8465 (p < 0.001 ***)	2.845 (p < 0.001 ***)	2.845 (p < 0.001 ***)	2.845 (p < 0.001 ***)
21.63 (p < 0.001 ***)		2.329 (p = 0.2746)	26.60 (p < 0.001 ***)	38.31 (p < 0.001 ***)	-15.59 (p < 0.001 ***)
19.34 (p < 0.001 ***)	19.34 (p < 0.001 ***)	-7.275 (p < 0.001 ***)	15.04 (p < 0.001 ***)	20.09 (p < 0.001 ***)	2.612 (p = 0.0217 *)
12.19 (p < 0.001 ***)	12.19 (p < 0.001 ***)				

S18	0.807	0.4355	685 ($p < 0.001$ ***)	-0.0002916 ($p = 0.808$)		0.485 ($p = 0.330$)		0.91 ($p = 0.311$)	-1.325 ($p < 0.001$ ***)					-98 ($p < 0.001$ ***)	2.845 ($p < 0.001$ ***)	-15.97 ($p < 0.001$ ***)	13.62 ($p < 0.001$ ***)	
S19	0.807	0.4355	-54.40 ($p = 0.014$ *)	-0.0002916 ($p = 0.808$)		0.485 ($p = 0.330$)		9.207 ($p < 0.001$ ***)	-2.362 ($p < 0.001$ ***)						2.845 ($p < 0.001$ ***)	21.63 ($p < 0.001$ ***)	19.34 ($p < 0.001$ ***)	12.19 ($p < 0.001$ ***)
S20	0.807	0.4355	-54.40 ($p = 0.014$ *)	-0.0002916 ($p = 0.808$)		0.485 ($p = 0.330$)		9.207 ($p < 0.001$ ***)	-2.362 ($p < 0.001$ ***)						2.845 ($p < 0.001$ ***)	21.63 ($p < 0.001$ ***)	19.34 ($p < 0.001$ ***)	12.19 ($p < 0.001$ ***)

Table S3.3. Subset analysis of the Microbiome data. Subsets obtained from "BVSTEP" routine. PERMANOVA of these subsets were also performed against sources of variations including Time, Sample Type (where applicable), and qPCR of *N. perurans*. For comparative purposes, PERMANOVA, using the full OTU table, data is also provided to highlight loss in variability with the subsets. Two cases were considered: Gill Longitudinal Analysis (white background) and Gill vs Mucous Cross-sectional Analysis (grey background). For each case, the abundance tables of the resulting subset of OTUs were obtained, normalised (log-relative normalisation), and then correlated (Kendall Correlation) with extrinsic parameters. The resulting p-values were then adjusted for multiple comparisons (Bonferroni-Hochberg procedure) for the OTUs found for the two cases and if significant, the correlation values (R) along with adjusted P-values are provided. The positive and negative correlations of these OTUs are then highlighted in different colours. For Gill vs Mucous Cross-sectional analysis, the correlations were performed separately for Gill and Mucous and together by collating the samples (as Gill + Mucous).

Gill Longitudinal Analysis				
Subset of top 1000 most abundant OTUs		**Correlation with full OTUs table**	**PERMANOVA full OTU table**	
			Time and Sample Type	**Log10(qPCR of *N. perurans*)**
			Time: R^2 = 0.22 (p = 0.001 ***) Type: R^2 = 0.04 (p = 0.001 ***)	R^2 = 0.05 (p = 0.001 ***)
			PERMANOVA subsets	
S1	OTU_268 + OTU_145 + OTU_62 + OTU_154 +OTU_136 + OTU_347 + OTU_353 + OTU_335 + OTU_363	0.922	R^2 = 0.208 (p = 0.001 ***)	R^2 = 0.037 (p = 0.006 **)
S2	OTU_268 + OTU_145 + OTU_62 + OTU_154 + OTU_136 + OTU_148 + OTU_347 + OTU_353 + OTU_335 + OTU_363	0.922	R^2 = 0.231 (p = 0.001 ***)	R^2 = 0.028 (p = 0.015 *)
S3	OTU_268 + OTU_145 + OTU_62 + OTU_154 + OTU_136 + OTU_353 + OTU_188 + OTU_335 + OTU_3156 + OTU_1011	0.922	R^2 = 0.224 (p = 0.001 ***)	R^2 = 0.046 (p = 0.004 **)
S4	OTU_268 + OTU_145 + OTU_62 + OTU_154 + OTU_136 + OTU_347 + OTU_353	0.915	R^2 = 0.224 (p = 0.001 ***)	R^2 = 0.046 (p = 0.009 **)
S5	OTU_268 + OTU_145 + OTU_62 + OTU_154 + OTU_347 + OTU_353	0.909	R^2 = 0.231 (p = 0.001 ***)	R^2 = 0.047 (p = 0.005 **)
S6	OTU_268 + OTU_145 + OTU_62 + OTU_154 + OTU_353	0.900	R^2 = 0.231 (p = 0.001 ***)	R^2 = 0.047 (p = 0.006 **)
S7	OTU_268 + OTU_145 + OTU_62 + OTU_154	0.889	R^2 = 0.231 (p = 0.001 ***)	R^2 = 0.048 (p = 0.008 **)
S8	OTU_268 + OTU_62 + OTU_154	0.873	R^2 = 0.238 (p = 0.001 ***)	R^2 = 0.051 (p = 0.004 **)

S9	OTU_268 + OTU_154	0.832	R^2 = 0.427 (p = 0.93)	R^2 = 0.061 (p = 0.937)
Correlations with environmental factors and fish features				
OTU_268: Lactobacillaceae;Lactobacillus OTU_145: Erysipelotrichaceae;Turicibacter OTU_62: Xanthomonadaceae;Stenotrophomonas OTU_154: Lactobacillaceae;Lactobacillus OTU_136: Bifidobacterium;Bifidobacterium sp. AGR2158 OTU_347: Erysipelotrichaceae;Allobaculum OTU_353: Clostridiaceae1;Clostridiumsensustricto 1 OTU_335: Lactobacillaceae;Lactobacillus OTU_363: Xanthomonada-les;Xanthomonadaceae;Stenotrophomonas OTU_148: Propionibacteriaceae;Propionibacterium			OTU_363: Clarity (previous month): R = -0.292 (Adj.p = 0.013 *) [Gill]	
Gill vs Mucous Cross-sectional Analysis				
Subset of top 1000 most abundant OTUs		**Correlation with full OTUs table**	**PERMANOVA full OTU table**	
			Time and Sample Type	**Log10 (qPCR of *N. perurans*)**
			Time: R^2 = 0.22 (p = 0.001 ***) Type: R^2 = 0.04 (p = 0.001 ***)	R^2 = 0.05 (p = 0.001 ***)
			PERMANOVA Subsets	
S1	OTU_268 + OTU_145 + OTU_62 + OTU_154 + OTU_136 + OTU_148 + OTU_353 + OTU_796 + OTU_188 + OTU_335 + OTU_3156 + OTU_1011	0.914	Time: R^2 = 0.14 (p = 0.001 ***) Type: R^2 = 0.08 (p = 0.001 ***)	R^2 = 0.024 (p = 0.023 *)
S2	OTU_268 + OTU_145 + OTU_62 + OTU_154 +	0.912	Time: R^2 = 0.14 (p = 0.001 ***)	R^2 = 0.029 (p = 0.014 *)

	OTU_136 + OTU_353 + OTU_796 + OTU_188 + OTU_335 + OTU_3156 + OTU_1011		Type: R^2 = 0.09 (p = 0.001 ***)	
S3	OTU_268 + OTU_145 + OTU_62 + OTU_154 + OTU_136 + OTU_353 + OTU_188 + OTU_335 + OTU_3156 + OTU_1011	0.912	Time: R^2 = 0.15 (p = 0.001 ***) Type: R^2 = 0.09 (p = 0.001 ***)	R^2 = 0.030 (p = 0.014 *)
S4	OTU_268 + OTU_145 + OTU_62 + OTU_154 + OTU_136 + OTU_353 + OTU_188 + OTU_335 + OTU_1011	0.903	Time: R^2 = 0.15 (p = 0.001 ***) Type: R^2 = 0.09 (p = 0.001 ***)	R^2 = 0.30 (p = 0.007 **)
S5	OTU_268 + OTU_145 + OTU_62 + OTU_154 + OTU_136 + OTU_353 + OTU_188 + OTU_335	0.896	Time: R^2 = 0.095 (p = 0.002 **) Type: R^2 = 0.089 (p = 0.001 ***)	R^2 = 0.032 (p = 0.011 *)
S6	OTU_268 + OTU_145 + OTU_62 + OTU_154 + OTU_136 + OTU_353 + OTU_188	0.883	Time: R^2 = 0.094 (p = 0.001 ***) Type: R^2 = 0.089 (p = 0.001 ***)	R^2 = 0.032 (p = 0.014 *)
S7	OTU_268 + OTU_62 + OTU_154 + OTU_136 + OTU_353 + OTU_188	0.865	Time: R^2 = 0.097 (p = 0.001 ***) Type: R^2 = 0.089 (p = 0.001 ***)	R^2 = 0.033 (p = 0.011 *)
S8	OTU_268 + OTU_62 + OTU_136 + OTU_353 + OTU_188	0.848	Time: R^2 = 0.100 (p = 0.001 ***) Type: R^2 = 0.090 (p = 0.001 ***)	R^2 = 0.35 (p = 0.006 **)
S9	OTU_268 + OTU_62 + OTU_136 + OTU_188	0.825	Time: R^2 = 0.100 (p = 0.001 ***) Type: R^2 = 0.090 (p = 0.001 ***)	R^2 = 0.035 (p = 0.012 *)
S10	OTU_268 + OTU_136 + OTU_188	0.770	Time: R^2 = 0.134 (p = 0.076) Type: R^2 = 0.048 (p = 0.064)	R^2 = 0.050 (p = 0.072)
S11	OTU_268 + OTU_62 + OTU_188	0.763	Time: R^2 = 0.106 (p = 0.001 ***) Type: R^2 = 0.090 (p = 0.001 ***)	R^2 = 0.038 (p = 0.004 **)
S12	OTU_268 + OTU_62	0.702	Time: R^2 = 0.090 (p = 0.003 **)	R^2 = 0.041 (p = 0.008 **)

			Type: R^2 = 0.114 (p = 0.001 ***)	
Correlations with environmental factors and fish features				
OTU_268: Lactobacillaceae;Lactobacillus OTU_145: Erysipelotrichaceae;Turicibacter OTU_62: Xanthomonadaceae;Stenotrophomonas OTU_154: Lactobacillaceae;Lactobacillus OTU_136: Bifidobacterium;Bifidobacterium sp. AGR2158 OTU_148: Propionibacteria-ceae;Propionibacterium OTU_353: Clostridiaceae1;Clostridiumsensustricto 1 OTU_796: Lactobacillaceae;Lactobacillus OTU_188: Bifidobacteriaceae;Gardnerella OTU_335: Lactobacillaceae;Lactobacillus OTU_3156: Acidimicrobiaceae;Illumatobacter OTU_1011: Comamonadaceae;Delftia	OTU_148: Temperature (previous month): R = 0.288 (Adj.p = 0.004 **) [Gill] OTU_188: Temperature (previous month): R = 0.50 (Adj.p<0.001 ***) [Gill] OTU_188: Salinity (previous month): R = -0.459 (Adj.p<0.001 ***) [Gill] OTU_188: Temperature (previous month): R = 0.50 (Adj.p<0.001 ***) [Gill+Mucous] OTU_188: Salinity (previous month): R = -0.459 (Adj.p<0.001 ***) [Gill+Mucous] OTU_188: Temperature (same day): R = 0.484 (Adj.p<0.001 ***) [Gill] OTU_188: Clarity (same day): R = -0.319 (Adj.p = 0.033 *) [Gill] OTU_188: Temperature (same day): R = 0.379 (Adj.p<0.001 ***) [Gill+Mucous] OTU_188: Clarity (same day): R = -0.295 (Adj.p = 0.016 *) [Gill+Mucous] OTU_188: AGD score of the fish: R = 0.297(Adj.p = 0.037 *) [Gill] OTU_188: Weight of the fish: R = -0.240 (Adj.p = 0.018 *) [Gill+Mucous] OTU_188: AGD score of the fish: R = 0.268 (Adj.p = 0.015 *) [Gill+Mucous] OTU_3156: Oxygen Levels (previous month): R = -0.295 (Adj.p = 0.019 *) [Gill] OTU_3156: Oxygen Levels (previous month): R = -0.242 (Adj.p = 0.032 *) [Gill+Mucous] OTU_3156: Temperature (same day): R = -0.227 (Adj.p = 0.036 *) [Gill+Mucous] OTU_3156: Oxygen Levels (same day): R = -0.267 (Adj.p = 0.025 *) [Gill+Mucous] OTU_3156: Temperature (same day): R = -0.270 (Adj.p = 0.027 *) [Gill] OTU_1011: Temperature (previous month): R = 0.626 (Adj.p<0.001 ***) [Gill] OTU_1011: Salinity (previous month): R = -0.396 (Adj.p<0.001 ***) [Gill] OTU_1011: Oxygen Levels (previous month): R = 0.255 (Adj.p = 0.019 *) [Gill] OTU_1011: Temperature (previous month): R = 0.395 (Adj.p<0.001 ***) [Gill+Mucous] OTU_1011: Salinity (previous month): R = -0.310 (Adj.p<0.001 ***) [Gill+Mucous] OTU_1011: Oxygen Levels (previous month): R = 0.257 (Adj.p = 0.006 **) [Gill+Mucous] OTU_1011: Temperature (same day): R = 0.419 (Adj.p<0.001 ***) [Gill+Mucous] OTU_1011: Temperature (same day): R = 0.568 (Adj.p<0.001 ***) [Gill]			

1
2
3
4
5
6

CHAPTER 4

Geographical impact on gill microbiome from farmed Atlantic salmon along the western Irish coast and its connection with Amoebic Gill Disease

4.1 - Introduction

Amoebic Gill Disease (AGD) is an infectious gill pathology affecting various fish, including salmonids (Oldham *et al.*, 2016), Ballan wrasse (*Labrus bergylta*) (Karlsbakk *et al*., 2013), lumpfish (*Cyclopterus lumpus*) (Haugland *et al.*, 2017) and rainbow trout (*Oncorhynchus mykiss*) (Munday *et al*., 2001). While AGD infected fish experience lethargy and respiratory distress (Munday *et al*., 2001; Kube *et al*., 2012; Oldham *et al*., 2016) white gill patches provide the clearest symptom (Munday *et al*., 2001; Oldham *et al*., 2016; Marcos-López *et al.*, 2017) and are widely used to track the severity of AGD episodes evaluated as an AGD gill score (Taylor *et al.*, 2009). Gene assays targeting the first aetiological agent of AGD, the free-living amoeba *Neoparamoeba perurans* (Young *et al*., 2007; Young *et al*., 2008), detect and track AGD using DNA samples from water or biological tissues (i.e. gill or skin) (Young *et al*., 2007; Downes *et al.*, 2015). Once AGD is confirmed based on histological inspection or genetic approaches, the most common treatment is to use freshwater baths for the infected fish (Munday *et al*., 2001; Oldham *et al*., 2016), as *N. perurans* is susceptible to low salinity.

AGD has become a major concern for salmonid fish farms (Rodger, 2014; English *et al.*, 2019; Robledo *et al.*, 2020) as typical AGD outbreaks cause salmon mortalities ranging from 10 to 20% of the stock, but losses of up to 80% were reported in Scotland, Norway and Ireland (Shinn *et al.*, 2015). Seasonal variations, showing more AGD episodes during summer (Oldham *et al.*, 2016) and in relatively warm waters (Oldham *et al.*, 2016; Boerlage *et al.* 2020) are observed, in addition, the frequency of AGD outbreaks seems to differ between salmon-producing regions (Oldham *et al.*, 2016). This variation may be explained by multiple, combined factors, such as variations in the intrinsic resistance of salmon populations to the parasite (Vincent *et al.*, 2006; Taylor *et al*., 2007; Wynne *et al.*, 2007; Kube *et al*., 2012), the availability of effective AGD treatments, the stocking density of fish farms (Crosbie *et al*., 2010), or, importantly, environmental conditions like temperature and salinity (Douglas-Helders *et al.*, 2001; Oldham *et al.*, 2016; Boerlage *et al.* 2020). The physico-chemical and microbiological parameters characterising certain locations likely influence *N. perurans* colonisation of fish gills. Therefore, the success of AGD mitigation strategies will at least partly depend on localised fish farm conditions.

Conventional techniques used to diagnose AGD, including AGD gill scoring and quantitative PCR assays, do not facilitate prevention of the disease since they rely on observable symptoms

(Taylor *et al.*, 2009) or high *N. perurans* concentrations (Young *et al*., 2007; Downes *et al.*, 2015), respectively. We previously found that the gill microbiome of farmed salmon was influenced by AGD episodes at a fish farm on the western Irish coast (Chapter 3 of the present thesis, manuscript submitted (Birlanga *et al*., 2021)). We hypothesised that the gill microbiomes of Atlantic salmon from disparate fish farms would correlate significantly, though distinctly, with AGD development. Our objective in the present study was to characterise the prokaryotic microbiome on gills from farmed Atlantic salmon (*Salmo salar* L.) at six disparate fish farms over the course of AGD episodes, also including AGD gill scores, fish features, *N. perurans* gill concentrations, major environmental variables, and historical microbiome data from one year before were also tracked.

4.2 - Materials and methods

4.2.1 - Atlantic salmon gill sampling and environmental data collection

Six fish farms along the western coast of Ireland were sampled from June to December 2018 (**Fig. 4.1a, b**) divided into five rounds (R1 to R5). One sampling timepoint from each fish farm was included in each sampling round. The fish farm in Roancarrig could not be sampled until November, owing to the absence of fish until that month.

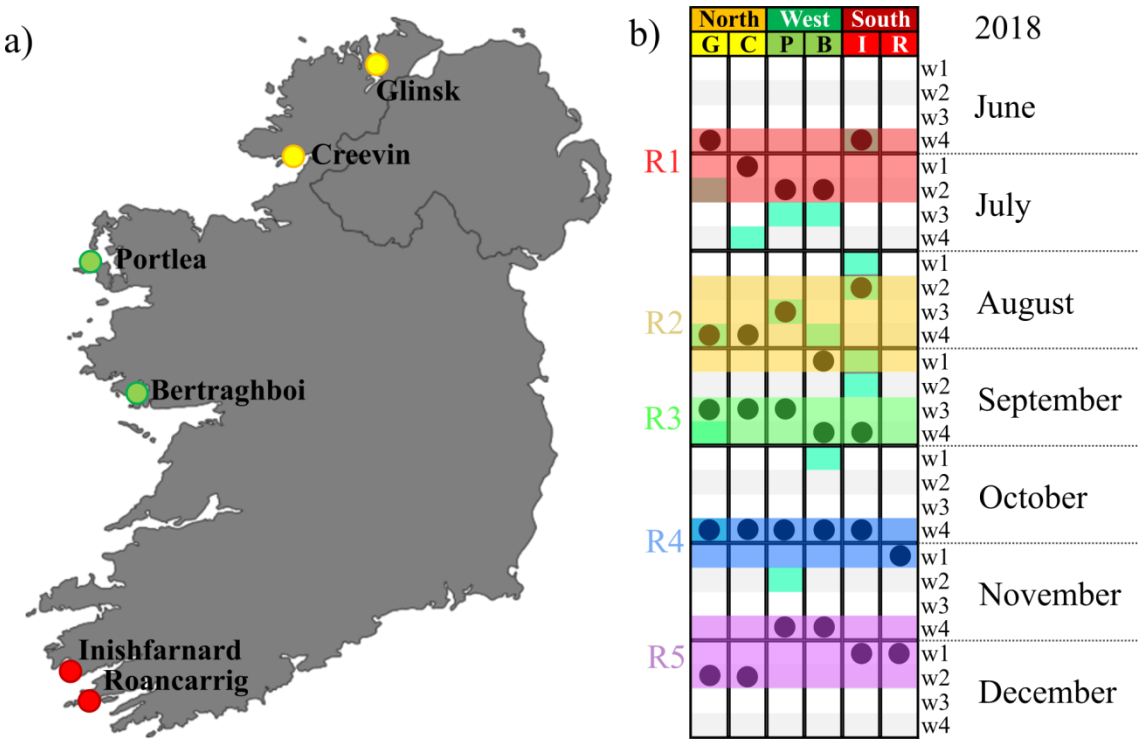

Figure 4.1. a) Location along the western Irish coast of the fish farms sampled, including those in the north: Glinsk (G) and Creevin (C); mid-west: Portlea (P) and Bertraghboi (B); and south: Inishfarnard (I) and Roancarrig (R). **b)** Sampling time points and freshwater treatments at each of the fish farms (G, C, P, B, I, R). Each of the sampling points of every fish farm is represented by a dot at the corresponding week. Turquoise cells represent weeks when the fish farm applied freshwater treatments.

At each farm and sampling round, five Atlantic salmon (*Salmo salar* L.) were sampled from each fish farm from one randomly selected fish cage. All fish were dispatched with an over-dose of anaesthetic (Tricaine Methanosulfonate MS-222, 200 mg/L). Weight (g), length (cm) and AGD gill score (Taylor *et al.*, 2009) were recorded. Each operculum was removed, and the second brachial arch was then excised using sterile scissors and forceps, placed in sterile labelled tubes, and frozen on dry ice.

Environmental data from each fish farm were collected including, water temperature (ºC), salinity (‰), oxygen (%), and turbidity (Secchi depth, metres) were measured daily at a depth of 5 meters near cages using a Conductivity-Temperature-Depth (CTD) measuring device (YSI 2030 device; ID: 12391).

4.2.2 - DNA recovery from salmon gills

Genomic DNA the microbial community on salmon gills was extracted using the DNA extraction protocol from (Chapter 3 of the present thesis, manuscript submitted (Birlanga *et al*., 2021)). This procedure included consecutive multiple washes of individual gill with 0.5% trypsin [w/v] in 6.8 mM EDTA (Sigma-Aldrich, Saint Louis, USA), followed by DNA precipitation from the pooled washes, and a DNA isolation step using a commercial DNA and RNA purification kit (Allprep DNA/RNA extraction QIAGEN kit, Hilden, Germany). The double-stranded DNA concentrations from each extraction were determined using a Qubit dsDNA BR Assay Kit (ThermoFisher Scientific, Paisley, UK), following manufacturer's instructions.

4.2.3 - Sequencing of 16S rRNA genes and quantification of *N. perurans* 18S rRNA genes

To characterise the prokaryotic community, the V4 and ITS-1 regions of 16S rRNA genes were amplified from DNA extractions using the primers 515F (5'-GTGCCAGCMGCCGCGGTAA-3') and 806R (5'-GGACTACHVGGGTWTCTAAT-3') (Caporaso *et al*., 2011; Dittmann *et al*., 2019; Dittmann *et al*., 2020). The first PCR (25 µl final volume) contained: 12.5 ng of genomic DNA, a final concentration of 0.2 µM of each of the primers (515F and 806R), and a final concentration of 12.5 µM 2X KAPA HiFi Hot Start Ready Mix (0.25 U; Roche). The PCR cycles were as follows: denaturation at 95ºC for 3 min; 25 cycles of 95ºC for 30 s, 55ºC for 30 s and 72ºC for 30 s; and final elongation for 72ºC for 5 min. PCR products were then purified (AMPure XP for PCR Purification, Beckman Coulter, USA) following manufacturer's instructions. Illumina sequencing adapters were added to the clean PCR products, along with specific indices using a NextEra XT Index Kit (Cambridge, United Kingdom) according to manufacture instructions. PCR products with adapters and indices were purified a second time following the same protocol, prior to DNA quantification using a 2100 Bioanalyzer system (Agilent Technologies). The DNA concentration was normalised (to 4 nM), after libraries with unique indices were pooled. The pooled libraries were denatured (0.2 N NaOH), diluted and denatured by a heat shock before sequencing. Sequencing was using an Illumina MiSeq platform (Caporaso *et al.*, 2012) 5% PhiXas as internal control, as recommended by Illumina.

In addition, to track the abundance of the *N. perurans* on salmon gills, a specific region of the 18S rRNA gene was targeted in quantitative PCR assays. The concentration in DNA samples was determined using primers 'NP1' (5'-AAAAGACCATGCGATTCGTAAAGT-3') and 'NP2'

(5'-CATTCTTTTCGGAGAGTGGAAATT-3'), and the 'NPP' probe (6-FAM-ATCATGATTCACCATATGTT-MGB) (Downes *et al.*, 2015). Each reaction (25 µl) had 25 ng of genomic DNA, 12.5 µl TaqMan® Universal 2 Master Mix (Applied Biosystems), and final concentrations of 300 nM primer NP1, 900 nM primer NP2 and 200 nM probe NPP. The qPCR program comprised of initial denaturation at 95ºC for 15 min, and 45 cycles of 95°C for 15 s and 56°C for 30 s, in a real-time PCR thermocycler (Applied Biosystems AB7500). As a control measurement, positive controls, negative controls, and internal and external process controls, were also included in each of the runs. The conditions of the parameters in the qPCR were arranged as established by Downs *et al.* (2015) (Downes *et al.*, 2015).

4.2.4 - Year-on-year data at the Bertraghboi Bay site

A previous sampling campaign, one year previous, at the Bertraghboi Bay fish farm ('B' in **Fig. 4.1**) was divided across six different timepoints (T1 in June through T6 in October). The sampling and analyses were described by Birlanga *et al*. (Chapter 3 of the present thesis, manuscript submitted (Birlanga *et al*., 2021)). Those data were integrated to some of the analysis in this study to allow comparisons at the Bertraghboi Bay site over both years.

4.2.5 - Bioinformatics on the microbiome data

The software VSEARCH v2.3.4 (steps documented in http://github.com/torognes/vsearch/wiki/VSEARCH-pipeline) was used to generate the abundance table by constructing operational taxonomic units (OTUs), a proxy for species. Prior to using VSEARCH, the paired-end reads were preprocessed according to the recommendations given in author's recent publications (Schirmer *et al*., 2015; D'Amore *et al.*, 2016) which results in significant reduction of substitution errors. Briefly, the paired-end reads were trimmed and filtered using Sickle v1.200 (Joshi & Fass) by using a sliding window approach and trimming the reads where the average base quality drops below 20. Only the reads that were above 10 bp length were kept after trimming. Next, BayesHammer (Nikolenko *et al*., 2013) was used from the Spades v2.5.0 assembler, which error-corrected the paired-end reads. Following this, pandaseqv(2.4) (Masella *et al*., 2012) was used to assemble the forward and reverse reads into a single sequence spanning the entire V4 region with a minimum overlap of 10 bp. The preprocessed reads (overlapped) from each sample were pooled together while barcodes were added to keep track of which sample the read originated from. The reads were then dereplicated,

sorted in order of decreasing abundance and singletons were discarded. Next, reads were clustered based on 97% similarity followed by a removal of clusters which had chimeric models built from more abundant reads (--uchime_denovo option in vsearch). To remove any chimeras that may have been missed, particularly in the case that they had parents that were absent from the reads or were present in very low abundance, a reference-based chimera filtering step (--uchime_ref option in vsearch) using a gold database (https://www.mothur.org/w/images/f/f1/Silva.gold.bacteria.zip) was applied. Finally, the OTU table was generated by matching the original barcoded reads against clean OTUs (a total of 20,299 OTUs for n=244 samples) at 97% similarity (a proxy for species-level separation). Having obtained the OTUs, we then used DeConseq (Schmieder & Edwards, 2011) to identify OTUs that were contaminants, hitting on *Salmo salar* reference genome. This step identified 12,220 OTUs as contaminants bringing the total OTUs down to 8,079 OTUs. The summary read statistics for n=244 samples are as follows: [1st Quantile: 20,302, Median: 70,980, Mean: 77,039, 3rd Quantile: 117,192, Max: 326, 452].

The Qiime2 workflow (Bolyen *et al*., 2019) was employed to import the abundance table as well OTU sequences. Within the workflow, we have used qiime feature-classifier to classify the OTUs against SILVA SSU Ref NR database release v132, and then used qiime phylogeny align-to-tree-mafft-fast tree to generate the rooted phylogenetic tree. The biom file for the OTUs was then generated by combining the abundance table with taxonomy information using biom utility available in qiime2 workflow.

For ensuing statistical analysis, any sample was dropped with total reads <5000, excluding further contaminants based on taxonomy (Chloroplast, Microchondria, and OTUs unassigned at Phylum level) and that resulted in a 210 (samples) X 6,786 (OTUs) abundance table.

4.2.6 - Statistical analyses

Statistical analyses were performed in R using the combined data generated from the bioinformatics as well as meta data associated with the study (environmental factors, fish features, and qPCR results). The vegan package (Oksanen *et al.*, 2007) was used for alpha and beta diversity analyses. For alpha diversity measures we have used: Shannon entropy – a commonly used index to measure balance within a community, and rarefied richness (exponential of Shannon entropy) – the estimated number of species, and both indices after

rarefying the abundance table to minimum library size. Ordination of OTU table in reduced space (beta diversity) was done using Principal Coordinate Analysis (PCoA) plots of OTUs using three different distance measures were made using Vegan's cmdscale() function: (1) Bray-Curtis is a distance metric which considers only OTU abundance counts, (2) Unweighted Unifrac is a phylogenetic distance metric which calculates the distance between samples by taking the proportion of the sum of unshared branch lengths in the sum of all the branch lengths of the phylogenetic tree for the OTUs observed in two samples, and without taking into account their abundances and, (3) Weighted Unifrac is a phylogenetic distance metric combining phylogenetic distance with relative abundances. This places emphasis on dominant OTUs or taxa. Unifrac distances were calculated using the phyloseq package (McMurdie & Holmes, 2013).

Analysis of variance for explanatory variables (or sources of variation) was performed using Vegan's adonis() against distance matrices (Bray-Curtis/Unweighted UniFrac/Weighted UniFrac). This function, referred to as PERMANOVA, fit linear models to distance matrices and used a permutation test with pseudo-F ratios. To give an account of environmental filtering (phylogenetic overdispersion versus clustering), phylogenetic distances within each sample were further characterised by calculating the nearest taxa index (NTI) and net relatedness index (NRI). This analysis helped determine whether the community structure was stochastic (overdispersion and driven by competition among taxa) or deterministic (clustering and driven by strong environmental pressure). The NTI was calculated using mntd() and ses.mntd(), and the mean phylogenetic diversity (MPD) and NRI were calculated using mpd() and ses.mpd() functions from the picante package (Kembel *et al.*, 2010). NTI and NRI represent the negatives of the output from ses.mntd() and ses.mpd(), respectively. Additionally, they quantify the number of standard deviations that separate the observed values from the mean of the null distribution (999 randomisation using null.model-'richness' in the ses.mntd() and ses.mpd() functions and only considering taxa as either present or absent regardless of their relative abundance). Based upon the recommendations given in Stegen *et al*. (2012), only the top 1000 most abundant OTUs were used for the calculations.

To find genera that are significantly different between different categories (locations or sampling rounds), we used DESeqDataSetFromMatrix() function from DESeq2 (Love *et al*., 2014) package with the adjusted p-value significance cut-off of 0.05 and log2 fold change cut-off of 2. This function uses negative binomial GLM to obtain maximum likelihood estimates for OTUs

log fold change between two conditions. Then Bayesian shrinkage is applied to obtain shrunken log fold changes subsequently employing the Wald test for obtaining significances.

We performed Local Contribution to Beta Diversity (LCBD) analysis (Legendre & De Cáceres, 2013) by using LCBD.comp() from adespatial package (Dray *et al*., 2018). We used the Bray-Curtis (abundances), unweighted (phylogenetic distance) and weighted Unifrac (phylogenetic distance weighted by abundance) dissimilarities. LCBD gives the sample-wise local contributions to beta diversity that could be derived as a proportion of the total beta diversity. The measure provides a mean to show how markedly different the microbial community structure of a single sample is from the average (with higher LCBD values representing outliers).

We performed subset regression against different microbiome metrics by testing all possible combination of the explanatory variables, and then selecting the best model according to some statistical criteria, with recommendations given in Kassambara (2018) and code available at http://www.sthda.com/english/articles/37-model-selection-essentials-in-r/155-best-subsets-regression-essentials-in-r/. The R function regubsets() from leaps (Lumley & Miller, 2009) package was used to identify different best models of different sizes, by specifying the option nvmax, set to the maximum number of predictors to incorporate the model. Having obtained the best possible subsets, the k-fold cross-validation consisted of first dividing the data into k subsets. Each subset (10%) served successively as test data set and the remaining subset (90%) as training data. The average cross-validation error is then computed as the model prediction error. This was all done using a custom function utilising R's train() function from the caret package (Kuhn, 2008). Finally R's tab_model() function from sjPlot package (Lüdecke, 2018) was used to obtain the statistics for each model. For qPCR data, Log10 normalisation was used.

To find the core microbiome, we have used R's microbiome package (Lahti *et al*., 2017) and the prevalence of 85% of OTUs to be tagged as core microbiome, by following recommendations given in Shetty *et al*. (2017).

In majority of the figures displaying boxplots, pair-wise ANOVA was performed taking two categories at a time, and where significant ($p \leq 0.05$), joined them together by a line and plotting significance on top (*: $0.01 \leq p < 0.05$; **: $0.001 \leq p < 0.01$; ***: $p < 0.001$).

The sequencing data is available on the European Nucleotide Archive under the study accession number: PRJEB32307 (http://www.ebi.ac.uk/ena/data/view/PRJEB32307) with the details given in "supplementary_data_information.xls" for the 2017 data. And under the accession number: number (link) with the details given in "file" for the 2018 data.

4.3 - Results

4.3.1 Environmental conditions, AGD gill scores and qPCR results

The water temperature profiles indicated a gradual decrease from southern to northern fish farms at the beginning and at the end of the year. Water cooling appeared to be slower than warming, resulting in higher average temperatures in January than in December (**Fig. 4.2**) and extending the period with warm water.

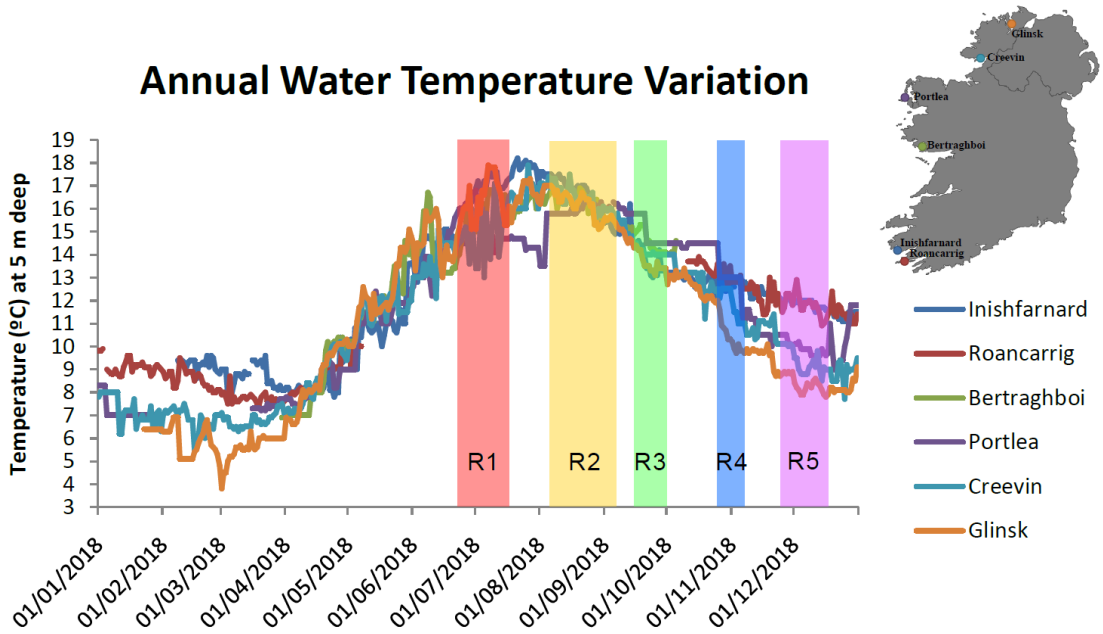

Figure 4.2. Annual Water Temperature Variation (Degrees Celsius) at 5 meters depth from each fish farm location through 2018 (Ireland). Labels at the Y axis show the first day of each month (dd/mm/yyyy). A different coloured strip represents each of the sampling rounds (R1, R2, R3, R4 and R5). A map of the Republic of Ireland with the location of every fish farm is shown to help understanding the figure.

Similar AGD gill scores and *N. perurans* trends were apparent at each of the locations during the sampling campaign (**Fig. 4.3**), but the magnitudes differed with location (**Fig. S4.1**). However,

unlike in the rest of the sites, salmon from Inishfarnard had high AGD gill scores and abundant *N. perurans* at the last sampling round (**Fig. 4.3**).

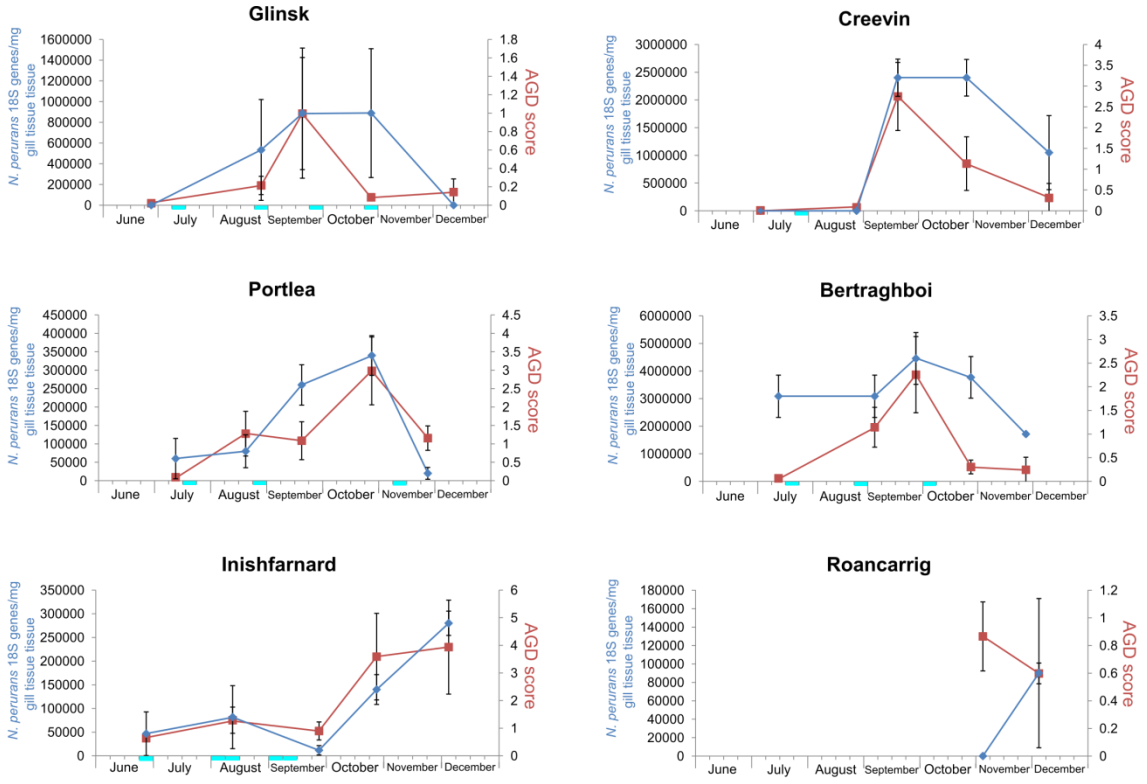

Figure 4.3. Development of the *N. perurans* abundance (*N. perurans* 18S genes / mg of gill tissue; blue line) and AGD gill scores (red line) on gills from each of the Irish fish farms during the sampling campaign (divided in 4 parts in each month, one per week). Weeks highlighted in blue at the Y axis represent the week when the fish farm treated their salmon with freshwater baths. The fish farm placed in **Roancarrig** could not be sampled until November, due to the lack of salmon in the facility.

N. perurans abundance on gill samples from Glinsk (at R1) and Creevin (at R1 and R2) was very low, and those fish did not show any AGD symptoms (AGD gill score 0) during those sampling rounds. Therefore, it was possible to categorise gills from salmon sampled before and during an AGD episode in Glinsk and Creevin (**Fig. 4.3**).

4.3.2 - Prokaryotic diversity and environmental impact on gill microbiome

Salmon reads were removed from the dataset, revealing a diverse gill prokaryotic microbiome (**Fig. S4.2**), with significant geographical differences (**Table S4.2**). In addition, differences were observed in alpha-diversity analysis, resulting in a gradually decreasing richness and Shannon entropy values from northern to southern fish farms at R2 and R3 (**Fig. 4.4**). In terms of temporal variation, alpha-diversity and environmental filtering (NTI and NRI) analysis significantly increased at R2, prior to significant reductions at R3 and a relative stable period at R4 and R5 (**Fig. 4.4**).

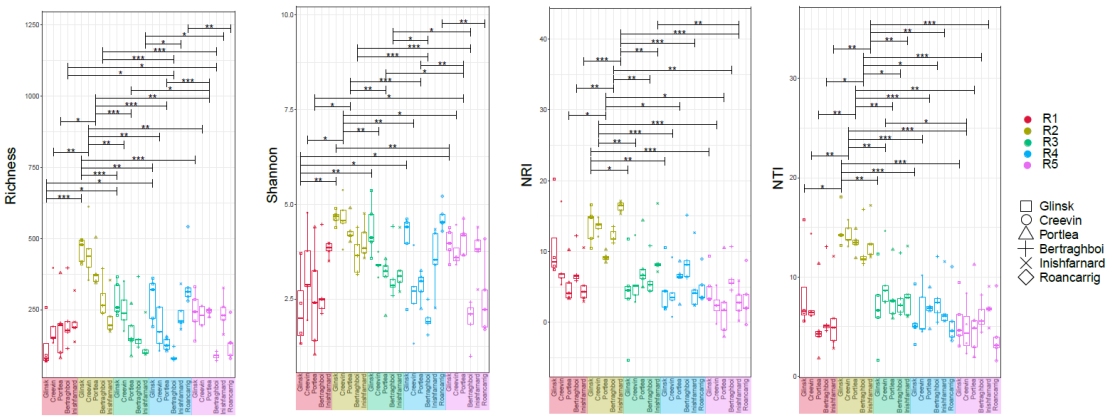

Figure 4.4. Prokaryotic alpha-diversity (Richness and Shannon Entropy) and environmental filtering (NRI and NTI) analyses from salmon gills from every fish farm in each sampling round (R1, R2, R3, R4 and R5). Fish farms are organised from the most northern locations on the left, to the most southern locations on the right in each of the sampling rounds (Glinsk, Creevin, Portlea, Bertraghboi, Inishfarnard and Roancarrig). Lines between points that connect two categories where the differences were significant (ANOVA) with * ($p < 0.05$), ** ($p < 0.01$), or *** ($p < 0.001$).

Beta-diversity analyses showed that samples from R2 clustered together, apart from the other sampling rounds (**Fig. 4.5**). Location and time were significant driving factors in the prokaryotic microbiome (**Fig. 4.5**), even when each sampling round and location was analysed separately (**Fig. S4.3, S4.4 and S4.5)**.

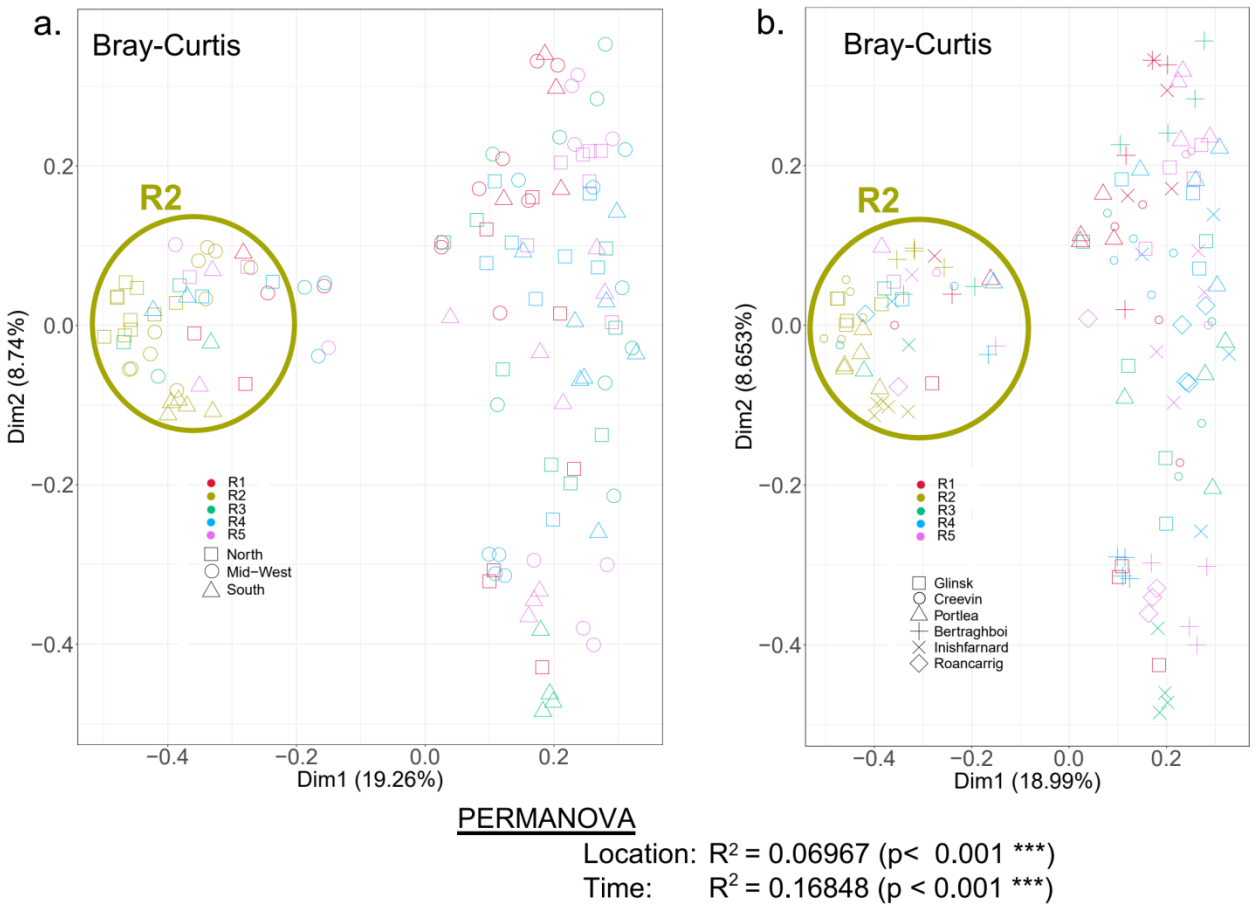

Figure 4.5. a. Prokaryotic beta diversity (based on the Bray-Curtis distance algorithm) grouping fish farms by their location on the Irish West coast (**Fig. 4.1**). Each of the points represents a group of fish farms from the North, Mid-West or the South on a specific sampling round. **b.** Prokaryotic beta diversity (based on the Bray-Curtis distance algorithm) keeping separated each fish farm. Each of the points represents a fish farm on a specific sampling round. Notice that all samples from R2 clustered separately from the rest of the sampling rounds in **a)** and **b)** (all R2 samples surrounded by a yellow circle). The influence of the time and the location was determined by PERMANOVA analyses with * ($p < 0.05$), ** ($p < 0.01$), or *** ($p < 0.001$).

4.3.3 - Gill microbiomes before and during AGD

Samples from Glinsk and Creevin included both before-AGD infection and after-AGD infection gills, making these two locations suitable for a prokaryotic microbiome comparison between before and during AGD. Alpha-diversity analyses showed that gills from Glinsk and Creevin followed the same trend as samples from the rest of the fish farms (**Fig. 4.4**). Gill samples from Glinsk presented richness and Shannon entropy values that significantly increased at R2, when the AGD episode had already started (AGD gill score and *N. perurans* abundance increased (**Fig.**

4.3). The richness and Shannon entropy values of gill microbiomes from Creevin also increased significantly at R2 (**Fig. 4.4**), but salmon from this sampling round were still not infected with AGD (**Fig. 4.3**). Once fish at Creevin were infected by R3, the alpha-diversity significantly decreased (**Fig. 4.4**). Many taxa significantly changed their relative abundance from before to during AGD infected gills from Creevin and Glinsk fish farms, including the genus *Shewanella*, *Endozoicomonas*, *Pseudomonas*, *Rubritalea*, and *Psychromonas* among them.

Fish farms from Creevin and Glinsk had a stable environmental pressure during the sampling campaign (**Fig. 4.4**), except in R2 when NTI and NRI values were significantly higher.

4.3.4 - Regression analyses with the prokaryotic microbiome

These regression analyses were performed including many prokaryotic microbiome features as dependent variables against all recorded possible explanatory variables obtaining many regression models (**Table S4.1**). Some sampling points, especially at R2 and T2, and the location of every fish farm were significant microbiome-driving factors in most of the regression analyses. However, between salmon features (weight and length), only the length of the fish could be correlated with the richness and the LCBD Weighted Unifrac (LCBD WUnifrac) data (**Table S4.1**). It seemed that the two sampling years (year 1 and year 2) did not have a major influence on the prokaryotic microbiome, as they were detected as significant time periods in the best regression models of only two microbiome characteristics (LCBD Bray-Curtis, and LCBD WUnifrac; **Table S4.1**). The environmental pressure (NTI) that influenced the microbial community on gills was correlated with all the measured environmental factors (temperature, salinity, oxygen and clarity in water; **Fig. 4.6, a**). In addition, some sampling rounds (including R2) and one fish farm location (Bertraghboi) were detected as relevant time/space points that explain environmental filtering trends (**Fig. 4.6a**).

On the other hand, regression analyses on NRI data detected the *N. perurans* abundance as a significant factor that influenced the environmental filtering data variability (**Fig. 4.6b**). A couple of sampling points (T2 from year 1, and R2 from year 2) were also picked up to be relevant in this regression model.

The best regression model that fit LCBD Unifrac variability (**Fig. 4.6c**) included not only different sampling points in year 1, but also the AGD scoring data as significant factors that

impacted the beta-diversity of the prokaryotic microbiome on farmed Atlantic salmon gills.

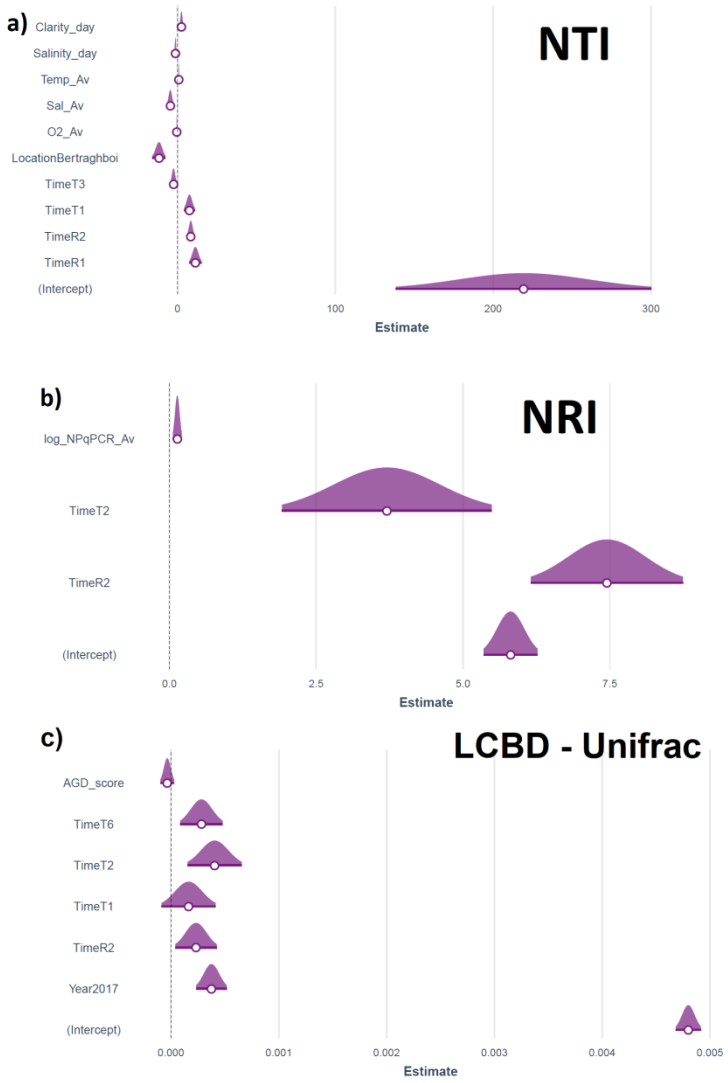

Figure 4.6. Part of the entire subset regression analyses with microbiome characteristic (NTI in **a)**, NRI in **b)**, and LCBD – Unifrac in **c)**). All environmental factors were considered in these analyses (temperature, oxygen, salinity and clarity), also the *N. perurans* abundance data (expressed like "log_NPqPCR_Av"), fish features (weight, length and AGD gill scores), the different fish farm locations and the different sampling rounds. Factors that appear in **a), b)** and **c)** regressions were picked up to be significant influencers in the best regression model. If the picked factor presents a value above zero, that factor has a significant positive correlation with the analysed microbiome characteristic. If the picked factor presents a value below zero, that factor has a significant negative correlation with the analysed microbiome characteristic. For further results related with the subset regression analyses, please consult **Table S4.1**.

4.3.5 - Prokaryotic core microbiome on farmed Atlantic salmon gills

Core microbiome analyses from gills from every sampling round and location revealed that five bacterial taxa were present in, at least, 85% of all samples from year 2 (**Fig. 4.7**). These bacterial taxa were: *Psychrobacter, Pseudomonas, Vibrio, Rubritalea* and the Order Alteromonadales (this Order includes *Shewanella* sp. for example) (**Table S4.2**). In concrete, the genus *Rubritalea* was also found to be part of the core microbiome when data from the year 1 was also included (**Fig. S4.6**). However, in year 2, the prokaryotic core microbiome members in each independent sampling round were different from the others (**Fig. S4.7**), especially at R2. At the second sampling round, there was a very clear increase in the number of prokaryotes in the core microbiome, but this number decreased from R3 until the end of the campaign. Although a clear time-dependent prokaryotic core microbiome was detected (**Fig. S4.7**), it was not possible to find any relevant difference between fish farms when the prokaryotic core microbiome from each of them were analysed (**Fig. S4.8**).

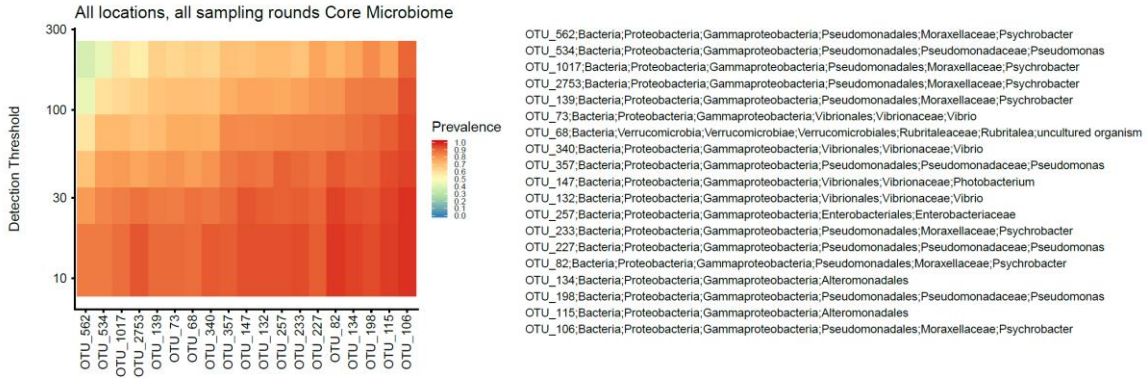

Figure 4.7. Prokaryotic core microbiome on gills from all locations and sampling rounds in the year 1 sampling campaign. To be part of the core microbiome, bacterial taxa must have at least 85% prevalence in all considered samples. Bacteria are arranged from a small relative abundance to a high relative abundance (from left to right), all of them with at least 85% prevalence. Although some prokaryotic taxa are repeated in more than one OTU, they could be considered as the same bacteria species.

4.3.6 - Comparison between the year 1 and the year 2 gill prokaryotic microbiome in Bertraghboi

Richness and Shannon entropy showed very similar profiles between years (**Fig. 4.8**), both significantly increasing their values at T2 (year 1) and R2 (year 2). However, it could be observed that year 2 samples were influenced by a higher environmental pressure (NRI data). On the other hand, T2 from year 1 was also impacted by a high environmental pressure, reaching R2

values (NTI data, **Fig. 4.8**). Although year 2 samples were exposed to a higher environmental pressure, no clear differences in alpha diversity were found between those and year 1 samples.

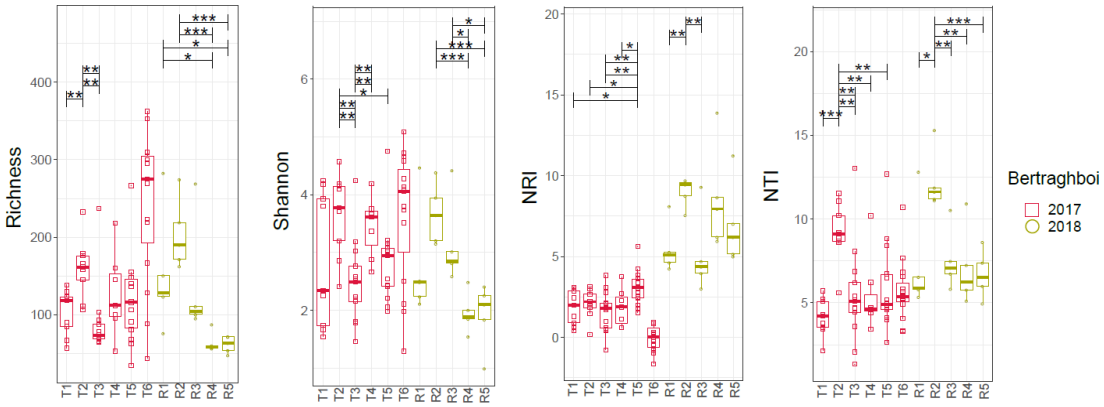

Figure 4.8. Prokaryotic alpha-diversity (Richness and Shannon Entropy) and environmental filtering (NRI and NTI) analyses from Bertraghboi fish farm comparing year 1 (red boxes) with year 2 (yellow boxes) gill samples. The year 1 sampling campaign includes samples from T1 until T6. The year 2 sampling campaign includes samples from R1 until R5. Lines between points that connect two categories where the differences were significant (ANOVA) with * ($p < 0.05$), ** ($p < 0.01$), or *** ($p < 0.001$).

Results from beta-diversity analyses (using the Bray-Curtis algorithm) showed that gill samples from T2 and R2 clustered together, away from the rest of the sampling points (inside the green ellipse in **Fig. 4.9**). PERMANOVA results showed that both possible influencing factors, the year of the sampling period and the sampling points, have a significant impact on the prokaryotic microbiome beta-diversity (**Fig. 4.9**).

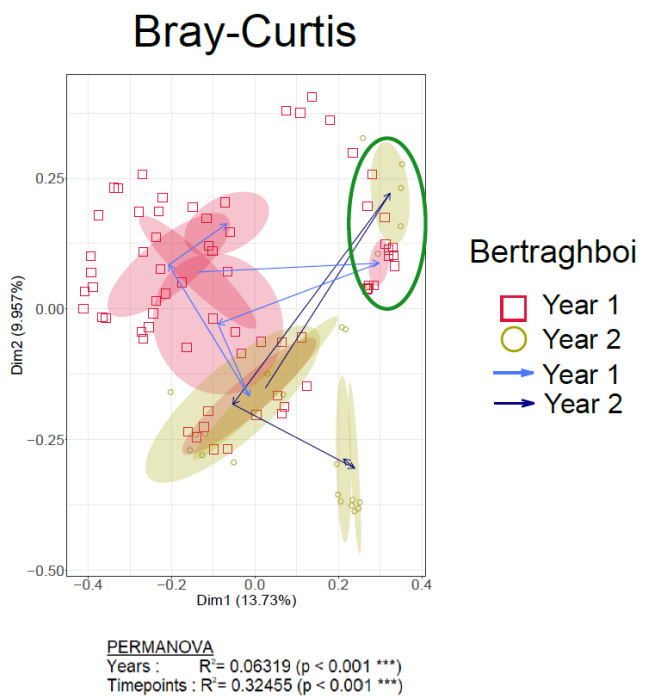

Figure 4.9. Prokaryotic beta-diversity analysis based on the Bray-Curtis distance algorithm comparing year 1 with year 2 gill samples from the Bertraghboi fish farm. Each of the squares and circles represents a gill from a specific sampling point from year 1 (red square) or year 2 (yellow circle). Red ellipses (sampling point of year 1) and yellow ellipses (sampling round of year 2) are drawn at 95% confidence interval of standard error with lines from T1 to T6 and from R1 to R5 plotted at the mean of the ordination values at each sampling point. Notice that gills from T2 and R2 clustered together (in a green ellipse (It was added in using an image editor software)). The possible significant influences of the timepoints and the year of the sampling period were determined by PERMANOVA analyses with * ($p < 0.05$), ** ($p < 0.01$), or *** ($p < 0.001$).

4.4 - Discussion

4.4.1 - Description of the AGD episode

Since the start of the sampling campaign, almost every fish farm presented symptoms of the AGD (AGD gill scores in **Fig. 4.3**) until the end. Therefore, and supported by the *N. perurans* qPCR data (*N. perurans* abundance in **Fig. 4.3**), it was reasonable to determine that most of the sampled fish farms were impacted by the AGD during the entire sampling period. All these results were probably due to the date when this campaign started (end of June 2018). At this time, the microbial community on gills was already exposed to a gradual increase in the water temperature in each location for a couple of months (**Fig. 4.2**). As explained in literature (Rodger & McArdle, 1996; Bustos *et al*., 2011; Oldham *et al*., 2016), severe AGD episodes in salmon

stocks were correlated positively with the water temperature and salinity. In addition, the slower cooling down of the water temperature after the annual maximum (**Fig. 4.2**) extended the period of time with warm waters. Hence, the wide AGD presence in most of the fish farms during the whole sampling campaign was probably due to a combination between the date of the start of the sampling period, and the unusual water temperature profile of year 1. Although AGD is normally considered to have its maximum impact during the warmest season (Rodger & McArdle, 1996; Bustos *et al*., 2011; Oldham *et al*., 2016), previous reports have shown clear symptoms of the disease during the coldest one (Douglas-Helders *et al.*, 2001; Steinum *et al*., 2008; Rodger, 2014). Thus, the high AGD gill scores that salmon from Inishfarnard showed in December (**Fig. S4.1**), at R5, is not unusual.

On the other hand, gill samples from Glinsk and Creevin did not show any AGD symptoms or *N. perurans* 18S rRNA gene copy at the beginning of the campaign (**Fig. 4.3**). Thus, it was concluded that salmons from these two fish farms were not impacted by the AGD until further in the sampling period (R2 in Glinsk, and R3 in Creevin). These two fish farms are located on the North coast of Ireland, thus it was possible that the colder water at the beginning of the year surpressed *N. perurans* for a longer time or the amoeba was not present in the water during R1. After the annual maximum water temperature (**Fig. 4.2**), *N. perurans* abundance and AGD gill score values started rising in Glinsk and Creevin, allowing the pathogen to begin colonising and spreading on gills.

Nowadays, the abundance of *N. perurans* is still the best target for a molecular assay to diagnose AGD on fish gills (Downes *et al.*, 2015; English *et al.*, 2019), as it is considered to be the first aetiological agent of AGD (Young *et al*., 2007; Young *et al*., 2008). Through the presented sampling period, *N. perurans* abundance overlapped with the AGD gill score in every fish farm (**Fig. 4.3**). Thus, the utility of AGD scoring was again corroborated to be a good method to record the ongoing of the gill disease. However, compared with gill sampling for *N. perurans* qPCR, AGD scoring is inherently a less invasive and non-lethal procedure with a very small cost and time required, making it a better alternative when clinical signs may be present (Taylor *et al.*, 2009). On the other side, molecular diagnosis tests, such as *N. perurans* qPCR, fit as an early warning and monitoring tool, when the AGD did not produce the typical symptoms on gills (Downes *et al.*, 2015).

4.4.2 - Temporal prokaryotic gill community development across all locations

Regarding the prokaryotic microbiome on gills (**Fig. 4.4**), the alpha-diversity (richness and Shannon entropy) was relatively even along the West coast of Ireland at R1. Nevertheless, alpha-diversity values increased significantly at R2 in most of the fish farm locations. It was hypothesised that the higher water temperature experienced before R2 (the annual maximum water temperature, see **Fig. 4.2**) could have drive the prokaryotic microbiome in each fish farm towards a more diverse community. NTI and NRI results (**Fig. 4.4**) suggested that environmental factors strongly influenced the prokaryotic community on R2, supporting the hypothesis that gill microbial community diversity is partially driven by water temperatures, as happens in gut microbiome (Vasemägi *et al*., 2017; Jones *et al*., 2018).

Although there were many similarities between the microbiomes from across the West coast of Ireland in alpha-diversity and environmental filtering results, the first difference could be noticed at the gradual decrease in richness and Shannon entropy from northern to southern fish farms, at R2 and R3 (**Fig. 4.4**). It was hypothesised that this decreasing bacterial diversity from North to South was again due to the influence of the water temperature, as the annual maximum water temperature was before R2 (**Fig. 4.2**). However, the water temperature before R2 was not distinct between locations, thus it is uncertain what could cause these gill microbiome dissimilarities between locations.

Regarding beta-diversity analyses, the differential clustering of the R2 samples from the rest when applying in Bray-Curtis analyses (**Fig. 4.5**) happened after the water temperature peak. As the temperature is one of the top fish microbiome-shifting factors (Minich *et al*., 2019; Horlick *et al.*, 2020; Krotman *et al.*, 2020; Sepulveda & Moeller, 2020), it possibly drove the prokaryotic gill community from every location towards the same direction, making the geographical differences less remarkable and clustering all gill samples closer in beta-diversity analyses (**Fig. 4.5**). Nevertheless, based on all PERMANOVA results (**Fig. 4.5, S4.3, S4.4 and S4.5**), there was a significant geographical dependence of the prokaryotic community structure in every sampling round, even at R2 when the gill microbiome showed less difference between fish farms.

4.4.3 - Identification of the microbiome influencing factors

Fish microbiome was been previously reported to develop along with the age of the animal (Llewellyn *et al.*, 2014; Minich *et al*., 2019). However, no typical ageing indicators (increasing in length and weight) from this dataset correlated with most of the microbiome descriptors (only the length correlated with richness and LCBD WUnifrac, **Table S4.1**). The sampling campaign in this study lasted for six months (**Fig. 4.1b**), not covering an entire Atlantic salmon growth cycle in sea fish farms, that is up from 10 to 15 months (FAO, 2020). Whether future studies aim to characterise the gill microbiome from farmed Atlantic salmon at different ages in sea water fish farms, it is recommendable to sample those salmon for more than six months.

On the other hand, as could be expected, some sampling rounds (mainly R2) were picked up to have a significant impact in many regression analyses on the explanatory variables (**Table S4.1**). This time dependant variation in gill microbiome might be explained by the environmental changes following seasonality, as described in many microbiome studies (Llewellyn *et al.*, 2014; Minich *et al*., 2019; Horlick *et al.*, 2020; Krotman *et al.*, 2020). In addition, fish farms locations were a significant factor on most of the microbiome descriptors (**Table S4.1**). The correlation with some fish farm locations, in combination with the PERMANOVA results (previous section), confirmed the geographical dependency of the prokaryotic microbiome (**Table S4.2**).

The environmental pressure that the microbiome in this study experienced was also a very determinant factor in its structure (NTI and NRI in **Fig. 4.4**), specially at R2. These environmental filtering results correlated significantly with the values of all physico-chemical properties of the water that were measured during the ongoing sampling campaign (**Fig. 4.6a**). In addition, regression analysis from the NRI data (**Fig. 4.6b**) concluded that the abundance of *N. perurans* correlated with environmental pressure on the gill prokaryotic microbiome. AGD gill scores were also correlated with the beta-diversity of the prokaryotic microbiome on gills (**Fig. 4.6c**). All these results (**Fig. 4.6**) suggested that the environmental pressure that drove the prokaryotic microbiome on farmed Atlantic salmon gills could be explained by a combination between: all measured environmental factors (including the water temperature), the time and fish farm when/where samples were taken, and the abundance of *Neoparamoeba perurans* on gills. This explanation would support previous results in this field (Chapter 3 of the present thesis, manuscript submitted (Birlanga *et al*., 2021)) but including samples from multiple fish farms in Ireland.

4.4.4 - Relevancy of the environmental pressure and AGD on Bertraghboi's salmon population in year 1 and year 2

Environmental filtering results suggested that the overall environmental pressure on year 2 salmon was higher than on salmon from year 1 (NRI in **Fig. 4.8**). As both years had similar AGD gill scores and the water temperature played a very important role in this study, we hypothesised that distinct water temperature profiles may partially contributed to these differences in the environmental pressure. Nevertheless, the water temperature records did not present clear variance between the two years (**Fig. S4.10**). Therefore, we concluded that differences in the non-measured environmental factors, in combination with the considered ones, determined the distinct environmental pressure that the gill prokaryotic microbiomes experienced in both years. These pressures at T2 and R2 made those gill communities more similar (**Fig. 4.9**). However, gills from T2 belonged to a salmon cohort that was infected with AGD 12 days after (Chapter 3 of the present thesis, manuscript submitted (Birlanga *et al*., 2021)); while R2 gills already had symptoms of AGD. Therefore, these results suggested that high environmental pressures have a higher impact on the gill microbiome than the AGD.

4.4.5 - Impact of environment and AGD on gills at Glinsk and Creevin

Although salmon from Glinsk and Creevin were not infected with AGD until R2 in Glinsk and R3 in Creevin (**Fig. 4.3)**, the alpha-diversity of gills from Glinsk and Creevin followed the same trend as samples from the rest of the fish farms (**Fig. 4.4**). Richness and Shannon entropy values increased when the AGD episode started, contrary to what happened in previous literature (Chapter 3 of the present thesis, manuscript submitted (Birlanga *et al*., 2021)). Therefore, and following the explanation from previous sections, the significant increase in alpha-diversity values from Glinsk and Creevin gills was due to a combination of all the environmental factors, specially the water temperature, which reached its annual maximum peak before R2. Therefore, the number of different bacteria and the balance of the prokaryotic community on gill would not change after the AGD onset, but mainly because the combination of all the environmental factors.

On the other hand, AGD infected salmon from Glinsk and Creevin experienced a change in their beta-diversity (Unifrac and Weighted Unifrac) compared with salmon before the infection. In

Glinsk, the gill microbiome shifted to a new area between R1 to R2, happening the same in Creevin between R2 to R3 (**Fig. S4.4 and S4.5**), when the AGD started spreading in those populations (**Fig. 4.3**). Even though Glinsk and Creevin salmons were influenced by a high environmental pressure, these results suggested that the onset of AGD also impacted the prokaryotic community on gills, as reported in previously (Chapter 3 of the present thesis, manuscript submitted (Birlanga *et al*., 2021)).

It was also possible to corroborate that many taxa significantly changed their relative abundance from pre- to AGD infected gills in Glinsk and Creevin. As it shown previously (Chapter 3 of the present thesis, manuscript submitted (Birlanga *et al*., 2021)), a number of OTUs associated with the genera *Shewanella* appeared to be sensitive to the AGD onset, with certain OTUs decreasing while others increase at both fish farms. This supports the possible relationship between *Shewanella* and the development of AGD on farmed Atlantic salmon, but further evidence is needed to be understood. Future studies should include functional descriptions of the gill microbiome, along with *in vitro* assays of co-existence between potential AGD relevant prokaryotes and *N. perurans*, in order to elucidate their relationships.

4.4.6 - Prokaryotic core microbiome on gills from Atlantic salmon farmed on West Ireland

The five bacterial taxa that were classified as the prokaryotic core microbiome from this study (*Psychrobacter*, *Pseudomonas*, *Vibrio*, *Rubritalea* and the Order Alteromonadales) were suggested to be the prokaryotic core microbiome on gills from Atlantic salmon with AGD (**Fig. 4.7**). Their wide presence in most of the samples suggested that they probably play an important role, positively or negatively, on the farmed Atlantic salmon during the ongoing of the Amoebic Gill Disease in every fish farm (as the core microbiome did not change between them, **Fig. S4.8**). These genera were also very abundant in our previous field study, where we characterised the gill microbiome from salmon in one Irish fish farm (Chapter 3 of the present thesis, manuscript submitted (Birlanga *et al*., 2021)). Additionally, the genera *Vibrio*, *Rubritalea* and the Order Alteromonadales were also found in the gill microbiome from AGD-affected Atlantic salmon in previous studies (Bowman & Nowak, 2004; Slinger *et al*., 2020).

On the other hand, the genera *Pseudomonas* and *Rubritalea* were equally abundant on gill samples from AGD infected and non-AGD infected salmon (Chapter 3 of the present thesis, manuscript submitted (Birlanga *et al*., 2021)), suggesting that they have a remarkable relevance

on farmed Atlantic salmon gills. However, the details of the relationship of the core microbiome with Atlantic salmon, the rest of the gill microbiome, and AGD are still unknown.

The importance of the environmental factors in this dataset could also be noted when each sampling round was treated individually, and core microbiome analyses were applied on them (**Fig. S4.7**). The core microbiome membership increased at R2, when the environmental pressure on those samples was at its maximum (**Fig. 4.4**). This pressure resulted in the gill microbiome from all location to become more similar (**Fig. 4.5**), sharing more of the same bacterial taxa between all farms; resulting in a higher number of core microbiome members results at R2.

4.5 - Conclusions

We were able to conclude that the AGD scoring was still the least invasive and costly procedure to determine the impact of the AGD on salmon gills when there are clear symptoms of the disease. Although the quantification of the *Neoparamoeba perurans* 18S rRNA genes from gill samples was still the most accurate methodology for an early diagnosis of the AGD on gills without clear symptoms.

The environment factors played a more relevant role than expected in shifting the prokaryotic microbiome, specifically, driving gill microbiome towards a more diverse, but similar community between locations. Especially, water temperature can be considered as one of the main microbiome drivers in the West coast of Ireland during 2018, producing, during the hottest time of the year, a decreasing gradient from northern to southern fish farms of the prokaryotic microbiome diversity on farmed Atlantic salmon gills. In addition, the location of each fish farm was a significant influencing factor on the bacterial community, concluding that the individual environmental conditions of each place determine the prokaryotic microbiome on farmed Atlantic salmon gills. However, the development of the AGD was still detected to impact significantly the microbiome on gills from every fish farm, suggesting its connection with the microorganisms on that organ.

Although the possible connection between the development of AGD and the gill prokaryotic microbiome was supported in various fish farms, the strong influence of the different environmental factors made it difficult to discern clear patterns. Further gill microbiome studies in a controlled mesocosm are needed, to isolate the impact of AGD on the gill microbiome to the

environment. In addition, the analytical part of that research should involve a functional study of the gill microbiome members (using metagenomics for example), in order to elucidate their potential role on that organ, and on the AGD onset and ongoing. Nevertheless, the present study can mean the next step towards a more comprehensive and effective way to treat the AGD, especially in fish farms on the West coast of the Republic of Ireland.

4.6 - References

Birlanga, V. B., McCormack, G., Ijaz, U. Z., McCarthy, E., Smith, C., & Collins, G. (2021). Dynamic Gill and Mucous Microbiomes Track an Amoebic Gill Disease Episode in Farmed Atlantic Salmon. (https://assets.researchsquare.com/files/rs-29747/v1/33663208-b035-433d617 bf44-59125d163937.pdf)

Boerlage, A. S., Ashby, A., Herrero, A., Reeves, A., Gunn, G. J., & Rodger, H. D. (2020). Epidemiology of marine gill diseases in Atlantic salmon (*Salmo salar*) aquaculture: a review. *Reviews in Aquaculture*, 12(4), 2140-2159.

Bolyen, E., Rideout, J. R., Dillon, M. R., Bokulich, N. A., Abnet, C. C., Al-Ghalith, G. A., Alexander, H., Alm, E.J., Arumugam, M., Asnicar, F. & Caporaso, J. G. (2019). Reproducible, interactive, scalable and extensible microbiome data science using QIIME 2. *Nature biotechnology*, 37(8), 852-857.

Bowman, J. P., & Nowak, B. (2004). Salmonid gill bacteria and their relationship to amoebic gill disease. *Journal of Fish Diseases*, 27(8), 483-492.

Bustos, P. A., Young, N. D., Rozas, M. A., Bohle, H. M., Ildefonso, R. S., Morrison, R. N., & Nowak, B. F. (2011). Amoebic gill disease (AGD) in Atlantic salmon (*Salmo salar*) farmed in Chile. *Aquaculture*, 310(3-4), 281-288.

Caporaso, J. G., Lauber, C. L., Walters, W. A., Berg-Lyons, D., Lozupone, C. A., Turnbaugh, P. J., Fierer, N. & Knight, R. (2011). Global patterns of 16S rRNA diversity at a depth of millions of sequences per sample. *Proceedings of the national academy of sciences*, 108(Supplement 1), 4516-4522.

Caporaso, J. G., Lauber, C. L., Walters, W. A., Berg-Lyons, D., Huntley, J., Fierer, N., Owens, S.M., Betley, J., Fraser, L., Bauer, M. & Knight, R. (2012). Ultra-high-throughput microbial community analysis on the Illumina HiSeq and MiSeq platforms. *The ISME journal*, 6(8), 1621-1624.

Crosbie, P. B., Bridle, A. R., Leef, M. J., & Nowak, B. F. (2010). Effects of different batches of *Neoparamoeba perurans* and fish stocking densities on the severity of amoebic gill disease in experimental infection of Atlantic salmon, *Salmo salar* L. *Aquaculture research*, 41(10), e505-e516.

D'Amore, R., Ijaz, U. Z., Schirmer, M., Kenny, J. G., Gregory, R., Darby, A. C., Shakya, M., Podar, M., Quince, C. & Hall, N. (2016). A comprehensive benchmarking study of protocols and sequencing platforms for 16S rRNA community profiling. *BMC genomics*, 17(1), 1-20.

Dittmann, K. K., Sonnenschein, E. C., Egan, S., Gram, L., & Bentzon-Tilia, M. (2019). Impact of *Phaeobacter inhibens* on marine eukaryote-associated microbial communities. *Environmental microbiology reports*, 11(3), 401-413.

Dittmann, K. K., Rasmussen, B. B., Melchiorsen, J., Sonnenschein, E. C., Gram, L., & Bentzon-Tilia, M. (2020). Changes in the microbiome of mariculture feed organisms after treatment with a potentially probiotic strain of *Phaeobacter inhibens*. *Applied and environmental microbiology*, 86(14), e00499-20.

Douglas-Helders, M., Saksida, S., Raverty, S., & Nowak, B. F. (2001). Temperature as a risk factor for outbreaks of amoebic gill disease in farmed Atlantic salmon (*Salmo salar*). *Bulletin of the European Association of Fish Pathologists*, 21(3), 114-116.

Downes, J. K., Henshilwood, K., Collins, E. M., Ryan, A., Connor, I. O., Rodger, H. D., MacCarthy, E. & Ruane, N. M. (2015). A longitudinal study of amoebic gill disease on a marine Atlantic salmon farm utilising a real-time PCR assay for the detection of *Neoparamoeba perurans*. *Aquaculture Environment Interactions*, 7(3), 239-251.

Dray, S., Blanchet, G., Borcard, D., Guenard, G., Jombart, T., Legendre, P., & Wagner, H. (2018). Package 'adespatial': multivariate multiscale spatial analysis. See https://cran. r-project. org/web/packages/adespatial/index. html.

English, C. J., Swords, F., Downes, J. K., Ruane, N. M., Botwright, N. A., Taylor, R. S., Barnes, A.C., Wynne, J.W., Lima, P.C. & Cook, M. T. (2019). Prevalence of six amoeba species colonising the gills of farmed Atlantic salmon with amoebic gill disease (AGD) using qPCR. *Aquaculture Environment Interactions*, 11, 405-415.

Food and Agriculture Organization of the United Nations: Aquaculture Feed and Fertilizer Resources Information System. http://www.fao.org/fishery/affris/species-profiles/atlantic-salmon/growth/en/ (2020). Accessed 10 April 2021.

Haugland, G. T., Olsen, A. B., Rønneseth, A., & Andersen, L. (2017). Lumpfish (*Cyclopterus lumpus* L.) develop amoebic gill disease (AGD) after experimental challenge with *Paramoeba perurans* and can transfer amoebae to Atlantic salmon (*Salmo salar* L.). *Aquaculture*, 478, 48-55.

Horlick, J., Booth, M. A., & Tetu, S. G. (2020). Alternative dietary protein and water temperature influence the skin and gut microbial communities of yellowtail kingfish (*Seriola lalandi*). *PeerJ*, 8, e8705.

Jones, J., DiBattista, J. D., Stat, M., Bunce, M., Boyce, M. C., Fairclough, D. V., Travers, M.J. & Huggett, M. J. (2018). The microbiome of the gastrointestinal tract of a range-shifting marine herbivorous fish. *Frontiers in microbiology*, 9, 2000.

Joshi NA, Fass JN. Sickle: A sliding-window, adaptive, quality-based trimming tool for FastQ files (Version 1.33)[Software].

Karlsbakk, E., Olsen, A. B., Einen, A. C. B., Mo, T. A., Fiksdal, I. U., Aase, H., Kalgraff, C., Skår, S.Å. & Hansen, H. (2013). Amoebic gill disease due to *Paramoeba perurans* in ballan wrasse (*Labrus bergylta*). *Aquaculture*, 412, 41-44.

Kassambara, A. (2018). Machine learning essentials: Practical guide in R. Sthda.

Kembel, S. W., Cowan, P. D., Helmus, M. R., Cornwell, W. K., Morlon, H., Ackerly, D. D., Blomberg, S.P. & Webb, C. O. (2010). Picante: R tools for integrating phylogenies and ecology. *Bioinformatics*, 26(11), 1463-1464.

Kuhn, M. (2008). Building predictive models in R using the caret package. *J Stat Softw*, 28(5), 1-26.

Krotman, Y., Yergaliyev, T. M., Shani, R. A., Avrahami, Y., & Szitenberg, A. (2020). Dissecting the factors shaping fish skin microbiomes in a heterogeneous inland water system. *Microbiome*, 8(1), 1-15.

Kube, P. D., Taylor, R. S., & Elliott, N. G. (2012). Genetic variation in parasite resistance of Atlantic salmon to amoebic gill disease over multiple infections. *Aquaculture*, 364, 165-172.

Lahti, L., Shetty, S., Blake, T., & Salojarvi, J. (2017). Microbiome R package. *Tools Microbiome Anal R*.

Legendre, P., & De Cáceres, M. (2013). Beta diversity as the variance of community data: dissimilarity coefficients and partitioning. *Ecology letters*, 16(8), 951-963.

Llewellyn, M. S., Boutin, S., Hoseinifar, S. H., & Derome, N. (2014). Teleost microbiomes: the state of the art in their characterization, manipulation and importance in aquaculture and fisheries. *Frontiers in microbiology*, 5, 207.

Love, M. I., Huber, W., & Anders, S. (2014). Moderated estimation of fold change and dispersion for RNA-seq data with DESeq2. *Genome biology*, 15(12), 1-21.

Lüdecke, D. (2018). sjPlot: Data visualization for statistics in social science. *R package version*, 2(1).

Lumley, T., & Miller, A. (2009). Leaps: regression subset selection. R package version, 2, 2366.

Marcos-López, M., Ruiz, C. E., Rodger, H. D., O'Connor, I., MacCarthy, E., & Esteban, M. Á. (2017). Local and systemic humoral immune response in farmed Atlantic salmon (*Salmo salar* L.) under a natural amoebic gill disease outbreak. *Fish & shellfish immunology*, 66, 207-216.

Masella, A. P., Bartram, A. K., Truszkowski, J. M., Brown, D. G., & Neufeld, J. D. (2012). PANDAseq: paired-end assembler for illumina sequences. *BMC bioinformatics*, 13(1), 1-7.

McMurdie, P. J., & Holmes, S. (2013). phyloseq: an R package for reproducible interactive analysis and graphics of microbiome census data. *PloS one*, 8(4), e61217.

Minich, J. J., Petrus, S., Michael, J. D., Michael, T. P., Knight, R., & Allen, E. E. (2020). Temporal, environmental, and biological drivers of the mucosal microbiome in a wild marine fish, *Scomber japonicus*. *Msphere*, 5(3).

Munday, B. L., Zilberg, D., & Findlay, V. (2001). Gill disease of marine fish caused by infection with *Neoparamoeba pemaquidensis*. *Journal of Fish Diseases*, 24(9), 497-507.

Nikolenko, S. I., Korobeynikov, A. I., & Alekseyev, M. A. (2013, January). BayesHammer: Bayesian clustering for error correction in single-cell sequencing. *In BMC genomics* (Vol. 14, No. 1, pp. 1-11). BioMed Central.

Oksanen, J., Kindt, R., Legendre, P., O'Hara, B., Stevens, M. H. H., Oksanen, M. J., & Suggests, M. A. S. S. (2007). The vegan package. *Community ecology package*, *10*(631-637), 719.

Oldham, T., Rodger, H., & Nowak, B. F. (2016). Incidence and distribution of amoebic gill disease (AGD)—an epidemiological review. *Aquaculture*, 457, 35-42.

Robledo, D., Hamilton, A., Gutiérrez, A. P., Bron, J. E., & Houston, R. D. (2020). Characterising the mechanisms underlying genetic resistance to amoebic gill disease in Atlantic salmon using RNA sequencing. *BMC genomics*, 21, 1-11.

Rodger, H. D., & McArdle, J. F. (1996). An outbreak of amoebic gill disease in Ireland. *Veterinary record*, 139, 348-348.

Rodger, H. D. (2014). Amoebic gill disease (AGD) in farmed salmon (*Salmo salar*) in Europe. *Fish Veterinary Journal*, (14), 16-27.

Schirmer, M., Ijaz, U. Z., D'Amore, R., Hall, N., Sloan, W. T., & Quince, C. (2015). Insight into biases and sequencing errors for amplicon sequencing with the Illumina MiSeq platform. *Nucleic acids research*, 43(6), e37-e37.

Schmieder, R., & Edwards, R. (2011). Fast identification and removal of sequence contamination from genomic and metagenomic datasets. *PloS one*, 6(3), e17288.

Sepulveda, J., & Moeller, A. H. (2020). The effects of temperature on animal gut microbiomes. *Frontiers in microbiology*, 11.

Shetty, S. A., Hugenholtz, F., Lahti, L., Smidt, H., & de Vos, W. M. (2017). Intestinal microbiome landscaping: insight in community assemblage and implications for microbial modulation strategies. *FEMS microbiology reviews*, 41(2), 182-199.

Shinn, A. P., Pratoomyot, J., Bron, J. E., Paladini, G., Brooker, E. E., & Brooker, A. J. (2015). Economic costs of protistan and metazoan parasites to global mariculture. *Parasitology*, 142(1), 196-270.

Slinger, J., Adams, M. B., & Wynne, J. W. (2020). Bacteriomic profiling of branchial lesions induced by *Neoparamoeba perurans* challenge reveals commensal dysbiosis and an association with *Tenacibaculum dicentrarchi* in AGD-affected Atlantic salmon (*Salmo salar* L.). *Microorganisms*, 8(8), 1189.

Stegen, J. C., Lin, X., Konopka, A. E., & Fredrickson, J. K. (2012). Stochastic and deterministic assembly processes in subsurface microbial communities. *The ISME journal*, 6(9), 1653-1664.

Steinum, T., Kvellestad, A., Rønneberg, L. B., Nilsen, H., Asheim, A., Fjell, K., Nygård, S.M.R., Olsen, A.B. & Dale, O. B. (2008). First cases of amoebic gill disease (AGD) in Norwegian seawater farmed Atlantic salmon, *Salmo salar* L., and phylogeny of the causative amoeba using 18S cDNA sequences. *Journal of fish diseases*, 31(3), 205-214.

Taylor, R. S., Wynne, J. W., Kube, P. D., & Elliott, N. G. (2007). Genetic variation of resistance to amoebic gill disease in Atlantic salmon (*Salmo salar*) assessed in a challenge system. *Aquaculture*, 272, S94-S99.

Taylor, R. S., Muller, W. J., Cook, M. T., Kube, P. D., & Elliott, N. G. (2009). Gill observations in Atlantic salmon (*Salmo salar*, L.) during repeated amoebic gill disease (AGD) field exposure and survival challenge. *Aquaculture*, 290(1-2), 1-8.

Vasemägi, A., Visse, M., & Kisand, V. (2017). Effect of environmental factors and an emerging parasitic disease on gut microbiome of wild salmonid fish. *MSphere*, 2(6).

Vincent, B. N., Morrison, R. N., & Nowak, B. F. (2006). Amoebic gill disease (AGD)-affected Atlantic salmon, *Salmo salar* L., are resistant to subsequent AGD challenge. *Journal of Fish Diseases*, 29(9), 549-559.

Wynne, J. W., Cook, M. T., Nowak, B. F., & Elliott, N. G. (2007). Major histocompatibility polymorphism associated with resistance towards amoebic gill disease in Atlantic salmon (*Salmo salar* L.). *Fish & shellfish immunology*, 22(6), 707-717.

Wynne, J. W., Stratford, C., Slinger, J., Samsing, F., Rigby, M., McCulloch, R., Quezada-Rodriguez, P. & Taylor, R. S. (2020). The interaction between temperature and dose on the efficacy and biochemical response of Atlantic salmon to hydrogen peroxide treatment for amoebic gill disease. *Journal of fish diseases*, 43(1), 39-48.

Young, N. D., Crosbie, P. B. B., Adams, M. B., Nowak, B. F., & Morrison, R. N. (2007). *Neoparamoeba perurans* n. sp., an agent of amoebic gill disease of Atlantic salmon (*Salmo salar*). *International journal for parasitology*, 37(13), 1469-1481.

Young, N. D., Dyková, I., Snekvik, K., Nowak, B. F., & Morrison, R. N. (2008). *Neoparamoeba perurans* is a cosmopolitan aetiological agent of amoebic gill disease. *Diseases of aquatic organisms*, 78(3), 217-223.

4.7 - Supplementary Figures and Tables

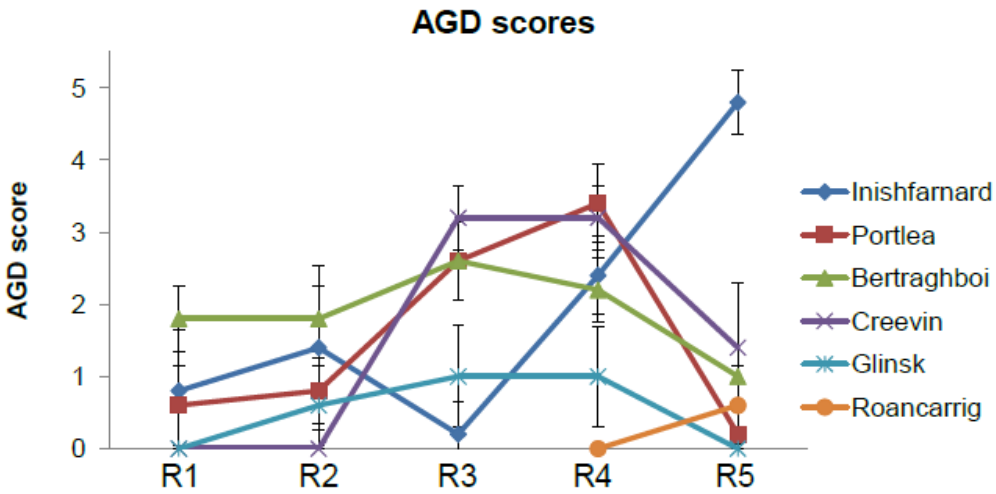

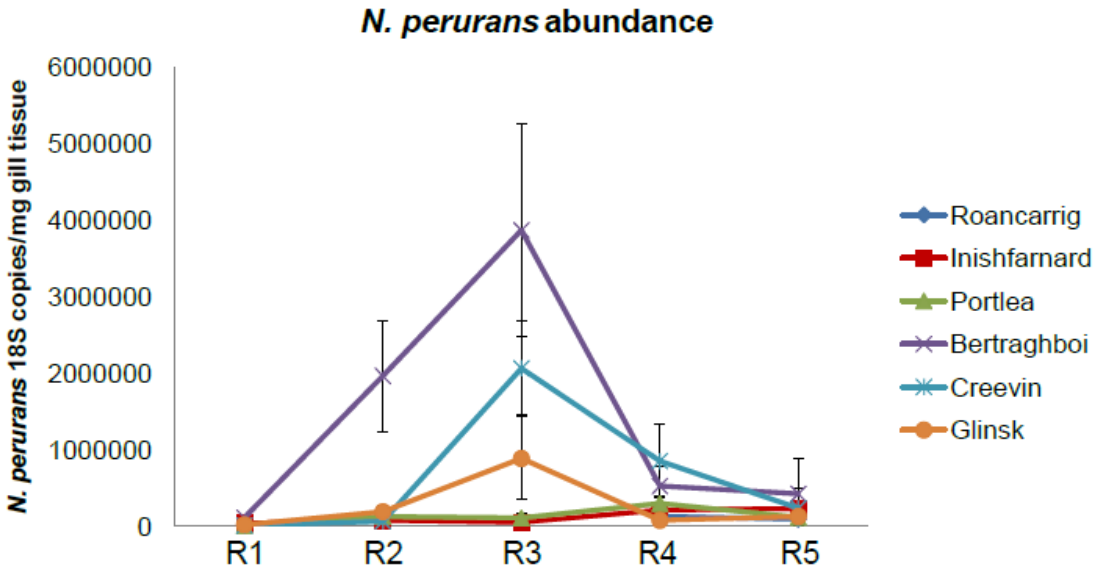

Figure S4.1. Amoebic Gill Disease impact and development on farmed Atlantic salmon gills in 2018. AGD score. Changes in the AGD score through the sampling campaign in each of the sampling rounds in every fish farm. *N. perurans* abundance data: Changes in the concentrations of *N. perurans* 18S rRNA genes in DNA extractions from salmon gills. It was measured by qPCR assays through the sampling campaign in each of the sampling rounds in every fish farm. This data was normalised for a mg of gill tissue to avoid differences in the amoeba abundance because of the size of the gill.

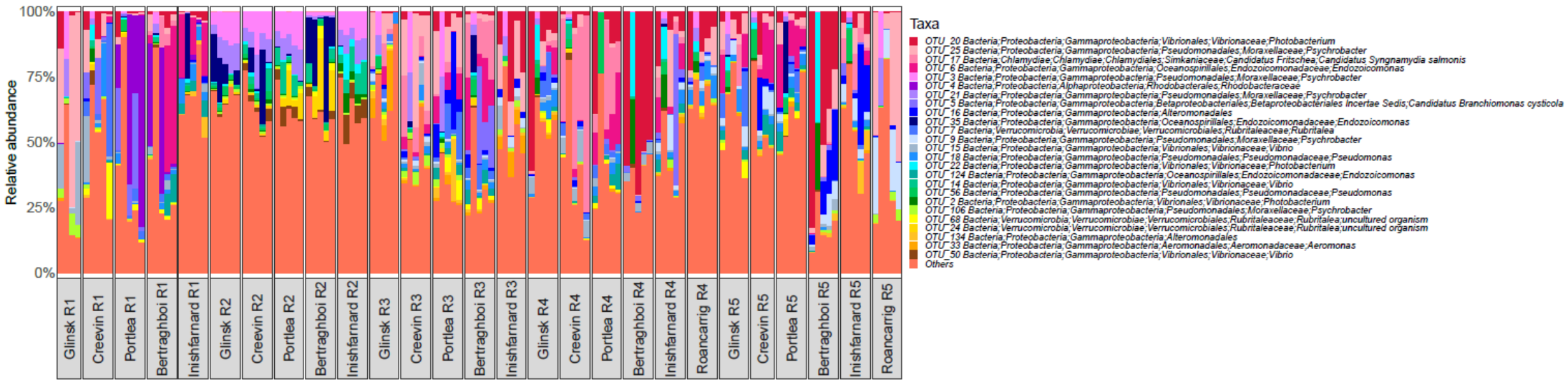

Figure S4.2. Community structure of each of the replicates from every fish farm in every sampling round in 2018. Each of the coloured bars represents the relative abundance of the top 25 most relatively abundant OTUs from across each combination of fish farm and sampling round. 'Others' refers to all OTUs not included in the top 25 most relatively abundant. The legend is on the right, where each colour represents one of the OTUs.

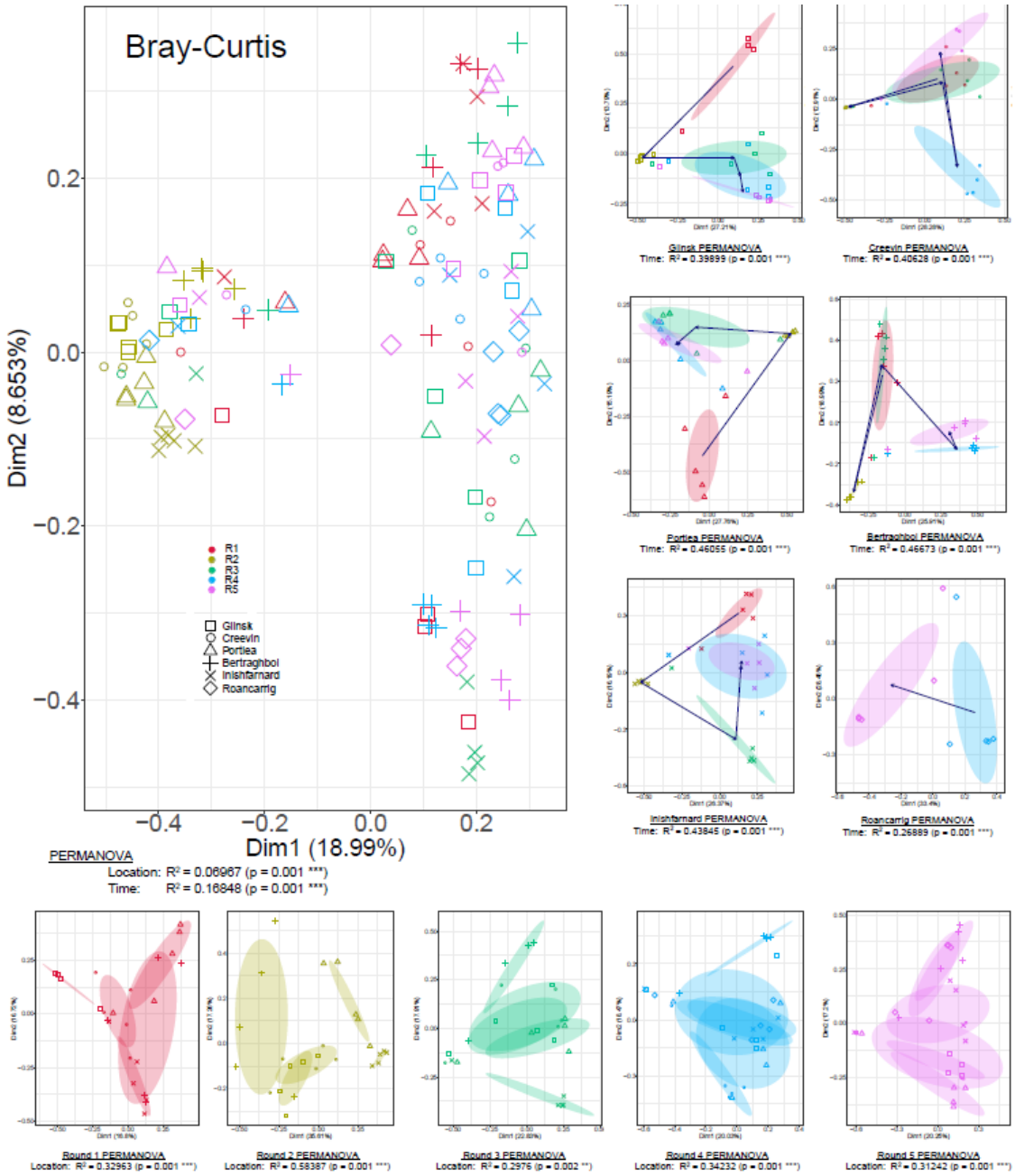

Figure S4.3. Beta-diversity analyses using the Bray-Curtis algorithm in 2018. The biggest graph includes all replicates from each fish farm in each sampling rounds colour and shape coded. Please notice that all samples from R2 are clustered closely in a different area from the majority of the rest of the samples. PERMANOVA analyses consider the *Location* and *Time* as parameters in this part. Ellipses in the rest of the graphics are drawn at 95% confidence interval of standard error with the lines going from sampling round R1 to R5 plotted at mean of the ordination values at each sampling round. Graphs at the right of the biggest one (6 graphs with fish farm's names below) consider changes in the beta-diversity between sampling rounds in each location separately. PERMANOVA analyses consider the *Time* as a parameter in this part However, graphs at the bottom (5 graphs with sampling round's numbers below) consider changes in the beta-diversity between locations in each sampling round separately. PERMANOVA analyses consider the *Location* as a parameter in this part. Please notice that, independently of the sampling round, the *Location* always plays a significant role in the prokaryotic microbiome structure.

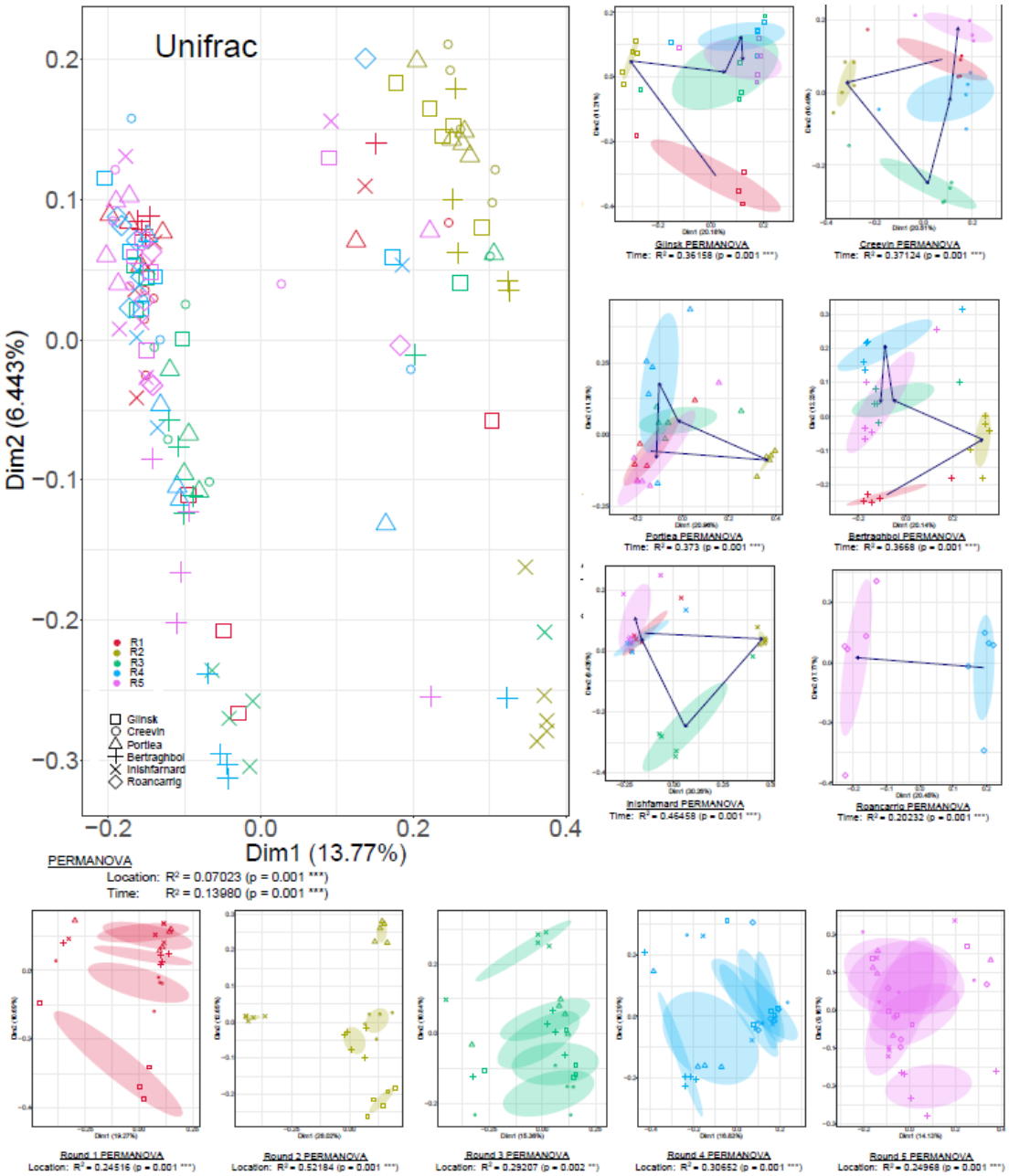

Figure S4.4. Beta-diversity analyses using the Unifrac algorithm in 2018. The biggest graph includes all replicates from each fish farm in each sampling rounds colour and shape coded. PERMANOVA analyses consider the *Location* and *Time* as parameters in this part. Ellipses in the rest of the graphics are drawn at 95% confidence interval of standard error with the lines going from sampling round R1 to R5 plotted at mean of the ordination values at each sampling round. Graphs at the right of the biggest one (6 graphs with fish farm's names below) consider changes in the beta-diversity between sampling rounds in each location separately. PERMANOVA analyses consider the *Time* as a parameter in this part However, graphs at the bottom (5 graphs with sampling round's numbers below) consider changes in the beta-diversity between locations in each sampling round separately. PERMANOVA analyses consider the *Location* as a parameter in this part. Please notice that, independently of the sampling round, the *Location* always plays a significant role in the prokaryotic microbiome structure.

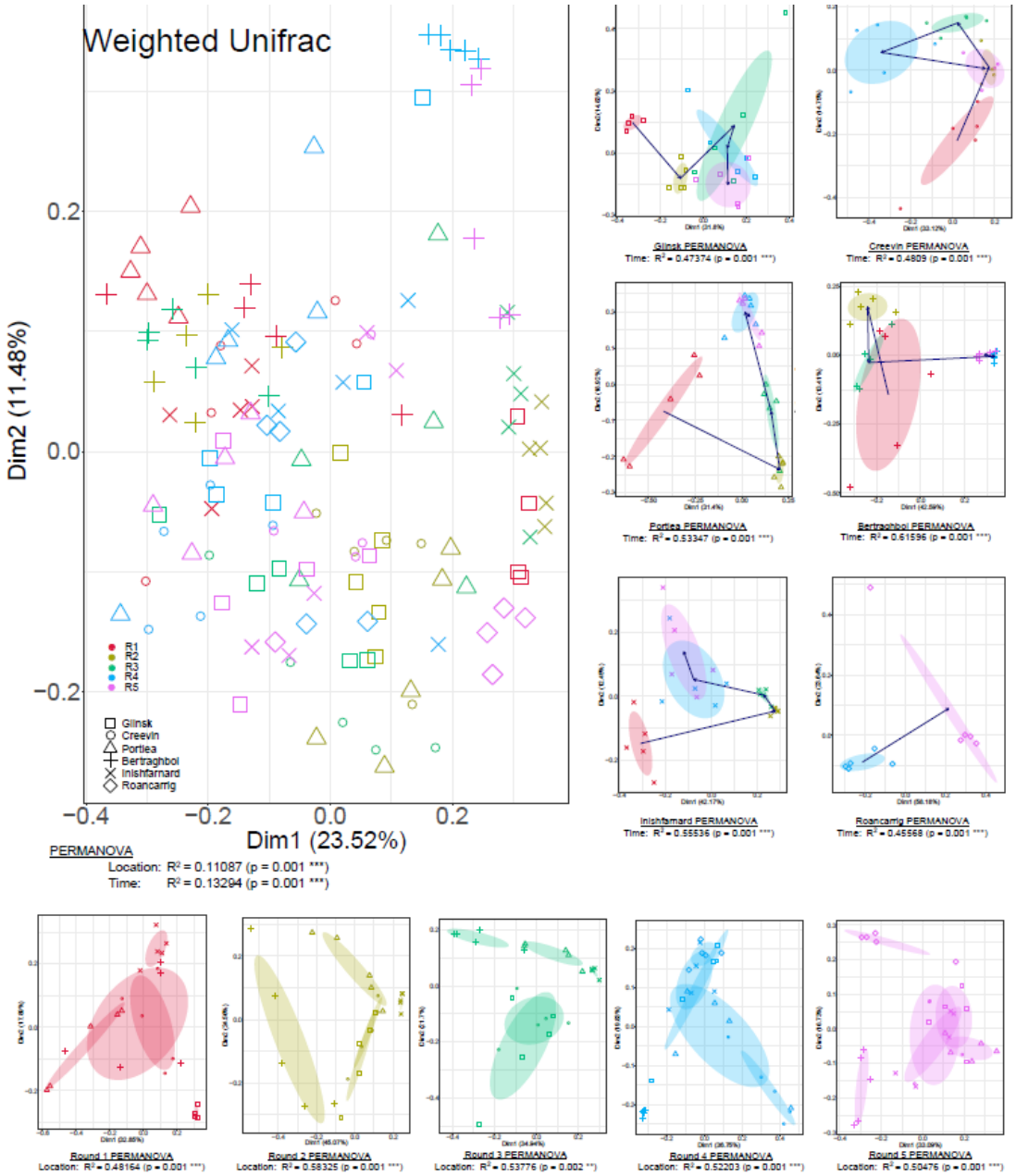

Figure S4.5. Beta-diversity analyses using the Weighted Unifrac algorithm in 2018**.** The biggest graph includes all replicates from each fish farm in each sampling rounds colour and shape coded. PERMANOVA analyses consider the *Location* and *Time* as parameters in this part. Ellipses in the rest of the graphics are drawn at 95% confidence interval of standard error with the lines going from sampling round R1 to R5 plotted at mean of the ordination values at each sampling round. Graphs at the right of the biggest one (6 graphs with fish farm's names below) consider changes in the beta-diversity between sampling rounds in each location separately. PERMANOVA analyses consider the *Time* as a parameter in this part However, graphs at the bottom (5 graphs with sampling round's numbers below) consider changes in the beta-diversity between locations in each sampling round separately. PERMANOVA analyses consider the *Location* as a parameter in this part. Please notice that, independently of the sampling round, the *Location* always plays a significant role in the prokaryotic microbiome structure.

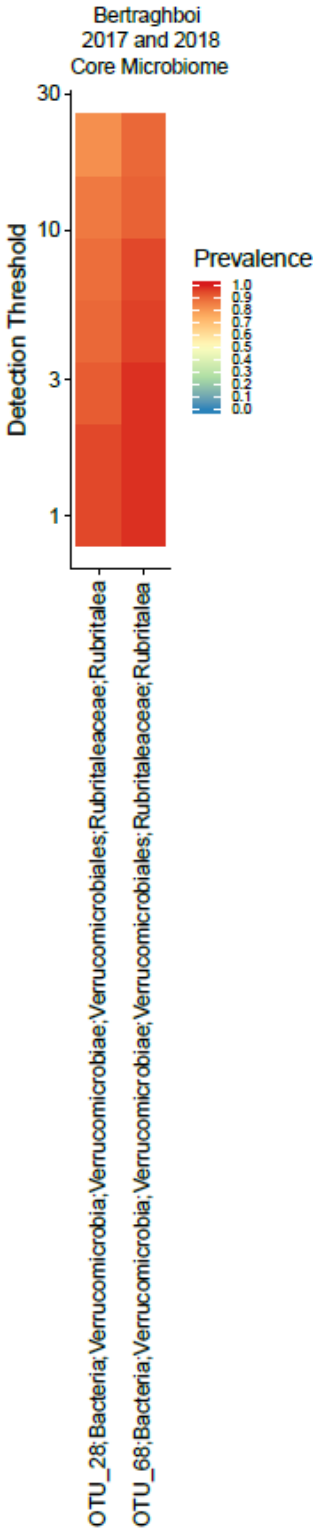

Figure S4.6. Prokaryotic core microbiome on gills from the Bertraghboi fish farm including all samples from 2017 and 2018. To be part of the core microbiome, bacterial taxa must have at least 85% prevalence in all considered samples. Bacteria are arranged from a small relative abundance to a high relative abundance, all of them with at least 85% prevalence. Although some prokaryotic taxa are repeated in more than one OTU, they could be considered as the same bacteria.

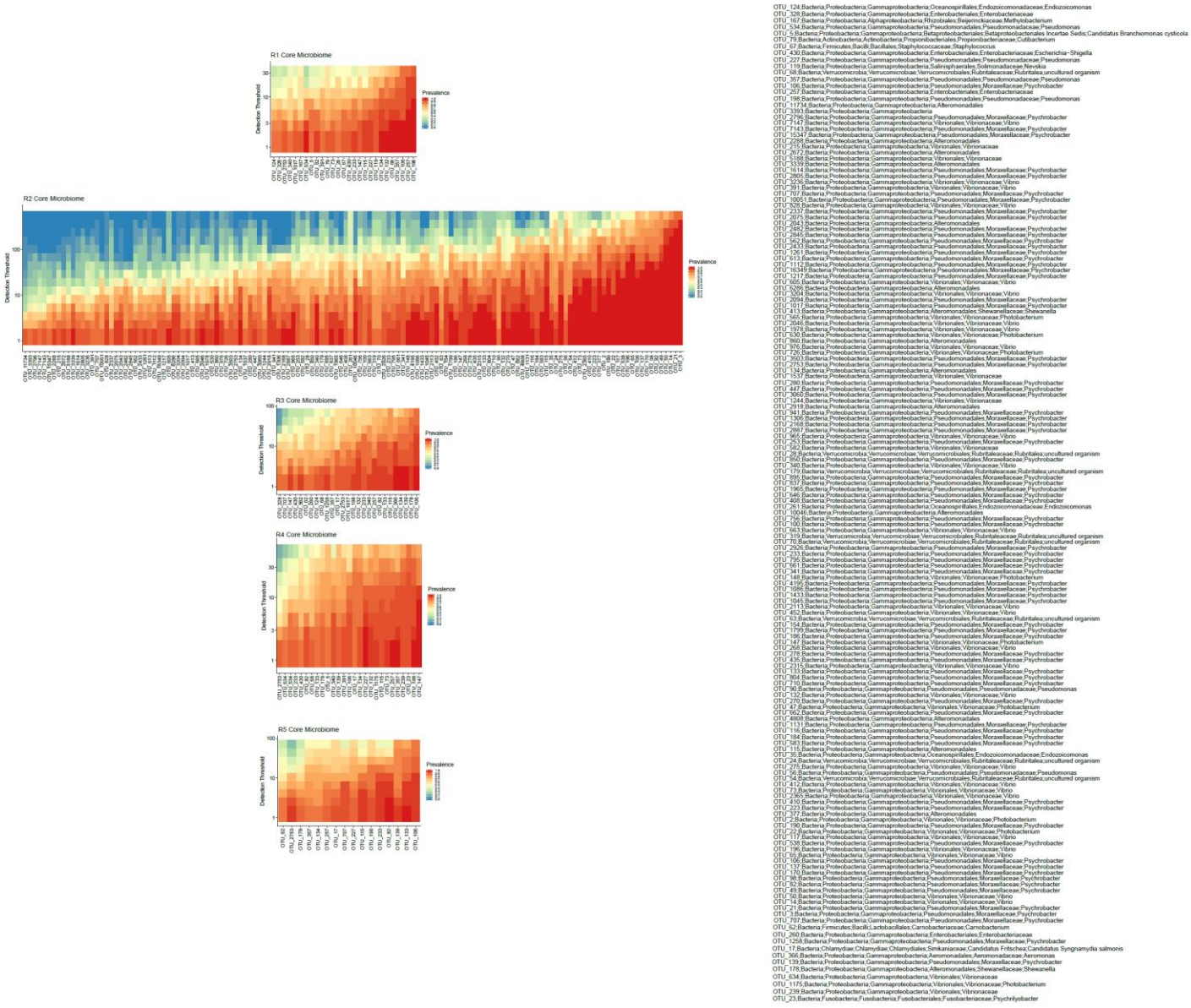

Figure S4.7. Prokaryotic core microbiome on gills from all locations in each of the sampling rounds separately in 2018. To be part of the core microbiome, bacterial taxa must have at least 85% prevalence in all considered samples. Bacteria are arranged from a small relative abundance to a high relative abundance (from left to right), all of them with at least 85% prevalence. Although some prokaryotic taxa are repeated in more than one OTU, they could be considered as the same bacteria. Please notice that the amount of bacteria with a higher 85% prevalence increase sharply at R2 compared with the rest of the sampling rounds.

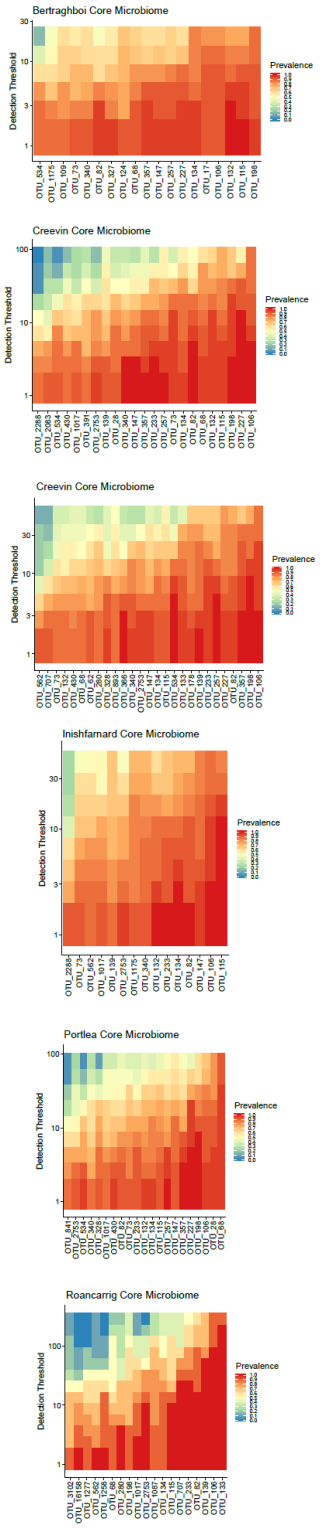

OTU_534;Bacteria;Proteobacteria;Gammaproteobacteria;Pseudomonadales;Pseudomonadaceae;Pseudomonas
OTU_1175;Bacteria;Proteobacteria;Gammaproteobacteria;Vibrionales;Vibrionaceae;Photobacterium
OTU_109;Bacteria;Proteobacteria;Gammaproteobacteria;Oceanospirillales;Endozoicomonadaceae;Endozoicomonas
OTU_73;Bacteria;Proteobacteria;Gammaproteobacteria;Vibrionales;Vibrionaceae;Vibrio
OTU_340;Bacteria;Proteobacteria;Gammaproteobacteria;Vibrionales;Vibrionaceae;Vibrio
OTU_82;Bacteria;Proteobacteria;Gammaproteobacteria;Pseudomonadales;Moraxellaceae;Psychrobacter
OTU_327;Bacteria;Proteobacteria;Gammaproteobacteria;Oceanospirillales;Halomonadaceae
OTU_124;Bacteria;Proteobacteria;Gammaproteobacteria;Oceanospirillales;Endozoicomonadaceae;Endozoicomonas
OTU_68;Bacteria;Verrucomicrobia;Verrucomicrobiae;Verrucomicrobiales;Rubritaleaceae;Rubritalea;uncultured organism
OTU_357;Bacteria;Proteobacteria;Gammaproteobacteria;Pseudomonadales;Pseudomonadaceae;Pseudomonas
OTU_147;Bacteria;Proteobacteria;Gammaproteobacteria;Vibrionales;Vibrionaceae;Photobacterium
OTU_257;Bacteria;Proteobacteria;Gammaproteobacteria;Enterobacteriales;Enterobacteriaceae
OTU_227;Bacteria;Proteobacteria;Gammaproteobacteria;Pseudomonadales;Pseudomonadaceae;Pseudomonas
OTU_134;Bacteria;Proteobacteria;Gammaproteobacteria;Alteromonadales
OTU_17;Bacteria;Chlamydiae;Chlamydiae;Chlamydiales;Simkaniaceae;Candidatus Fritschea;Candidatus Syngnamydia salmonis
OTU_106;Bacteria;Proteobacteria;Gammaproteobacteria;Pseudomonadales;Moraxellaceae;Psychrobacter
OTU_132;Bacteria;Proteobacteria;Gammaproteobacteria;Vibrionales;Vibrionaceae;Vibrio
OTU_115;Bacteria;Proteobacteria;Gammaproteobacteria;Alteromonadales
OTU_198;Bacteria;Proteobacteria;Gammaproteobacteria;Pseudomonadales;Pseudomonadaceae;Pseudomonas
OTU_2288;Bacteria;Proteobacteria;Gammaproteobacteria;Alteromonadales
OTU_2083;Bacteria;Proteobacteria;Gammaproteobacteria;Pseudomonadales;Pseudomonadaceae;Pseudomonas
OTU_430;Bacteria;Proteobacteria;Gammaproteobacteria;Enterobacteriales;Enterobacteriaceae;Escherichia−Shigella
OTU_1017;Bacteria;Proteobacteria;Gammaproteobacteria;Pseudomonadales;Moraxellaceae;Psychrobacter
OTU_391;Bacteria;Proteobacteria;Gammaproteobacteria;Vibrionales;Vibrionaceae;Vibrio
OTU_2753;Bacteria;Proteobacteria;Gammaproteobacteria;Pseudomonadales;Moraxellaceae;Psychrobacter
OTU_139;Bacteria;Proteobacteria;Gammaproteobacteria;Pseudomonadales;Moraxellaceae;Psychrobacter
OTU_28;Bacteria;Verrucomicrobia;Verrucomicrobiae;Verrucomicrobiales;Rubritaleaceae;Rubritalea;uncultured organism
OTU_233;Bacteria;Proteobacteria;Gammaproteobacteria;Pseudomonadales;Moraxellaceae;Psychrobacter
OTU_562;Bacteria;Proteobacteria;Gammaproteobacteria;Pseudomonadales;Moraxellaceae;Psychrobacter
OTU_707;Bacteria;Proteobacteria;Gammaproteobacteria;Pseudomonadales;Moraxellaceae;Psychrobacter
OTU_62;Bacteria;Firmicutes;Bacilli;Lactobacillales;Carnobacteriaceae;Carnobacterium
OTU_280;Bacteria;Proteobacteria;Gammaproteobacteria;Pseudomonadales;Moraxellaceae;Psychrobacter
OTU_328;Bacteria;Proteobacteria;Gammaproteobacteria;Enterobacteriales;Enterobacteriaceae
OTU_893;Bacteria;Proteobacteria;Gammaproteobacteria;Pseudomonadales;Moraxellaceae;Psychrobacter
OTU_366;Bacteria;Proteobacteria;Gammaproteobacteria;Aeromonadales;Aeromonadaceae;Aeromonas
OTU_133;Bacteria;Proteobacteria;Gammaproteobacteria;Pseudomonadales;Moraxellaceae;Psychrobacter
OTU_178;Bacteria;Proteobacteria;Gammaproteobacteria;Alteromonadales;Shewanellaceae;Shewanella
OTU_841;Bacteria;Proteobacteria;Gammaproteobacteria;Enterobacteriales;Enterobacteriaceae;Escherichia−Shigella
OTU_3102;Bacteria;Bacteroidetes;Bacteroidia;Flavobacteriales;Flavobacteriaceae;Flavobacterium
OTU_16158;Bacteria;Bacteroidetes;Bacteroidia;Flavobacteriales;Flavobacteriaceae;Flavobacterium
OTU_1277;Bacteria;Bacteroidetes;Bacteroidia;Flavobacteriales;Flavobacteriaceae;Gillisia
OTU_1258;Bacteria;Proteobacteria;Gammaproteobacteria;Pseudomonadales;Moraxellaceae;Psychrobacter
OTU_1087;Bacteria;Bacteroidetes;Bacteroidia;Flavobacteriales;Flavobacteriaceae;Flavobacterium

Figure S4.8. Prokaryotic core microbiome on gills from all sampling rounds in each of the locations separately in 2018. To be part of the core microbiome, bacterial taxa must have at least 85% prevalence in all considered samples. Bacteria are arranged from a small relative abundance to a high relative abundance (from left to right), all of them with at least 85% prevalence. Although some prokaryotic taxa are repeated in more than one OTU, they could be considered as the same bacteria.

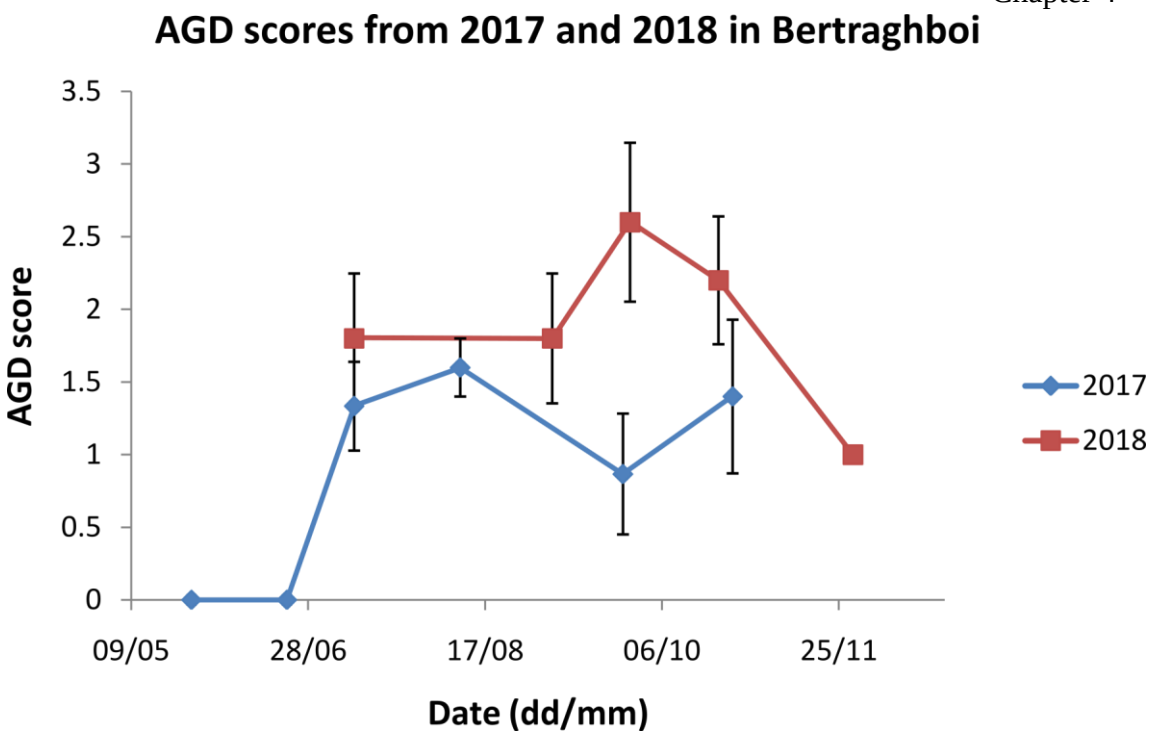

Figure S4.9. AGD scores comparing the two sampling campaigns (2017 in blue and 2018 in red) from the Bertraghboi fish farm. The period of time in the graph includes from May 09th until November 29th.

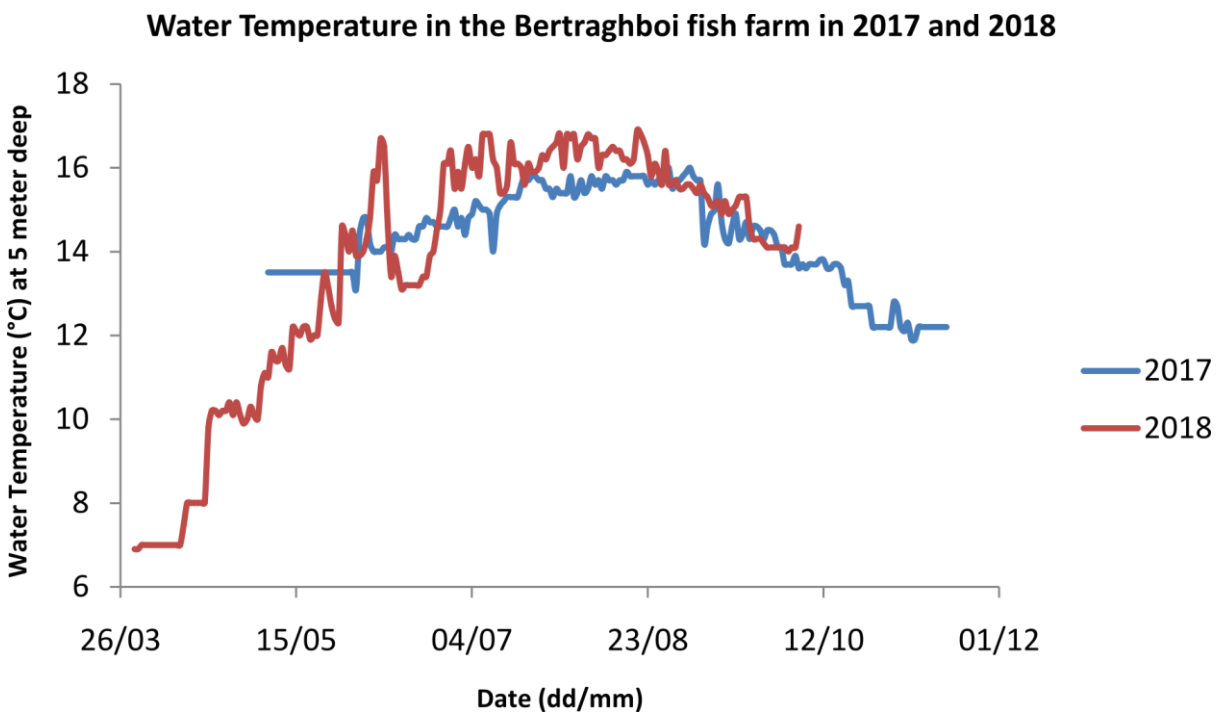

Figure S4.10. Water temperature profiles (Degrees Celsius) at 5 meters deep from 2017 (blue line) and 2018 (red line) from the Bertraghboi fish farm. The period of time in the graph includes from March 26th until December 1st.

Supplementary Tables

Table S4.1. Subset regression analyses. These analyses tried to correlate all recorded possible explanatory variables: environmental factors (Temperature, Salinity, Oxygen Level and Clarity from the sampling day and the average from the previous month), fish features (Weight, Length and AGD score), sampling points (from T1 to T6 in 2017, and from R1 to R5 in 2018), sampling years (2017 and 2018), fish farms locations (Inishfarnard, Roancarrig, Portlea, Bertraghboi, Glinsk and Creevin) and the logarithm of the *N. perurans* concentration (log_NPqPCR_Av); with the microbiome characteristics as dependent variables (Richness, NTI, NRI, LCBD Bray-Curtis, LCBD Unifrac, LCBD Weighted Unifrac, and the logarithm of the *N. perurans* concentration). The first table in each section lists various possible regression models that were created to try to fit the profile of the dependent variables with the lowest cross-validation error. The second table in each section gives details about the best performing regression model that fits with the profile of each dependent variable. This second table includes a figure where all significant factors are listed on the left. If the significant factor presents a value (represented as a box in the same raw as the factor) above zero (a dotted line from the zero value at the "Estimate" axis), that factor has a significant positive correlation with the analysed microbiome characteristic. If the significant factor presents a value below zero, that factor has a significant negative correlation with the analysed microbiome characteristic.

Richness

	Model	**Cross-validation Errors**
11	Richness ~ TimeR2 + TimeR3 + TimeT1 + TimeT2 + TimeT3 + LocationPortlea + LocationBertraghboi + Length + O2_Av + Temperature_day + Salinity_day	60.75302
10	Richness ~ TimeR2 + TimeR3 + TimeT1 + TimeT2 + LocationPortlea + LocationBertraghboi + Length + O2_Av + Temperature_day + Salinity_day	60.92862
9	Richness ~ TimeR2 + TimeR3 + TimeT2 + TimeT6 + LocationPortlea + Length + Temp_Av + Temperature_day + O2_day	61.14099
7	Richness ~ Year2017 + TimeR2 + TimeT2 + TimeT6 + LocationPortlea + Temp_Av + Temperature_day	62.17839
6	Richness ~ TimeR2 + TimeT2 + TimeT6 + LocationGlinsk + Length + Temperature_day	62.69192
5	Richness ~ TimeR2 + TimeT2 + TimeT6 + LocationGlinsk + Length	62.73126
8	Richness ~ TimeR2 + TimeT2 + TimeT6 + LocationGlinsk + Length + Temp_Av + Temperature_day + O2_day	62.75560
12	Richness ~ TimeR2 + TimeR3 + TimeT1 + TimeT2 + TimeT3 + LocationPortlea + LocationBertraghboi + Weight + Length + O2_Av + Temperature_day +	62.77956

	Salinity_day	
4	Richness ~ TimeR2 + TimeT6 + LocationGlinsk + Length	63.71462
13	Richness ~ TimeR2 + TimeR3 + TimeR4 + TimeT1 + TimeT2 + LocationPortlea + LocationBertraghboi + Weight + Length + O2_Av + Sal_Av + Temperature_day + Salinity_day	64.03372
3	Richness ~ TimeR2 + TimeT6 + Weight	64.26576
14	Richness ~ Year2017 + TimeR1 + TimeR3 + TimeR4 + TimeT2 + TimeT3 + TimeT6 + LocationPortlea + Weight + Length + O2_Av + Temp_Av + log_NPqPCR_Av + Temperature_day	65.44030
15	Richness ~ TimeR2 + TimeR3 + TimeR4 + TimeT1 + TimeT2 + TimeT3 + LocationPortlea + LocationGlinsk + Weight + Length + Clarity_Av + log_NPqPCR_Av + Temperature_day + Salinity_day + O2_day	65.70966
16	Richness ~ Year2018 + TimeR2 + TimeR3 + TimeR5 + TimeT1 + TimeT2 + TimeT5 + LocationPortlea + LocationBertraghboi + Weight + Length + Sal_Av + Clarity_Av + log_NPqPCR_Av + Temperature_day + Salinity_day	66.89566
17	Richness ~ Year2017 + TimeR2 + TimeR3 + TimeR5 + TimeT1 + TimeT2 + TimeT3 + TimeT5 + LocationPortlea + LocationBertraghboi + Weight + Length + Sal_Av + Clarity_Av + log_NPqPCR_Av + Temperature_day + Salinity_day	67.21001
20	Richness ~ Year2017 + TimeR2 + TimeR3 + TimeR4 + TimeT1 + TimeT2 + TimeT3 + TimeT4 + TimeT5 + TimeT6 + LocationBertraghboi + LocationCreevin + LocationGlinsk + Weight + AGD_score + Temp_Av + Clarity_Av + log_NPqPCR_Av + Temperature_day + Salinity_day	67.53046
2	Richness ~ TimeR2 + TimeT6	67.77784
18	Richness ~ TimeR1 + TimeR2 + TimeR3 + TimeR4 + TimeT1 + TimeT2 + TimeT4 + LocationPortlea + LocationBertraghboi + Weight + Length + AGD_score + Sal_Av + Clarity_Av + log_NPqPCR_Av + Temperature_day + Salinity_day + O2_day	67.93234
19	Richness ~ Year2018 + TimeR1 + TimeR2 + TimeR4 + TimeR5 + TimeT1 + TimeT2 + TimeT4 + LocationPortlea + LocationBertraghboi + Weight + Length + AGD_score + Sal_Av + Clarity_Av + log_NPqPCR_Av + Temperature_day + Salinity_day + O2_day	68.07079
21	Richness ~ TimeR1 + TimeR3 + TimeR5 + TimeT1 + TimeT2 + TimeT3 + TimeT4 + TimeT6 + LocationPortlea + LocationBertraghboi + Weight + Length + AGD_score + O2_Av + Sal_Av + Temp_Av	69.96122

	+ Clarity_Av + log_NPqPCR_Av + Temperature_day + O2_day + Clarity_day	
22	Richness ~ Year2017 + TimeR1 + TimeR2 + TimeR3 + TimeR4 + TimeT1 + TimeT2 + TimeT3 + TimeT4 + LocationPortlea + LocationBertraghboi + LocationGlinsk + Weight + Length + AGD_score + Temp_Av + Clarity_Av + log_NPqPCR_Av + Temperature_day + Salinity_day + O2_day + Clarity_day	70.38638
1	Richness ~ TimeR2	74.39326

129

	Richness						
Predictors	*Estimates*	*std. Error*	*std. Beta*	*CI*	*standardized CI*	*Statistic*	*p*
(Intercept)	-1812.44017 ***	417.44394		-2639.09282 – -985.78753		-4.34176	**<0.001**
TimeR2	196.47913 ***	25.55521	0.69939	145.87286 – 247.08540	0.52110 – 0.87769	7.68842	**<0.001**
TimeR3	72.06442 **	23.75119	0.21395	25.03060 – 119.09824	0.07575 – 0.35216	3.03414	**0.003**
TimeT1	-80.04863 **	25.62776	-0.22640	-130.79856 – -29.29869	-0.36846 – -0.08434	-3.12351	**0.002**
TimeT2	100.18261 ***	28.49232	0.28335	43.76007 – 156.60516	0.12540 – 0.44129	3.51613	**0.001**
TimeT3	-27.93978	19.81623	-0.09339	-67.18131 – 11.30174	-0.22321 – 0.03643	-1.40994	0.161
LocationPortlea	-82.70086 ***	20.84854	-0.36315	-123.98664 – -41.41508	-0.54258 – -0.18372	-3.96675	**<0.001**
LocationBertraghboi	81.27493 ***	19.72739	0.45014	42.20934 – 120.34053	0.23599 – 0.66428	4.11990	**<0.001**
Length	2.41321 *	1.11486	0.21656	0.20549 – 4.62092	0.02047 – 0.41265	2.16459	**0.032**
O2_Av	2.87682 **	1.08671	0.18188	0.72484 – 5.02880	0.04722 – 0.31655	2.64727	**0.009**
Temperature_day	-14.12916 ***	3.79752	-0.33963	-21.64929 – -6.60904	-0.51854 – -0.16072	-3.72063	**<0.001**
Salinity_day	56.84605 ***	12.42863	0.59687	32.23398 – 81.45812	0.34110 – 0.85264	4.57380	**<0.001**
Observations	130						
R^2 / R^2 adjusted	0.636 / 0.602						

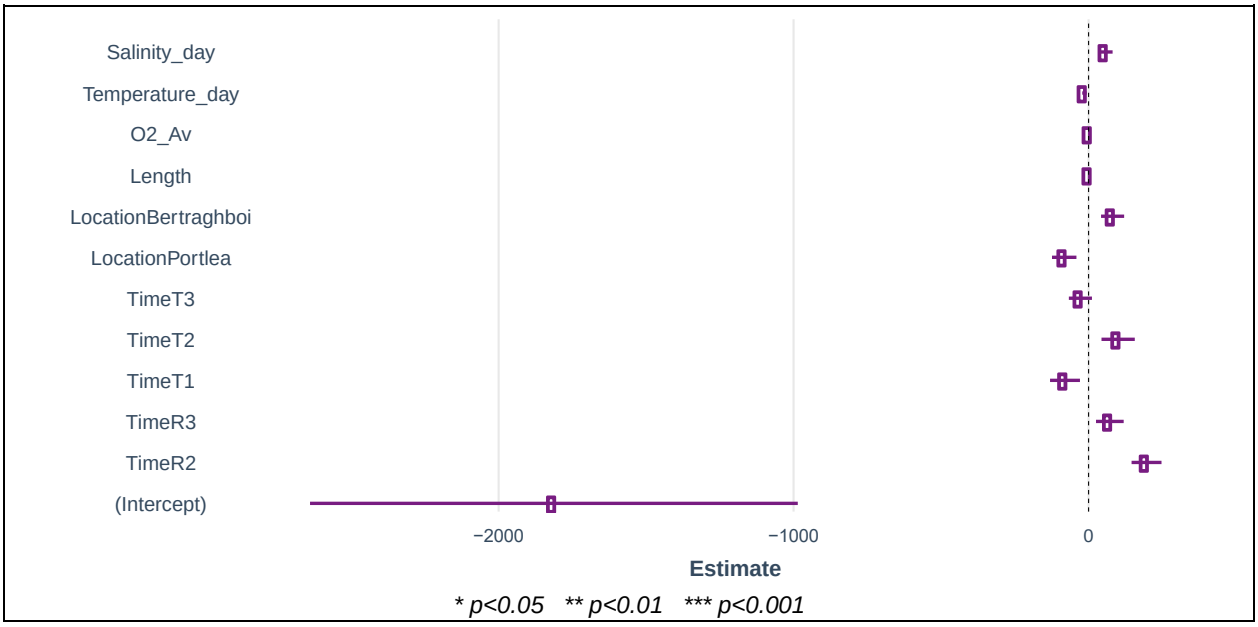
Salinity_day
Temperature_day
O2_Av
Length
LocationBertraghboi
LocationPortlea
TimeT3
TimeT2
TimeT1
TimeR3
TimeR2
(Intercept)
−2000
−1000
0
Estimate
* p<0.05 ** p<0.01 *** p<0.001

	Model	Cross-validation Errors
10	NRI ~ TimeR1 + TimeR2 + TimeT1 + TimeT3 + LocationBertraghboi + O2_Av + Sal_Av + Temp_Av + Salinity_day + Clarity_day	2.46293
13	NRI ~ TimeR1 + TimeR2 + TimeT1 + TimeT2 + TimeT3 + LocationBertraghboi + Length + O2_Av + Sal_Av + Temp_Av + log_NPqPCR_Av + Salinity_day + Clarity_day	2.46342
8	NRI ~ TimeR1 + TimeR2 + TimeR5 + TimeT6 + LocationCreevin + Weight + O2_Av + Clarity_Av	2.48858
9	NRI ~ TimeR1 + TimeR2 + TimeR5 + TimeT6 + LocationCreevin + Length + O2_Av + Clarity_Av + log_NPqPCR_Av	2.49917
7	NRI ~ TimeR1 + TimeR2 + TimeR5 + TimeT6 + LocationCreevin + O2_Av + Clarity_Av	2.50084
12	NRI ~ TimeR1 + TimeR2 + TimeR5 + TimeT1 + LocationPortlea + LocationCreevin + Length + O2_Av + Clarity_Av + log_NPqPCR_Av + Salinity_day + Clarity_day	2.51029
14	NRI ~ TimeR1 + TimeR2 + TimeT1 + TimeT5 + LocationPortlea + LocationCreevin + Length + O2_Av + Temp_Av + Clarity_Av + log_NPqPCR_Av + Temperature_day + Salinity_day + Clarity_day	2.51244
6	NRI ~ TimeR1 + TimeR2 + TimeT6 + LocationGlinsk + O2_Av + Temperature_day	2.52467
11	NRI ~ TimeR1 + TimeR2 + TimeT1 + LocationPortlea + LocationCreevin + O2_Av + Temp_Av + Clarity_Av + log_NPqPCR_Av + Salinity_day + Clarity_day	2.54397
17	NRI ~ Year2017 + TimeR3 + TimeR4 + TimeT1 + TimeT3 + TimeT4 + TimeT5 + LocationPortlea + LocationBertraghboi + Length + O2_Av + Sal_Av + Temp_Av + Clarity_Av + log_NPqPCR_Av + Salinity_day + O2_day	2.56760
15	NRI ~ TimeR1 + TimeR2 + TimeR3 + TimeT1 + TimeT5 + LocationPortlea + LocationCreevin + Length + O2_Av + Temp_Av + Clarity_Av + log_NPqPCR_Av + Temperature_day + Salinity_day + Clarity_day	2.56989
5	NRI ~ TimeR1 + TimeR2 + LocationGlinsk + O2_Av + Temperature_day	2.57168
18	NRI ~ Year2017 + TimeR3 + TimeR4 + TimeT1 + TimeT3 + TimeT4 + TimeT5 + LocationPortlea + LocationBertraghboi + Length + AGD_score + O2_Av + Sal_Av + Temp_Av + Clarity_Av + log_NPqPCR_Av + Salinity_day + O2_day	2.58467
4	NRI ~ Year2017 + TimeR2 + LocationPortlea + Temperature_day	2.58583
16	NRI ~ TimeR1 + TimeR2 + TimeR3 + TimeR5 + TimeT1 +	2.60545

	TimeT5 + TimeT6 + LocationCreevin + Length + O2_Av + Sal_Av + Clarity_Av + log_NPqPCR_Av + Temperature_day + Salinity_day + O2_day	
3	NRI ~ Year2017 + TimeR2 + Temperature_day	2.66750
19	NRI ~ Year2017 + TimeR1 + TimeR2 + TimeR4 + TimeR5 + TimeT1 + TimeT2 + TimeT4 + TimeT5 + TimeT6 + LocationBertraghboi + LocationCreevin + LocationGlinsk + Sal_Av + Temp_Av + Clarity_Av + Temperature_day + O2_day + Clarity_day	2.70562
21	NRI ~ Year2018 + TimeR3 + TimeR5 + TimeT1 + TimeT2 + TimeT4 + TimeT6 + LocationPortlea + LocationBertraghboi + LocationCreevin + LocationGlinsk + Length + AGD_score + O2_Av + Sal_Av + Temp_Av + Clarity_Av + Temperature_day + Salinity_day + O2_day + Clarity_day	2.70794
20	NRI ~ Year2018 + TimeR1 + TimeR2 + TimeR3 + TimeR4 + TimeT1 + TimeT2 + TimeT4 + TimeT5 + TimeT6 + LocationPortlea + LocationBertraghboi + LocationGlinsk + AGD_score + Temp_Av + Clarity_Av + Temperature_day + Salinity_day + O2_day + Clarity_day	2.71878
22	NRI ~ Year2017 + TimeR1 + TimeR2 + TimeR3 + TimeR4 + TimeT1 + TimeT2 + TimeT3 + TimeT4 + TimeT5 + LocationPortlea + LocationBertraghboi + LocationGlinsk + Weight + Length + AGD_score + O2_Av + Clarity_Av + log_NPqPCR_Av + Salinity_day + O2_day + Clarity_day	2.78137
2	NRI ~ Year2017 + Temperature_day	2.80718
1	NRI ~ TimeR2	2.89143

	NRI						
Predictors	*Estimates*	*std. Error*	*std. Beta*	*CI*	*standardized CI*	*Statistic*	*p*
(Intercept)	219.31881 ***	40.90291		138.32696 – 300.31066		5.36194	<0.001
TimeR1	11.29603 ***	1.90217	0.92851	7.52954 – 15.06252	0.62206 – 1.23496	5.93849	<0.001
TimeR2	8.35467 ***	1.17622	0.70777	6.02564 – 10.68370	0.51247 – 0.90307	7.10298	<0.001
TimeT1	7.51391 ***	1.72372	0.50576	4.10077 – 10.92704	0.27836 – 0.73317	4.35913	<0.001
TimeT3	-2.56773 *	1.02402	-0.20426	-4.59539 – -0.54007	-0.36392 – -0.04460	-2.50750	0.014
LocationBertraghboi	-11.78461 ***	2.09534	-1.55333	-15.93360 – -7.63563	-2.09465 – -1.01201	-5.62420	<0.001
O2_Av	-0.52164 ***	0.11008	-0.78490	-0.73961 – -0.30367	-1.10954 – -0.46026	-4.73873	<0.001

Sal_Av	-4.59971 ***	1.05033	-1.06059	-6.67947 – -2.51994	-1.53526 – -0.58592	-4.37929	<0.001
Temp_Av	0.75555 ***	0.16331	0.33301	0.43217 – 1.07893	0.19193 – 0.47409	4.62635	<0.001
Salinity_day	-1.35007 ***	0.36349	-0.33736	-2.06981 – -0.63033	-0.51538 – -0.15934	-3.71423	<0.001
Clarity_day	2.43915 ***	0.63406	0.60772	1.18366 – 3.69464	0.29809 – 0.91735	3.84690	<0.001
Observations	130						
R^2 / R^2 adjusted	0.629 / 0.598						

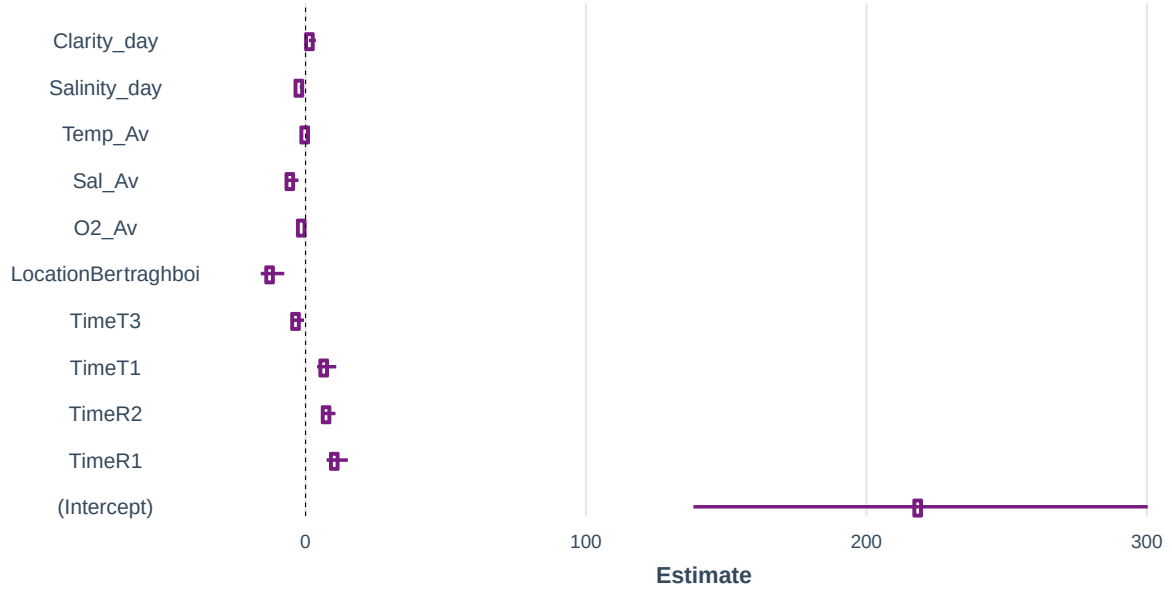

** p<0.05 ** p<0.01 *** p<0.001*

155 *NTI*

156

	Model	Cross-validation Errors
3	NTI ~ TimeR2 + TimeT2 + log_NPqPCR_Av	2.33515
5	NTI ~ TimeR2 + TimeT2 + Length + log_NPqPCR_Av + Temperature_day	2.36332
4	NTI ~ TimeR2 + TimeT2 + log_NPqPCR_Av + Temperature_day	2.36534
7	NTI ~ TimeR1 + TimeR2 + TimeR3 + TimeT2 + LocationCreevin + O2_Av + log_NPqPCR_Av	2.37181
6	NTI ~ TimeR2 + TimeT2 + TimeT4 + Length + log_NPqPCR_Av + Temperature_day	2.37718
8	NTI ~ TimeR1 + TimeR2 + TimeT2 + LocationCreevin + O2_Av + Clarity_Av + log_NPqPCR_Av + Temperature_day	2.42554
2	NTI ~ TimeR2 + TimeT2	2.43255
9	NTI ~ TimeR1 + TimeR2 + TimeT2 + TimeT4 + LocationCreevin + O2_Av + Clarity_Av + log_NPqPCR_Av + Temperature_day	2.43517
10	NTI ~ TimeR1 + TimeR2 + TimeT2 + TimeT4 + LocationCreevin + Weight + O2_Av + Clarity_Av + log_NPqPCR_Av + Temperature_day	2.46413
11	NTI ~ TimeR1 + TimeR2 + TimeT2 + TimeT4 + LocationCreevin + Weight + AGD_score + O2_Av + Clarity_Av + log_NPqPCR_Av + Temperature_day	2.46490
12	NTI ~ TimeR1 + TimeR2 + TimeT2 + TimeT4 + LocationCreevin + LocationGlinsk + Weight + AGD_score + O2_Av + Clarity_Av + log_NPqPCR_Av + Temperature_day	2.46601
13	NTI ~ TimeR1 + TimeR2 + TimeT2 + TimeT4 + LocationCreevin + LocationGlinsk + Weight + AGD_score + O2_Av + Clarity_Av + log_NPqPCR_Av + Temperature_day + Clarity_day	2.46737
14	NTI ~ TimeR1 + TimeR2 + TimeR3 + TimeT2 + TimeT4 + LocationCreevin + LocationGlinsk + Weight + AGD_score + O2_Av + Temp_Av + Clarity_Av + log_NPqPCR_Av + Temperature_day	2.50782
15	NTI ~ TimeR1 + TimeR2 + TimeR3 + TimeT2 + TimeT4 + LocationCreevin + LocationGlinsk + Weight + AGD_score + O2_Av + Temp_Av + Clarity_Av + log_NPqPCR_Av + Temperature_day + Clarity_day	2.50847
1	NTI ~ TimeR2	2.51173
16	NTI ~ TimeR1 + TimeR2 + TimeR3 + TimeR5 + TimeT2 + TimeT4 + LocationCreevin + LocationGlinsk + Weight + AGD_score + O2_Av + Temp_Av + Clarity_Av + log_NPqPCR_Av + Temperature_day + Clarity_day	2.54709
17	NTI ~ TimeR1 + TimeR2 + TimeR3 + TimeR5 + TimeT2 + TimeT4 + LocationCreevin + LocationGlinsk + Weight + Length + AGD_score + O2_Av + Temp_Av + Clarity_Av + log_NPqPCR_Av + Temperature_day + Clarity_day	2.57158

18	NTI ~ TimeR1 + TimeR2 + TimeR3 + TimeR5 + TimeT2 + TimeT4 + LocationCreevin + LocationGlinsk + Weight + Length + AGD_score + O2_Av + Temp_Av + Clarity_Av + log_NPqPCR_Av + Temperature_day + Salinity_day + Clarity_day	2.60475
19	NTI ~ TimeR1 + TimeR2 + TimeR3 + TimeR5 + TimeT2 + TimeT3 + TimeT4 + LocationCreevin + LocationGlinsk + Weight + Length + AGD_score + O2_Av + Temp_Av + Clarity_Av + log_NPqPCR_Av + Temperature_day + Salinity_day + Clarity_day	2.67400
20	NTI ~ TimeR1 + TimeR2 + TimeR3 + TimeR5 + TimeT1 + TimeT2 + TimeT4 + TimeT5 + TimeT6 + LocationPortlea + LocationCreevin + Weight + Length + AGD_score + Sal_Av + Clarity_Av + log_NPqPCR_Av + Temperature_day + O2_day + Clarity_day	2.69210
21	NTI ~ Year2017 + TimeR3 + TimeR4 + TimeR5 + TimeT1 + TimeT3 + TimeT4 + TimeT5 + TimeT6 + LocationCreevin + LocationGlinsk + Weight + Length + AGD_score + Temp_Av + Clarity_Av + log_NPqPCR_Av + Temperature_day + Salinity_day + O2_day + Clarity_day	2.70991
22	NTI ~ Year2017 + TimeR1 + TimeR2 + TimeR3 + TimeR4 + TimeT1 + TimeT2 + TimeT3 + TimeT4 + LocationPortlea + LocationBertraghboi + LocationGlinsk + Weight + Length + AGD_score + O2_Av + Sal_Av + Temp_Av + log_NPqPCR_Av + Salinity_day + O2_day + Clarity_day	2.75448

	NTI						
Predictors	*Estimates*	*std. Error*	*std. Beta*	*CI*	*standardized CI*	*Statistic*	*p*
(Intercept)	5.81018 ***	0.23222		5.35062 – 6.26974		25.01980	**<0.001**
TimeR2	7.45006 ***	0.65494	0.69288	6.15395 – 8.74617	0.57350 – 0.81227	11.37513	**<0.001**
TimeT2	3.70395 ***	0.90278	0.27371	1.91737 – 5.49053	0.14295 – 0.40446	4.10281	**<0.001**
log_NPqPCR_Av	0.13405 ***	0.03871	0.23029	0.05745 – 0.21065	0.09996 – 0.36063	3.46319	**0.001**
Observations	130						
R^2 / R^2 adjusted	0.537 / 0.526						

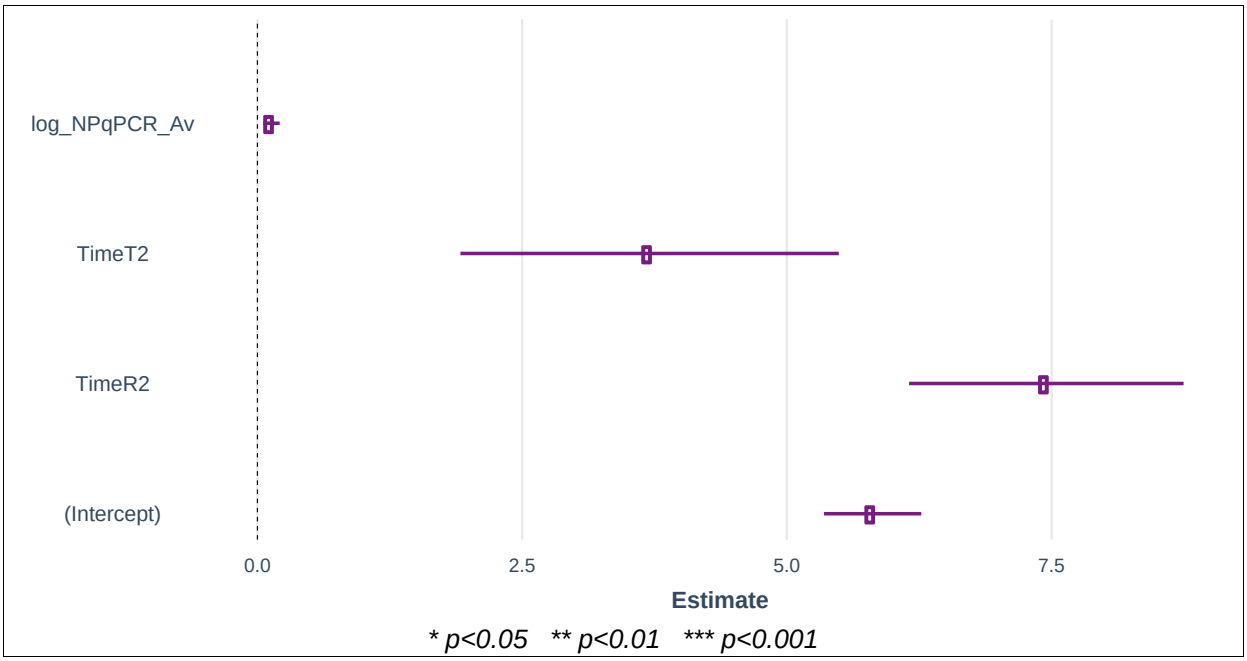
log_NPqPCR_Av
TimeT2
TimeR2
(Intercept)
0.0
2.5
5.0
7.5
Estimate
* p<0.05 ** p<0.01 *** p<0.001

160

LCBD – Bray-Curtis

	Model	Cross-validation Errors
5	LCBD ~ Year2017 + TimeT2 + O2_Av + Salinity_day + Clarity_day	0.00033
8	LCBD ~ TimeR1 + TimeT2 + TimeT5 + LocationPortlea + Sal_Av + Clarity_Av + Salinity_day + O2_day	0.00033
6	LCBD ~ Year2017 + TimeT2 + TimeT5 + O2_Av + Sal_Av + Clarity_day	0.00033
7	LCBD ~ Year2017 + TimeT2 + TimeT5 + O2_Av + Sal_Av + log_NPqPCR_Av + Clarity_day	0.00033
4	LCBD ~ Year2017 + TimeT2 + O2_Av + Clarity_day	0.00033
9	LCBD ~ TimeR1 + TimeT1 + TimeT5 + LocationPortlea + Weight + Sal_Av + Clarity_Av + Salinity_day + O2_day	0.00033
10	LCBD ~ TimeR1 + TimeT1 + TimeT4 + TimeT5 + LocationPortlea + Weight + Sal_Av + Clarity_Av + Salinity_day + O2_day	0.00034
3	LCBD ~ TimeT2 + TimeT6 + O2_Av	0.00034
11	LCBD ~ TimeR1 + TimeT1 + TimeT4 + TimeT5 + LocationPortlea + LocationBertraghboi + Weight + Sal_Av + Clarity_Av + Salinity_day + O2_day	0.00034
2	LCBD ~ TimeT2 + O2_Av	0.00034
12	LCBD ~ TimeR1 + TimeT1 + TimeT4 + TimeT5 + LocationPortlea + LocationBertraghboi + Weight + O2_Av + Sal_Av + Clarity_Av + Salinity_day + O2_day	0.00034
1	LCBD ~ TimeT2	0.00035
14	LCBD ~ TimeR1 + TimeR4 + TimeT1 + TimeT4 + TimeT5 + LocationPortlea + Weight + Length + Sal_Av + Clarity_Av + log_NPqPCR_Av + Salinity_day + O2_day + Clarity_day	0.00035
15	LCBD ~ TimeR1 + TimeR2 + TimeR4 + TimeT1 + TimeT4 + TimeT5 + LocationPortlea + Weight + Length + Sal_Av + Clarity_Av + log_NPqPCR_Av + Salinity_day + O2_day + Clarity_day	0.00036
13	LCBD ~ TimeR1 + TimeR2 + TimeR3 + TimeR5 + TimeT2 + TimeT6 + Weight + O2_Av + Sal_Av + Temp_Av + Temperature_day + Salinity_day + Clarity_day	0.00036
17	LCBD ~ TimeT1 + TimeT3 + TimeT4 + TimeT5 + LocationBertraghboi + LocationGlinsk + Weight + Length + O2_Av + Sal_Av + Temp_Av + Clarity_Av + log_NPqPCR_Av + Temperature_day + Salinity_day + O2_day + Clarity_day	0.00037
16	LCBD ~ TimeR1 + TimeR2 + TimeR3 + TimeR5 + TimeT2 + TimeT6 + LocationCreevin + Weight + Length + O2_Av + Sal_Av + Temp_Av + log_NPqPCR_Av + Temperature_day + Salinity_day + Clarity_day	0.00037
19	LCBD ~ TimeR1 + TimeR2 + TimeR4 + TimeT1 + TimeT3 +	0.00037

	TimeT4 + TimeT5 + LocationPortlea + LocationCreevin + LocationGlinsk + Weight + Length + AGD_score + Clarity_Av + log_NPqPCR_Av + Temperature_day + Salinity_day + O2_day + Clarity_day	
18	LCBD ~ TimeR1 + TimeR2 + TimeR3 + TimeR5 + TimeT2 + TimeT3 + TimeT6 + LocationCreevin + Weight + Length + AGD_score + O2_Av + Sal_Av + Temp_Av + log_NPqPCR_Av + Temperature_day + Salinity_day + Clarity_day	0.00038
21	LCBD ~ Year2018 + TimeR1 + TimeR3 + TimeR4 + TimeR5 + TimeT1 + TimeT2 + TimeT3 + TimeT5 + TimeT6 + LocationBertraghboi + LocationCreevin + LocationGlinsk + Length + O2_Av + Sal_Av + Temp_Av + Temperature_day + Salinity_day + O2_day + Clarity_day	0.00039
20	LCBD ~ Year2017 + TimeR2 + TimeR3 + TimeR4 + TimeR5 + TimeT1 + TimeT3 + TimeT5 + TimeT6 + LocationPortlea + LocationCreevin + LocationGlinsk + O2_Av + Sal_Av + Temp_Av + Clarity_Av + log_NPqPCR_Av + Temperature_day + O2_day + Clarity_day	0.00040
22	LCBD ~ Year2017 + TimeR1 + TimeR2 + TimeR3 + TimeR4 + TimeT1 + TimeT2 + TimeT3 + TimeT4 + TimeT5 + LocationPortlea + LocationGlinsk + Weight + Length + AGD_score + O2_Av + Sal_Av + Temp_Av + log_NPqPCR_Av + Temperature_day + O2_day + Clarity_day	0.00040

	LCBD						
Predictors	*Estimates*	*std. Error*	*std. Beta*	*CI*	*standardized CI*	*Statistic*	*p*
(Intercept)	-0.00121	0.00184		-0.00486 – 0.00244		-0.65776	0.512
Year2017	0.00034 ***	0.00010	0.42900	0.00015 – 0.00053	0.18708 – 0.67092	3.47563	**0.001**
TimeT2	0.00089 ***	0.00015	0.57520	0.00059 – 0.00119	0.38253 – 0.76787	5.85136	**<0.001**
O2_Av	0.00003 ***	0.00001	0.45963	0.00002 – 0.00004	0.28305 – 0.63622	5.10155	**<0.001**
Salinity_day	0.00011 *	0.00005	0.27288	0.00002 – 0.00021	0.03831 – 0.50745	2.28007	**0.024**
Clarity_day	-0.00012 **	0.00004	-0.29756	-0.00021 – -0.00004	-0.49951 – -0.09561	-2.88786	**0.005**
Observations	130						
R^2 / R^2 adjusted	0.336 / 0.309						

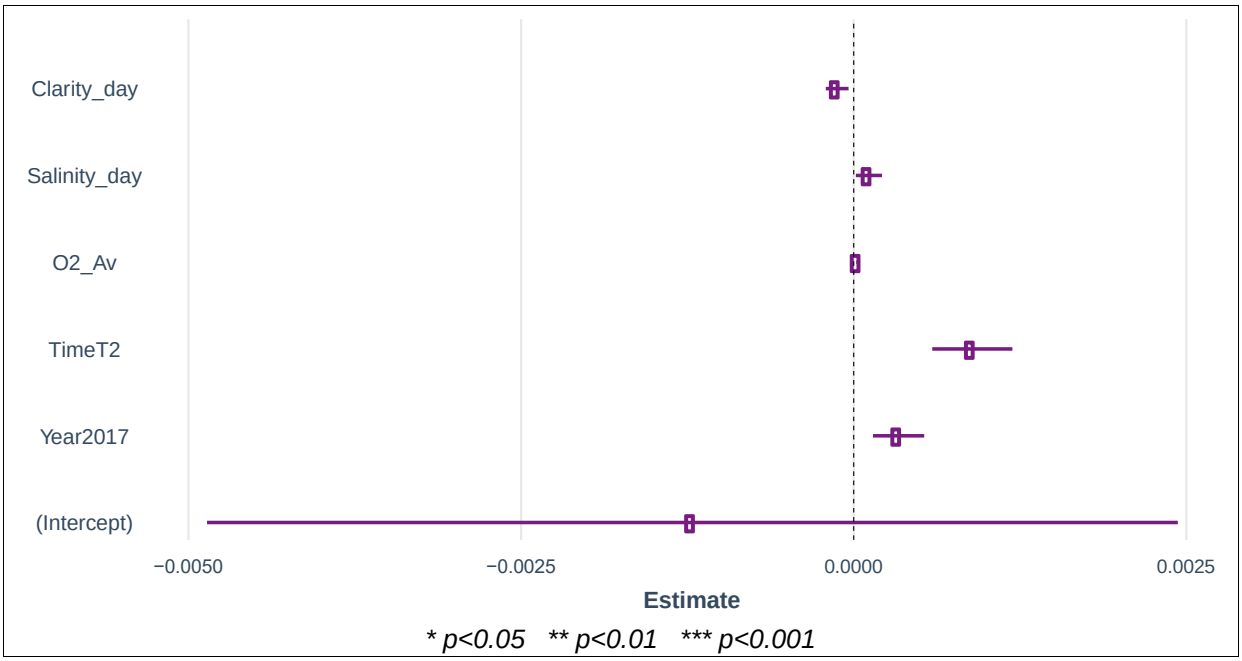
Clarity_day
Salinity_day
O2_Av
TimeT2
Year2017
(Intercept)
−0.0050
−0.0025
0.0000
0.0025
Estimate
* p<0.05 ** p<0.01 *** p<0.001

196 *LCBD – UniFrac*

197

	Model	Cross-validation Errors
6	LCBD ~ Year2017 + TimeR2 + TimeT1 + TimeT2 + TimeT6 + AGD_score	0.00032
5	LCBD ~ Year2017 + TimeR2 + TimeT1 + TimeT2 + TimeT6	0.00032
7	LCBD ~ Year2017 + TimeR2 + TimeR4 + TimeT1 + TimeT2 + TimeT6 + AGD_score	0.00032
4	LCBD ~ Year2017 + TimeR2 + TimeT2 + TimeT6	0.00032
3	LCBD ~ Year2018 + TimeR2 + TimeT2	0.00032
8	LCBD ~ TimeR1 + TimeR3 + TimeT6 + LocationBertraghboi + AGD_score + Sal_Av + Temperature_day + Salinity_day	0.00032
11	LCBD ~ TimeR3 + TimeR5 + LocationPortlea + LocationBertraghboi + LocationCreevin + AGD_score + O2_Av + Temp_Av + Clarity_Av + Temperature_day + Clarity_day	0.00032
10	LCBD ~ TimeT1 + TimeT6 + LocationPortlea + LocationBertraghboi + LocationCreevin + Temp_Av + Clarity_Av + Temperature_day + O2_day + Clarity_day	0.00033
12	LCBD ~ TimeR3 + TimeR4 + TimeT6 + LocationPortlea + LocationBertraghboi + LocationGlinsk + AGD_score + O2_Av + Temp_Av + Clarity_Av + Temperature_day + Clarity_day	0.00033
13	LCBD ~ TimeR3 + TimeR4 + TimeT6 + LocationPortlea + LocationBertraghboi + LocationGlinsk + AGD_score + O2_Av + Temp_Av + Clarity_Av + Temperature_day + Salinity_day + Clarity_day	0.00033
9	LCBD ~ TimeR1 + TimeR3 + TimeT3 + TimeT6 + LocationBertraghboi + AGD_score + Sal_Av + Temperature_day + Salinity_day	0.00033
14	LCBD ~ TimeR3 + TimeR4 + TimeT6 + LocationPortlea + LocationBertraghboi + LocationGlinsk + AGD_score + O2_Av + Temp_Av + Clarity_Av + Temperature_day + Salinity_day + O2_day + Clarity_day	0.00033
15	LCBD ~ TimeR3 + TimeR4 + TimeT6 + LocationBertraghboi + LocationCreevin + LocationGlinsk + AGD_score + O2_Av + Temp_Av + Clarity_Av + log_NPqPCR_Av + Temperature_day + Salinity_day + O2_day + Clarity_day	0.00033
2	LCBD ~ Year2017 + TimeT2	0.00033
16	LCBD ~ TimeR3 + TimeR4 + TimeT5 + TimeT6 + LocationPortlea + LocationBertraghboi + LocationCreevin + AGD_score + O2_Av + Temp_Av + Clarity_Av + log_NPqPCR_Av + Temperature_day + Salinity_day + O2_day + Clarity_day	0.00033
17	LCBD ~ Year2017 + TimeR3 + TimeR4 + TimeT5 + TimeT6 + LocationPortlea + LocationBertraghboi + LocationGlinsk + Length + AGD_score + O2_Av + Temp_Av + Clarity_Av +	0.00034

	log_NPqPCR_Av + Temperature_day + Salinity_day + Clarity_day	
18	LCBD ~ Year2018 + TimeR3 + TimeR4 + TimeT5 + TimeT6 + LocationBertraghboi + LocationCreevin + LocationGlinsk + Weight + Length + AGD_score + O2_Av + Temp_Av + Clarity_Av + log_NPqPCR_Av + Temperature_day + Salinity_day + Clarity_day	0.00034
1	LCBD ~ Year2017	0.00034
19	LCBD ~ Year2017 + TimeR1 + TimeR2 + TimeR5 + TimeT1 + TimeT2 + TimeT4 + TimeT5 + LocationPortlea + LocationGlinsk + Weight + Length + AGD_score + Sal_Av + Temp_Av + Clarity_Av + log_NPqPCR_Av + Temperature_day + O2_day	0.00035
21	LCBD ~ Year2018 + TimeR1 + TimeR2 + TimeR3 + TimeR5 + TimeT1 + TimeT2 + TimeT3 + TimeT4 + TimeT6 + LocationPortlea + LocationBertraghboi + LocationGlinsk + AGD_score + O2_Av + Temp_Av + log_NPqPCR_Av + Temperature_day + Salinity_day + O2_day + Clarity_day	0.00035
22	LCBD ~ Year2017 + TimeR1 + TimeR2 + TimeR3 + TimeR4 + TimeT1 + TimeT2 + TimeT3 + TimeT4 + LocationBertraghboi + LocationCreevin + LocationGlinsk + Weight + Length + AGD_score + O2_Av + Temp_Av + Clarity_Av + log_NPqPCR_Av + Temperature_day + O2_day + Clarity_day	0.00036
20	LCBD ~ Year2018 + TimeR2 + TimeR3 + TimeR4 + TimeR5 + TimeT2 + TimeT3 + TimeT4 + TimeT5 + TimeT6 + LocationPortlea + LocationBertraghboi + LocationGlinsk + Length + O2_Av + Temp_Av + Temperature_day + Salinity_day + O2_day + Clarity_day	0.00036

	LCBD						
Predictors	*Estimates*	*std. Error*	*std. Beta*	*CI*	*standardized CI*	*Statistic*	*p*
(Intercept)	0.00480 ***	0.00006		0.00468 – 0.00492		81.93583	**<0.001**
Year2017	0.00038 ***	0.00007	0.45420	0.00023 – 0.00052	0.28362 – 0.62479	5.21872	**<0.001**
TimeR2	0.00023 *	0.00010	0.17969	0.00004 – 0.00042	0.03264 – 0.32673	2.39499	**0.018**
TimeT1	0.00016	0.00013	0.10049	-0.00009 – 0.00041	-0.05217 – 0.25315	1.29022	0.199
TimeT2	0.00041 **	0.00013	0.24895	0.00015 – 0.00066	0.09629 – 0.40161	3.19626	**0.002**
TimeT6	0.00028 **	0.00010	0.21863	0.00009 – 0.00048	0.06802 – 0.36924	2.84518	**0.005**
AGD_score	-0.00003	0.00003	-0.08185	-0.00010 –	-0.23246 –	-1.06522	0.289

				0.00003	0.06875		
Observations	130						
R^2 / R^2 adjusted	0.431 / 0.404						

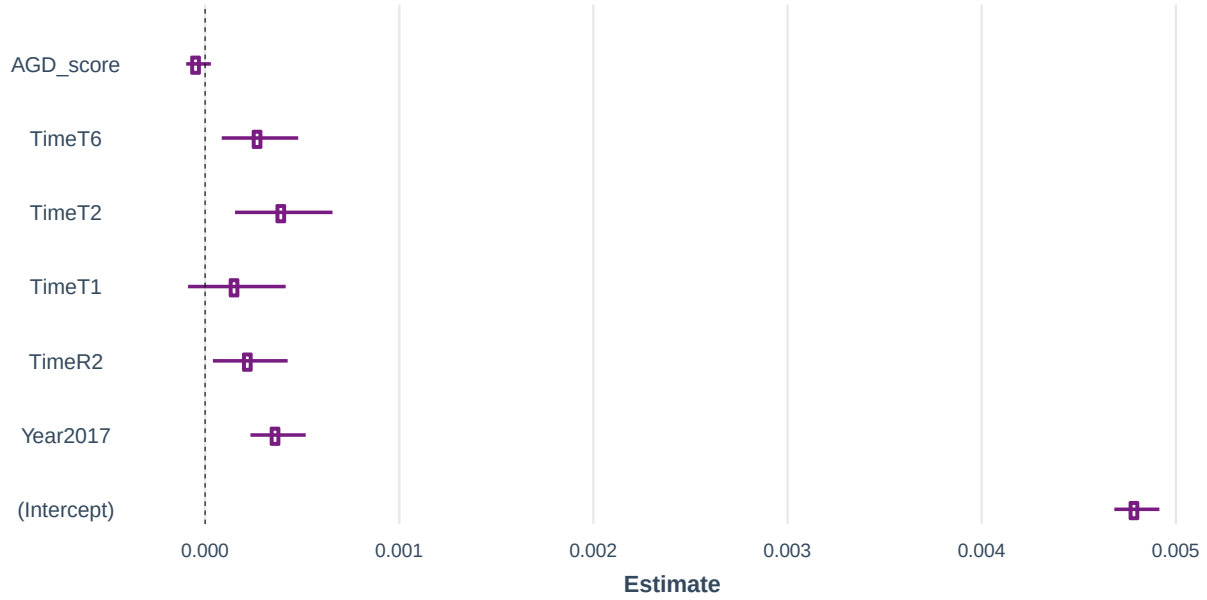

** p<0.05 ** p<0.01 *** p<0.001*

201

LCBD – Weighted UniFrac

	Model	Cross-validation Errors
8	LCBD ~ TimeR2 + TimeR3 + TimeT2 + TimeT4 + LocationCreevin + LocationGlinsk + Length + Clarity_Av	0.00093
7	LCBD ~ TimeR2 + TimeR3 + TimeT2 + LocationCreevin + LocationGlinsk + Length + Clarity_Av	0.00093
10	LCBD ~ TimeR2 + TimeT3 + TimeT4 + TimeT5 + LocationCreevin + LocationGlinsk + Length + Temp_Av + Clarity_Av + Salinity_day	0.00093
11	LCBD ~ TimeR2 + TimeR3 + TimeT3 + TimeT4 + TimeT5 + LocationCreevin + LocationGlinsk + Length + Temp_Av + Clarity_Av + Salinity_day	0.00093
9	LCBD ~ TimeR2 + TimeT3 + TimeT4 + TimeT5 + LocationCreevin + LocationGlinsk + Length + Temp_Av + Clarity_Av	0.00093
12	LCBD ~ TimeR2 + TimeT1 + TimeT4 + TimeT5 + LocationBertraghboi + Weight + Length + Sal_Av + Clarity_Av + log_NPqPCR_Av + Salinity_day + Clarity_day	0.00094
6	LCBD ~ TimeR2 + TimeT2 + LocationCreevin + LocationGlinsk + Length + Clarity_Av	0.00094
13	LCBD ~ Year2018 + TimeR1 + TimeR2 + TimeT1 + TimeT6 + LocationCreevin + LocationGlinsk + Length + AGD_score + Sal_Av + Clarity_Av + Temperature_day + Salinity_day	0.00094
14	LCBD ~ Year2017 + TimeR1 + TimeR2 + TimeT3 + TimeT6 + LocationPortlea + LocationGlinsk + Length + AGD_score + Sal_Av + Clarity_Av + Temperature_day + Salinity_day + Clarity_day	0.00095
5	LCBD ~ TimeR2 + LocationCreevin + LocationGlinsk + Length + Clarity_Av	0.00095
15	LCBD ~ Year2017 + TimeR1 + TimeR2 + TimeT3 + TimeT6 + LocationBertraghboi + Weight + Length + AGD_score + Sal_Av + Clarity_Av + log_NPqPCR_Av + Temperature_day + Salinity_day + Clarity_day	0.00096
18	LCBD ~ TimeR2 + TimeR3 + TimeR4 + TimeR5 + TimeT3 + TimeT6 + LocationBertraghboi + Weight + Length + AGD_score + O2_Av + Sal_Av + Temp_Av + Clarity_Av + log_NPqPCR_Av + Temperature_day + Salinity_day + Clarity_day	0.00097
17	LCBD ~ Year2018 + TimeR1 + TimeR2 + TimeT3 + TimeT4 + TimeT5 + LocationPortlea + LocationCreevin + LocationGlinsk + Weight + Length + AGD_score + Sal_Av + Clarity_Av + log_NPqPCR_Av + Temperature_day + O2_day	0.00097
4	LCBD ~ TimeR2 + LocationCreevin + Length + Clarity_Av	0.00097
16	LCBD ~ Year2018 + TimeR1 + TimeR2 + TimeT3 + TimeT4 + TimeT5 + LocationBertraghboi + LocationCreevin + Weight +	0.00097

	Length + AGD_score + Sal_Av + Clarity_Av + log_NPqPCR_Av + Temperature_day + O2_day	
19	LCBD ~ Year2018 + TimeR1 + TimeR2 + TimeT3 + TimeT4 + TimeT5 + LocationPortlea + LocationCreevin + LocationGlinsk + Weight + Length + AGD_score + Sal_Av + Temp_Av + Clarity_Av + log_NPqPCR_Av + Temperature_day + O2_day + Clarity_day	0.00098
20	LCBD ~ Year2018 + TimeR1 + TimeR2 + TimeT2 + TimeT3 + TimeT4 + TimeT6 + LocationBertraghboi + LocationGlinsk + Weight + Length + AGD_score + O2_Av + Sal_Av + Clarity_Av + log_NPqPCR_Av + Temperature_day + Salinity_day + O2_day + Clarity_day	0.00099
3	LCBD ~ TimeR1 + LocationGlinsk + Length	0.00099
21	LCBD ~ Year2018 + TimeR1 + TimeR3 + TimeR4 + TimeR5 + TimeT1 + TimeT2 + TimeT3 + TimeT4 + LocationBertraghboi + LocationCreevin + Weight + Length + O2_Av + Sal_Av + Temp_Av + Clarity_Av + Temperature_day + Salinity_day + O2_day + Clarity_day	0.00099
2	LCBD ~ TimeR1 + Length	0.00099
22	LCBD ~ Year2017 + TimeR1 + TimeR2 + TimeR3 + TimeR4 + TimeT1 + TimeT2 + TimeT3 + TimeT4 + TimeT5 + LocationPortlea + LocationBertraghboi + LocationCreevin + Weight + Length + AGD_score + O2_Av + Sal_Av + Clarity_Av + log_NPqPCR_Av + O2_day + Clarity_day	0.00100
1	LCBD ~ Length	0.00103

	LCBD						
Predictors	*Estimates*	*std. Error*	*std. Beta*	*CI*	*standardized CI*	*Statistic*	*p*
(Intercept)	-0.00476 *	0.00233		-0.00937 – -0.00016		-2.04698	**0.043**
TimeR2	-0.00190 ***	0.00037	-0.50889	-0.00263 – -0.00118	-0.70026 – -0.31752	-5.21198	**<0.001**
TimeR3	0.00069	0.00037	0.15296	-0.00005 – 0.00142	-0.00938 – 0.31530	1.84677	0.067
TimeT2	0.00064	0.00035	0.13523	-0.00005 – 0.00133	-0.00974 – 0.28019	1.82827	0.070
TimeT4	-0.00053	0.00037	-0.10066	-0.00127 – 0.00021	-0.23925 – 0.03793	-1.42360	0.157
LocationCreevin	0.00434 ***	0.00091	0.92279	0.00255 – 0.00613	0.54565 – 1.29994	4.79558	**<0.001**
LocationGlinsk	0.00151 ***	0.00042	0.48941	0.00067 – 0.00234	0.22117 – 0.75765	3.57597	**0.001**
Length	-0.00006 ***	0.00001	-0.42057	-0.00009 – -0.00004	-0.59872 – -0.24243	-4.62721	**<0.001**

Clarity_Av	0.00200 ***	0.00038	1.02225	0.00125 – 0.00276	0.64124 – 1.40325	5.25866	**<0.001**
Observations	130						
R^2 / R^2 adjusted	0.432 / 0.395						

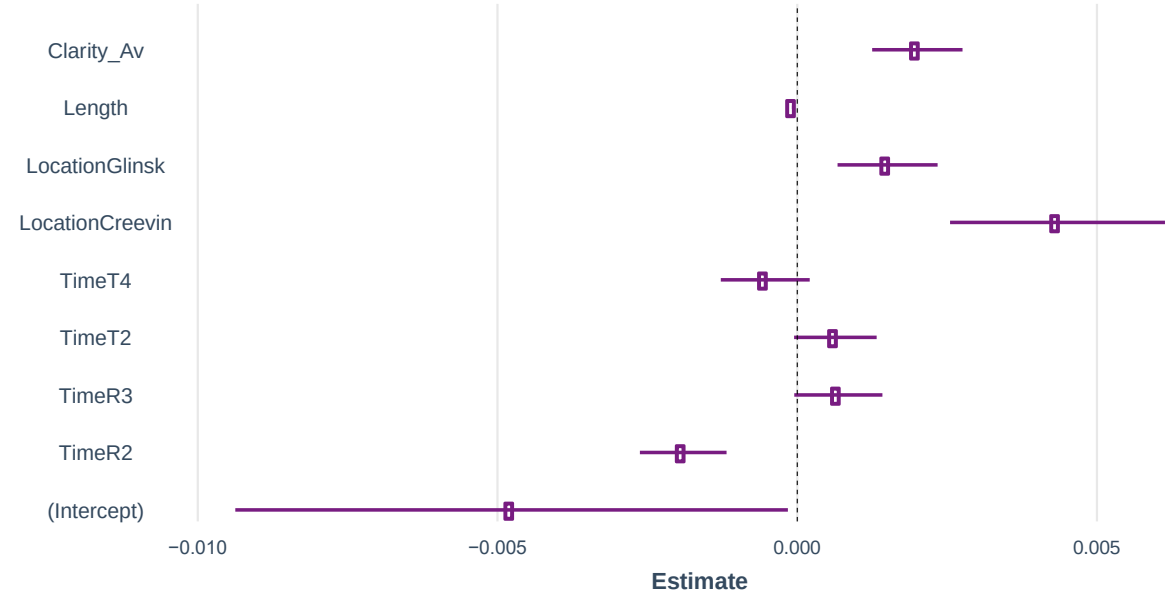

** p<0.05 ** p<0.01 *** p<0.001*

*Log_*Neoparamoeba perurans *qPCR*

	Model	Cross-validation Errors
9	log_NPqPCR_Av ~ TimeR3 + TimeR4 + TimeR5 + TimeT1 + TimeT2 + TimeT4 + O2_Av + Clarity_Av + O2_day	4.14320
11	log_NPqPCR_Av ~ TimeR3 + TimeR4 + TimeR5 + TimeT1 + TimeT2 + TimeT3 + TimeT4 + Weight + O2_Av + Clarity_Av + O2_day	4.14983
10	log_NPqPCR_Av ~ TimeR3 + TimeR4 + TimeR5 + TimeT1 + TimeT2 + TimeT3 + TimeT4 + O2_Av + Clarity_Av + O2_day	4.15788
5	log_NPqPCR_Av ~ TimeT1 + TimeT2 + TimeT4 + LocationGlinsk + AGD_score	4.15829
7	log_NPqPCR_Av ~ Year2018 + TimeR5 + TimeT1 + TimeT2 + TimeT4 + Clarity_Av + Clarity_day	4.17481
6	log_NPqPCR_Av ~ TimeR5 + TimeT1 + TimeT2 + TimeT4 + Clarity_Av + Clarity_day	4.20600
4	log_NPqPCR_Av ~ TimeT1 + TimeT2 + LocationGlinsk + AGD_score	4.26949
8	log_NPqPCR_Av ~ Year2018 + TimeR5 + TimeT1 + TimeT2 + TimeT4 + LocationPortlea + O2_Av + Clarity_day	4.29291
12	log_NPqPCR_Av ~ Year2018 + TimeR2 + TimeR5 + TimeT1 + TimeT2 + TimeT4 + TimeT5 + LocationPortlea + LocationCreevin + Weight + O2_Av + Clarity_day	4.34602
3	log_NPqPCR_Av ~ TimeT1 + TimeT2 + LocationGlinsk	4.38078
13	log_NPqPCR_Av ~ Year2017 + TimeR2 + TimeR5 + TimeT1 + TimeT2 + TimeT4 + TimeT5 + LocationBertraghboi + LocationCreevin + LocationGlinsk + Weight + O2_Av + Clarity_day	4.38897
14	log_NPqPCR_Av ~ Year2018 + TimeR2 + TimeR5 + TimeT1 + TimeT2 + TimeT4 + TimeT5 + LocationPortlea + LocationBertraghboi + LocationCreevin + Weight + AGD_score + O2_Av + Clarity_day	4.41551
17	log_NPqPCR_Av ~ TimeR3 + TimeR4 + TimeR5 + TimeT1 + TimeT2 + TimeT3 + TimeT4 + TimeT5 + LocationPortlea + LocationBertraghboi + LocationCreevin + Weight + AGD_score + O2_Av + Temperature_day + O2_day + Clarity_day	4.43987
20	log_NPqPCR_Av ~ Year2018 + TimeR1 + TimeR2 + TimeR3 + TimeR4 + TimeR5 + TimeT1 + TimeT2 + TimeT3 + TimeT4 + TimeT6 + LocationPortlea + LocationCreevin + LocationGlinsk + Weight + AGD_score + O2_Av + Temperature_day + O2_day + Clarity_day	4.44761
2	log_NPqPCR_Av ~ TimeT1 + TimeT2	4.45730
15	log_NPqPCR_Av ~ Year2018 + TimeR2 + TimeR5 + TimeT1 + TimeT2 + TimeT4 + TimeT5 + LocationPortlea + LocationCreevin + Weight + AGD_score + O2_Av + Sal_Av +	4.45948

	Salinity_day + Clarity_day	
16	log_NPqPCR_Av ~ Year2018 + TimeR1 + TimeR2 + TimeR5 + TimeT1 + TimeT2 + TimeT4 + TimeT5 + LocationPortlea + LocationGlinsk + Weight + AGD_score + O2_Av + Sal_Av + Salinity_day + Clarity_day	4.46309
19	log_NPqPCR_Av ~ Year2017 + TimeR2 + TimeR4 + TimeR5 + TimeT2 + TimeT3 + TimeT4 + TimeT5 + TimeT6 + LocationPortlea + LocationCreevin + LocationGlinsk + Weight + Length + AGD_score + O2_Av + Temp_Av + Clarity_Av + Clarity_day	4.49990
18	log_NPqPCR_Av ~ Year2018 + TimeR2 + TimeR3 + TimeR5 + TimeT3 + TimeT4 + TimeT5 + TimeT6 + LocationPortlea + LocationBertraghboi + Weight + Length + AGD_score + O2_Av + Sal_Av + Temp_Av + O2_day + Clarity_day	4.53162
21	log_NPqPCR_Av ~ Year2017 + TimeR1 + TimeR2 + TimeR3 + TimeR4 + TimeT1 + TimeT2 + TimeT3 + TimeT5 + TimeT6 + LocationCreevin + Weight + Length + AGD_score + O2_Av + Sal_Av + Temp_Av + Clarity_Av + Temperature_day + Salinity_day + O2_day	4.58615
1	log_NPqPCR_Av ~ TimeT1	5.42813

	log_NPqPCR_Av						
Predictors	*Estimates*	*std. Error*	*std. Beta*	*CI*	*standardized CI*	*Statistic*	*p*
(Intercept)	8.38985	6.80074		-5.05231 – 21.83202		1.23367	0.219
TimeR3	3.07463 *	1.41432	0.12171	0.27912 – 5.87014	0.01198 – 0.23144	2.17393	**0.031**
TimeR4	3.74368 **	1.35184	0.14819	1.07168 – 6.41569	0.04331 – 0.25307	2.76933	**0.006**
TimeR5	-4.81117 ***	1.31920	-0.22916	-7.41866 – -2.20368	-0.35232 – -0.10601	-3.64705	**<0.001**
TimeT1	-11.03216 ***	1.10157	-0.52548	-13.20950 – -8.85483	-0.62832 – -0.42264	-10.01496	**<0.001**
TimeT2	-11.51534 ***	1.10706	-0.54849	-13.70352 – -9.32717	-0.65185 – -0.44514	-10.40178	**<0.001**
TimeT4	-3.74946 ***	1.11013	-0.17859	-5.94371 – -1.55521	-0.28223 – -0.07496	-3.37751	**0.001**
O2_Av	-0.26631 *	0.10545	-0.22736	-0.47475 – -0.05788	-0.40382 – -0.05091	-2.52542	**0.013**
Clarity_Av	-1.84517 **	0.69163	-0.17400	-3.21222 – -0.47811	-0.30182 – -0.04617	-2.66786	**0.009**
O2_day	0.30272 ***	0.07318	0.34980	0.15807 – 0.44737	0.18406 – 0.51555	4.13646	**<0.001**
Observations	154						

R^2 / R^2 adjusted	0.640 / 0.618

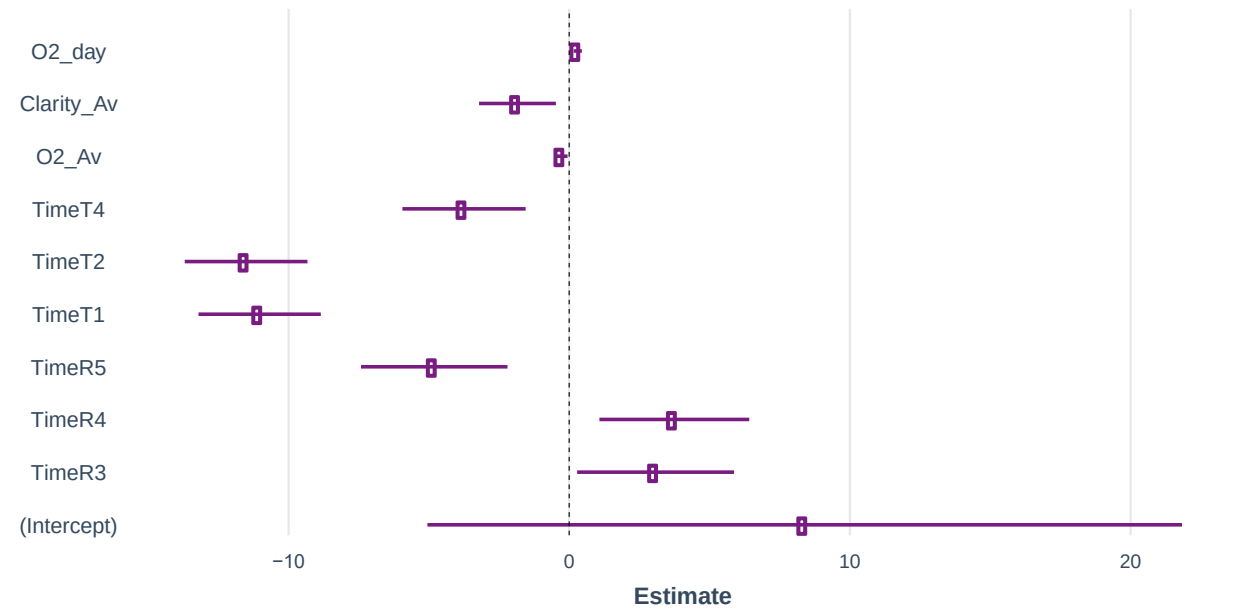

** p<0.05 ** p<0.01 *** p<0.001*

Table S4.2: Most Abundant and Relevant OTUs (Operational Taxonomical Units) Description. This table show the top 25 most abundant OTUs/Genus, the core prokaryotic microbiome, as well as some interesting taxa with significant geographical distribution from every sampled fish farm. The location of the fish farm where the taxa had a significantly higher relative abundance is showed in the "Fish farm" column.

OTU/Genera	Fish farm	Description
Rubritalea	Widely present. Significantly higher in Roancarrig, Creevin and Portlea.	It was found on Atlantic salmon, seabram and seabass gills, skin and guts [1, 2, 3, 4], even on some salmon affected by epitheliocystis [2] and AGD [1].
Photobacterium	Widely present. Very abundant at every sampling round, except at R2.	This taxa was identified as the most probable causative agent of a disease on skin and gills in seabass [4], also present in AGD mucous microbiome from Atlantic salmon [1, 5]. Part of the core microbiome in guts from many bony fish [6, 7].
Aeromonas	Widely present. Significantly higher in Glinsk.	Present in the gut microbiome from semi-natural Atlantic salmons [8]. Also main causative genera (*A. salmonicida*) of furunculosis in salmonids [9].
Alteromonadales	Widely present.	Associated with the skin [10] and mucous microbiomes [1, 11] on Atlantic salmon in seawater.
Rhodobacteraceae	Widely present. Significantly higher in Portlea and Bertraghboi.	It is part of the core gut microbiome in Atlantic salmon [12, 13].
Endozoicomonas	Widely present. Significantly higher in Bertraghboi, Glinsk and Portlea.	First described as a causative agent for epitheliocystis [14], even on Atlantic salmon gills [5, 15].
C. Branchiomonas cysticola	Widely present. Significantly higher in Creevin.	Very common agent of Epitheliocystis on Atlantic salmon gills [16]. This genus was found associated with "Proliferative Gill Inflammation" (PGI) and "Complex Gill Disease" (CGD) [17].
Psychrobacter	Widely present.	This genus was found on affected and non-affected AGD Atlantic salmon [1, 5], gut [18], skin [10], and even kidney [19].
Tenacibaculum maritimum	Significantly higher in Creevin.	Is the causative agent of tenacibaculisis, especially at low water [17]. Was found on skin, gill and salmon fins [1, 20], even in freshwater [10].
Vibrio	Widely present. Very abundant at R2.	*Vibrio* sp. was found to appear on Atlantic salmon gills [1], epidermal mucous [21] and gastrointestinal microbiome [22].
Flavobacterium	Significantly higher in Roancarrig and Glinsk.	This genus appeared before on Atlantic salmon gills [1, 5], gut [3], and skin [10].
Pseudomonas	Widely present. Significantly higher in Roancarrig, Creevin and Glinsk.	Was present in Atlantic salmon [3], gills [1, 5], and even in freshwater salmon skin [10].

C. Fritschea	Widely present. Significantly higher in Bertraghboi.	Was found to be very close to other gill pathogens in Atlantic salmon [23], such as *Candidatus* Syngnamydia venezia and *Candidatus* Syngnamydia salmonis [24, 25], associated with *Paramoeba perurans*.
Shewanella	Widely present.	This genus was found in Atlantic cod intestine [26], and in other fish skin and gill microbiome studies [1, 27, 28].
Pedobacter	Significantly higher in Glinsk.	This genus appears in the gut microbiome of some tropical fish [29] with *Bacillus* and *Vibrio* species too.
Synechococcus	Significantly higher in Roancarrig.	This genus was found in Atlantic mackerel gills [27], and in Chinook salmon gut microbiome [30].
Marinobacter	Significantly higher in Glinsk and Creevin.	This genus was detected in AGD affected and non-affected Atlantic salmon gills [1, 5]. In another study [31], was associated with *Paramoeba perurans* cultures.
Lactobacillus	Significantly higher in Glinsk and Portlea.	Is a genus very commonly present with high abundance in skin [32] and gut [33] microbiome of different fish.
Bifidobacterium	Significantly higher in Roancarrig.	This bacteria was not related with fish microbiome before, but is commonly used as a potential probiotic for fish [34].
Dyadobacter	Significantly higher in Roancarrig.	This genus was found on the surface of Lake Sturgeon eggs after an iodine disinfection treatment [35].
Piscichlamydia	Significantly higher in Glinsk.	This genus was found to have a positive association with the "Proliferative Gill Inflammation" [15] on Atlantic salmon gills. Was also related with Epitheliocystis [36].

References

1. Birlanga, V. B., McCormack, G., Ijaz, U. Z., McCarthy, E., Smith, C., & Collins, G. (2021). Dynamic Gill and Mucous Microbiomes Track an Amoebic Gill Disease Episode in Farmed Atlantic Salmon. (https://assets.researchsquare.com/files/rs-29747/v1/33663208-b035-433d617bf44-59125d163937.pdf).

2. Soto MG, Vidondo B, Vaughan L, Seth-Smith HM, Nufer L, Segner H, Rubin JF, Schmidt-Posthaus H. The emergence of epitheliocystis in the upper Rhone region: evidence for Chlamydiae in wild and farmed salmonid populations. Archives of microbiology. 2016;198(4):315-24.

3. Wang C, Sun G, Li S, Li X, Liu Y. Intestinal microbiota of healthy and unhealthy Atlantic salmon *Salmo salar* L. in a recirculating aquaculture system. Journal of Oceanology and Limnology. 2018;36(2):414-26.

4. Rosado D, Perez-Losada M, Severino R, Cable J, Xavier R. Characterization of the skin and gill microbiomes of the farmed seabass (*Dicentrarchus labrax*) and seabream (*Sparus aurata*). Aquaculture. 2019;500:57-64.

5. Bowman JP, Nowak B. Salmonid gill bacteria and their relationship to amoebic gill disease. Journal of Fish Diseases. 2004;27(8):483-92.

6. Givens CE, Ransom B, Bano N, Hollibaugh JT. Comparison of the gut microbiomes of 12 bony fish and 3 shark species. Marine Ecology Progress Series. 2015;518:209-23.

7. Sullam KE, Essinger SD, Lozupone CA, O'CONNOR MP, Rosen GL, Knight RO, Kilham SS, Russell JA. Environmental and ecological factors that shape the gut bacterial communities of fish: a meta-analysis. Molecular ecology. 2012;21(13):3363-78.

8. Uren Webster TM, Rodriguez-Barreto D, Castaldo G, Gough P, Consuegra S, Garcia de Leaniz C. Environmental plasticity and colonisation history in the Atlantic salmon microbiome: a translocation experiment. Molecular ecology. 2020;29(5):886-98.

9. Jutfelt F, Olsen RE, Glette J, Ringø E, Sundell K. Translocation of viable Aeromonas salmonicida across the intestine of rainbow trout, *Oncorhynchus mykiss* (Walbaum). Journal of fish diseases. 2006;29(5):255-62.

10. Lokesh J, Kiron V. Transition from freshwater to seawater reshapes the skin-associated microbiota of Atlantic salmon. Scientific reports. 2016;6:19707.

11. Llewellyn MS, Leadbeater S, Garcia C, Sylvain FE, Custodio M, Ang KP, Powell F, Carvalho GR, Creer S, Elliot J, Derome N. Parasitism perturbs the mucosal microbiome of Atlantic Salmon. Scientific reports. 2017;7:43465.

12. He X, Chaganti SR, Heath DD. Population-specific responses to interspecific competition in the gut microbiota of two Atlantic Salmon (*Salmo salar*) populations. Microbial ecology. 2018;75(1):140-51.

13. Webster TM, Consuegra S, Hitchings M, de Leaniz CG. Interpopulation variation in the Atlantic salmon microbiome reflects environmental and genetic diversity. Appl. Environ. Microbiol.. 2018;84(16):e00691-18.

14. Mendoza M, Güiza L, Martinez X, Caraballo X, Rojas J, Aranguren LF, Salazar M. A novel agent (*Endozoicomonas elysicola*) responsible for epitheliocystis in cobia *Rachycentrum canadum* larvae. Diseases of aquatic organisms. 2013;106(1):31-7.

15. Steinum T, Sjåstad K, Falk K, Kvellestad A, Colquhoun DJ. An RT PCR-DGGE survey of gill-associated bacteria in Norwegian seawater-reared Atlantic salmon suffering proliferative gill inflammation. Aquaculture. 2009;293(3-4):172-9.

16. Mitchell SO, Steinum TM, Toenshoff ER, Kvellestad A, Falk K, Horn M, Colquhoun DJ. 'Candidatus *Branchiomonas cysticola*' is a common agent of epitheliocysts in seawater-farmed Atlantic salmon *Salmo salar* in Norway and Ireland. Diseases of aquatic organisms. 2013;103(1):35-43.

17. Herrero A, Thompson KD, Ashby A, Rodger HD, Dagleish MP. Complex gill disease: an emerging syndrome in farmed Atlantic salmon (*Salmo salar* L.). Journal of comparative pathology. 2018;163:23-8.

18. Askarian F, Zhou Z, Olsen RE, Sperstad S, Ringø E. Culturable autochthonous gut bacteria in Atlantic salmon (*Salmo salar* L.) fed diets with or without chitin. Characterization by 16S rRNA gene sequencing, ability to produce enzymes and in vitro growth inhibition of four fish pathogens. Aquaculture. 2012;326:1-8.

19. McCarthy Ú, Stagg H, Donald K, Garden A, Weir SJ. *Psychrobacter* sp. isolated from the kidney of salmonids at a number of aquaculture sites in Scotland. Bull Eur Assoc Fish Pathol. 2013;33:67-72.

20. Downes JK, Collins EM, Morrissey T, Hickey C, O'Connor I, Rodger HD, MacCarthy E, Palmer R, Ruttledge M, Ruane NM. Confirmation of *Neoparamoeba perurans* on the gills of Atlantic salmon during the earliest outbreaks of amoebic gill disease in Ireland. Bull. Eur. Assoc. Fish Pathol.. 2018;38(1).

21. Llewellyn MS, Leadbeater S, Garcia C, Sylvain FE, Custodio M, Ang KP, Powell F, Carvalho GR, Creer S, Elliot J, Derome N. Parasitism perturbs the mucosal microbiome of Atlantic Salmon. Scientific reports. 2017;7:43465.

22. Zarkasi KZ, Abell GC, Taylor RS, Neuman C, Hatje E, Tamplin ML, Katouli M, Bowman JP. Pyrosequencing-based characterization of gastrointestinal bacteria of Atlantic salmon (*Salmo salar* L.) within a commercial mariculture system. Journal of applied microbiology. 2014;117(1):18-27.

23. Pawlikowska-Warych M, Deptuła W. Characteristics of chlamydia-like organisms pathogenic to fish. Journal of applied genetics. 2016;57(1):135-41.

24. Nylund S, Steigen A, Karlsbakk E, Plarre H, Andersen L, Karlsen M, Watanabe K, Nylund A. Characterization of '*Candidatus* Syngnamydia salmonis'(Chlamydiales, Simkaniaceae), a bacterium associated with epitheliocystis in Atlantic salmon (*Salmo salar* L.). Archives of microbiology. 2015;197(1):17-25.

25. Nylund A, Pistone D, Trösse C, Blindheim S, Andersen L, Plarre H. Genotyping of Candidatus Syngnamydia salmonis (chlamydiales; Simkaniaceae) co-cultured in *Paramoeba perurans* (amoebozoa; Paramoebidae). Archives of microbiology. 2018;200(6):859-67.

26. Riiser ES, Haverkamp TH, Borgan Ø, Jakobsen KS, Jentoft S, Star B. A single Vibrionales 16S rRNA oligotype dominates the intestinal microbiome in two geographically separated Atlantic cod populations. Frontiers in Microbiology. 2018;9:1561.

27. Svanevik CS, Lunestad BT. Characterisation of the microbiota of Atlantic mackerel (*Scomber scombrus*). International Journal of Food Microbiology. 2011;151(2):164-70.

28. Brown RM, Wiens GD, Salinas I. Analysis of the gut and gill microbiome of resistant and susceptible lines of rainbow trout (*Oncorhynchus mykiss*). Fish & shellfish immunology. 2019;86:497-506.

29. Rasheeda MK, Rangamaran VR, Srinivasan S, Ramaiah SK, Gunasekaran R, Jaypal S, Gopal D, Ramalingam K. Comparative profiling of microbial community of three economically important fishes reared in sea cages under tropical offshore environment. Marine genomics. 2017;34:57-65.

30. Ciric M, Waite D, Draper J, Jones JB. Characterisation of gut microbiota of farmed Chinook salmon using metabarcoding. bioRxiv: The Preprint server for Biology. 2018.

31. Benedicenti O, Secombes CJ, Collins C. Effects of temperature on *Paramoeba perurans* growth in culture and the associated microbial community. Parasitology. 2019;146(4):533-42.

32. Nikouli E, Meziti A, Antonopoulou E, Mente E, Kormas KA. Gut bacterial communities in geographically distant populations of farmed sea bream (*Sparus aurata*) and sea bass (*Dicentrarchus labrax*). Microorganisms. 2018;6(3):92.

33. Hovda MB, Fontanillas R, McGurk C, Obach A, Rosnes JT. Seasonal variations in the intestinal microbiota of farmed Atlantic salmon (*Salmo salar* L.). Aquaculture Research. 2012;43(1):154-9.

34. Tacchi L, Bickerdike R, Douglas A, Secombes CJ, Martin SA. Transcriptomic responses to functional feeds in Atlantic salmon (*Salmo salar*). Fish & shellfish immunology. 2011;31(5):704-15.

35. Chalupnicki M, Dittman D, Starliper CE, Iwanowicz DD. Efficacy of iodine for disinfection of lake sturgeon eggs from the St. Lawrence River, New York. North American Journal of Aquaculture. 2015;77(1):82-9.

36. Draghi A, Popov VL, Kahl MM, Stanton JB, Brown CC, Tsongalis GJ, West AB, Frasca S. Characterization of "*Candidatus* Piscichlamydia salmonis"(order Chlamydiales), a chlamydia-like bacterium associated with epitheliocystis in farmed Atlantic salmon (*Salmo salar*). Journal of clinical microbiology. 2004;42(11):5286-97.

CHAPTER 5

Amoebic Gill Disease and Functional Diets alter the Gill Microbiome in Atlantic Salmon

5.1 - Introduction

Since the first description of amoebic gill disease (AGD) in the 1980s (Munday, 1986), this gill disorder has been reported to be prevalent in global aquaculture (Oldham *et al.*, 2016). AGD is considered one of the most concerning disorders impacting Atlantic salmon (*Salmo salar* L.) production in terms of both prevalence and economic impact (Marcos-López *et al*., 2017; Boerlage *et al*., 2020). While AGD-affected fish experience lethargy, higher ventilation rates and increased production of gill mucus (Munday *et al*., 1990; Clark and Novak, 1999), the most recognisable sign of AGD is the presence of white mucoid patches on the gills, as consequence of hyperplasia and lamellar fusion (Clark and Novak, 1999; Taylor *et al.*, 2009; Bridle *et al*., 2010). The abundance and size of these white patches is used as a quantitative measurement (AGD gill score) of the AGD severity in gross pathological assessments (Taylor *et al.*, 2009) to monitor the gill condition in routine checking (Rodger, 2014). However, since most common gill diseases share similar signs (Rozas-Serri, 2019), AGD gill scoring is inherently unable to diagnose the specific disorder, and therefore to identify the first aetiological agent of AGD, *Neoparamoeba perurans* (Young *et al*., 2007; Crosbie *et al*., 2012). Thus, specific quantitative-PCR (qPCR) assays were developed to diagnose AGD and track *N. perurans* abundance in gill samples (Bridle *et al*., 2010; Downes *et al.*, 2015). Once AGD is confirmed, the most commonly used treatment is freshwater bathing of infected fish, since *N. perurans* is susceptible to low salinity (Oldham *et al.*, 2016; Boerlage *et al*., 2020).

The onset and development of AGD on Atlantic salmon are influenced by many factors, of which environmental conditions and host genetics are the most studied (Taylor *et al.*, 2007; Bustos *et al*., 2011; Oldham *et al.*, 2016; Rozas-Serri, 2019; Robledo *et al*., 2020). Nevertheless, specific functional diets were also recently shown to have a positive impact on the survival, and physiological response to AGD, of Atlantic salmon (Mullins *et al*., 2020). Such diets are formulated as inexpensive preventive treatments for various disorders or diseases (Mullins *et al*., 2020; Waagbø & Remø, 2020). Indeed, one of the least well studied possible factors in AGD is the gill microbiome (Nowak & Archibald, 2018; Rozas-Serri, 2019). However, some published studies addressed this topic, finding changes using high-throughput and culture-independent approaches in the microbiome diversity and structure due to AGD (Slinger *et al*., 2020a; Chapter 3 of the present thesis, manuscript submitted (Birlanga *et al*., 2021)). In this study, we investigated the connection between the whole-gill microbiome and AGD by describing the impact of the disease on the bacterial community on gills over a longitudinal *in-vivo* laboratory

trial. We also tested the effect of various functional diets on fish performance, AGD severity and the gill microbiome in Atlantic salmon during an AGD episode. Additionally, water samples were taken from experimental tanks to compare the gill and water microbiome.

We hypothesised that the gill microbiome may be influenced by AGD onset, becoming less diverse in AGD-affected Atlantic salmon and deviating from the microbiome in the surrounding water. Equally, we hypothesised that the various functional diets would impact on the water and gill microbiomes.

5.2 - Materials and Methods

5.2.1 - Fish husbandry and conditions of the challenge

Atlantic salmon were reared on a land-based freshwater hatchery in the north-west of Ireland. Following smoltification, they were transferred to a land-based indoor, marine recirculating facility at the Marine and Freshwater Research Centre (MFRC) at the Galway-Mayo Institute of Technology (GMIT) in Galway, Ireland. The MFRC was equipped with TMC2500 filtration/closed recirculation systems each with two 1,000-litre tanks, in an indoor, temperature-controlled, simulated marine environment with artificial seawater. All environmental conditions (ambient and tank water temperature, dissolved oxygen, carbon dioxide, photoperiod) were controlled and monitored from a computerised control centre, with additional water parameters (nitrites/ammonia, salinity) measured using a HACH DR2800 and a refractometer, respectively.

Fish (*n* = 180, average weight 80 g) were distributed into each of four independent systems (S1-4; *n* = 45 fish per system), with the following conditions: stocking density per system, 3.6 kg/m^3;water temperature, 12ºC; water oxygen maintained at 90% saturation; artificial salinity,30 ppt (Coral Pro salt, Red Sea);and light cycle,14 h light, 8 h dark. A control feed type (feed type A - FTA) was tested with two novel-formula feeds, feed type B (FTB) and feed type C (FTC). Salmon from S1 and S2 were fed with FTA, salmon from S3 with FTB, and salmon from S4 with FTC. The compositions of these diets were unknown, as the company that provided them kept that information. Fish were fed with the respective feed type at 1% body weight per day. The whole salmon cohort had an acclimatisation period of 6 d prior to the start of the conditioning phase with the different feed types (21 days). After conditioning phase, AGD challenge phase started (**Fig. 5.1**).

5.2.2 - *Neoparamoeba perurans* culture

To establish cultures, *N. perurans* were sampled from naturally infected Atlantic salmon on a commercial farm based on the west coast of Ireland. Gill mucus containing the amoeba was collected using a sterile cotton swab and transferred into 10 ml sterile seawater. Following transport to the laboratory, saline solution containing the amoeba was plated onto marine malt yeast agar (MMYA; 0.01% malt, 0.01% yeast, 2% agar, sterile seawater at 27 practical salinity units (PSU)) and incubated at 16°C. Agar plates were washed every two days by replacing the overlay water with new sterile seawater. To sub-culture the amoeba, floating amoeba in seawater overlay were poured onto fresh marine malt yeast agar plates. The species was confirmed by real-time polymerase chain reaction (PCR), as described by Downes *et al*. (2015). Time from collection and seeding of amoebae until the *in-vivo* challenge was 89 d.

5.2.3 - Inoculation with the *N. perurans* culture

Prior to starting the *in-vivo* challenge, the water level of the four tanks containing the salmon was reduced from 1,000 L to 300 L. Three systems (S2, S3 and S4) were inoculated with 500 amoebae/L. Another system (S1) was used as negative control, and fish from this system experienced a water bath without amoeba to mimic the stress of inoculation. Following this, the experimental and control systems were maintained for 4 h with volumes of 300 L and at oxygen saturation, whilst fish behaviour and welfare were closely monitored. After this, the fish from each system were moved into new respective tanks, each containing 1,000 L artificial seawater and kept under same conditions for further sampling. This work was authorised by the Health Products Regulatory Authority (HPRA) in Ireland under project authorisation number AE19137/P003, following the Animals Scientific Procedures Act 1986 (Directive 2010/ 63/EU transposed into Irish law by S.I. No 543 of 2012).

5.2.4 - Gill and water samples collection

The sampling was divided into four timepoints (**Fig. 5.1**): T0 (at beginning of conditioning phase), T1 (at end of conditioning phase and before AGD challenge), T2 (14 days post-infection (dpi)) and T3 (21 days post-infection (dpi)). A total of eight salmon were sampled at T0, before experiencing differential treatment, and were thus considered to be biological replicates.

However, six salmon replicates were sampled from each system at the remaining timepoints (**Fig. 5.1**). All fish were euthanised by overdose of anaesthetic (400 mg/L of tricaine methane-sulfonate (MS-222)) prior to measuring length and weight, and scoring the gill health based on the guidelines of Taylor *et al.*(2009). Upon sampling, and after removing the operculum, the first brachial arch from the right side, and the fourth brachial arch of the left side, of each fish was aseptically excised and flash frozen in liquid nitrogen.

Following standard operating procedures from GMIT, laboratory cohorts in which salmon reach AGD gill scores of ≥2 should be euthanised by overdose of anaesthetic (400 mg/L of tricaine methane-sulfonate (MS-222)).For this reason, S2 was stopped at T2. Thus, a total of 148 gill arches (74 from the left first arch and 74 from the right fourth arch) were sampled, frozen and stored at -80ºC for downstream DNA extraction and analyses.

Water samples were taken from each of the systems at T1, T2 and T3. Respective sterile 2-L glass bottles were filled with water from the four systems and maintained at 4ºC in the dark until filtration. Within 24 h, water samples were each divided into three technical replicates (approx. 650 mL each, **Fig. 5.1**), which were filtered through 0.22-µm cellulose nitrate filters (Sartorius, Germany). Two unused filters, and three filters used to filter sterile distilled water, were included as negative control samples. Since S2 was stopped after T2, the total number of filters, which were stored at -80ºC for downstream DNA extraction, was 38 (33 filtered water samples and 5 negative control filters).

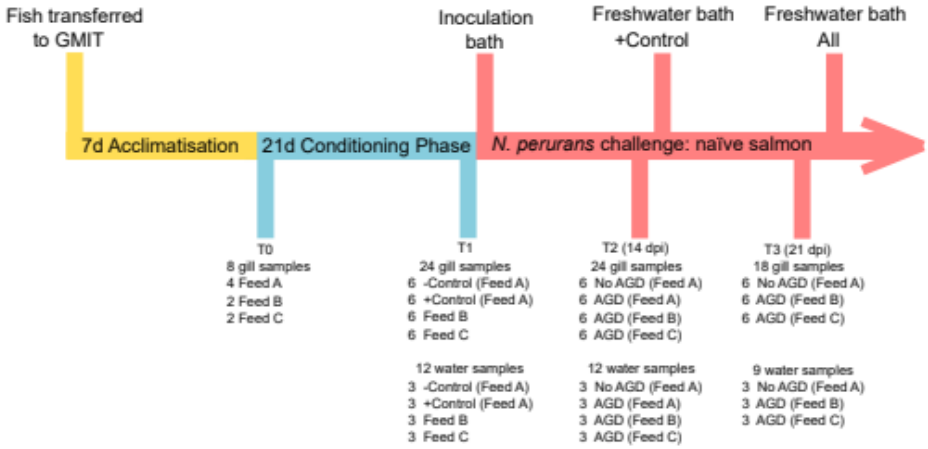

Figure 5.1. Timeline of the main events and sampling points during the challenge. Seven days after the Atlantic salmon arrived to GMIT (acclimatisation phase), the sampling point T0 included eight gill samples. Following 21 d of conditioning, the next sampling point was T1, when 24 gills and 12 water samples were obtained. The AGD challenge started after T1. Fourteen days post-infection (dpi) (T2), gills (24) and water (12) samples were obtained. Finally, 21 dpi (T3,) 18 gill and nine water samples were obtained. After T3, all remaining salmon were treated with freshwater bathing (4 h in desalinated water at 12.0 ºC with 100% oxygen saturation) and humanely euthanised.

5.2.5 - DNA extraction procedures for gill and water samples

The DNA from gill samples to characterise the microbiome (right, first brachial arch) was extracted following the optimised protocol from Birlanga *et al.* (Chapter 3 of the present thesis, manuscript submitted (Birlanga *et al*., 2021)): **1)** 50 µl trypsin-EDTA (0.5% trypsin [w/v] in 6.8 mM EDTA; Sigma-Aldrich, Saint Louis, USA) were added along with 450 µl 0.5 M EDTA to a gill in a 2-ml microcentrifuge tube prior to sonication for 5 min (Kerry Ultrasonic Baths, model PUL-125). The gill was then removed to a fresh tube, repeating the process five times; **2)** the liquid phase from each wash step was pooled in a 15-ml tube, and the gill was discarded. An equal volume of ice-cold isopropanol was added along with a 0.1 volume of 3 M sodium acetate to precipitate free DNA, which was then recovered with microbial cells by centrifuging for 30 min at > 8,000 g (4°C) to form three layers; **3)** an extraction kit (AllPrep DNA/RNA extraction kit, QIAGEN, Hilden, Germany) was used to recover nucleic acids from the bottom layer following the manufacturer's instructions without any modifications. In total (including extractions from gill samples and from negative-control extractions without gill material) 77 preparations for microbiome analysis were processed (74 gill arches and three control samples).

Total DNA from gill samples to estimate the *N. perurans* abundance (left, fourth brachial arch) was recovered using a QIAamp DNA Mini kit (QIAGEN) according to the manufacturer's instructions for animal tissue, and the eluted DNA from the 74 gill samples was stored at -20°C.

To extract the microbial DNA from the filters, each was placed, using sterile forceps, in respective, sterile 15-mL tubes each containing 3 mL lysis buffer (RLT plus buffer, QIAGEN, Hilden, Germany) and sterile glass bead (1 g beads with 1-mm diameter, and 1 g beads with 0.1-mm diameter). The tubes were then vortexed at maximum speed for 45 s, prior incubating at room temperature with constant orbital shaking for 30 min. After the first incubation, vortexing and incubation was repeated. Proteinase K (final concentration, 2 mg/L) was then added to each tube, before vortexing again for 15 s. Samples were then incubated at room temperature horizontally on a rolling plate for 2 h. After homogenising by briefly vortexing, the tubes were centrifuged at 3,220 x*g*at room temperature for 5 m. The filters were removed from tube using sterile forceps and discarded. As much lysate as possible was then pipetted from the respective tubes, avoiding the beads, and placed on a DNA extraction column (QIAGEN, Hilden, Germany). The remaining steps were following the AllPrep DNA and RNA extraction kit (QIAGEN, Hilden, Germany) instructions. DNA samples from filters were then stored at -80ºC prior to sequencing.

Concentrations of double-stranded DNA from every sample were determined using a Qubit dsDNA BR Assay Kit (ThermoFisher Scientific, Paisley, UK), following the instructions provided.

5.2.6 - 16S rRNA gene sequencing and *N. perurans* 18S rRNA gene quantification

The V4 and OutTS1-spanning regions of 16S rRNA genes from gill and filter DNA samples were amplified using the oligonucleotide primers 515F (5'-GTGCCAGCMGCCGCGGTAA-3') and 806R (5'-GGACTACHVGGGTWTCTAAT-3') (Caporaso *et al.*, 2011). A set of two pre-amplification controls without any DNA sample were included as negative controls. PCR mixtures (25 µl final volume) contained: 12.5 ng genomic DNA, 0.2 µM (final concentration) of each primer (515F and 806R), and 12.5 µl 2X KAPA HiFi Hot Start Ready Mix (0.25 U; Roche). The PCR comprised of initial denaturation at 95°C for 3 min; 25 cycles of 95°C for 30 s, 55°C for 30 s and 72°C for 30 s; and a final incubation at 72°C for 5 min. PCR products were purified (AMPure XP for PCR Purification, Beckman Coulter, USA) before adding Illumina sequencing adapters and indices using a Nextera XT Index Kit (Cambridge, United Kingdom) following the

manufacturer's instructions. A second PCR purification was done before quantifying the DNA using a 2100 Bioanalyzer system (Agilent Technologies), normalising the DNA concentration (to 4 nM) and pooling the libraries with unique indices. Pooled libraries and controls were denatured (0.2 N NaOH), diluted and heat-denatured before sequencing. Amplicons were sequenced using an Illumina MiSeq platform (Caporaso *et al*., 2012) using 5% PhiXas as internal control, following Illumina's recommendations.

The concentration of *N. perurans* in gill samples was estimated in qPCR assays targeting partial 18S rRNA gene sequences specific to the amoeba and using the primers NP1 (5'-AAAAGACCATGCGATTCGTAAAGT-3') and NP2 (5'-CATTCTTTTCGGAGAGTGGAAATT-3'), with the NPP (6-FAM-ATCATGATTCACCATATGTT-MGB) probe, according to the procedure as described in detail by Downes *et al.* (2015). Each PCR mixture (25 µl) contained: 5 µl microbial genomic DNA (5 ng/µl), 12.5 µl TaqMan® Universal 2 Master Mix (Applied Biosystems), and final concentrations of 300 nM primer NP1, 900 nM primer NP2 and 200 nM probe NPP. Each qPCR program comprised of an initial denaturation at 95°C for 15 min, followed by 45 cycles of 95°C for 15 s and 56°C for 30 s in a real-time PCR thermocycler (Applied Biosystems AB7500). Positive and negative controls were added into each run, as well as internal and external process controls (Downes *et al.*, 2015). Results from qPCR runs (expressed as Cq) were annotated to be included in subset regressions.

5.2.7 - Bioinformatics and Statistical Analyses

We have used deblur algorithm from Qiime2 (Bolyen *et al*., 2019) to generate the Amplicon Sequencing Variants (ASVs). Briefly, after importing the multiplexed samples into Qiime2 environment, we quality trimmed the data using a minimum Phred quality score of 20 using qiime quality-filter q-score plugin. Afterwards, we used qiime deblur denoise-16S plugin with the parameters -p-trim-length 115, --p-min-size 0**,** and --p-min-reads 1 to generate the ASVs abundance table and the representative sequences (by retaining singletons). The choice of trimming length was obtained based on the recommendations given in the benchmarking analysis given at https://qiita.ucsd.edu/static/doc/html/deblur_quality.html. Having obtained the ASVs, we then used DeConseq (Masella *et al.*, 2012) to identify ASVs that were contaminants, hitting on the *Salmo salar* reference genome. Afterwards, we used qiime feature-classifier classify-sklearn plugin for the filtered ASVs against SILVA SSU Ref NR database release v138,

and then used qiime phylogeny align-to-tree-mafft-fasttree to generate the rooted phylogenetic tree. The biom file for the ASVs was then generated by combining the abundance table with taxonomy information using biom utility available in qiime2 workflow.

After this, we obtained 80,579 ASVs (including singletons) for *n* = 117 samples with summary statistics of reads as follows: [1st Quantile: 32,348, Median: 43,895, Mean: 58,487, 3rd Quantile: 90,040, Max: 228,483]. Out of these 117 samples, we had 10 samples for control/blanks (6 for water samples and 4 for gill samples), which we used R decontam package (Davis *et al.*, 2018) using the "prevalence" method to filter out ASVs (991 for water samples, and 963 for gill samples, respectively). For ensuing statistical analysis and to further exclude contaminants based on taxonomy (Chloroplast, Microchondria, and ASVs unassigned at Phylum level), any sample was dropped with total reads <5000, leaving 68 samples from gills sampling (6 less than the initial amount: three from S1 at T1, one from S1 at T2, one from S2 at T1, and one from S4 at T1) and 33 samples from water sampling (same as the initial amount). Thus, the final amount of analysed samples was *n* = 101.

Statistical analyses were performed in R using the combined data generated from the bioinformatics as well as meta data associated with the study (environmental factors, fish features, and qPCR results). The vegan package (Oksanen *et al*., 2007) was used for alpha and beta diversity analyses. For alpha diversity measures we have used: Shannon entropy, Simpson's Index, Inverse Simpsons Index, Pileou's Evenness, and Fisher's Alpha, and Richness metrics, that are default in the function diversity() from vegan package. Ordination of ASV table in reduced space (beta diversity) was done using Principal Coordinate Analysis (PCoA) plots of ASVs using three different distance measures were made using Vegan's cmdscale() function: (1) Bray-Curtis is a distance metric which considers only ASVs abundance counts, (2) Unweighted Unifrac is a phylogenetic distance metric which calculates the distance between samples by taking the proportion of the sum of unshared branch lengths in the sum of all the branch lengths of the phylogenetic tree for the ASVs observed in two samples, and without taking into account their abundances and, (3) Weighted Unifrac is a phylogenetic distance metric combining phylogenetic distance with relative abundances. This places emphasis on dominant ASVs or taxa. Unifrac distances were calculated using the phyloseq package (McMurdie & Holmes, 2013).

Analysis of variance for explanatory variables (or sources of variation) was performed using Vegan's adonis() against distance matrices (Bray-Curtis/Unweighted UniFrac/Weighted

UniFrac). This function, referred to as PERMANOVA, fit linear models to distance matrices and used a permutation test with pseudo-F ratios. To give an account of environmental filtering (phylogenetic overdispersion versus clustering), phylogenetic distances within each sample were further characterised by calculating the nearest taxa index (NTI) and net relatedness index (NRI). This analysis helped determine whether the community structure was stochastic (overdispersion and driven by competition among taxa) or deterministic (clustering and driven by strong environmental pressure). The NTI was calculated using mntd() and ses.mntd(), and the mean phylogenetic diversity (MPD) and NRI were calculated using mpd() and ses.mpd() functions from the picante package (Kembel *et al.*, 2010). NTI and NRI represent the negatives of the output from ses.mntd() and ses.mpd(), respectively. Additionally, they quantify the number of standard deviations that separate the observed values from the mean of the null distribution (999 randomisation using null.model-'richness' in the ses.mntd() and ses.mpd() functions and only considering taxa as either present or absent regardless of their relative abundance). Based upon the recommendations given (Stegen *et al*., 2012), only the top 2000 most abundant ASVs were used for the calculations. We performed Local Contribution to Beta Diversity (LCBD) analysis (Legendre & De Cáceres, 2013) by using LCBD.comp() from adespatial package (Dray *et al.*, 2018). We used the Bray-Curtis (abundances), unweighted (phylogenetic distance) and weighted Unifrac (phylogenetic distance weighted by abundance) dissimilarities. LCBD gives the sample-wise local contributions to beta diversity that could be derived as a proportion of the total beta diversity. The measure provides a mean to show how markedly different the microbial community structure of a single sample is from the average (with higher LCBD values representing outliers).

To find ASVs that are significantly different between different categories (locations or sampling rounds), we used DESeqDataSetFromMatrix() function from DESeq2 (Love *et al.*, 2014) package with the adjusted p-value significance cut-off of 0.05 and log2 fold change cut-off of 2. This function uses negative binomial GLM to obtain maximum likelihood estimates for OTUs log fold change between two conditions. Then Bayesian shrinkage is applied to obtain shrunken log fold changes subsequently employing the Wald test for obtaining significances.

We performed subset regression against different microbiome metrics by testing all possible combination of the explanatory variables, and then selecting the best model according to some statistical criteria, with recommendations from the Kassambara work (2018) and code available at http://www.sthda.com/english/articles/37-model-selection-essentials-in-r/155-best-subsets-

regression-essentials-in-r/. The R function regubsets() from leaps package (Lumley & Miller, 2009) was used to identify different best models of different sizes, by specifying the option nvmax, set to the maximum number of predictors to incorporate the model. Having obtained the best possible subsets, the k-fold cross-validation consisting of first dividing the data into k subsets. Each subset (10%) served successively as test data set and the remaining subset (90%) as training data. The average cross-validation error is then computed as the model prediction error. This was all done using a custom function utilising R's train() function from the caret package (Kuhn, 2008). Finally R's tab_model() function from sjPlot package (Lüdecke, 2018) was used to obtain the statistics for each model. To find the core microbiome, we have used R's microbiome package (Lahti *et al*., 2017) and the prevalence of 85% of OTUs to be tagged as core microbiome, by following recommendations given in Shetty *et al*. (2017).

In a majority of the figures displaying boxplots, pair-wise ANOVA was performed taking two categories at a time and, where significant ($p \leq 0.05$), these were joined together by a line, plotting significance on top (*: $0.01 \leq p < 0.05$; **: $0.001 \leq p < 0.01$; ***: $p < 0.001$).

The sequencing data are available in the European Nucleotide Archive under the study accession number PRJEB41326 (http://www.ebi.ac.uk/ena/data/view/PRJEB41326).

5.3 - Results

5.3.1 - Description of AGD episode on salmon

The condition factor profile of the salmon cohort from each system was similar (**Fig. 5.2**), with a decreasing overall tendency regardless of the system, shifting from approximately 1.0 at T0 to 0.95 at T3.

The average observed AGD gill scores in S2, S3 and S4 14 dpi (T2) ranged 1.0-2.5 (**Fig. 5.2**). The gill score of S2 salmon at T2 was 2.0 and the challenge was stopped for this cohort, which was then unavailable for sampling at T3. However, the challenge for S3 and S4 continued until T3, when AGD gill scores on those salmon were close to 2. Meanwhile, the unexposed cohort (S1) did not show any sign of AGD throughout the trial. The same pattern was observed in *N. perurans* qPCR data, with no *N. perurans* detected at T0 or T1 in any system, but amplification of *N. perurans* 18S rRNA genes observed at T2 and T3 in S2, S3 and S4 (**Fig. 5.2**).

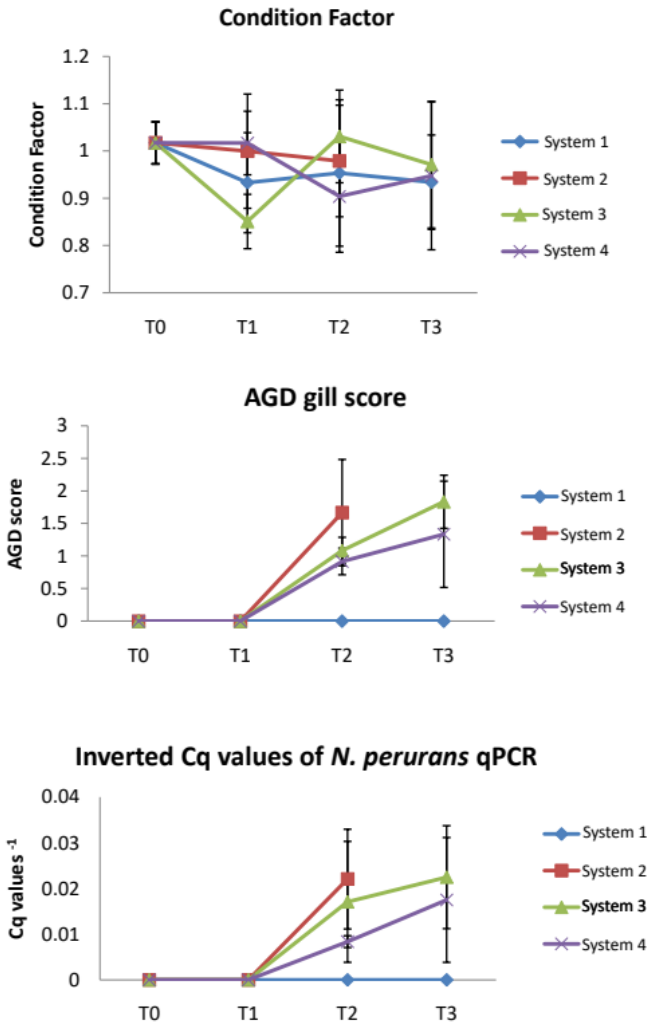

Figure 5.2. Condition factors, AGD gill scores, and qPCR results (inverted Cq). Salmon from System 1 (AGD-unaffected) and System 2 (AGD-affected) were fed with food type A, salmon from System 3 (AGD-affected) with feed type B, and salmon from System 4 (AGD-affected) with feed type C. There were no data for System 2 at T3.

5.3.2 - Influence of AGD and different functional diets on the gill microbiome

The relatively most abundant bacterial taxa overall in gill samples included: the classes Bacteroidia and Alphaproteobacteria, the families Chlorobiaceae and Rubritaleaceae, and the genera *Synechococcus* and *Streptococcus*, all of which were present in every sample (**Fig. 5.3**). The most-abundant bacterial taxa were similarly abundant across the systems and between timepoints, except for the Flavobacteriaceae family, which were relatively more abundant in

AGD-challenged salmon fed with FTA, and the *Owenweeksia* genus, which was relatively more abundant in AGD-challenged salmon fed with FTB and FTC.

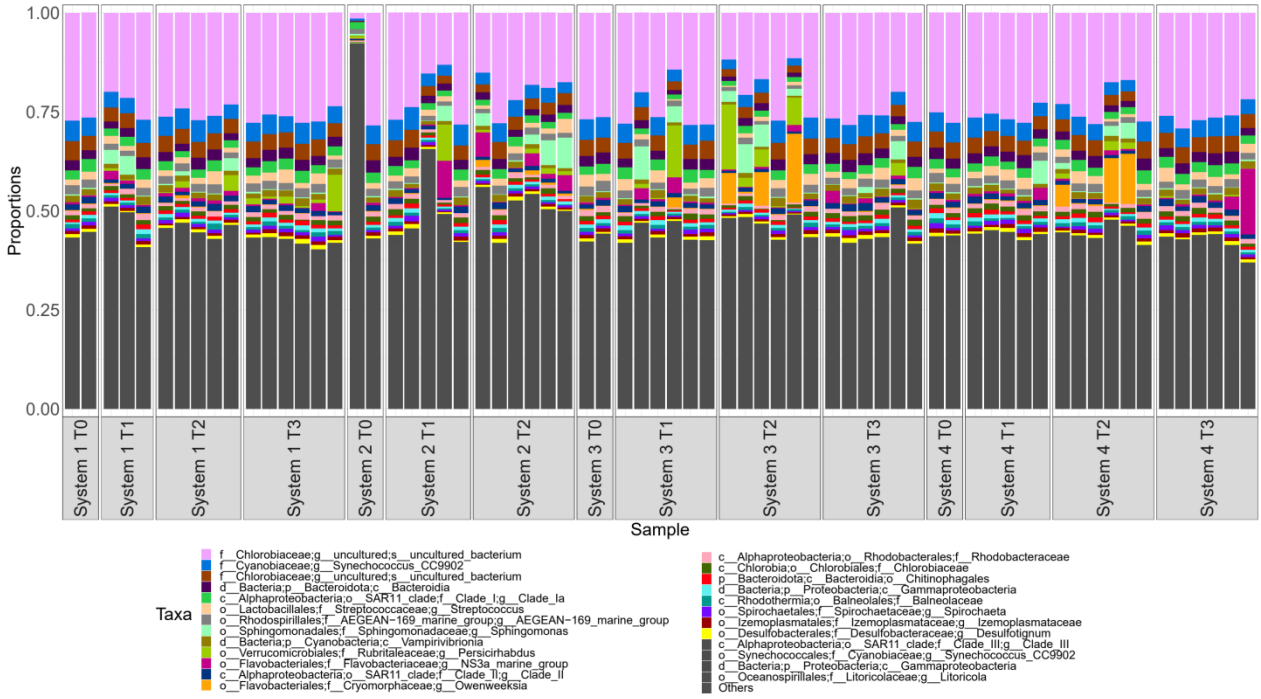

Figure 5.3. Community structure of the top 25 most relatively abundant ASVs from across each timepoint and system from gill samples, where 'others' refers to all ASVs not included in the top 25. Letter before taxonomic names reference their taxonomic ranks (d: Domain, p: Phylum, c: Class, o: Order, f: Family, g: Genus, s: Species). Salmon from System 1 (AGD-unaffected) and System 2 (AGD-affected) were fed with food type A, salmon from System 3 (AGD-affected) with feed type B, and salmon from System 4 (AGD-affected) with feed type C. There were no data for System 2 at T3.

The core microbiome analyses from gill samples (**Fig. S5.1**) resulted in a wide range of microbial taxa, which had a prevalence higher than 85% in gill samples. Some of the taxa included in the core microbiome were: the classes Bacteroidia and Alphaproteobacteria, the order Flavobacteriales, the families Chlorobiaceae, Rubritaleaceae and Rhodobacteriaceae, and the genera *Synechococcus*, *Streptococcus*, and *Owenweeksia*.

The alpha-diversity analyses used to compare diversity in gill microbiomes between systems across timepoints, indicated similar diversity along the trial, showing only some significant differences between systems at T2 (**Fig. 5.4**). Specifically, using Pielou's evenness and Shannon diversity, the gill microbial community from S2 at T2 was significantly more diverse than in S3 orS4 at the same time (**Fig. 5.4**). Similarly, diversity measured using Pielou's evenness and Simpson's diversity was higher in S2 than S1 at T2. Therefore, AGD-affected salmon fed with

FTA had a significantly more even gill prokaryotic microbiome than either healthy salmon or salmon fed with FTB or FTC. Indeed, during this time, the gill microbiomes from the distinct systems did not experience different levels of environmental pressure (**Fig. 5.5**).

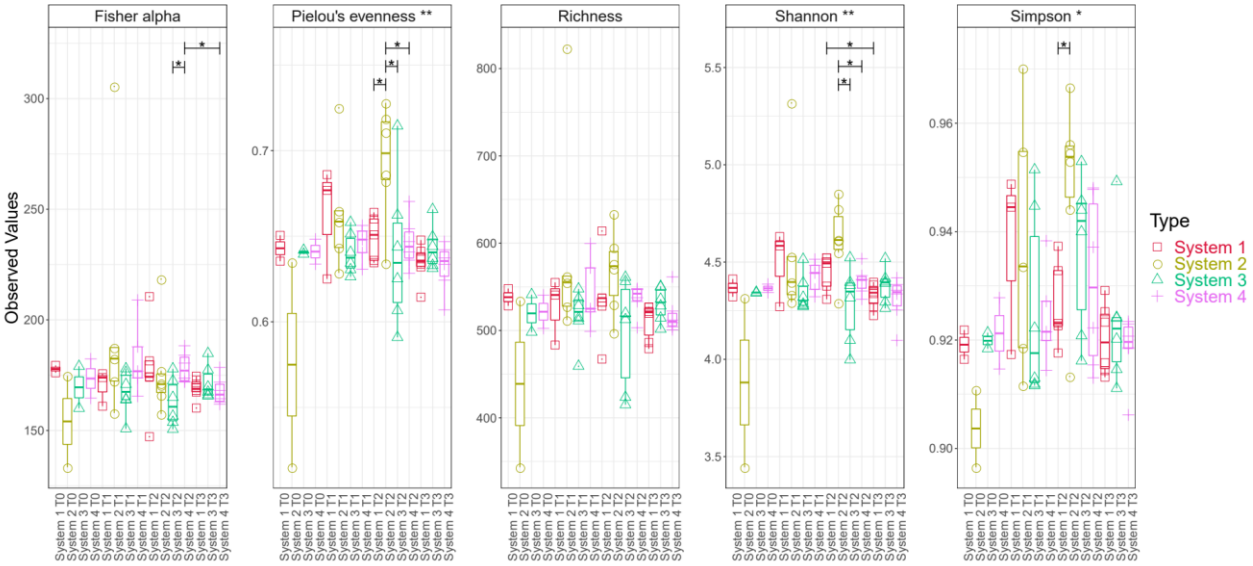

Figure 5.4. Alpha-diversity (Fisher's alpha parameter, Pielou's evenness, richness, Shannon diversity index, and Simpson's diversity index) of the gill prokaryotic community from each system at each timepoint. Symbol shapes and symbol/box colours represent the different systems, S1-S4. The lines at the top of each chart connect two categories where the differences were significant (ANOVA) with * ($p < 0.05$), ** ($p < 0.01$), or *** ($p < 0.001$). Salmon from System 1 (AGD-unaffected) and System 2 (AGD-affected) were fed with food type A, salmon from System 3 (AGD-affected) with feed type B, and salmon from System 4 (AGD-affected) with feed type C. There were no data for System 2 at T3.

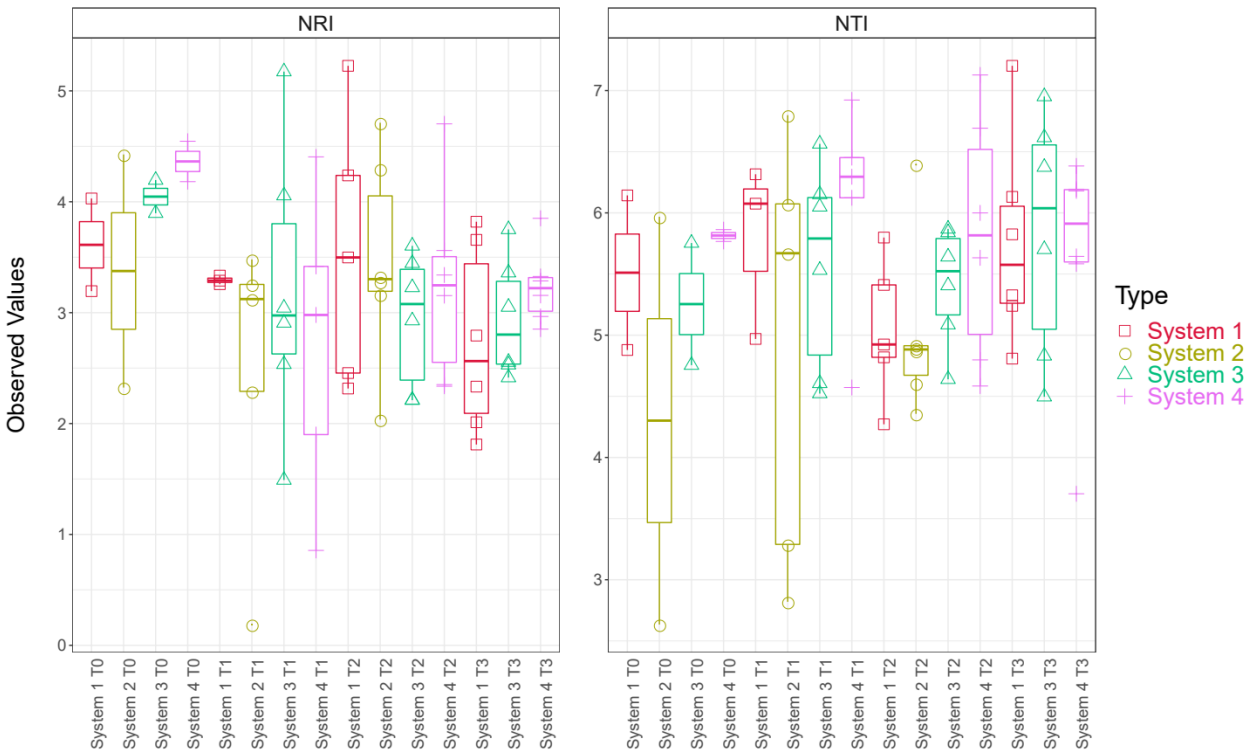

Figure 5.5. Environmental filtering analyses (Nearest Taxa Index (NTI) and Net Relatedness Index (NRI)) of the gill prokaryotic community from each system at each timepoint. Symbol shapes and symbol/box colours represent the different systems, S1-S4. ANOVA analyses did not show any significant difference in any of the pair wise analyses. Salmon from System 1 (AGD-unaffected) and System 2 (AGD-affected) were fed with food type A, salmon from System 3 (AGD-affected) with feed type B, and salmon from System 4 (AGD-affected) with feed type C. There were no data for System 2 at T3.

Beta-diversity, and local contribution to beta-diversity (LCBD), analyses used to compare microbiome structure between gill samples did not indicate discernible patterns in beta diversity or clustering either between systems or across timepoints (**Figs. 5.6 and 5.7**). However, PERMANOVA results suggested that time was a significant factor influencing the beta-diversity when any of the three indices were used (**Fig. 5.6**). Nonetheless, the different systems, S1-S4, significantly impacted beta-diversity though only using the UniFrac algorithms (**Fig. 5.6**). Comparing all beta-diversity indices between systems and timepoints using LCBD, S1 was significantly different to S4 at T1 using the Bray-Curtis and the Weighted UniFrac approaches (**Fig. 5.7**). S2 appeared to also be significantly different to S4 at T1 using the Weighted UniFrac approach (**Fig. 5.7**). In other words, the gill microbiome structure of FTA-fed salmon was significantly different than in FTC-fed salmon before the AGD challenge.

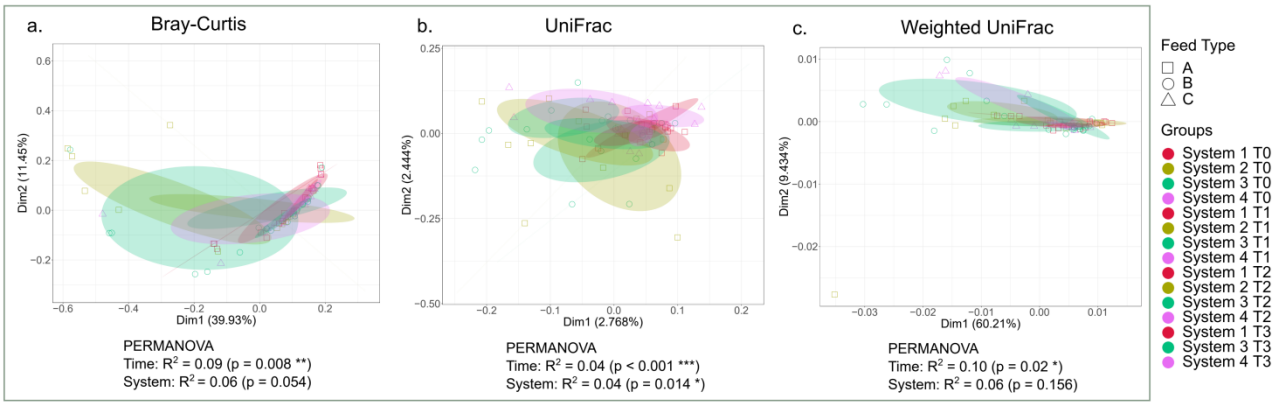

Figure 5.6. Representation of the beta-diversity indices (a. Bray-Curtis, b. UniFrac, c. Weighted UniFrac) of the gill prokaryotic community from each system at each timepoint. Ellipses are drawn at 95% confidence interval of standard error from the replicates of each system in each timepoint. PERMANOVA analyses considered temporal changes in the gill microbiome ('Time') and the changes comparing gill microbiomes from different systems ('System'). Salmon from System 1 (AGD-unaffected) and System 2 (AGD-affected) were fed with food type A, salmon from System 3 (AGD-affected) with feed type B, and salmon from System 4 (AGD-affected) with feed type C. There were no data for System 2 at T3.

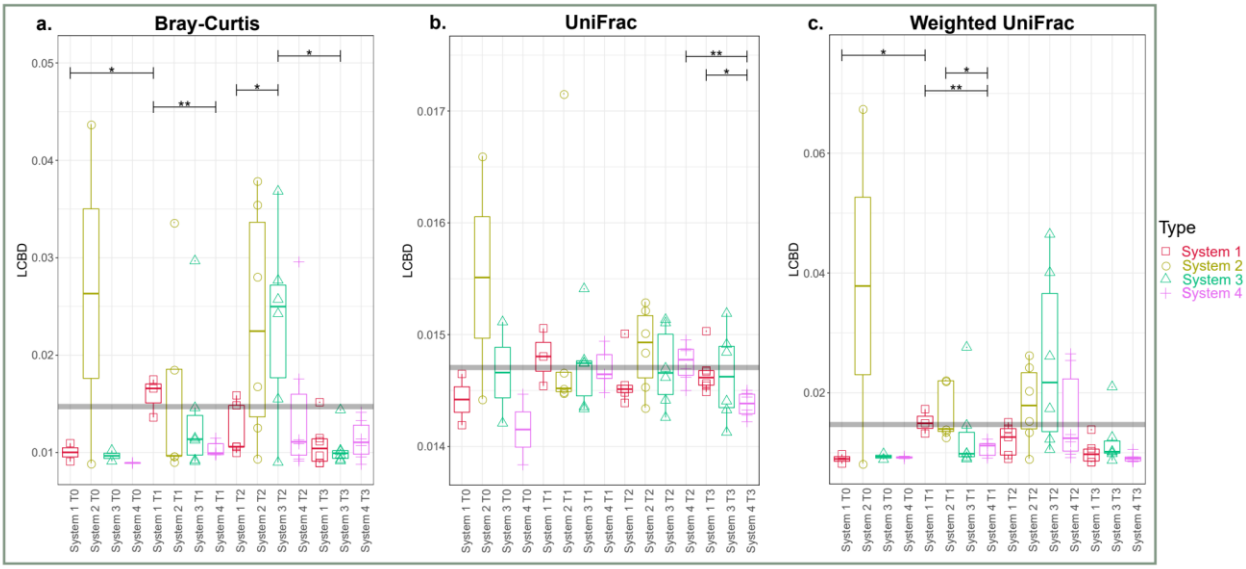

Figure 5.7. Local Contribution to Beta-Diversity (LCBD) (a. Bray-Curtis, b. UniFrac, c. Weighted UniFrac) of the gill prokaryotic community from each system at each timepoint. Symbol shapes and symbol/box colours represent the different systems, S1-S4. The lines at the top of each chart connect two categories where the differences were significant (ANOVA) with * ($p < 0.05$), ** ($p < 0.01$), or *** ($p < 0.001$). Salmon from System 1 (AGD-unaffected) and System 2 (AGD-affected) were fed with food type A, salmon from System 3 (AGD-affected) with feed type B, and salmon from System 4 (AGD-affected) with feed type C. There were no data for System 2 at T3.

All the available metadata compiled in the present study (fish features, AGD gill scores, qPCR data) were included in subset regression analyses to search for correlations to explain variability in different attributes of the microbiome (**Fig. 5.8**). Some alpha-diversity descriptors (Pielou's evenness and Simpson's diversity index) correlated positively with timepoints T1 and T2 (**Fig. 5.8**). Samples from S2 also showed significantly positive regressions with most of the alpha-diversity descriptors (except for Simpson's diversity index) and with all beta-diversity approaches. Hence, the microbiomes from salmon gills taken at T1 and T2, and from AGD-affected salmon fed with FTA, more likely had diverse gill microbiomes. The AGD gill score data positively correlated with some alpha-diversity descriptors (Pielou's evenness and Simpson's diversity index), one of the environmental filtering indices (NRI), and the Bray-Curtis approach from the beta-diversity analyses (**Fig. 5.8**).

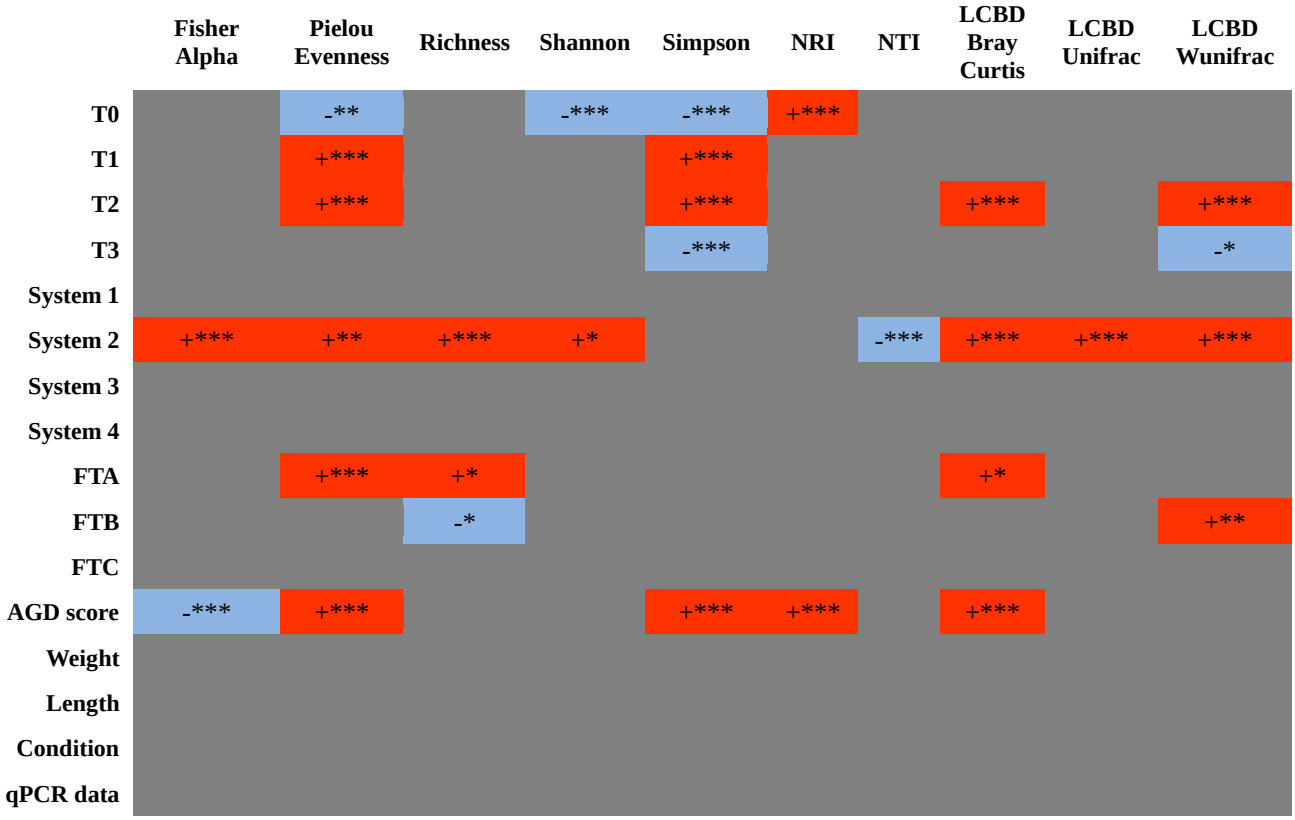

Figure 5.8. Heatmap of the explanatory parameters potentially influencing the gill microbiome, based on subset regressions. Red or blue shading indicate significant positive or negative beta coefficients from regression models. Asterisks at the significant regressions (a plus for a positive and a minus for a negative) indicate frequency the regression was significant in the different models: *in one model, **in two models or *** in three, or more, models. Significant regressions from categorical variables (T0, T1, T2, T3, System 1 to 4, and Feed type A, B, and C) could be interpreted as the samples from those variables having positive/negative influence on the respective microbiome attribute. Salmon from System 1 (AGD-unaffected) and System 2 (AGD-affected) were fed with food type A, salmon from System 3 (AGD-affected) with feed type B, and salmon from System 4 (AGD-affected) with feed type C. There were no data for System 2 at T3.

5.3.3 - Comparison of the gill microbiome with the microbial community in the surrounding water

The most relatively abundant bacterial taxa in water samples were: the class Gammaproteobacteria, order Sphingobacteriales, families Flavobacteriaceae, Rhodobacteriaceae, Rubritaleaceae, Alteromonadaceae and Rhizobiaceae, and the genus *Owenweeksia* (**Fig. 5.9**).

However, the relative abundance greatly differed between systems and timepoints. As within gill samples, the family Chlorobiaceae was present in most of the water samples, but at very low relative abundance (**Fig. 5.9**).

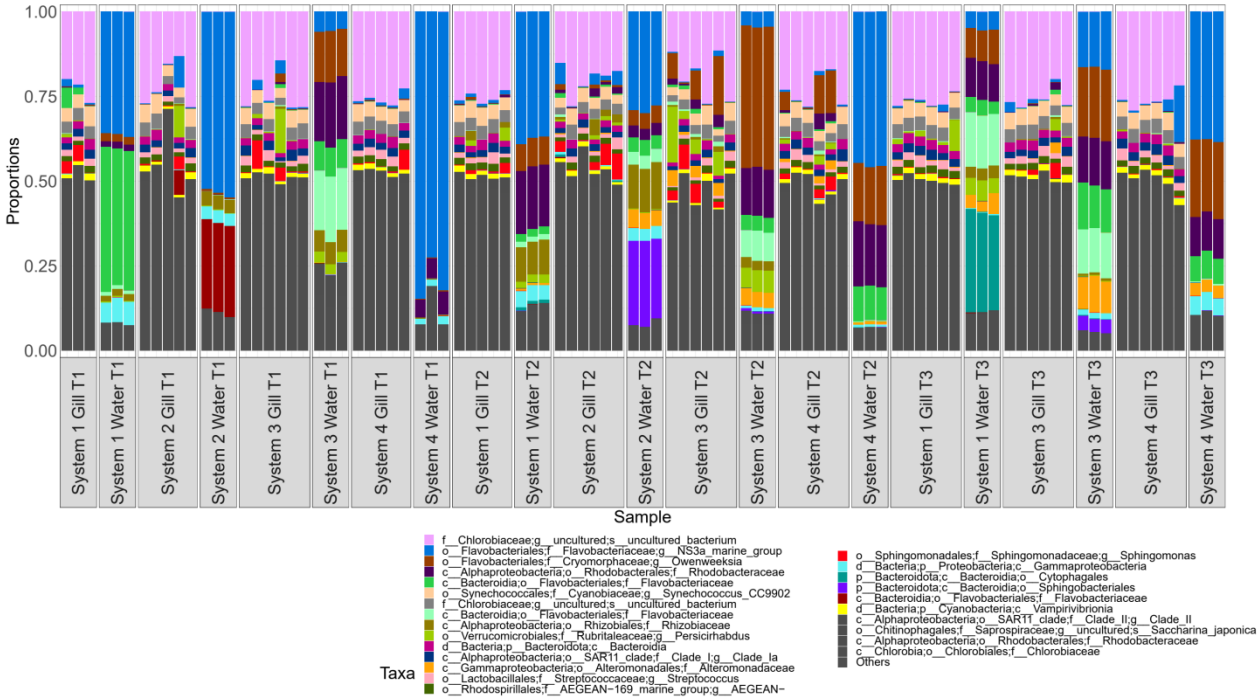

Figure 5.9. Community structure of the top 25 most relatively abundant ASVs from across each timepoint and system from gill and water samples, where 'others' refers to all ASVs not included in the top 25. Letter before taxonomic names reference their taxonomic ranks (d: Domain, p: Phylum, c: Class, o: Order, f: Family, g: Genus, s: Species). Salmon from System 1 (AGD-unaffected) and System 2 (AGD-affected) were fed with food type A, salmon from System 3 (AGD-affected) with feed type B, and salmon from System 4 (AGD-affected) with feed type C. There were no data for System 2 at T3.

The bacteria that appeared with prevalence higher than 85% in gill and water samples were considered as the shared core microbiome (**Fig. S5.2**). Thosetaxa included: the classes Alphaproteobacteria and Bacteroidia, families Flavobacteriaceae, Chlorobiaceae, Rhodobacteriaceae, Rubritaleaceae and Rhizobiaceae, and the genera *Blastopirellula*, *Owenweeksia*, and *Synechococcus.*

Four separate analyses were used to compare the gill microbiome with the surrounding water microbiome: alpha-diversity, environmental filtering, beta-diversity, and PERMANOVA analyses. All gill samples were significantly more diverse (**Fig. 5.10**), and experienced a higher environmental pressure (NTI, **Fig. 5.11**), than water samples from the same respective systems

and timepoints. In addition, the beta-diversity of gill and water samples were very different (**Fig. 5.12**). This was significant in PERMANOVA analyses (**Fig. 5.12**), where the influence of time and system was significant in some of analyses.

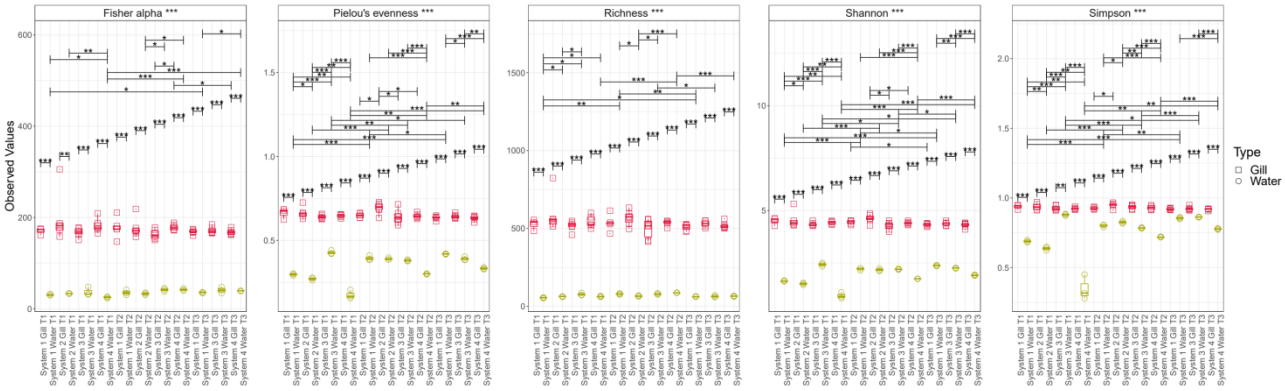

Figure 5.10. Alpha-diversity descriptors (Fisher's alpha parameter, Pielou's evenness, richness, Shannon diversity index, and Simpson's diversity index) of the gill and water prokaryotic community from each system at each timepoint (T1, T2 and T3). Symbol shapes and symbol/box colours represents either gill or water samples. The lines at the top of each chart connect two categories where the differences were significant (ANOVA) with * ($p < 0.05$), ** ($p < 0.01$), or *** ($p < 0.001$). Salmon from System 1 (AGD-unaffected) and System 2 (AGD-affected) were fed with food type A, salmon from System 3 (AGD-affected) with feed type B, and salmon from System 4 (AGD-affected) with feed type C. There were no data for System 2 at T3.

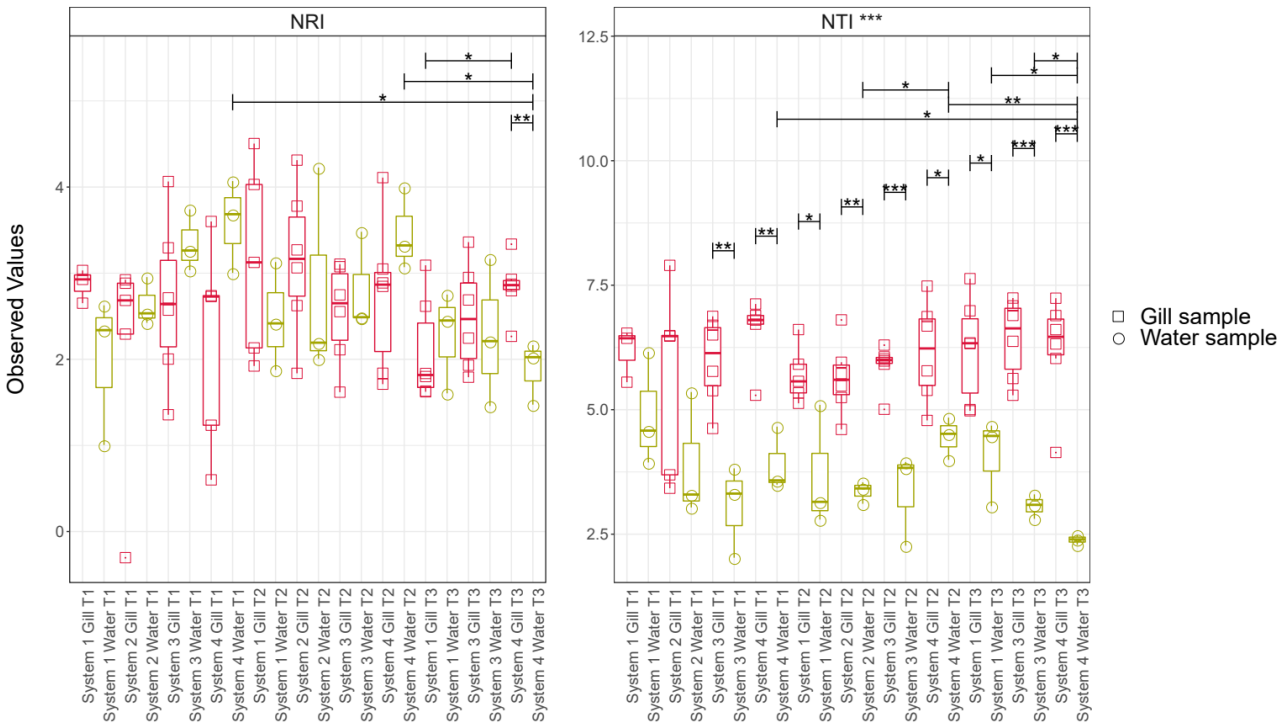

Figure 5.11. Environmental filtering analyses (NRI and NTI) from each gill (red squares) and water (yellow circles) sample. The lines at the top of each chart connect two categories where the differences were significant (ANOVA) with * ($p < 0.05$), ** ($p < 0.01$), or *** ($p < 0.001$). Salmon from System 1 (AGD-unaffected) and System 2 (AGD-affected) were fed with food type A, salmon from System 3 (AGD-affected) with feed type B, and salmon from System 4 (AGD-affected) with feed type C. There were no data for System 2 at T3.

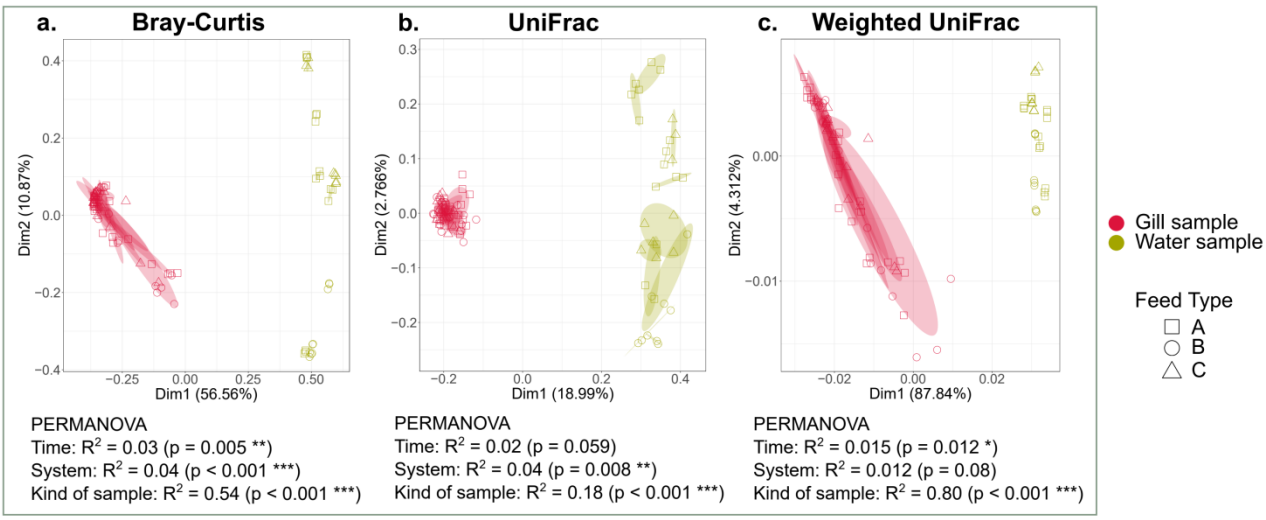

Figure 5.12. Representation of the beta-diversity indices (a. Bray-Curtis, b. UniFrac, c. Weighted UniFrac) of the gill (in red) and water (in yellow) prokaryotic community from each system at each timepoint. Ellipses are drawn at 95% confidence interval of standard error from the replicates of each system at each timepoint. PERMANOVA analyses considered temporal changes in the bacterial community ('time'),

changes comparing microbial communities from different systems ('system'), and changes when comparing prokaryotic communities from types of sample ('kind of sample').

5.3.4 - Differences between bacterial communities of surrounding water

Bacterial diversity in the water was very different depending on the system and timepoint (**Fig. 5.13**). Samples from S3 and S4 were significantly more diverse (than S1 or S2) at T2, but were less even at T2 and T3 (**Fig. 5.13**). Thus, the water microbiome in tanks in which salmon were fed with FTB and FTC was more diverse, and less even, than in tanks in which salmon were fed with FTA. Beta-diversity analyses also showed significant differences in the water community structure, but without any recognisable trend based on the time and the system (**Fig. S5.3**). Although differences in alpha and beta-diversity were observed between systems, the most abundant taxa were common between systems and included the families Flavobacteriaceae and Rhodobacteriaceae, and the genus *Owenweeksia* (**Fig. S5.4**).

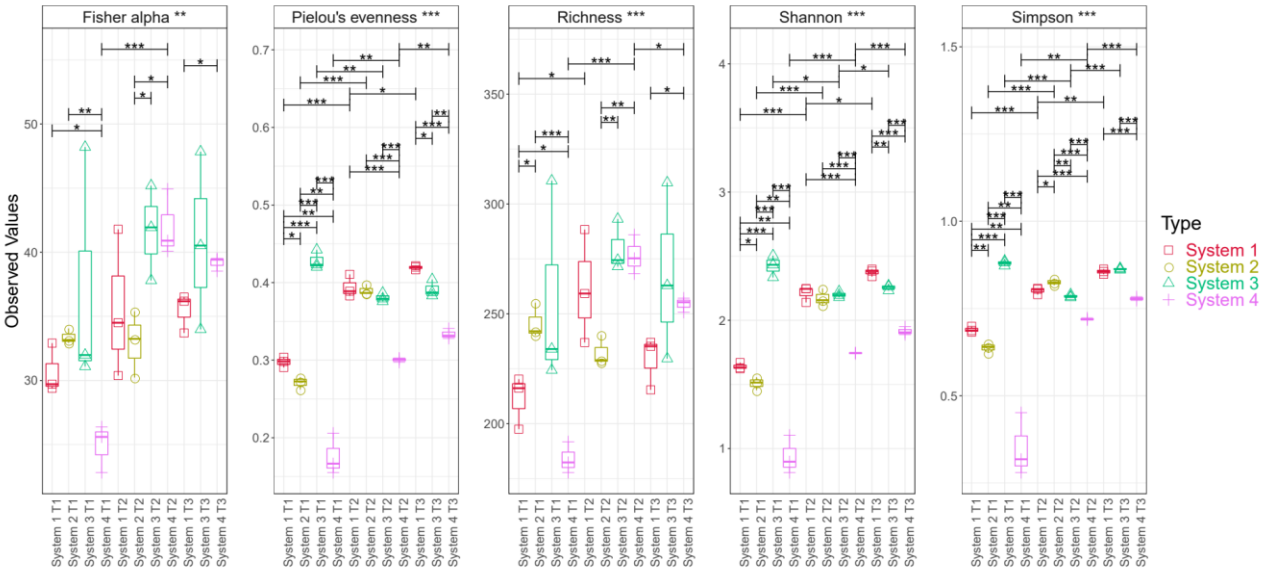

Figure 5.13. Alpha-diversity descriptors (Fisher's alpha parameter, Pielou's evenness, richness, Shannon's diversity index, and Simpson's diversity index) of the water prokaryotic community from each system at each timepoint. Symbol shapes and symbol/box colours represent the different systems, S1-S4. The lines at the top of each chart connect two categories where the differences were significant (ANOVA) with * ($p < 0.05$), ** ($p < 0.01$), or *** ($p < 0.001$). Salmon from System 1 (AGD-unaffected) and System 2 (AGD-affected) were fed with food type A, salmon from System 3 (AGD-affected) with feed type B, and salmon from System 4 (AGD-affected) with feed type C. There were no data for System 2 at T3.

5.4 - Discussion

5.4.1 - Most abundant bacteria in gill and water samples

The premise of the present study was that the gill microbiome is relevant in AGD onset and development (Bowman and Nowak, 2004; Slinger *et al*., 2020a; Chapter 3 of the present thesis, manuscript submitted (Birlanga *et al*., 2021)), but that not much is known about the gill microbiome in Atlantic salmon, and that thus a description of the gill microbiome is desirable. The most abundant bacteria in gill samples, and also part of the core gill microbiome, were also found in previous studies and included: members of the Rubritaleaceae family (Slinger *et al*., 2020a; Slinger *et al*., 2020b; Chapter 3 of the present thesis, manuscript submitted (Birlanga *et al*., 2021)); members of the phyla Bacteroidetes and Proteobacteria (classes Bacteroidia and Alphaproteobacteria, respectively) (Schmidt *et al*., 2016; Minich *et al*., 2020; Slinger *et al*., 2020a; Slinger *et al*., 2020b); and the genus *Streptococcus* (Bowman & Nowak, 2004; Schmidt *et al*., 2016). The family Chlorobiaceae was abundant across gill samples (**Fig. 5.3**), and was also part of the core gill microbiome (**Fig. S5.1**). Only Minich *et al*. (2020) previously found the phylum Chlorobi (including the family Chlorobiaceae) in the gill microbiome; however, we could not find that phylum in our previous gill microbiome studies in Irish fish farms. The high relative abundance of the Chlorobiaceae family on gills, compared with the very low abundance in surrounding water, suggests this group was selected to be part of the gill microbiome.

The Chlorobi phylum, also known as green sulfur bacteria, was initially described as anoxygenic photosynthesisers, capable of using hydrogen sulfide for reducing power (Gupta *et al*., 2004). The genus *Chlorobium* was found to include phosphorus-removing bacteria in anaerobic zones of eutrophic lakes (Li *et al*., 2018). As hydrogen sulfide is a common toxic molecule in aquariums and fish tanks (Roberts & Palmeiro, 2008), the possible selection of the Chlorobiaceae family in the microbiome suggests a role in hydrogen sulfide consumption near gills.

Although the phylum Chlorobi was first described as anaerobic, some members were found in bacterial communities from activated sludge in aerobic bioreactors (Cortés-Lorenzo *et al*., 2014; Zhang *et al*., 2016; He *et al*., 2020), and as aerobic photoheterotrophs in microbial mats (Liu *et al*., 2012; Stamps *et al*., 2014; Roy *et al*., 2019). Considering the findings of Minich *et al*. (2020), the literature on aerobic Chlorobi members, and the measured oxygen concentrations in S1-S4,

the high abundance of Chlorobiaceae in gill samples appears to preclude low oxygen availability in the water near brachial arches.

Members of the family Flavobacteriaceae were abundant in Atlantic salmon gill microbiome studies, including *Flavobacterium* sp. (Bowman & Nowak, 2004; Steinum *et al.*, 2009; Schmidt *et al*., 2016; Slinger *et al*., 2020a, Chapter 3 of the present thesis, manuscript submitted (Birlanga *et al*., 2021)), *Winogradskyella* sp. (Embar-Gopinath *et al*., 2005; Chapter 3 of the present thesis, manuscript submitted (Birlanga *et al*., 2021)), *Psychroserpens* sp. (Bowman & Nowak, 2004; Chapter 3 of the present thesis, manuscript submitted (Birlanga *et al*., 2021)), and *Tenacibaculum* sp. (Slinger *et al*., 2020a, Chapter 3 of the present thesis, manuscript submitted (Birlanga *et al*., 2021)), and were suggested as important in AGD episodes or to be opportunistic pathogens.

Owenweeksia, which appeared more abundant in gill samples from S3 and S4, and in most of the water samples (**Fig. 5.9**), was identified by Cottrell & Kirchman (2000), and Jiang *et al*. (2020), to be important marine heterotrophs and was previously found recirculation aquaculture systems (RAS) by Ruan *et al*. (2015). The presence of this group in the core water and gill microbiomes (**Fig. S5.2**) may indicate an important role in carbon cycling in the trial.

The taxa found in the water samples (**Fig. 5.9**) were not previously reported as occurring together in Atlantic salmon RAS. However, each of the most abundant taxa were found individually in previous studies: Flavobacteriaceae (Schmidt *et al*., 2016; Karlsen *et al*., 2017; Rud *et al*., 2017), Rhodobacteriaceae (Karlsen *et al*., 2017; Rud *et al*., 2017; Minich *et al*., 2020), Alteromonadaceae (Karlsen *et al*., 2017; Rud *et al*., 2017), Rhizobiaceae (Schmidt *et al*., 2016; Rud *et al*., 2017), Gammaproteobacteria (Rud *et al*., 2017; Kuang *et al*., 2020) and Sphingobacteriales (Schmidt *et al*., 2016). Such variances are likely due to the many factors influencing RAS water microbiomes (Blancheton *et al*., 2013; Bentzon‐Tilia *et al*., 2016), including the impact of fish microbiomes; the quantity and quality of available organic and inorganic nutrients; and the presence or absence of microorganisms capable of nitrogen, carbon and sulfur cycling (Itoi *et al*., 2006).

5.4.2 - Gill microbiomes are more diverse than the surrounding water microbiome

Although beta-diversity of gill microbiomes was partially driven by time (**Fig. 5.6**), the various conditions (in S1-S4) impacted community structure. On the other hand, diversity of the water microbiome was significantly driven by both time and system (**Fig. S5.3**). The water and gill microbiomes included 13 taxa considered to be a shared, core microbiome (**Fig. S5.2**), although many significant differences were apparent in microbiome features (alpha-diversity, environmental filtering, and beta-diversity) between water and gill samples (**Fig. 5.10, 5.11, 5.12,** respectively). Although the water microbiome from each system was significantly different, the gill microbiome was similar between systems. This supports the idea of a selective development of the gill microbiome, probably shaped and constrained by the gill microbiome already established prior to the experiment, and the host immunological system. Karlsen *et al*. (2017) and Minniti *et al.* (2017) also found different microbiomes in seawater and skin from Atlantic salmon. In addition, Minich *et al*. (2020) found the gill microbiome from freshwater Atlantic salmon did not correlate with the surrounding water or the tank biofilms, contrary to the conventional assumption that the gill microbiome is seeded from the surrounding water. Further studies should be done to better understand the connection and dynamics of the gill and skin microbiome in pre- and post-smolted Atlantic salmon.

5.4.3 - Diet types influenced the surrounding water microbiome

Water microbiome analyses showed different bacterial communities between systems (**Fig. 5.13, S5.3, and S5.4**). The possible influence of the fish diet on the surrounding water microbiome has not been demonstrated yet, but the results in this study supported this hypothesis. On the other hand, the impact of diet on the gut microbiome was demonstrated by Silva *et al*. (2011), Piazzon *et al*. (2017) and Yukgehnaish *et al*. (2020). Alteration of the gut microbiome likely shapes the faecal microbiome (Silva *et al*., 2011), impacting the surrounding water and, in turn, likely the gill microbiome. However, this phenomenon would likely only be relevant in closed environments with relatively low volumes, such as in a laboratory-scale trials, and would seem unlikely at the scale of fish farms.

5.4.4 - Gill microbiomes were significantly influenced by AGD

Although the gill microbiome remained stable along the timepoints (**Fig. 5.4**), samples from AGD-affected salmon fed with FTA were significantly more even and diverse at 14 dpi compared with control salmon fed with FTA, which was counter to our hypothesis. The results also do not correlate with the findings of Slinger *et al*. (2020a), the only previous study with similar objectives and methodologies, which aimed to characterise the gill microbiome of AGD-affected and healthy salmon 21 dpi in a laboratory trial. In fact, Slinger *et al*. (2020a) found a less diverse and less even bacterial community in AGD-related lesions compared with healthy samples. Although that study is the closest to the present study in terms of objectives and methodologies, the DNA recovery procedure used gill filaments without confirming that partial gills could adequately represent the whole-gill microbiome. As we used entire gill arches (Chapter 3 of the present thesis, manuscript submitted (Birlanga *et al*., 2021)), we suggest the possible difference in representativeness may partly explain the discrepancy in the findings. In addition, as we could not obtain gill samples at 21 dpi, the different sampling time may also explain the different observation.

The gill microbiome, as with the gut microbiome, participates in numerous metabolic and immunological pathways (Llewellyn *et al.*, 2014; Ghanbari *et al*., 2015; Talwar *et al*., 2018). Among the factors influencing this relationship is the colonisation history (Llewellyn *et al.*, 2014), which influences resistance of fish to diseases since the microbiome is the first line of defence against pathogens (Boutin *et al*., 2012). The different gill microbiomes at the start of the experiments of Slinger *et al*. (2020a) and the present study likely also influenced the contradictory findings. Despite all these methodological and microbial differences, all these studies found a significant impact on the gill microbiome from AGD-affected Atlantic salmon when compared with healthy fish. Results from Birlanga *et al*. (Chapter 3 of the present thesis, manuscript submitted (Birlanga *et al*., 2021)) also supported this conclusion, after comparing the gill microbiome between farmed salmon before and during an AGD episode (12 dpi).

Another possible explanation for the unexpected rise in the gill microbiome evenness in AGD-affected samples can be related to a dysregulation in the host immune response. Literature already confirmed the participation of the host immune system in the regulation of the gut microbiome composition in fish (Smith *et al.*, 2015; Yukgehnaish *et al*., 2020), being probable to have a similar regulation of the gill microbiome. Having in mind that a high environmental stress

on fish may compromise the performance of the immunological response (Xiong *et al*., 2019), we suggested that the combination between AGD development might leaded to a decrease in the immunological control of the gill microbiome. This would allow preselected gill microbes to spread easily, and it would also allow microorganisms in the surrounding water to more easily colonise the gills. However, gill microbiome from AGD-affected salmon fed with FTB and FTC had lower diversity and evenness when compared with AGD-affected salmon fed with FTA at T2 (**Fig. 5.4**). This discrepancy can be probably due to the only difference between those treatments: the distinct formulation of the feeds that those salmon ate. These different functional components in FTB and FTC may helped maintaining the immunological regulation of the gill microbiome during AGD, inhibiting certain bacteria to colonise gills and keeping bacterial diversity and evenness levels closer to the gill microbiome from unexposed salmon from S1. The presence of AGD-negative controls for S3 and S4 would help supporting or denying these explanations, but, unfortunately, we could not establish those treatments in the *in-vivo* trial.

5.4.5 - Functional diets may influence the gill microbiome

AGD gill scores, *N. perurans* abundance, and condition factor results did not evidence that tested functional diets differently influenced AGD severity and fish performance (**Fig. 5.2**). More research should be done to further elucidate the possible role of new formulated functional diets to mitigate AGD on Atlantic salmon.

Gill microbiome structure from Atlantic salmon fed with FTA was significantly different when compared with salmon fed with FTC at T1 (**Fig. 5.7c**). These observed differences in beta-diversity were due to the variations in the functional diets, as samples at T1 were collected after 21 days feeding the fish with their respective diets, and before *N. perurans* inoculation (**Fig. 5.1**). There could be two possible explanations: **i)** FTA and FTC formulations differentiate the gut microbiome and the overall Atlantic salmon health, as fish gut microbiome is actively involved in numerous metabolic and immunological pathways (Llewellyn *et al.*, 2014; Ghanbari *et al*., 2015; Talwar *et al*., 2018). As was observed in the gut microbiome (Smith *et al.*, 2015; Yukgehnaish *et al*., 2020), the immunological response may also influence the gill microbiome, thus, as a consequence of the different diets, an altered immunological response may impact the gill microbiome differently; **ii)** FTA and FTC formulations differentiate the gut microbiome, thus faeces from FTA-fed salmon and FTC-fed salmon contain different bacteria that seed distinctly the surrounding water microbiome. These different water microbiomes would then play as

bacteria reservoirs, differently influencing the gill microbiome. We find more plausible the first possible explanation, as modifying the water microbiome due to faecal bacteria would be more difficult, especially in a sea farm.

The genus *Reyranella*, and a member of the family Flavobacteriaceae had significant higher abundance in gill samples from FTC-fed salmon at T1; while other members of the family Flavobacteriaceae, the genera *Prevotella*, and members of the families Rubritaleaceae, Rhodobacteriaceae, and Halomonadaceae were more abundant in gill microbiome from FTA-fed salmon. All mentioned bacteria were previously found in other fish microbiome studies, mainly focused on guts (Wang *et al*., 2018; Tyagi *et al*., 2019; Foysal *et al*., 2020; Minich *et al.*, 2020; Mukherjee *et al*., 2020; Rimoldi *et al*., 2020; Slinger *et al*., 2020a), but their role and dynamics in the gill microbiome require further research.

Results from subset regression analyses showed that changes in alpha-diversity from gill samples correlated with the timepoints T1 and T2 (**Fig. 5.8**). This suggested that variation in the gill microbiome evenness (even though those variations were not significant at T1) may be due to the effect of the various functional diets that salmon experienced at T1; and the combination between the various functional diets and the AGD at T2. Alpha- and beta-diversity showed positive correlations with samples from S2 (**Fig. 5.8**), suggesting that the combination of FTA and AGD significantly influenced the gill microbiome, making the community more even and diverse, and differentiating the gill microbiome from salmon in S2 from salmon in other systems. Although differences in diversity were proved in samples from S2 (**Fig. 5.4**), the bacterial community on gills from salmon in S2 was very similar to salmon in other systems (**Fig. 5.6**). Thus, even though the combination of FTA and AGD had a significant correlation with alpha- and beta-diversity, these factors were not enough to produce a significant difference in the gill microbiome structure when compared with the other treatments.

Although the present research provides initial evidences of the possible impact of functional diets on the gill microbiome in Atlantic salmon, more research should be done to further evidence the possible impact of functional diets on the gill microbiome and whether the immunological system plays a role.

5.5 - Conclusions

The present study concluded that the gill prokaryotic microbiome from Atlantic salmon was significantly impacted by the AGD onset. Unexpectedly, the diversity and evenness of the gill microbiome increased after 14 dpi in AGD-affected salmon. However, the different treatments did not clearly influence the gill microbiome beta-diversity, being the time factor the main driver. Nevertheless, the gill microbiome from salmon fed with feed type A was significantly different from salmon fed with feed type C before AGD. Additionally, the gill microbiome from AGD-affected salmon which were fed with feed type A positively correlated with most of the alpha- and beta-diversity descriptors. These correlations could not be observed in AGD-affected salmon fed with the other functional diets.

The core microbiome taxa in gill samples were the families Chlorobiaceae, Flavobacteriaceae, and Rubritaleaceae, the genera *Synechococcus*, *Owenweeksia*, and *Streptococcus*, and the classes Bacteroidia and Alphaproteobacteria. Bacterial communities from gill samples had higher diversity than communities from water samples in the same system, having very different microbiome structures.

These results further evidenced the impact of the AGD on the gill microbiome of Atlantic salmon, and also provided some initial evidence of the influence of the diet on both, the gill and the water microbiome. Further research on this topic should focus on applying ‘omics approaches, such as metagenomics, to try to better understand the AGD impact and the role of the gill microbiome.

5.6 - References

Bentzon‐Tilia, M., Sonnenschein, E. C., & Gram, L. (2016). Monitoring and managing microbes in aquaculture‐Towards a sustainable industry. *Microbial biotechnology*, 9(5), 576-584.

Birlanga, V. B., McCormack, G., Ijaz, U. Z., McCarthy, E., Smith, C., & Collins, G. (2021). Dynamic Gill and Mucous Microbiomes Track an Amoebic Gill Disease Episode in Farmed Atlantic Salmon. (https://assets.researchsquare.com/files/rs-29747/v1/33663208-b035-433d617 bf44-59125d163937.pdf)

Blancheton, J. P., Attramadal, K. J. K., Michaud, L., d'Orbcastel, E. R., & Vadstein, O. (2013). Insight into bacterial population in aquaculture systems and its implication. *Aquacultural engineering*, 53, 30-39.

Boerlage, A. S., Ashby, A., Herrero, A., Reeves, A., Gunn, G. J., & Rodger, H. D. (2020). Epidemiology of marine gill diseases in Atlantic salmon (*Salmo salar*) aquaculture: a review. *Reviews in Aquaculture*, 12(4), 2140-2159.

Bolyen, E., Rideout, J. R., Dillon, M. R., Bokulich, N. A., Abnet, C. C., Al-Ghalith, G. A., Alexander, H., Alm, E.J., Arumugam, M., Asnicar, F. & Caporaso, J. G. (2019). Reproducible, interactive, scalable and extensible microbiome data science using QIIME 2. *Nature biotechnology*, 37(8), 852-857.

Boutin, S., Bernatchez, L., Audet, C., & Derôme, N. (2012). Antagonistic effect of indigenous skin bacteria of brook charr (*Salvelinus fontinalis*) against *Flavobacterium columnare* and *F. psychrophilum*. *Veterinary microbiology*, 155(2-4), 355-361.

Bowden, A. J. (2018). The effects of temperature and ploidy on the metabolism and energetics of Atlantic salmon (*Salmo salar*) infected with amoebic gill disease (*Doctoral dissertation, University of Tasmania*).

Bowman, J. P., & Nowak, B. (2004). Salmonid gill bacteria and their relationship to amoebic gill disease. *Journal of Fish Diseases*, 27(8), 483-492.

Bustos, P. A., Young, N. D., Rozas, M. A., Bohle, H. M., Ildefonso, R. S., Morrison, R. N., & Nowak, B. F. (2011). Amoebic gill disease (AGD) in Atlantic salmon (*Salmo salar*) farmed in Chile. *Aquaculture*, 310(3-4), 281-288.

Bridle, A. R., Crosbie, P. B. B., Cadoret, K., & Nowak, B. F. (2010). Rapid detection and quantification of *Neoparamoeba perurans* in the marine environment. *Aquaculture*, 309(1-4), 56-61.

Caporaso, J.G., Lauber, C.L., Walters, W.A., Berg-Lyons, D., Lozupone, C.A., Turnbaugh, P.J., Fierer, N. & Knight, R. (2011). Global patterns of 16S rRNA diversity at a depth of millions of sequences per sample. *Proceedings of the national academy of sciences*. 108(Supplement 1), 4516-22.

Caporaso, J.G., Lauber, C.L., Walters, W.A., Berg-Lyons, D., Huntley, J., Fierer, N., Owens, S.M., Betley, J., Fraser, L., Bauer, M. & Gormley, N. (2012). Ultra-high-throughput microbial community analysis on the Illumina HiSeq and MiSeq platforms. *The ISME journal*. 6(8), 1621-4.

Clark, A., & Nowak, B. F. (1999). Field investigations of amoebic gill disease in Atlantic salmon, *Salmo salar* L., in Tasmania. *Journal of Fish Diseases*, 22(6), 433-443.

Cortés-Lorenzo, C., Sipkema, D., Rodríguez-Díaz, M., Fuentes, S., Juárez-Jiménez, B., Rodelas, B., Smidt, H. & González-López, J. (2014). Microbial community dynamics in a submerged fixed bed bioreactor during biological treatment of saline urban wastewater. *Ecological engineering*, 71, 126-132.

Cottrell, M. T., &Kirchman, D. L. (2000). Natural assemblages of marine proteobacteria and members of the Cytophaga-Flavobacter cluster consuming low-and high-molecular-weight dissolved organic matter. *Applied and environmental microbiology*, 66(4), 1692-1697.

Crosbie, P. B. B., Bridle, A. R., Cadoret, K., & Nowak, B. F. (2012). In vitro cultured *Neoparamoeba perurans* causes amoebic gill disease in Atlantic salmon and fulfils Koch's postulates. *International journal for parasitology*, 42(5), 511-515.

Davis, N. M., Proctor, D. M., Holmes, S. P., Relman, D. A., & Callahan, B. J. (2018). Simple statistical identification and removal of contaminant sequences in marker-gene and metagenomics data. *Microbiome*, 6(1), 1-14.

Downes, J.K., Henshilwood, K., Collins, E.M., Ryan, A., Connor, I.O., Rodger, H.D., MacCarthy, E. & Ruane, N.M. (2015). A longitudinal study of amoebic gill disease on a marine Atlantic salmon farm utilising a real-time PCR assay for the detection of *Neoparamoeba perurans*. *Aquaculture Environment Interactions*. 7(3), 239-51.

Dray, S., Bauman, D., Blanchet, G., Borcard, D., Clappe, S., Guenard, G., Jombart, T., Larocque, G., Legendre, P., Madi, N. & Wagner, H. H. (2018). adespatial: Multivariate multiscale spatial analysis. *R package version* 0.3-2.

Embar-Gopinath, S., Butler, R., & Nowak, B. (2005). Influence of salmonid gill bacteria on development and severity of amoebic gill disease. *Diseases of aquatic organisms*, 67(1-2), 55-60.

Foysal, M. J., Alam, M., Kawser, A. R., Hasan, F., Rahman, M. M., Tay, C. Y., Prodhan, M.S.H. & Gupta, S. K. (2020). Meta-omics technologies reveals beneficiary effects of Lactobacillus plantarum as dietary supplements on gut microbiota, immune response and disease resistance of Nile tilapia (*Oreochromis niloticus*). *Aquaculture*, 520, 734974.

Ghanbari, M., Kneifel, W., &Domig, K. J. (2015). A new view of the fish gut microbiome: advances from next-generation sequencing. *Aquaculture*, 448, 464-475.

Gjerde, B., Boison, S. A., Aslam, M. L., Løvoll, M., Bakke, H., Rey, S., & Lillehammer, M. (2019). Estimates of genetic correlations between susceptibility of Atlantic salmon to amoebic gill disease in a bath challenge test and a field test. *Aquaculture*, 511, 734265.

Gupta, R. S. (2004). The phylogeny and signature sequences characteristics of Fibrobacteres, Chlorobi, and Bacteroidetes. *Critical reviews in microbiology*, 30(2), 123-143.

He, Q., Wang, H., Chen, L., Gao, S., Zhang, W., Song, J., & Yu, J. (2020). Elevated salinity deteriorated enhanced biological phosphorus removal in an aerobic granular sludge sequencing batch reactor performing simultaneous nitrification, denitrification and phosphorus removal. *Journal of hazardous materials*, 390, 121782.

Itoi, S., Niki, A., & Sugita, H. (2006). Changes in microbial communities associated with the conditioning of filter material in recirculating aquaculture systems of the pufferfish *Takifuguru bripes*. *Aquaculture*, 256(1-4), 287-295.

Jiang, W., Ren, W., Li, L., Dong, S., & Tian, X. (2020). Light and carbon sources addition alter microbial community in biofloc-based *Litopenaeus vannamei* culture systems. *Aquaculture*, 515, 734572.

Karlsen, C., Ottem, K. F., Brevik, Ø. J., Davey, M., Sørum, H., &Winther-Larsen, H. C. (2017). The environmental and host-associated bacterial microbiota of Arctic seawater-farmed Atlantic salmon with ulcerative disorders. *Journal of fish diseases*, 40(11), 1645-1663.

Kassambara, A. (2018). Machine learning essentials: Practical guide in R. *Sthda*.

Kembel, S. W., Cowan, P. D., Helmus, M. R., Cornwell, W. K., Morlon, H., Ackerly, D. D., Blomberg, S.P. & Webb, C. O. (2010). Picante: R tools for integrating phylogenies and ecology. *Bioinformatics*, 26(11), 1463-1464.

Kuhn, M. (2008). Building predictive models in R using the caret package. *J Stat Softw*, 28(5), 1-26.

Kuang, T., He, A., Lin, Y., Huang, X., Liu, L., & Zhou, L. (2020). Comparative analysis of microbial communities associated with the gill, gut, and habitat of two filter-feeding fish. *Aquaculture Reports*, 18, 100501.

Lahti, L., Shetty, S., Blake, T., &Salojarvi, J. (2017). Microbiome R package. *Tools Microbiome Anal R.*

Legendre, P., & De Cáceres, M. (2013). Beta diversity as the variance of community data: dissimilarity coefficients and partitioning. *Ecology letters*, 16(8), 951-963.

Li, X., Li, Y., Li, Y., & Wu, J. (2018). Diversity and distribution of bacteria in a multistage surface flow constructed wetland to treat swine wastewater in sediments. *Applied microbiology and biotechnology*, 102(24), 10755-10765.

Liu, Z., Klatt, C. G., Ludwig, M., Rusch, D. B., Jensen, S. I., Kühl, M., Ward, D.M. & Bryant, D. A. (2012). 'Candidatus *Thermochlorobacter aerophilum*:'an aerobic chlorophotoheterotrophic member of the phylum Chlorobi defined by metagenomics and metatranscriptomics. *The ISME journal*, 6(10), 1869-1882.

Llewellyn, M. S., Boutin, S., Hoseinifar, S. H., &Derome, N. (2014). Teleost microbiomes: the state of the art in their characterization, manipulation and importance in aquaculture and fisheries. *Frontiers in microbiology*, 5, 207.

Love, M. I., Huber, W., & Anders, S. (2014). Moderated estimation of fold change and dispersion for RNA-seq data with DESeq2. *Genome biology*, 15(12), 1-21.

Lüdecke, D. (2018). sjPlot: Data visualization for statistics in social science. *R package version*, 2(1).

Lumley, T., & Miller, A. (2009). Leaps: regression subset selection. *R package version*, 2, 2366.

Masella, A. P., Bartram, A. K., Truszkowski, J. M., Brown, D. G., & Neufeld, J. D. (2012). PANDAseq: paired-end assembler for illumina sequences. *BMC bioinformatics*, 13(1), 1-7.

Marcos-López, M., Ruiz, C. E., Rodger, H. D., O'Connor, I., MacCarthy, E., & Esteban, M. Á. (2017). Local and systemic humoral immune response in farmed Atlantic salmon (*Salmo salar* L.) under a natural amoebic gill disease outbreak. *Fish & shellfish immunology*, 66, 207-216.

McMurdie, P. J., & Holmes, S. (2013). phyloseq: an R package for reproducible interactive analysis and graphics of microbiome census data. *PloS one*, 8(4), e61217.

Minich, J. J., Poore, G. D., Jantawongsri, K., Johnston, C., Bowie, K., Bowman, J., Knight, R., Nowak, B. & Allen, E. E. (2020). Microbial ecology of Atlantic salmon (*Salmo salar*) hatcheries: impacts of the built environment on fish mucosal microbiota. *Applied and environmental microbiology*, 86(12).

Minniti, G., Hagen, L. H., Porcellato, D., Jørgensen, S. M., Pope, P. B., &Vaaje-Kolstad, G. (2017). The skin-mucus microbial community of farmed Atlantic salmon (*Salmo salar*). *Frontiers in microbiology*, 8, 2043.

Mukherjee, A., Rodiles, A., Merrifield, D. L., Chandra, G., & Ghosh, K. (2020). Exploring intestinal microbiome composition in three Indian major carps under polyculture system: a high-throughput sequencing based approach. *Aquaculture*, 524, 735206.

Mullins, J., Nowak, B., Leef, M., Røn, Ø., Eriksen, T. B., & McGurk, C. (2020). Functional diets improve survival and physiological response of Atlantic salmon (*Salmo salar*) to amoebic gill disease. *Journal of the World Aquaculture Society*, 51(3), 634-648.

Munday, B. L. (1986). Diseases of salmonids. In Proceedings of the workshop on diseases of Australian fish and shellfish (pp. 127-141). *Australian Fish Health Reference Laboratory*.

Munday, B. L., Foster, C. K., Roubal, F. R., & Lester, R. J. G. (1990). Paramoebic gill infection and associated pathology of Atlantic salmon, *Salmo salar* and rainbow trout, *Salmo gairdneri* in Tasmania. In Pathology in marine science. *Proceedings of the Third International Colloquium on Pathology in Marine Aquaculture*, held in Gloucester Point, Virginia, USA, October 2-6, 1988. (pp. 215-222). Academic Press Inc..

Nowak, B. F., & Archibald, J. M. (2018). Opportunistic but lethal: the mystery of paramoebae. *Trends in Parasitology*, 34(5), 404-419.

Oksanen, J., Kindt, R., Legendre, P., O'Hara, B., Stevens, M. H. H., Oksanen, M. J., & Suggests, M. A. S. S. (2007). The vegan package. *Community ecology package*, 10(631-637), 719.

Oldham, T., Rodger, H., & Nowak, B. F. (2016). Incidence and distribution of amoebic gill disease (AGD)—an epidemiological review. *Aquaculture*, 457, 35-42.

Piazzon, M. C., Calduch-Giner, J. A., Fouz, B., Estensoro, I., Simó-Mirabet, P., Puyalto, M., Karalazos, V., Palenzuela, O., Sitjà-Bobadilla, A. & Pérez-Sánchez, J. (2017). Under control: how a dietary additive can restore the gut microbiome and proteomic profile, and improve disease resilience in a marine teleostean fish fed vegetable diets. *Microbiome*, 5(1), 164.

Rimoldi, S., Gini, E., Koch, J. F. A., Iannini, F., Brambilla, F., &Terova, G. (2020). Effects of hydrolyzed fish protein and autolyzed yeast as substitutes of fishmeal in the gilthead sea bream (*Sparus aurata*) diet, on fish intestinal microbiome. *BMC veterinary research*, 16, 1-13.

Roberts, H., & Palmeiro, B. S. (2008). Toxicology of aquarium fish. *Veterinary clinics of North America: exotic animal practice*, 11(2), 359-374.

Robledo, D., Hamilton, A., Gutiérrez, A. P., Bron, J. E., & Houston, R. D. (2020). Characterising the mechanisms underlying genetic resistance to amoebic gill disease in Atlantic salmon using RNA sequencing. *BMC genomics*, 21, 1-11.

Rodger, H. D. (2014). Amoebic gill disease (AGD) in farmed salmon (*Salmo salar*) in Europe. *Fish Veterinary Journal*, (14), 16-27.

Ross, N. W., Firth, K. J., Wang, A., Burka, J. F., & Johnson, S. C. (2000). Changes in hydrolytic enzyme activities of naive Atlantic salmon *Salmo salar* skin mucus due to infection with the salmon louse *Lepeophtheirus salmonis* and cortisol implantation. *Diseases of aquatic organisms*, 41(1), 43-51.

Roy, C., Bakshi, U., Rameez, M. J., Mandal, S., Haldar, P. K., Pyne, P., & Ghosh, W. (2019). Phylogenomics of an uncultivated, aerobic and thermophilic, photoheterotrophic member of Chlorobia sheds light into the evolution of the phylum Chlorobi. *Computational biology and chemistry*, 80, 206-216.

Rozas-Serri, M. (2019). Gill diseases in marine salmon aquaculture with an emphasis on amoebic gill disease. *Atlantic*, 32(33), 34-35.

Ruan, Y. J., Guo, X. S., Ye, Z. Y., Liu, Y., & Zhu, S. M. (2015). Bacterial community analysis of different sections of a biofilter in a full-scale marine recirculating aquaculture system. *North American Journal of Aquaculture*, 77(3), 318-326.

Rud, I., Kolarevic, J., Holan, A. B., Berget, I., Calabrese, S., &Terjesen, B. F. (2017). Deep-sequencing of the bacterial microbiota in commercial-scale recirculating and semi-closed aquaculture systems for Atlantic salmon post-smolt production. *Aquacultural Engineering*, 78, 50-62.

Schmidt, V., Amaral-Zettler, L., Davidson, J., Summerfelt, S., & Good, C. (2016). Influence of fishmeal-free diets on microbial communities in Atlantic salmon (*Salmo salar*) recirculation aquaculture systems. *Applied and Environmental Microbiology*, 82(15), 4470-4481.

Shetty, S. A., Hugenholtz, F., Lahti, L., Smidt, H., & de Vos, W. M. (2017). Intestinal microbiome landscaping: insight in community assemblage and implications for microbial modulation strategies. *FEMS microbiology reviews*, 41(2), 182-199.

Silva, F. C. D. P., Nicoli, J. R., Zambonino-Infante, J. L., Kaushik, S., &Gatesoupe, F. J. (2011). Influence of the diet on the microbial diversity of faecal and gastrointestinal contents in gilthead sea bream (*Sparus aurata*) and intestinal contents in goldfish (*Carassius auratus*). *FEMS microbiology ecology*, 78(2), 285-296.

Slinger, J., Adams, M. B., & Wynne, J. W. (2020a). Bacteriomic profiling of branchial lesions induced by *Neoparamoeba perurans* challenge reveals commensal dysbiosis and an association with T*enacibaculum dicentrarchi* in AGD-affected Atlantic salmon (*Salmo salar* L.). *Microorganisms*, 8(8), 1189.

Slinger, J., Adams, M. B., & Wynne, J. W. (2020b). Comparison of bacterial diversity and distribution on the gills of Atlantic salmon (*Salmo salar* L.); an evaluation of sampling techniques. *Journal of Applied Microbiology*.

Smith, C. C., Snowberg, L. K., Caporaso, J. G., Knight, R., & Bolnick, D. I. (2015). Dietary input of microbes and host genetic variation shape among-population differences in stickleback gut microbiota. *The ISME journal*, 9(11), 2515-2526.

Stamps, B. W., Corsetti, F. A., Spear, J. R., & Stevenson, B. S. (2014). Draft genome of a novel Chlorobi member assembled by tetranucleotide binning of a hot spring metagenome. *Genome announcements*, 2(5).

Stegen, J. C., Lin, X., Konopka, A. E., & Fredrickson, J. K. (2012). Stochastic and deterministic assembly processes in subsurface microbial communities. *The ISME journal*, 6(9), 1653-1664.

Steinum, T., Sjåstad, K., Falk, K., Kvellestad, A., & Colquhoun, D. J. (2009). An RT PCR-DGGE survey of gill-associated bacteria in Norwegian seawater-reared Atlantic salmon suffering proliferative gill inflammation. *Aquaculture*, 293(3-4), 172-179.

Talwar, C., Nagar, S., Lal, R., & Negi, R. K. (2018). Fish gut microbiome: current approaches and future perspectives. *Indian journal of microbiology*, 58(4), 397-414.

Taylor, R. S., Wynne, J. W., Kube, P. D., & Elliott, N. G. (2007). Genetic variation of resistance to amoebic gill disease in Atlantic salmon (*Salmo salar*) assessed in a challenge system. *Aquaculture*, 272, S94-S99.

Taylor, R.S., Muller, W.J., Cook, M.T., Kube, P.D. & Elliott, N.G. (2009). Gill observations in Atlantic salmon (*Salmo salar*, L.) during repeated amoebic gill disease (AGD) field exposure and survival challenge. *Aquaculture*. 290(1-2), 1-8.

Tyagi, A., Singh, B., Thammegowda, N. K. B., & Singh, N. K. (2019). Shotgun metagenomics offers novel insights into taxonomic compositions, metabolic pathways and antibiotic resistance genes in fish gut microbiome. *Archives of microbiology*, 201(3), 295-303.

Vendramin, N., Alencar, A. L. F., Iburg, T. M., Dahle, M. K., Wessel, Ø., Olsen, A. B., Rimstad, E. & Olesen, N. J. (2018). Piscine orthoreovirus infection in Atlantic salmon (*Salmo salar*) protects against subsequent challenge with infectious hematopoietic necrosis virus (IHNV). *Veterinary research*, 49(1), 1-12.

Waagbø, R., & Remø, S. C. (2020). Functional diets in fish health management. In Aquaculture Health Management (pp. 187-234). *Academic Press.*

Wang, C., Sun, G., Li, S., Li, X., & Liu, Y. (2018). Intestinal microbiota of healthy and unhealthy Atlantic salmon *Salmo salar* L. in a recirculating aquaculture system. *Journal of Oceanology and Limnology*, 36(2), 414-426.

Wynne, J. W., Stratford, C., Slinger, J., Samsing, F., Rigby, M., McCulloch, R., Quezada-Rodriguez, P. & Taylor, R. S. (2020). The interaction between temperature and dose on the efficacy and biochemical response of Atlantic salmon to hydrogen peroxide treatment for amoebic gill disease. *Journal of fish diseases*, 43(1), 39-48.

Xiong, J. B., Nie, L., & Chen, J. (2019). Current understanding on the roles of gut microbiota in fish disease and immunity. *Zoological research*, 40(2), 70.

Young, N. D., Crosbie, P. B. B., Adams, M. B., Nowak, B. F., & Morrison, R. N. (2007). *Neoparamoeba perurans* n. sp., an agent of amoebic gill disease of Atlantic salmon (*Salmo salar*). *International journal for parasitology*, 37(13), 1469-1481.

Yukgehnaish, K., Kumar, P., Sivachandran, P., Marimuthu, K., Arshad, A., Paray, B. A., & Arockiaraj, J. (2020). Gut microbiota metagenomics in aquaculture: Factors influencing gut microbiome and its physiological role in fish. *Reviews in Aquaculture*, 12(3), 1903-1927.

Zhang, Y., Li, B., Xu, R. X., Wang, G. X., Zhou, Y., &Xie, B. (2016). Effects of pressurized aeration on organic degradation efficiency and bacterial community structure of activated sludge treating saline wastewater. *Bioresource technology*, 222, 182-189.

5.7 - Supplementary Figures and Tables

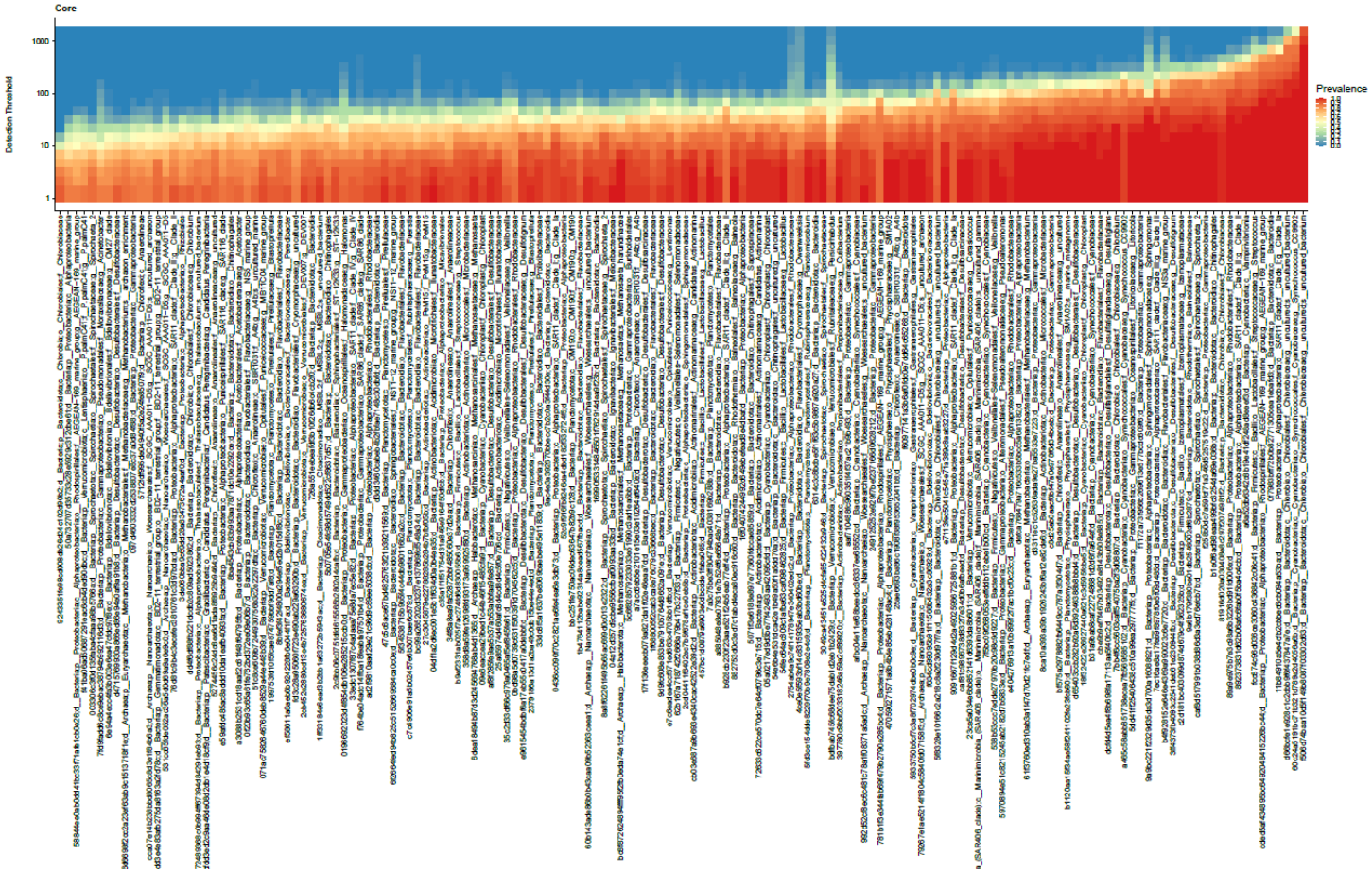

Figure S5.1. Prokaryotic core microbiome from gill samples from every system and every sampling point. To be part of the core microbiome, bacterial taxa must have at least 85% prevalence in all considered samples. Bacteria are arranged from a small relative abundance to a high relative abundance (from left to right), all of them with at least 85% prevalence. Although some prokaryotic taxa are repeated in more than one OTU, they could be considered as the same bacteria.

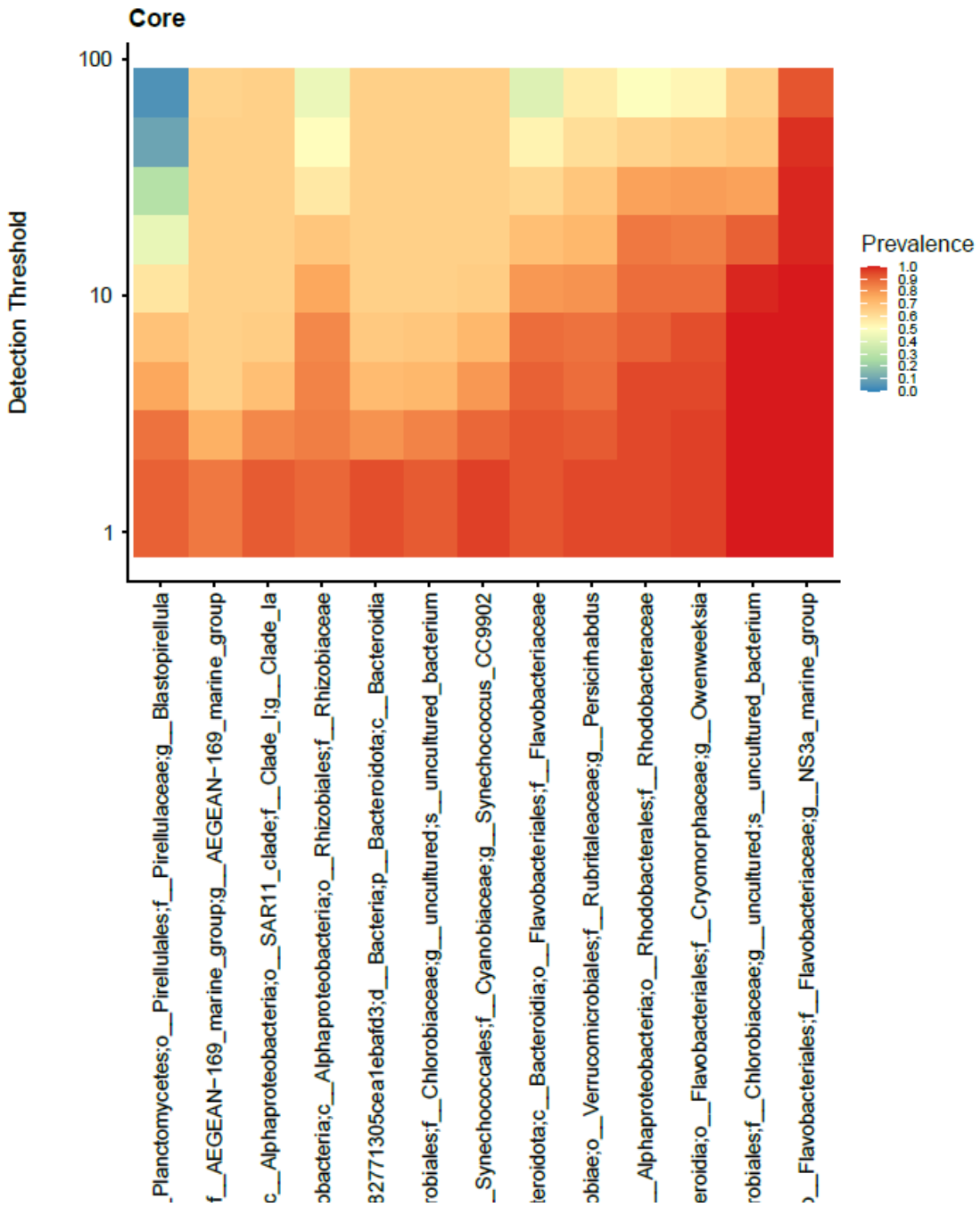

Figure S5.2. Shared prokaryotic core microbiome from gill and water samples from every system and every sampling point. To be part of the core microbiome, bacterial taxa must have at least 85% prevalence in all considered samples. Bacteria are arranged from a small relative abundance to a high relative abundance (from left to right), all of them with at least 85% prevalence. Although some prokaryotic taxa are repeated in more than one OTU, they could be considered as the same bacteria.

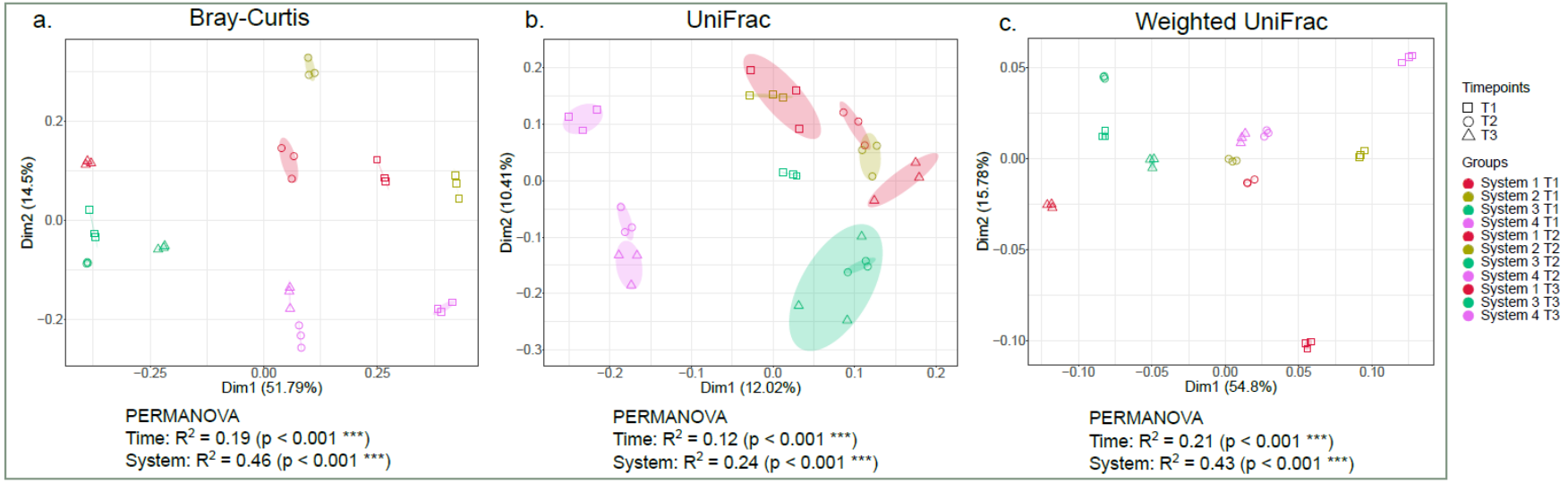

Figure S5.3. Representation of the beta-diversity descriptors (a. Bray-Curtis, b. UniFrac, c. Weighted UniFrac) of the water prokaryotic community from every system in every timepoint (T1, T2 and T3). Ellipses are drawn at 95% confidence interval of standard error from the replicates of each system in each timepoint. PERMANOVA analyses considered temporal changes in the water microbiome ("Time") and the changes comparing water microbiomes from different systems ("System")

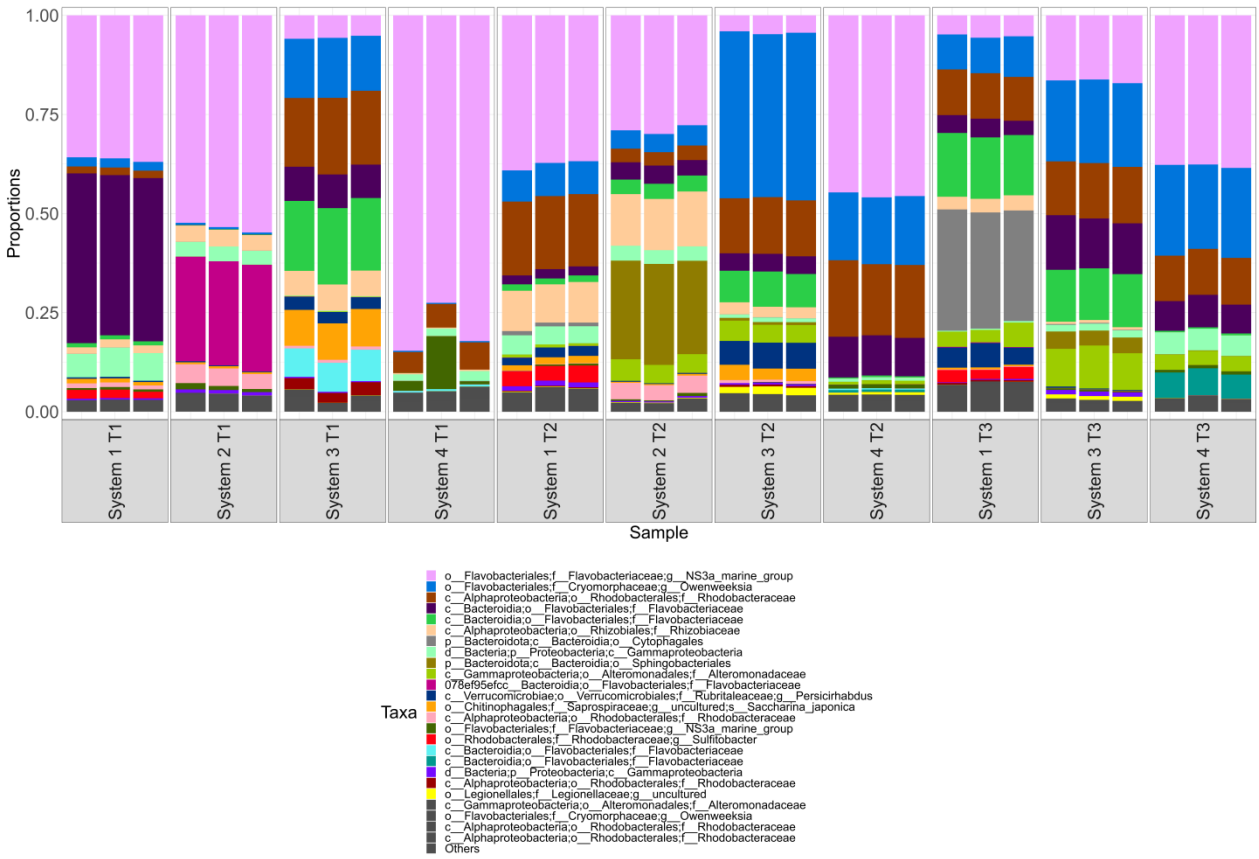

Figure S5.4. Community structure of the top 25 most relatively abundant ASVs from across each timepoint and system from water samples, where 'others' refers to all ASVs not included in the top 25. Letter before taxonomic names reference their taxonomic ranks (d: Domain, p: Phylum, c: Class, o: Order, f: Family, g: Genus, s: Species).

CHAPTER 6

General Discussion, Future Research and Recommendations for the Aquaculture Industry

The average annual mortality rate due to AGD in Irish production of Atlantic salmon is estimated to be 12%, comprising 1,200 tonnes worth €11.4 million in 2018 (BIM Annual Aquaculture Survey, 2019). The most common and best-studied way to treat salmon after AGD diagnoses is by freshwater bathing of infected fish, usually 2-4 h in water with salinity <3 ppt, before returning them to seacages. Despite relative expense and labour associated with freshwater bathing, this approach is still the most common AGD treatment, followed by hydrogen peroxide bathing (Wynne *et al*., 2020). In Ireland, the high availability of freshwater encourages fish farms to apply this treatment on their salmon, sometimes combined with other treatments (such as hydrogen peroxide). Indeed, the impact of low-salinity baths on the survival of AGD-affected fish has been widely demonstrated (Parsons *et al*., 2001; Adams & Nowak, 2004). Numerous studies have addressed the influence of many other factors, including temperature, biofouling, different possible treatments, the presence of specific kind of fish, fish stocking density in farms, and salmon genetic resistance (Oldham *et al.*, 2016), on the prevalence of AGD and abundance on gills of the initial aetiological agent, *Neoparamoeba perurans*.. However, the possible influence on AGD development and *N. perurans* abundance on gills of certain bacteria or the gill bacterial community has been less widely studied (e.g., Bowman & Nowak, 2004; Embar-Gopinath *et al*., 2005; Embar-Gopinath *et al*., 2006; Slinger *et al.*, 2020; Slinger *et al.*, 2021), and even fewer publications addressed this topic using high-throughput DNA sequencing studies (Slinger *et al.*, 2020; Slinger *et al.*, 2021). Most of the relevant literature hypothesised the possible role of the gill microbiome in the resistance of salmon to AGD, since the fish microbiome is considered to be the first line of defence against pathogens (Boutin *et al*., 2012). Thus, a better comprehension of the connection between the microbiome and AGD could mean the first steps towards the development of molecular tools to estimate the susceptibility of fish to AGD before *N. perurans* colonisation. Chapters 3, 4, and 5 hypothesised that the onset of AGD impacts the gill microbiome of farmed salmon, and aimed to characterise the gill microbiome before and during AGD episodes.

6.1 - Main findings and difficulties faced

First two experimental chapters (Chapters 3 and 4) included samples from Irish fish farms, out of our control, and thus we could only describe the gill microbiome whilst monitoring signs of AGD. These commercial fish farms applied freshwater baths to treat AGD on their salmon when and however they considered appropriate. These uncontrolled events interfered with the natural development of the gill microbiome during AGD, as the exposition to low-salinity water impacts bacteria and *N. perurans* abundance on gills (Adams & Nowak, 2004; Wright *et al*., 2018).

Hence, I expected not to see significant correlations between AGD development and the gill microbiome. However, the *N. perurans* abundance on gills significantly correlated with gill microbiome changes in both field campaigns. These results included samples from across six farms in two years; indeed, adding to this the conclusions from Chapter 5, the connection between AGD and the salmon gill microbiome has been demonstrated by the work of this thesis.

Slinger *et al.* (2020) and the findings of Chapter 3 support the conclusion that the gill microbiome from healthy salmon may be more diverse, and even, than the gill microbiome from AGD-affected salmon. However, the results reported in Chapter 5 described a less diverse and less even gill microbiome on the gills of control (non-AGD) salmon than AGD-affected salmon. This discrepancy may be due to our different sampling procedures, and our different sampling times (14 days post infection (dpi) in this thesis, and 21 dpi in Slinger *et al*. (2020)). Thus, I would extend the sampling period and increase the sampling frequency in future similar experiments. In this way I would be able to more easily compare those results with the literature, and to achieve a more detailed description of temporal changes in the gill microbiome.

Another difficulty that we faced was the long distance between the sampled fish farms described in Chapter 4. Although an intrinsic advantage of this sampling study was the wide territory used, the logistics were complicated. We needed to entrust fish features measurements, AGD gill scoring, gill arches sampling, and sample transportation to other people, thus risking consistency in sampling dates and procedures between locations. We ensured consistency and appropriate handling and transportation by providing each sampler with detailed guidelines and kits comprising of tubes and sampling consumables. Future similar campaigns should include an initial face-to-face training for samplers, and a planned simultaneous sampling that would start before summer, to have gill samples prior to AGD onset at each location. Despite these difficulties, we consider this campaign a success in describing the gill microbiome from AGD-affected salmon in fish farms, and in further evidence the connection between AGD and the gill microbiome in salmon. However, another factor that seemed to impact the diversity and structure of the gill microbiome to a greater extent was the water temperature. Coinciding with the hottest time of the year, we found a decreasing gradient of the gill microbiome diversity from northern to southern fish farms. Additionally, gill microbiome structure in samples taken during the hottest time of the year greatly differed from the rest of the microbiomes. The influence of the water temperature and seasonality on the fish microbiome has been demonstrated in the literature (Larsen *et al*., 2015; Vasemägi *et al*., 2017; Jones *et al*., 2018; Legrand *et al*., 2020), which was

mainly focused on the skin and gut microbiome, and thus we suggest that water temperature and seasonality are also important drivers impacting the gill microbiome.

During the sampling campaign described in Chapter 3, we obtained gill samples from before and during an AGD episode in one fish farm. This allowed us to describe significant temporal changes in the relative abundance of certain bacteria in gill microbiomes from before and during AGD. The relative abundance in the genera *Dyadobacter*, *Pedobacter* and *Shewanella* significantly decreased in T3, 12 dpi. Thus, we hypothesised that these three genera could be connected with the onset and development of AGD, offering possible AGD markers. As *Shewanella* was part of the top-25 relatively most abundant bacteria in healthy salmon, we suggested this genus as a possible target in the development of a qPCR assay to predict AGD susceptibility prior to *N. perurans* colonisation. On the other hand, the possible relationship between *Shewanella* and AGD was not as simple in the study described in Chapter 4. The relative abundance of *Shewanella* significantly changed between before and during AGD in two fish farms (Glinsk and Creevin). However, the high impact of the environmental factors on the gill microbiome during that sampling campaign impeded us in associating these changes in the *Shewanella* relative abundance with AGD onset. In the last experimental chapter of the thesis, we aimed to isolate the impact of the AGD on the gill microbiome from the environmental variability inherent in Chapters 3 and 4. After comparing the gill microbiome from healthy salmon with the microbiome from AGD-affected salmon, the relative abundance of some *Shewanella* amplicon sequencing variants (ASVs) were significantly different. Nevertheless, the relative abundance of some *Shewanella* ASVs increased while other *Shewanella* ASVs decreased, constraining us from clear conclusions on the relationship between *Shewanella* and AGD. Although we suggested that the genera *Dyadobacter*, *Pedobacter* and, especially, *Shewanella* are somehow connected with the AGD onset, further investigation should be carried out to better elucidate this possibility before the development of a molecular tool for AGD susceptibility prediction.

Apart from the gill and water microbiome characterisation in laboratory conditions in Chapter 5, we hypothesised that two functional diets would significantly impact on the water and gill microbiomes from AGD-affected fish. The tested functional diets (Feed type B (FTB) and feed type C (FTC)) did not decrease the AGD gill scores or impact the gill microbiome diversity from AGD-affected salmon, but FTC impacted the gill microbiome from AGD-unaffected salmon. Unfortunately, we did not know the composition of the two diets due to the company policy that provided them, making more difficult to interpret these results. However, previous literature

demonstrated the impact of specific functional diets on shifting the salmon gut microbiome (Gajardo *et al*., 2017; Wang *et al*., 2021), and on modulating the immune system (Waagbø, 1994; Abid *et al*., 2013; Djordjevic *et al*., 2021).Thus, we suggested that functional diets could partially drive the gill microbiome through modulating the immunological system, as happens with gut microbiome (Smith *et al*., 2015; Yukgehnaish *et al*., 2020), but these microbiome changes could not decrease the AGD signs on salmon. Although we provided initial evidence of the impact of functional diets on the gill microbiome, the AGD influence could have obscured that impact in challenged salmon. Research should be done to further explore the possible impact of functional diets and specific components of the diet on the gill microbiome and whether the immunological system plays a role. On the other hand, FTB, FTC, and the control diet differently shifted the water microbiome. We hypothesised that the various functional diets shifted the gut microbiome, which seeded the surrounding water in each tank differently and impacted its diversity. This phenomenon would hardly happen at fish farm scale, as high water circulation would spread the faecal bacteria into the sea, but it could be relevant in relatively low volume tanks in laboratory trials.

Results from the laboratory trial also demonstrated that the gill microbiome was more diverse than the water microbiome in every system, having very different microbiome structures. Additionally, it was also evidenced that the water microbiome in each system was different from the rest, and the gill microbiome was very similar between systems. Gathering these results, we hypothesised that the gill microbiome experienced a selective development, probably shaped and constrained by the gill microbiome already established prior to the experiment, and the host immunological system. Our study is not the first describing different gill or skin microbiomes and the surrounding water microbiome in Atlantic salmon (Karlsen *et al*., 2017; Minniti *et al*., 2017; Minich *et al*., 2020a), thus a selective development of the gill microbiome can be possible in Atlantic salmon. However, we do not have evidence that these differences between water microbiome and gill microbiome in Atlantic salmon happen in a field sampling. Further studies should be done to confirm gill and water microbiome differences, and to better understand whether/how the Atlantic salmon immunological system regulates the bacterial community on gills.

6.2 - Discussion on the methodology used

Previous studies have addressed gill microbiome characterisation based on using parts of the gill or gill swabs as samples (Steinum *et al*., 2009; Schmidt *et al*., 2016; Legrand *et al*., 2018; Slinger

et al., 2020; Slinger *et al*., 2021). Nevertheless, it was still not determined whether genetic material extracted from a part of a gill arch or from gill swabs would be representative of the microbiome from the entire gill arch. Thus, we successfully optimised in Chapter 3 a modified DNA extraction protocol from entire gill arches for microbiome studies. However, around 75% of the reads we got after sequencing each sample belonged to Atlantic salmon (the host), while this ranged between 10 and 14 % in samples from Chapters 4 and 5. We did not include any gill disruption step to try to avoid as much host DNA as possible. However, we needed to cope with host DNA contamination by automatically removing those sequences prior to bioinformatic analyses. Host DNA contamination is one of the most significant challenges that host-microbiome studies face (Marotz *et al*., 2018), as a high abundance of host DNA may obscure patterns in microbial community analyses due to competition with microbiome DNA for PCR amplification (Lefèvre *et al*., 2020; Reigel *et al.*, 2020). Thus, various researchers have proposed using, for instance, blocking primers (Arenz *et al*., 2015), propidium monoazide (Marotz *et al*., 2018) or methylation-based enrichments (Chiou & Bergey, 2018) for host DNA depletion. We suggest that future modifications of the novel DNA extraction procedure that we optimised in Chapter 3 should include one of the mentioned host DNA depletion techniques. Additionally, further studies describing the gill microbiome should determine how similar the microbiome DNA extracted from a part of a gill arch and the microbiome DNA extracted from an entire gill arch are. Unfortunately, we could not determine the utility of a part of a gill arch in charactering the microbiome from entire gill arches due to our limited resources.

Another concern that we had while optimising the DNA extraction procedure for the gill microbiome in Chapter 3 was whether the resulting DNA samples are representative of the gill microbiome. The first step of that procedure consisted on multiple consecutive washes of the gill in a trypsin solution, to try to detach as much microbes as possible from the gill surface. However, we were unsure about how many times we should wash the gill. To ensure that we do not miss any abundant taxa on gills, we decided to wash various gills a total of seven times and to characterise and compare the bacteria in each separated wash. There was no increase in the bacterial diversity along with the washes, and the bacterial community structure obtained in each wash was indistinguishable from the others. In conclusion, the most relatively abundant bacteria were equally represented in each of the washes; hence, we decided to keep a total of five consecutive washes for the DNA extraction from gills. Although extracting the DNA from more than seven washes would likely increase the representativeness of the procedure, the proteolytic effect of the trypsin (Wang *et al*., 2008) already started disintegrating the gill tissue at the

seventh wash, raising the abundance of salmon DNA in the resulting sample. Despite the inherent limitations in discriminating between close taxa using amplicon sequencing (Poretsky *et al*., 2014), we consider that the DNA extraction procedure that we developed, in combination with the sequencing approach and the bioinformatic pipeline that we used, ensured a good representativeness in describing the gill prokaryotic microbiome.

We conducted a parallel experiment in Chapter 3, where we tested mucus sampling from gills as a non-lethal substitute of branchial arch sampling in microbiome studies. To ensure enough DNA concentration in our samples, I sampled mucus by gently scraping the surface of the gill using a sterile spatula and pooling mucus from the same fish cage in the same tube. Thus, our sampling method can be named as mucus scraping. This method only differs in one thing from the typical mucus swabbing (Legrand *et al.*, 2018; Minich *et al*., 2020a; Minich *et al*., 2020b; Slinger *et al*., 2021): the tool used to collect the gill mucus. Hence, these two methods are similar enough to extrapolate our results from mucus scraping to mucus swabbing. Results from Chapter 3 evidenced that microbiomes from branchial arch sampling and mucus scraping were slightly different. However, we concluded that mucus scrapping was a suitable non-lethal substitute for gill sampling for partial characterisation of the whole-gill prokaryotic community. We did not implement mucus sampling in the other sampling campaigns, as salmon we got the gills from in Chapters 4 and 5 were also sampled for other studies after been euthanised. Thus, we decided to keep the sampling simple and to excise the gills. However, future gill microbiome studies aiming to describe or quantify the most relatively abundant part of the bacterial community could sample mucus by scraping or swabbing, a non-lethal approach that would allow the salmon to continue living.

Although this thesis successfully characterised the gill microbiome from AGD-affected and AGD-unaffected salmon in multiple environments, we could only speculate as to the possible functionality of the gill bacteria and their role in AGD due to the sequencing procedure we used. There are currently many culture-independent tools available to help characterising microbial communities, for instance denaturing, or temperature, gradient gel electrophoresis (DGGE or TGGE)(Muyzer & Smalla, 1998; Xu, 2006; Boughner & Singh, 2016), terminal restriction fragment length polymorphism (TRFLP)(Xu, 2006; Boughner & Singh, 2016), fluorescence *in situ* hybridization (FISH)(Xu, 2006), microautoradiography with FISH (MAR-FISH)(Okabe *et al*., 2004), and DNA or RNA stable-isotope probing (DNA/RNA-SIP) (Bernard *et al*., 2007), among others. However, DGGE, TGGE, and TRFLP are laborious and technically-complex, as well as increasingly outdated, assays that are not able to identify from which microorganism the

separated amplicons come. Thus, for these approaches, a sequencing of the amplicons also required if the genotypes are to be identified (Liu *et al*., 1997), increasing the complexity of the entire procedure for the user. FISH, MAR-FISH and DNA/RNA-SIP are used to label parts of the microbial cell. Hence, the researcher is able to detect and enumerate those microorganisms, to study their metabolic functions, and even their spatial-temporal interactions within the community (Okabe *et al*., 2004; Neufeld *et al*., 2007). Nevertheless, FISH and MAR-FISH require having initial information about the genetic sequence or metabolic pathways of the microorganisms of interest (Xu, 2006; Okabe *et al*., 2004), making them less suitable for the description of undefined microbiomes. In addition, DNA/RNA-SIP and MAR-FISH use isotopes (Neufeld *et al*., 2007), thus increasing the costs and, in the case of using radioisotopes, increasing the risk on the user. We decided not to use any of the previously mentioned approaches to characterise the gill microbiome from AGD-affected salmon, which was quite under-studied when we made that decision.

On the other hand, high-throughput sequencing technologies have been used for years to study microbiomes, as they are relatively easy and increasingly inexpensive approaches (Sinclair *et al.*, 2015). Among these, amplicon sequencing platforms, such as Illumina MiSeq or HiSeq, allows for descriptions of microbial communities and the relative abundance of their components based on sequencing one gene, normally the ribosomal RNA gene, which is common between the microorganisms of interest (Sinclair *et al.*, 2015). Many microbiome features could be easily obtained from the short reads that amplicon sequencing provides in MiSeq and HiSeq, named: alpha and beta-diversity descriptors, environmental filtering, subset regressions, core microbiome, or differential taxa analyses among others.

However, amplicon sequencing provides no evidence of the metabolic activity or functionality of specific taxa in the microbiome, due to sequencing only one gene. In contrast, the study of potential metabolic activities in mixed microbial communities can be addressed by sequencing the genome from the entire community using Illumina MiSeq or HiSeq (Ayling *et al*., 2020), and assembling those genomes in a complex bioinformatic process, this kind of research is known as metagenomics. The development of new technologies allowed obtaining longer reads in sequencing, making metagenomic studies easier to perform and more reliable (Wommack *et al*., 2008). Thus, future gill microbiome research should include sequencing from longer reads targeting entire genomes (like, for example, Oxford Nanopore (James *et al*., 2020), or MinIon (Brown *et al*., 2017) technologies) if authors also want to be able to characterise the potential metabolic activity of particular microbes. Additionally, metatranscriptomics, metaproteomics

and metabolomics would further elucidate the relationships between gill microbiome members, and their connection with AGD and other environmental factors (as water temperature). Despite the obvious benefits of taking such genome-centric approaches, we decided to use Illumina MiSeq amplicon sequencing of rRNA genes in our sampling campaigns, as MiSeq outcomes fit with the aims in this thesis, and the sequencing price was affordable for our available budget.

6.3 - Future research and recommendations for the aquaculture industry

This thesis addressed some knowledge gaps associated with the gill microbiome from Atlantic salmon, and the relationship between the gill microbiome and AGD. Several novel findings were presented which could have implications for Atlantic salmon aquaculture. However, future research is required to better understand the role of the gill microbiome on AGD, and on other gill diseases (such as Complex Gill Disease (CGD), for example). These investigations should further describe and compare the gill microbiome from various aquaculture areas worldwide, to determine if our results are reproducible and to obtain findings that could be extrapolated to other farms with AGD-affected fish. In combination with more laboratory challenges, the role of certain members of the gill microbiome on the onset and development of AGD could be better unveiled. This may provide further evidence for the development of a qPCR assay to assess the vulnerability of salmon to AGD prior to *Neoparamoeba perurans* colonisation; or even to develop a preventive treatment for AGD through the gill microbiome manipulation (with pro- or prebiotics, for instance). However, we recommend that future research on the gill microbiome should use metagenomic approaches to sequence the microbiome DNA. This would allow not only to identify members in the gill microbiome, but also to describe the potential metabolism of specific microorganisms, probably improving our comprehension of their role on the gill microbial community and on the development of gill diseases. Additionally, studying the same fish cohort during a long period of time (more than one year) and sampling every week or two weeks using non-lethal sampling (like mucus scraping or swabbing) would be desirable. We also recommend that the ideal research on the gill microbiome in AGD-affected salmon in fish farms should sample the surrounding water, and should describe the fish immunological response during AGD to better explain dynamics in gill microbial communities.

The aquaculture industry has been using freshwater baths to treat AGD for several years now, and in the present thesis we suggested that freshwater bathing also had an impact on the gill microbiome from the farmed Atlantic salmon described in Chapter 3. The positive effects of this treatment on treating AGD have been widely proved (Oldham *et al*., 2016), but it may delay the

development of the gill microbiome towards a stable community, which probably acts as the first line of defence against gill pathogens (Boutin *et al*., 2012). Thus, over-treating salmon with freshwater baths for AGD may increase the susceptibility of those fish to other gill diseases. Therefore, we recommend not treating salmon too often with freshwater baths, but only when there is clear evidence of AGD in the salmon cohort.

Various AGD diagnostic methodologies have been under development in recent years (Downes *et al*., 2017; Cano *et al*., 2020; Fernandez-Senac *et al*., 2020), all targeting *N. perurans*. Cano *et al*. (2020) suggested that their loop-mediated isothermal amplification (LAMP) assay could be used as a test for the on-site identification of *N. perurans*. However, we correlated the abundance of *N. perurans* on gills with the AGD gill scoring in most of the sampled farms described in Chapter 4. Thus, we support that on-site evaluation of the AGD gill scores is better to assess the severity of the gill disease, while other molecular tools are better to confirm the presence of *N. perurans* on gills. Hence, a collaboration with a R&D institution (like a local research institute or university), where the molecular analyses could be performed, is desirable. Additionally, the R&D institution could help with the farm monitoring, scoring, and molecular assays development, while fish farm could provide the institution with educational and research-related activities.

The currently AGD-associated mortalities range between 10 and 20% worldwide, and AGD is still considered one of the main health concerns in salmonid production (Oldham *et al*., 2016). Although the most commonly used treatment for AGD is relatively inexpensive and available in salmon production areas, further research on AGD will likely provide better diagnostic methodologies, treatments, and even preventive therapies. Conclusions from the present thesis could help move a step closer to improving AGD diagnostics and prevention whilst targeting the gill microbiome in Atlantic salmon.

6.4 - References

Abid, A., Davies, S. J., Waines, P., Emery, M., Castex, M., Gioacchini, G., Carnevali, O., Bickerdike, R., Romero, J. & Merrifield, D. L. (2013). Dietary synbiotic application modulates Atlantic salmon (*Salmo salar*) intestinal microbial communities and intestinal immunity. *Fish & shellfish immunology*, 35(6), 1948-1956.

Adams, M. B., & Nowak, B. F. (2004). Sequential pathology after initial freshwater bath treatment for amoebic gill disease in cultured Atlantic salmon, *Salmo salar* L. *Journal of Fish Diseases*, 27(3), 163-173.

Arenz, B. E., Schlatter, D. C., Bradeen, J. M., & Kinkel, L. L. (2015). Blocking primers reduce co-amplification of plant DNA when studying bacterial endophyte communities. *Journal of microbiological methods*, 117, 1-3.

Ayling, M., Clark, M. D., & Leggett, R. M. (2020). New approaches for metagenome assembly with short reads. *Briefings in bioinformatics*, 21(2), 584-594.

Bernard, L., Mougel, C., Maron, P. A., Nowak, V., Lévêque, J., Henault, C., Haichar, F.E.Z., Berge, O., Marol, C., Balesdent, J.,&Ranjard, L. (2007). Dynamics and identification of soil microbial populations actively assimilating carbon from 13C-labelled wheat residue as estimated by DNA-and RNA-SIP techniques. *Environmental Microbiology*, 9(3), 752-764.

BIM (Bord IascaighMhara) Annual Aquaculture Survey (2019) Ireland's Seafood Development Agency. http://www.bim.ie/our-publications/aquaculture/

Boughner, L. A., & Singh, P. (2016). Microbial Ecology: Where are we now?.*Postdoc journal: a journal of postdoctoral research and postdoctoral affairs*, 4(11), 3.

Boutin, S., Bernatchez, L., Audet, C., &Derôme, N. (2012). Antagonistic effect of indigenous skin bacteria of brook charr (*Salvelinus fontinalis*) against *Flavobacterium columnare* and *F. psychrophilum*. *Veterinary microbiology*, 155(2-4), 355-361.

Bowman, J. P., & Nowak, B. (2004). Salmonid gill bacteria and their relationship to amoebic gill disease. *Journal of Fish Diseases*, 27(8), 483-492.

Brown, B. L., Watson, M., Minot, S. S., Rivera, M. C., & Franklin, R. B. (2017). MinION™ nanopore sequencing of environmental metagenomes: a synthetic approach. *GigaScience*, 6(3), gix007.

Cano, I., McCullough, R., Mulhearn, B., Gunning, S., Waine, A., Joiner, C., & Paley, R. (2020). Non-lethal loop-mediated isothermal amplification assay as a point-of-care diagnostics tool for *Neoparamoebaperurans*, the causative agent of amoebic gill disease. *Journal of fish diseases*, 43(7), 779-790.

Chiou, K. L., &Bergey, C. M. (2018). Methylation-based enrichment facilitates low-cost, noninvasive genomic scale sequencing of populations from feces. *Scientific reports*, 8(1), 1-10.

Djordjevic, B., Morales-Lange, B., Øverland, M., Mercado, L., & Lagos, L. (2021). Immune and proteomic responses to the soybean meal diet in skin and intestine mucus of Atlantic salmon (*Salmo salar* L.). *Aquaculture Nutrition*.

Downes, J. K., Rigby, M. L., Taylor, R. S., Maynard, B. T., MacCarthy, E., O'Connor, I., Marcos-Lopez, M., Rodger, H.D., Collins, E., Ruane, N.M. & Cook, M. T. (2017). Evaluation of Non-destructive Molecular Diagnostics for the Detection of *Neoparamoebaperurans*. *Frontiers in Marine Science*, 4, 61.

Embar-Gopinath, S., Butler, R., & Nowak, B. (2005). Influence of salmonid gill bacteria on development and severity of amoebic gill disease. *Diseases of aquatic organisms*, 67(1-2), 55-60.

Embar-Gopinath, S., Crosbie, P., & Nowak, B. F. (2006). Concentration effects of *Winogradskyella* sp. on the incidence and severity of amoebic gill disease. *Diseases of aquatic organisms*, 73(1), 43-47.

Fernandez-Senac, C., Fridman, S., Sokolowska, J., Monaghan, S. J., Garzon, T., Betancor, M., Paladini, G., Adams, A. &Bron, J. E. (2020). A comparison of the use of different swab materials for optimal diagnosis of amoebic gill disease (AGD) in Atlantic salmon (*Salmo salar* L.). *Journal of Fish Diseases*, 43(11), 1463-1472.

Gajardo, K., Jaramillo-Torres, A., Kortner, T. M., Merrifield, D. L., Tinsley, J., Bakke, A. M., &Krogdahl, Å. (2017). Alternative protein sources in the diet modulate microbiota and functionality in the distal intestine of Atlantic salmon (*Salmo salar*). *Applied and environmental microbiology*, 83(5), e02615-16.

James, R. S., Rangama, S., Clark, V., & Wellington, E. M. (2020). Genetic characterisation of a large antibiotic resistant environmental ST131 *E. coli* plasmid using a long read hybrid assembly approach. *BioRxiv*.

Jones, J., DiBattista, J. D., Stat, M., Bunce, M., Boyce, M. C., Fairclough, D. V., Travers, M.J. & Huggett, M. J. (2018). The microbiome of the gastrointestinal tract of a range-shifting marine herbivorous fish. *Frontiers in microbiology*, 9, 2000.

Karlsen, C., Ottem, K. F., Brevik, Ø. J., Davey, M., Sørum, H., &Winther-Larsen, H. C. (2017). The environmental and host-associated bacterial microbiota of Arctic seawater-farmed Atlantic salmon with ulcerative disorders. *Journal of fish diseases*, 40(11), 1645-1663.

Larsen, A. M., Bullard, S. A., Womble, M., & Arias, C. R. (2015). Community structure of skin microbiome of gulf killifish, *Fundulus grandis*, is driven by seasonality and not exposure to oiled sediments in a Louisiana salt marsh. *Microbial ecology*, 70(2), 534-544.

Lefèvre, E., Gardner, C.M. and Gunsch, C.K. (2020). A novel PCR-clamping assay reducing plant host DNA amplification significantly improves prokaryotic endo-microbiome community characterization. *FEMS Microbiology Ecology*, 96(7), p.fiaa110.

Legrand, T. P., Catalano, S. R., Wos-Oxley, M. L., Stephens, F., Landos, M., Bansemer, M. S., Stone, D.A., Qin, J.G. & Oxley, A. (2018). The inner workings of the outer surface: skin and gill microbiota as indicators of changing gut health in yellowtail kingfish. *Frontiers in microbiology*, 8, 2664.

Legrand, T. P., Wynne, J. W., Weyrich, L. S., & Oxley, A. P. (2020). A microbial sea of possibilities: current knowledge and prospects for an improved understanding of the fish microbiome. *Reviews in Aquaculture*, 12(2), 1101-1134.

Liu, W. T., Marsh, T. L., Cheng, H., & Forney, L. J. (1997). Characterization of microbial diversity by determining terminal restriction fragment length polymorphisms of genes encoding 16S rRNA. *Applied and environmental microbiology*, 63(11), 4516-4522.

Minich, J. J., Poore, G. D., Jantawongsri, K., Johnston, C., Bowie, K., Bowman, J., Knight, R., Nowak, B. & Allen, E. E. (2020a). Microbial ecology of Atlantic salmon (*Salmo salar*) hatcheries: impacts of the built environment on fish mucosal microbiota. *Applied and Environmental Microbiology*, 86(12).

Minich, J. J., Petrus, S., Michael, J. D., Michael, T. P., Knight, R., & Allen, E. E. (2020b). Temporal, environmental, and biological drivers of the mucosal microbiome in a wild marine fish, *Scomber japonicus*. *Msphere*, 5(3).

Minniti, G., Hagen, L. H., Porcellato, D., Jørgensen, S. M., Pope, P. B., &Vaaje-Kolstad, G. (2017). The skin-mucus microbial community of farmed Atlantic salmon (*Salmo salar*). *Frontiers in microbiology*, 8, 2043.

Mullins, J., Nowak, B., Leef, M., Røn, Ø., Eriksen, T. B., & McGurk, C. (2020). Functional diets improve survival and physiological response of Atlantic salmon (*Salmo salar*) to amoebic gill disease. *Journal of the World Aquaculture Society*, 51(3), 634-648.

Muyzer, G., &Smalla, K. (1998). Application of denaturing gradient gel electrophoresis (DGGE) and temperature gradient gel electrophoresis (TGGE) in microbial ecology. *Antonie van Leeuwenhoek*, 73(1), 127-141.

Neufeld, J. D., Dumont, M. G., Vohra, J., & Murrell, J. C. (2007). Methodological considerations for the use of stable isotope probing in microbial ecology. *Microbial Ecology*, 53(3), 435-442.

Okabe, S., Kindaichi, T., & Ito, T. (2004). MAR-FISH—An ecophysiological approach to link phylogenetic affiliation and in situ metabolic activity of microorganisms at a single-cell resolution. *Microbes and environments*, 19(2), 83-98.

Oldham, T., Rodger, H., & Nowak, B. F. (2016). Incidence and distribution of amoebic gill disease (AGD)—an epidemiological review. *Aquaculture*, 457, 35-42.

Parsons, H., Nowak, B., Fisk, D., & Powell, M. (2001). Effectiveness of commercial freshwater bathing as a treatment against amoebic gill disease in Atlantic salmon. *Aquaculture*, 195(3-4), 205-210.

Poretsky, R., Rodriguez-R, L. M., Luo, C., Tsementzi, D., & Konstantinidis, K. T. (2014). Strengths and limitations of 16S rRNA gene amplicon sequencing in revealing temporal microbial community dynamics. *PloS one*, 9(4), e93827.

Reigel, A.M., Owens, S.M. and Hellberg, M.E. (2020). Reducing host DNA contamination in 16S rRNA gene surveys of anthozoan microbiomes using PNA clamps. *Coral Reefs*, 39(6), 1817-1827.

Schmidt, V., Amaral-Zettler, L., Davidson, J., Summerfelt, S., & Good, C. (2016). Influence of fishmeal-free diets on microbial communities in Atlantic salmon (*Salmo salar*) recirculation aquaculture systems. *Applied and environmental microbiology*, 82(15), 4470-4481.

Sinclair, L., Osman, O. A., Bertilsson, S., &Eiler, A. (2015). Microbial community composition and diversity via 16S rRNA gene amplicons: evaluating the illumina platform. *PloS one*, 10(2), e0116955.

Slinger, J., Adams, M. B., & Wynne, J. W. (2020). Bacteriomic profiling of branchial lesions induced by *Neoparamoebaperurans* challenge reveals commensal dysbiosis and an association with *Tenacibaculumdicentrarchi* in AGD-affected Atlantic salmon (*Salmo salar* L.). *Microorganisms*, 8(8), 1189.

Slinger, J., Adams, M. B., Stratford, C. N., Rigby, M., & Wynne, J. W. (2021). The Effect of Antimicrobial Treatment upon the Gill Bacteriome of Atlantic Salmon (*Salmo salar* L.) and Progression of Amoebic Gill Disease (AGD) In Vivo. *Microorganisms*, 9(5), 987.

Smith, C. C., Snowberg, L. K., Caporaso, J. G., Knight, R., &Bolnick, D. I. (2015). Dietary input of microbes and host genetic variation shape among-population differences in stickleback gut microbiota. *The ISME journal*, 9(11), 2515-2526.

Steinum, T., Sjåstad, K., Falk, K., Kvellestad, A., & Colquhoun, D. J. (2009). An RT PCR-DGGE survey of gill-associated bacteria in Norwegian seawater-reared Atlantic salmon suffering proliferative gill inflammation. *Aquaculture*, 293(3-4), 172-179.

Vasemägi, A., Visse, M., &Kisand, V. (2017). Effect of environmental factors and an emerging parasitic disease on gut microbiome of wild salmonid fish. *MSphere*, 2(6).

Waagbø, R. (1994). The impact of nutritional factors on the immune system in Atlantic salmon, *Salmo salar* L.: a review. *Aquaculture Research*, 25(2), 175-197.

Wang, Y., Luo, W., & Reiser, G. (2008). Trypsin and trypsin-like proteases in the brain: proteolysis and cellular functions. *Cellular and Molecular Life Sciences*, 65(2), 237-252.

Wang, J., Jaramillo-Torres, A., Li, Y., Kortner, T. M., Gajardo, K., Brevik, Ø. J., Jakobsen, J.V. & Krogdahl, Å. (2021). Microbiota in intestinal digesta of Atlantic salmon (*Salmo salar*), observed from late freshwater stage until one year in seawater, and effects of functional ingredients: a case study from a commercial sized research site in the Arctic region. *Animal microbiome*, 3(1), 1-16.

Wommack, K. E., Bhavsar, J., & Ravel, J. (2008). Metagenomics: read length matters. *Applied and environmental microbiology*, 74(5), 1453-1463.

Wright, D. W., Nowak, B., Oppedal, F., Crosbie, P., Stien, L. H., & Dempster, T. (2018). Repeated sublethal freshwater exposures reduce the amoebic gill disease parasite, *Neoparamoebaperurans*, on Atlantic salmon. *Journal of fish diseases*, 41(9), 1403-1410.

Wynne, J. W., Stratford, C., Slinger, J., Samsing, F., Rigby, M., McCulloch, R., Quezada-Rodriguez, P., & Taylor, R. S. (2020). The interaction between temperature and dose on the efficacy and biochemical response of Atlantic salmon to hydrogen peroxide treatment for amoebic gill disease. *Journal of Fish Diseases*, 43(1), 39-48.

Xu, J. (2006). Invited review: microbial ecology in the age of genomics and metagenomics: concepts, tools, and recent advances. *Molecular ecology*, 15(7), 1713-1731.

Yukgehnaish, K., Kumar, P., Sivachandran, P., Marimuthu, K., Arshad, A., Paray, B. A., &Arockiaraj, J. (2020). Gut microbiota metagenomics in aquaculture: Factors influencing gut microbiome and its physiological role in fish. *Reviews in Aquaculture*, 12(3), 1903-1927.